EVALUATING INHIBITION OF DNA METHYLATION AND ALDH1A3 AS BREAST CANCER THERAPIES

by

Margaret Lois Dahn

Submitted in partial fulfilment of the requirements
for the degree of Doctor of Philosophy

at

Dalhousie University
Halifax, Nova Scotia
June 2020

TABLE OF CONTENTS

LIST OF TABLES

LIST OF FIGURES

ABSTRACT

Breast cancer is the most common form of cancer among Canadian women. Patients with triple-negative breast cancer (TNBC) have poor prognoses, with inherently more aggressive disease and limited treatment options. New modalities for treating TNBC are required. Here, I investigate a precision medicine approach to applying DNA hypomethylating therapy and assess the potential benefits of targeting breast cancer stem cell (CSC) marker aldehyde dehydrogenase 1A3 (ALDH1A3).

Dysregulation of DNA methylation is an established feature of breast cancers. DNA hypomethylating therapies like decitabine are proposed for the treatment of TNBC yet indicators of response need to be identified. I demonstrate the requirement of deoxycytidine kinase (DCK) for decitabine response in breast cancer cells; however, no predictive features or other mediators of decitabine response were identified. An shRNA-based genome-wide screen was performed to detect potent hypermethylated genes or novel mediators of decitabine. I found that loss of methylene tetrahydrofolate dehydrogenase 2 (MTHFD2) conferred decitabine resistance to TNBC cells likely by suppressing cell proliferation via limiting nucleotide biosynthesis. Therefore, while hypermethylated genes that predict hypomethylating therapy response were not obtained, the relevance of emerging drug target MTHFD2 to TNBC was confirmed.

CSCs are a highly aggressive subpopulation of cells within breast tumours and are identified by their high ALDH1A3 activity. In addition to its role as an established CSC marker, ALDH1A3 plays a key role in the progression and metastasis of breast cancer. Therefore, ALDH1A3 represents a druggable anti-cancer target of interest. Nanoparticle encapsulation of ALDH1A3 inhibitor citral reduced ALDH1A3-mediated growth of MDA-MB-231 TNBC tumours. Metabolomic and gene expression analyses identified γ-aminobutyric acid (GABA) signaling/metabolism as a dysregulated pathway in ALDH1A3-hi breast tumours. In mice treated with systemic GABA there was higher rates of lung metastasis. Patient dataset analyses revealed that metastatic breast cancer has a distinct GABA metabolism profile.

Together, these results suggest two new approaches for TNBC therapy: 1) use MTHFD2 to stratify patients for hypomethylating therapy or directly inhibit MTHFD2 and 2) inhibit ALDH1A3 to potentially control GABA-mediated metastasis.

LIST OF ABBREVIATIONS AND SYMBOLS USED

°C	degrees Celsius
µg	micrograms
µm	micrometres
µM	micromoles per litre
13cRA	13-cis retinoic acid
2D	2-dimensional
3D	3-dimensional
3'UTR	3' untranslated region
5,10-mTHF	5,10-methylenetetrahydrofolate
5mC	5-methylcytosine
5mhC	5-hydroxymethylcytosine
5'UTR	5' untranslated region
7-AAD	7-aminoactinomycin D
A	adenine (nucleotide)
AA	antibiotic-antimycotic
ABAT	γ-aminobutyrate transaminase
ABC	ATP-Binding cassette drug efflux transporters (ABCB1, C1, G2, A3)
ABCB1	ATP Binding Cassette Subfamily B Member 1
ACRC	acidic repeat containing
ADH1A	alcohol dehydrogenase 1A
ADH1B	alcohol dehydrogenase 1B
AJCC	American Joint Committee on Cancer
aka	also known as
AKT	protein kinase B
ALDH	aldehyde dehydrogenase (isoforms 1A1, 1A2, 1A3, 2, 5A1)
ALDH+	high ALDH activity; Aldefluor positive
ALDH5A1	succinic semialdehyde dehydrogenase
ALDHi	ALDH inhibitor
AML	acute myeloid leukemia
ANOVA	analysis of variance
AOX1	aldehyde oxidase
APL	acute promyelocytic leukemia
APOD	apolipoprotein D
ATARiS	Analytic Technique for Assessment of RNAi by Similarity
ATCC	American Type Culture Collection
ATP	adenosine triphosphate
ATRA	all-trans retinoic acid
AU	arbitrary units

B2M	β-2 microglobulin
BAD	Bcl-2 associated agonist of cell death
BAK	Bcl-2 homologous antagonist/killer
BALB/C	Bagg-albino inbred mouse model
BAX	Bcl-2-like protein 4
BCL-2	B-cell CLL/lymphoma 2
BCR-ABL	fusion gene; breakpoint cluster region-Abelson murine leukemia viral oncogene homolog 1
BEH Amide	ethylene bridged hybrid amide column
BIM	Bcl-2-like protein 11
BODIPY	boron-dipyrromethene
bp	base pair
BRCA	breast cancer susceptibility gene type 1
C	cytosine (nucleotide)
Ca^{2+}	calcium ion
$CaCl_2$	calcium chloride
CAF	cancer associated fibroblast
CCAC	Canadian Council on Animal Care
CCL20	chemokine (C-C motif) ligand 20
CD24	cluster of differentiation 24
CD44	cluster of differentiation 44
CDH2	cadherin-2; N-cadherin
CDKN2A	cyclin-dependent kinase inhibitor 2A
cDNA	complementary deoxyribonucleic acid
Citral-NP	nanoparticle encapsulated citral
Cl^-	chloride ion
cm^2	square centimetre
CML	chronic myeloid leukemia
CMML	chronic monomyelocytic leukemia
CMPK1	cytidine/uridine monophosphate kinase 1
CO_2	carbon dioxide
COL16A1	collagen type XVI alpha 1 chain
COX-1	cyclooxygenase-1 encoded by PTGS1
COX-2	cyclooxygenase-2 encoded by PTGS2
CpG	5'—cytosine—phosphate—guanine—3'
Cq	quantification cycle
CRISPR	clustered regularly interspaced short palindromic repeats
CROCC	ciliary rootlet coiled-coil, rootletin
CSC	cancer stem cell
CTC	circulating tumour cell

CTLA4	cytotoxic T-lymphocyte-associated protein 4
Cy3	indocarbocyanine
Cy5	indodicarbocyanine
CYP	cytochromes P450
DAC	decitabine, 5-aza-2'-deoxycytidine
DCK	deoxycytidine kinase
DDX58	DEAD-box helicase 5
DEAB	N,N-diethylaminobenzaldehyde
DHF	7,8-dihydrofolate
DHRS3	dehydrogenase/reductase 3
DIMATE	4-dimethylamino-4- methylepent-2-ynthioic acid-S-methylester
DMEM	Dulbecco’s modified Eagle's medium
DMSO	dimethylsulfoxide
DNA	deoxyribonucleic acid
DNAJB9	DNAJ heat shock protein family (Hsp40) member B9
DNMT	DNA methyltransferase
DNMTi	DNA methyltransferase inhibitor
ECM	extracellular matrix
ELF3	E74-like ETS transcription factor 3
ELISA	enzyme-linked immunosorbent assay
EMP	epithelial to mesenchymal plasticity
envE	endogenous retroviral element envelope-like
EP4	prostaglandin E2 cell surface receptor type 4
ER	estrogen receptor (α, β)
ERK1/2	extracellular signal-regulated kinases 1/2
ERVFRD1	endogenous retrovirus group FRD member 1, envelope
ERVs	endogenous retroviral elements
ESR1	estrogen receptor 1
F12	Ham's F12 nutrient mixture
FACS	fluorescence-activated cell sorting
FBS	fetal bovine serum
FDA	U.S. Food and Drug Administration
FHIT	fragile histidine triad gene
FSC	forward scatter
fTHF	10-formyltetrahydrofolate
G	guanine (nucleotide)
g	gram
G6PD	glucose-6-phosphate dehydrogenase
GABA	γ-aminobutyric acid
GABRA3	γ-aminobutyric acid receptor subunit α3

GABRA6	γ-aminobutyric acid receptor subunit α-6
GABRE	γ-aminobutyric acid receptor subunit ε
GABRP	γ-aminobutyric acid receptor subunit π
GAD1	glutamate decarboxylase 1
GAPDH	glyceraldehyde 3-phosphate dehydrogenase
GEO	Gene Expression Omnibus
GFP	green fluorescent protein
Gly	glycine
GSEA	Gene Set Enrichment Analysis
GSH	glutathione
GSSG	glutathione disulfide
H#K#	histone #, lysine #
H&E	hematoxylin & eosin
H-2Kd	MHC class I alloantigen haplotype d
HAT	histone acetyltransferase
HDAC	histone deacetylase
HEK293T	human embryonic kidney cells 293
HEPES	4-(2-hydroxyethyl)-1-piperazineethanesulfonic acid
HER2	human epidermal growth factor receptor 2, see also ERBB2/neu
HERV-K	human endogenous retrovirus type K
HILIC	hydrophilic interaction liquid chromatography
HIST1H2BA	histone H2B type 1-A
HM450	human methylation 450K Illumina bead chip array
HOXA5	homeobox A5
HPLC	high performance liquid chromatography
HRP	horseradish peroxidase
IC_{50}	inhibitory concentration, 50%
IDH1/2	isocitrate dehydrogenase 1/2
IFIT1	interferon induced protein with tetratricopeptide repeats 1
IP	intraperitoneal
IRF7	interferon regulatory factor 7
ISG15	interferon-stimulated gene 15
ITGA6	integrin alpha-6
kb	kilobase
KD	knockdown
kDa	kilodalton
KLHL3	kelch like family member 3
L-15	Leibovitz's medium
LINE1	class 1 long interspersed nuclear element
lncRNA	long non-coding RNA

LumA	luminal A
LumB	luminal B
MAPK	mitogen-activated protein kinase
Matrigel-HC	high concentration matrigel
MAVS	mitochondrial anti-viral signaling protein
MBD	methyl-CpG binding domain
MDA5	melanoma differentiation-associated protein; encoded by IFIT1
MDR	multidrug resistance
MDR1	multidrug resistance 1 aka P-glycoprotein encoded by ABCB1
MDS	myelodysplastic syndrome
Me-DIP	methyl-DNA immunoprecipitation assay
MEM	minimum essential media
METABRIC	Molecular Taxonomy of Breast Cancer International Consortium
MFI	mean fluorescence intensity
mg	milligrams
$MgCl_2$	magnesium chloride
MGMT	O-6-methylguanine-DNA methyltransferase
miRNA	micro RNA
mL	millilitre
mm^3	cubic millimetre
MMP	matrix metalloproteinase
MMTV-PyMT	mouse mammary tumour virus-polyoma middle tumour-antigen
MOI	multiplicity of infection
MRM	multiple reaction monitoring
mRNA	messenger RNA
MS	mass spectrometer
MS-PCR	methylation-specific PCR
MSTUS	MS total useful signals
mTHF	5-methyl-THF
MTHFD1	methylenetetrahydrofolate dehydrogenase, cyclohydrolase and formyltetrahydrofolate synthetase 1
MTHFD2	methylenetetrahydrofolate dehydrogenase 2
MTHFD2L	methylenetetrahydrofolate dehydrogenase 2 like
N.B.	nota bene
n.s.	not significant
NAD	nicotinamide adenine dinucleotide
NADH	reduced nicotinamide adenine dinucleotide
NADP	nicotinamide adenine dinucleotide phosphate

NADPH	reduced nicotinamide adenine dinucleotide phosphate
NANOG	homeobox transcription factor nanog
NCBI	National Center for Biotechnology Information
NEAA	non-essential amino acids solution
ng	nanogram
NHR	nuclear hormone receptor
nM	nanomole per litre
NME#	nucleoside diphosphate kinase #
NOD/SCID	nonobese diabetic/severe combined immunodeficiency
NOREVA	NORmalization and EVAluation of Metabolomics Data
ns	not significant
NSAID	nonsteroidal anti-inflammatory drug
NT	no treatment
nt	nucleotide
O6-MeG	O6-methylguanine
OASL	2'-5'-oligoadenylate synthetase-like
OCT4	octamer-binding transcription factor 4 (aka POU5F1)
OE	overexpression
OGT	O-GlcNAc transferase
PAM50	prediction analysis of microarray 50
PBS	phosphate buffered saline
PCA	principal component analysis
PCR	polymerase chain reaction
PD1	programmed cell death protein 1
PDL1	programmed death-ligand 1
PDX	patient derived xenograft
PEG-b-PC	polyethylene glycol-block-polycaprolactone
PFS	progression-free survival
PGE2	prostaglandin E2
pGIPZ	GIPZ lentiviral vector plasmid
PI3K	phosphoinositide 3-kinases
PLAT	tissue plasminogen activator; see tPA
PLAU	plasminogen activator, urokinase; see uPA
PLAUR	plasminogen activator urokinase receptor; see uPAR
PML	promyelocytic leukemia
p-NA	p-nitroanilide
POU5F1	POU class 5 homeobox 1; see OCT4
PR	progesterone receptor
PTGES	prostaglandin E synthase
PTGS1	prostaglandin-endoperoxide synthase 1
PTGS2	prostaglandin-endoperoxide synthase 2

Q1/Q3	parent ion / product ion
RA	retinoic acid
RARE	retinoic acid response element
RARRES1	retinoic acid receptor responder protein 1
RARβ	retinoic acid receptor β
RASSF1A	ras Association domain family protein 1
RefSeq	reference sequence database
RFP	red fluorescence protein
RIG-I	retinoic acid-inducible gene I; encoded by DDX58
RNA	ribonucleic acid
RNAi	RNA interference
RPL29	ribosomal protein L29
RPMI	Roswell Park Memorial Institute
RSEM	RNA-Seq by expectation-maximization
RT-qPCR	reverse transcriptase quantitative polymerase chain reaction
RUNX3	runt-related transcription factor 3
SAM	S-adenosylmethionine
SD	standard deviation
SEM	standard error of the mean
Ser	serine
SERPINB2	plasminogen activator inhibitor-2
SERPINE1	plasminogen activator inhibitor-1
SHMT	serine hydroxymethyltransferase
shRNA	short hairpin RNA
siRNA	short interfering RNA
SLC#A1	sodium/nucleoside co-transporters solute carrier family x member 1
snoRNA	small nucleolar RNA
SOX2	sex determining region Y-box 2
SP	side population
SSC	side scatter
T	thymine (nucleotide)
TAC	transcriptome analysis console
Taxol-res	taxane resistant MDA-MB-231 cell line
TCA	tricarboxylic acid
TCGA	the cancer genome atlas
TDRD1	tudor domain containing 1
TET	ten eleven translocation
THF	tetrahydrofolate
TMBIM4	transmembrane BAX inhibitor motif-containing protein 4
TNBC	triple-negative breast cancer

TNM	staging
tPA	tissue plasminogen activator; encoded by PLAT
TRPC4	transient receptor potential cation channel subfamily C member 4
TSG	tumour suppressor gene
TSS	transcription start site
TSS1500	within 1500 base pairs of the transcription start site
TSS200	within 200 base pairs of the transcription start site
TU	transfection units
TXNRD1	thioredoxin reductase 1
U	units
uPA	plasminogen activator, urokinase; see PLAU
uPAR	plasminogen activator urokinase receptor; encoded by PLAUR
UPLC	ultra performance liquid chromatography
Verap	verapamil
x g	times gravity
XRCC4	X-ray repair cross complementing 4
ZNF595	zinc finger protein 595

ACKNOWLEDGEMENTS

To my supervisor, Dr. Paola Marcato, thank you for agreeing to have coffee with me all those years ago. Our conversation then—and the many subsequent discussions—changed the course of my life and I will be forever grateful. Thank you for always being generous with your time, ideas, and kindness. Thank you for being right so many times. Thank you for always having your students' backs. I am also grateful to all my fellow Marcato lab members who have contributed pep talks, useful feedback, and a sense of community.

I am grateful towards all the talented and generous collaborators who have made this work possible. For Roberto who gave me a full summer of mentorship and support; and for Alejandro, Mike, and Pat who made my mass spectrometry dreams come true: thank you! For Krysta who challenged me and got us involved in many fun schemes over the years. To my talented undergraduate students, I am honoured to have benefitted from your clever ideas and hard work. Phil, Celia, Ainsleigh, Mona, and Hayley are all over this manuscript. To lil B, who became a sister to me and contributes so much to my work and my life, I can't imagine this without you.

Thank you to the members of my supervisory committee, Drs Carman Giacomantonio, Ian Weaver, Roy Duncan, and David Hoskin. Your diverse perspectives and guidance have made me a better scientist. I have been gifted with many scientific mentors in my life who have taught me that science can be as emotionally fulfilling as great art or music.

To my family and friends who have shown me love, encouragement, and laughter whenever I needed it. For my parents who believed in me and this day. Much gratitude to my Jackson who is impossibly supportive and loving, and to the rest of the Dahn clan.

I would like to acknowledge financial support from Dalhousie University, the Killam Trusts, Beatrice Hunter Cancer Research Institute, Nova Scotia Health Research Foundation, Alberta Advanced Education, the Government of Nova Scotia Department of Labour and Advanced Education, and the Canadian Institutes of Health Research.

CHAPTER 1: INTRODUCTION

Copyright statement

Portions of this chapter have been previously published in the following manuscripts. The corresponding text has been edited for length, consistency, and to include recent findings.

Thomas ML, P Marcato. Epigenetic Modifications as Biomarkers of Tumour Development, Therapy Response, and Recurrence Across the Cancer Care Continuum (2018). *Cancers* doi:10.3390/cancers10040101

Thomas ML, Krysta M Coyle, Mohammad Sultan and Paola Marcato. (2015) Cancer Stem Cells and Chemoresistance: Strategies to Overcome Therapeutic Resistance (Chapter 26). Cancer Stem Cells: Emerging Concepts and Future Perspectives in Translational Oncology. Springer.

Contribution statement

I prepared the included manuscripts and figures for publication with the guidance of PM. KMC, MS, and AVK supported the writing of the respective manuscripts. All manuscripts were reviewed and edited by all indicated authors.

1.1 BREAST CANCER

Breast cancer is the most commonly diagnosed cancer among Canadian women with 27,400 women expected to receive a breast cancer diagnosis in 2020[1]. Overall, breast cancer is the fourth leading cause of cancer-related mortality in Canada, responsible for 6.1% of cancer-related deaths. This mortality rate is comparable to what is observed in other developed nations, and has been decreasing over time[2]. Since its peak mortality rate of 43 per 100,000 population in 1986 to ≈22 per 100,000 population in 2020; breast cancer mortality in Canada has declined by 49%[1]. This decline is attributed to the improved screening measures and treatment strategies that have been implemented.

Most women present with early stage breast cancer and have surgery. They may also receive radiotherapy as well as adjuvant systemic therapy to reduce their risk of relapse. Treatment paradigms for invasive breast cancer are based on different risk factors and histological features[3]. The most commonly used biomarkers for molecular classification of invasive breast carcinoma are estrogen receptor (ER), progesterone receptor (PR), and human epidermal growth factor receptor (HER2) which are assessed by immunohistochemistry[4]. The nuclear protein Ki-67 is also commonly assessed by immunohistochemistry, and is used as a proxy for proliferation rate and is positively associated with poor prognosis[5]. Gene expression profiling is another tool for breast cancer classification and overlaps well with existing hormone receptor profiles. The four intrinsic molecular subtypes of invasive breast carcinoma as determined by gene expression profiling are: luminal A, luminal B, Her2-enriched, and basal-like[6]. However, this molecular classification is not used in routine clinical practice.

While overall breast cancer mortality is decreasing over time, the benefits of new therapies are not felt by all patients. A particularly aggressive type of breast cancer that does not express the three hormone receptors (ER, PR, and HER2) is termed triple-negative breast cancer (TNBC). These patients are not eligible to receive the estrogen receptor-targeted (tamoxifen) or HER2-targeted (Herceptin) therapies that have been successfully applied to patients who do express those receptors. Studying the biology of TNBC will eventually translate to improved therapies for this underserved cancer population.

Triple-negative breast cancer accounts for 15-20% of all invasive breast carcinomas[7,8]. The risk of metastasis and death from breast cancer within 5 years of diagnosis is significantly higher in TNBC cases versus non-TNBC (Hazard ratio [HR] = 3.2)[8]. This increased relapse rate is partially attributed to TNBC having a higher percentage of an aggressive subpopulation of cancer cells know as cancer stem cells (CSCs) [9,10,19,11–18]. CSCs are highly tumourigenic, but most concerning in terms of mitigating recurrence is their intrinsic resistance to chemotherapy and their increased metastatic potential[20,21]. New therapeutic approaches which can effectively target TNBC and CSCs are required. Here, I investigate strategies to 1) apply DNA hypomethylating agents and 2) inhibit ALDH1A3-mediated growth and metastasis as breast cancer therapies with a focus on TNBC.

1.2 EPIGENETICS OF BREAST CANCER

Cancer has been referred to as “cellular chaos.” This is an appropriate description for a disease which is characterized by uncontrolled cell proliferation and avoiding the host’s strategies to eliminate aberrant cells. Part of the chaotic nature of cancer cells is that

while all cancers share certain hallmark traits, the driving forces and resulting phenotype of the aberrant cells can vary greatly[22]. While the role of genetic mutations as drivers of carcinogenesis has been firmly established, epigenetic modifications have more recently been proposed as important drivers of cancer as well[23].

The term epigenotype was first coined by C.H. Waddington in 1942 to describe the heritable alterations in gene expression which affect phenotype and do not change the DNA sequence itself [24]. Epigenetic modifications are key regulators of gene expression and contribute to genomic stability/chromatin structure.

1.2.1 *EPIGENETIC MODIFICATIONS*

Post-Translational Histone Modifications

The human genome consists of approximately 3 billion base pairs and can fit within a cell due to the tightly regulated process of DNA compaction, the first stage of which is based around the nucleosome[25]. The nucleosome is a core unit of chromatin consisting of an octamer of four histone proteins (H2A, H2B, H3, and H4) with approximately 147 bp of DNA wrapped twice around the complex[26]. An amino acid tail extends from each histone, and it is the post-translational modifications to these tails which affect histone–DNA interactions and nuclear architecture[27]. Over 60 distinct histone modifications exist, though most cancer-related research focuses on acetylation (mediated by histone deacetylases (HDACs) and histone acetyltransferases (HATs)) and methylation (mediated by several protein lysine methyl-transferases like polycomb repression complex)[28].

The presence of these modifications forms a histone "code" that can affect transcriptional activity of the associated DNA sequence via directly impacting DNA wrapping or through recruiting enzyme complexes to wrap the DNA[29]. Histone modifications which generally indicate areas of active transcription include H3K4me (methylation of histone 3 at lysine position 4), H3K36me, H3KAc, H4K16Ac, and H3KAc; while H3K27me and H3K20me are associated with gene repression[29–32]. Breast cancer cells display silencing histone modifications on tumour-suppressive genes and encourage active transcription histone modifications on oncogenes[33]. Global histone profiling revealed a general loss of H4K16Ac and H4K20me3 (trimethylation) in a variety of cancers[33,34].

Dysregulation of histone variants has also been observed in breast cancer. These proteins are functionally distinct from the canonical replication-coupled core histones and endow special properties to chromatin. For example, H2A.Bbd incorporation results in nucleosomes containing 118–130 bp; this less compact chromatin is potentially more transcriptionally active[35]. Histone variants can also be post-translationally modified; thus the many combinations of canonical and variant histones (with their associated post-translational modifications) form a "variant network" to epigenetically alter chromatin structure and transcription[36]. Expression or mutation of specific histone variants are prognostic biomarkers, as in the case of H2A.Z in breast cancer where overexpression confers a poor prognosis[37,38].

Non-Coding RNAs

With the discovery that only approximately 3% of transcribed RNAs were subsequently translated into proteins, there was a surge of interest in the role of the non-

coding RNA transcriptome[39]. There are several types of non-coding RNAs, such as small nucleolar RNAs (snoRNAs), and short interfering RNAs (siRNAs); but microRNAs (miRNAs) and long non-coding RNAs (lncRNAs) have been the most extensively characterized in breast cancer[40,41]. As their names suggest, miRNAs are small (18–20 nucleotides) while long non-coding RNAs are significantly longer (200–100,000 nucleotides). While these RNA species are divergent in their size and how they are post-transcriptionally processed, they share a common feature: a single miRNA or lncRNA is able to affect multiple genes/proteins[42,43]. Thus, deregulation of a single miRNA or lncRNA can influence many pathways and alter downstream processes such as apoptosis, proliferation, differentiation, etc. and act as either oncogene or tumour suppressor[44]. Many studies have described differential miRNA/lncRNA expression profiles between normal and cancerous human cells[45].

MicroRNAs repress protein production by binding to the 3′ untranslated region (3'-UTR) of their target messenger RNA (mRNA); this miRNA–mRNA duplex is actively degraded and also prevents translation initiation[43]. While miRNAs are canonically repressive, lncRNA functions are more diverse. There are four archetypes of lncRNA function (decoy, activator, guide, or scaffold) which help dictate the interactions between transcription factors or chromatin modifier complexes. LncRNAs ultimately change either the transcription of an mRNA or participate in post-transcriptional regulation of mRNA maturation processes[42].

DNA Methylation

The nucleotide alphabet has been expanded beyond ATGC with the discovery of modified bases, the best-characterized of which is 5-methylcytosine (5mC)[46]. In 5mC, a

methyl moiety, donated by *S*-adenosylmethionine (SAM), is added to the 5′ position of a cytosine residue in CpG dinucleotides. The maintenance and *de novo* generation of 5mC is mediated by DNA methyltransferases DNMT1/3A/3B. Genomic regions with high concentration of CpGs are known as CpG islands and seem to have an important role in gene expression regulation. Approximately 40–70% of human genes have CpG islands in the promoter region; and when these islands acquire 5mC, transcription of the gene is inhibited[47]. 5mC-mediated transcriptional repression was also observed in genes without promoter CpG islands[48–50]. A prototypical breast cancer phenotype consists of a globally hypomethylated genome (which disrupts genomic stability) concurrent with promoter-specific hypermethylation (which silences tumour suppressor genes)[23,51,52].

Several methods exist for assessing DNA methylation at a global or CpG site-specific level. Global methylation levels can be determined via liquid chromatography–electrospray ionization–tandem mass spectrometry, luminometric methylation assay, or using methylation of repetitive sequences like long interspersed nuclear element (LINE) as a proxy of global methylation[53–55]. Site-specific methylation assays are also prevalent and can use either genome-wide discovery/screening approaches (e.g., Illumina beadchip, reduced representation or whole genome bisulfite sequencing, or methylated DNA immunoprecipitation sequencing), or can be used to investigate a single region (e.g., pyrosequencing or methylation-specific polymerase chain reaction (MS-PCR))[56,57]. The most commonly used assays are MS-PCR and the Illumina HumanMethylation bead kits[58,59].

Stable gene silencing may occur when areas of the promoter region that are rich in CpG dinucleotide content (CpG islands) become methylated[60,61]. DNA methylation

silences gene expression through two mechanisms. In the direct mechanism, DNA methylation at transcription factor binding sites blocks the necessary transcription factors and this blockage effectively silences expression of the gene[62]. In the indirect mechanism, the methyl-CpG binding domain (MBD) proteins bind to the methylated DNA, recruit co-proteins and histone modification enzymes, and ultimately modify chromatin compaction.

Active demethylation in somatic cells has been observed in response to hormones, during tissue-specific differentiation, and during re-programming to re-activate pluripotency genes[63]. One striking discovery is that demethylation in somatic cells is far more common in CpG-poor regions than in CpG islands; implying that when aberrant methylation occurs on CpG islands, is it less likely to be removed through typical means. Demethylation can occur through a series of steps that culminate in the replacement of the 5-methylcytosine with an unmethylated cytosine. 5-Methylcytosine (5mC) is sequentially oxidized by ten eleven translocation (TET) enzymes to 5-formylcytosine or 5-carboxylcytosine, which is then removed by DNA glycosylases which are a group of enzymes involved in base excision repair[64,65]. The product of this reaction would then undergo DNA patch repair and an unmethylated cytosine would take the place of the 5mC. DNA methylation can also be passively lost through depletion of SAM levels or reduction of DNMT activity[66].

Before discussing the literature on breast cancer methylation, it should be noted that there are several DNA modifications that have recently been identified. Typically, DNA methylation refers to methylation of cytosine (5mC) or the hydroxymethylation of cytosine (5mhC); however, 5-carboxylcytosine and 5-formylcytosine are picked up by many methylation assays. To be consistent with primary publications, the term “DNA

methylation" is used, but it may be more appropriate to refer to the results of many studies as "DNA modifications."

1.3 DNA METHYLATION IN BREAST CANCER

1.3.1 *HYPERMETHYLATION OF SINGLE GENES & GENOME-WIDE HYPOMETHYLATION*

The human genome contains approximately 30 million CpG dinucleotides, and the portion of these cytosines that are methylated is 4-6%[67]. Interestingly, CpG islands are mostly unmethylated with the majority of methylation occurring in areas of CpG-poor DNA[63]. At this time however it is unknown exactly which features of a given sequence make it a target for DNA methylation[63]. Two general hypotheses have emerged: differential attraction of methylation machinery, or removal of the anti-methylation factors that protect the default state. Regardless of the exact mechanism, recent work has shown that the surrounding DNA sequence is vital in specifying the correct methylation status. Lienert *et al*. (2011) inserted a series of short DNA sequences into a murine pluripotent stem cell and determined that the integrated sequences gained the same methylation status as the local DNA[68]. Not only did these inserted elements obtain the correct methylation profile, but retained their status during differentiation, highlighting the importance of proximal DNA regions in specifying methylation status. Though methylation acts upon the CpG dinucleotide, it does not appear that the CpG density in the surrounding DNA is the most important factor in determining methylation status. A microarray analysis of human embryonic stem cells found that motifs associated with transcription start sites and not CpG density were most predictive of an unmethylated region[69]. While there are characteristics

of the DNA sequence that make a gene more susceptible to aberrant hypermethylation, there does not seem to be a universal rule to predict methylation status in mammals.

Silencing of specific genes has important effects on cell phenotype, but the overall methylation level also plays a role in regulation of gene expression. A genome-wide decrease in methylation accompanied by gene-specific increased methylation is associated with aging as well as breast cancer[70]. In all cancers, the general trend has been towards global hypomethylation with hypermethylation of specific genes at the promoter region[71]. This holds true for breast carcinomas where patient samples were revealed to have global hypomethylation that correlated with tumour grade[72]. Genome-wide analyses were developed with the goal of determining how the composition of methylated regions changes with gene expression and phenotype. For two commonly studied breast cancer cell lines (MDA-MB-231 and MCF-7) it was determined that methylation was significantly different between the cell lines for ≈300 genes[73]; which illustrates differences in methylation of individual genes. Interestingly, characterization of genome-wide methylation changes using a methyl-DNA immunoprecipitation assay (Me-DIP) combined with sequencing found that while there was differential methylation of individual genes, the global methylation pattern was the same for MCF-7 and MDA-MB-231 cells: overall hypomethylation with promoter-specific hypermethylation[74].

In normal cells, the majority of promoter region CpG islands are unmethylated; however, in breast cancer there is an increase in methylation at these regions. In breast cancer, the change from unmethylated to hypermethylated at promoter region CpG islands is contrasted against the total CpG content where the initial global methylation transitions to global hypomethylation. Hypermethylation in breast cancer is clearly prevalent in

promoter regions; however, the distribution of hypermethylation in other regions changes as well[74]. Increased methylation was observed at some introns and exons even while global methylation decreased in general. Overall, hypomethylation was the trend for total CpG content, with most regions showing decreased methylation in cancer cells.

Within a tumour, it is common to find hypermethylation of a CpG island on the promoter region of a tumour-suppressor gene and hypomethylation of normally silenced oncogenes and retrotransposons[75]. Genes associated with sustained angiogenesis, evading apoptosis, insensitivity to antigrowth signals, self-sufficiency in growth signals, limitless replicative potential, tissue invasion and metastasis, and DNA repair have been shown to be aberrantly methylated in breast cancer[76]. More than 200 genes have been identified as aberrantly methylated in breast cancers. There is, however, great variety in the methylome of different cell lines and tumour samples; this is perhaps attributable to the methylation mechanisms themselves which do not target specific genes. While the generation of the aberrant methylation status seems to be non-specific, there is a non-random association between the methylation status of specific genes and clinical or molecular characteristics[75]. This implies silencing or re-activation of certain genes provides tumour cells with a selective advantage.

With mounting evidence indicating an abnormal methylome in breast cancers, there is less evidence linking dysregulation of the methylation machinery to breast cancer. A study on 12 breast cancer cell lines implicated overexpression of the DNA methyltransferase DNMT3b protein in cell lines with increased hypermethylation[77]. When sporadic breast carcinomas were analyzed for overexpression of this DNMT3b protein, it was found that 30% of patients were overexpressing the protein and that these same

patients had shorter relapse-free survival[78]. It is likely that the excessive DNMT activity in these patients was driving increased hypermethylation of tumour suppressor genes relative to the low-DNMT3b patients which may account for the poor prognosis. However, this is correlative evidence, and it has not been shown directly that hypermethylation drives breast tumour growth.

1.3.2 *HYPERMETHYLATION OF RASSF1A*

Numerous studies have attempted to directly link hypermethylation of single genes to breast tumour establishment and growth. One of the best examples of a hypermethylated gene having a potent effect in breast cancer cells is RASSF1A. Cells within a breast tumour are able to escape apoptosis. Though the host targets malignant cells, breast cancer cells do not respond to the pro-apoptotic signals. This may be attributed to the silencing of important pro-apoptotic genes such as: RASSF1A (ras association domain family protein 1), CDKN2A (cyclin-dependent kinase inhibitor 2A), FHIT (fragile histidine triad gene), and HOXA5 (homeobox A5). The hypermethylation of RASSF1A is observed in many types of cancer including breast cancer[79]. When active, RASSF1A modulates many pro-apoptotic pathways and is involved in assembling tumour suppressor complexes. This tumour suppressor gene was found to be hypermethylated in 58%-88% of lobular breast carcinoma samples[80], and 11% of invasive ductal carcinoma samples[31]. The silencing of RASSF1A is associated with poor prognoses. Patients with hypermethylated RASSF1A had significantly shorter overall survival compared to unmethylated patients[31]. With these types of data alone it is not possible to claim that RASSF1A caused these poor outcomes,

but it sets the scene for using methylation of specific genes or CpGs as biomarkers or targets of DNA methylation-based therapies.

1.3.3 *DNA METHYLATION BIOMARKERS*

The presence of estrogen receptor (ER), progesterone receptor (PR), and epidermal growth factor receptor (HER2) in breast tumours directly impacts prognosis and treatment strategies[81]. Epigenetic profiling can complement ER/PR/HER2 status and further define subtypes; or there may be epigenetic markers that have prognostic relevance independent of our current subtyping. Epigenome-wide profiling of DNA methylation, histone modifications, miRNA expression, and lncRNA expression have generally found that unsupervised clustering of patients based on differential epigenome markers recapitulates the existing breast cancer subtypes[82,83]. Therefore, prognostic studies of DNA methylation profiles should be performed for each subtype separately. This was the case for ER+ patients, where hypomethylation of a selection of tumour suppressive pathways (e.g. Wnt signaling) was associated with longer overall survival[84].

Breast tumours that are immunohistochemically positive for ER expression are typically treated with the ER antagonist tamoxifen. It is unclear how methylation of the estrogen receptor 1 gene (*ESR1*) is connected to silencing of ER expression or response to tamoxifen. Unexpectedly, promoter hypermethylation of the *ER* gene is not generally predictive of decreased ER protein levels[85]; however, *ESR1* methylation in circulating DNA actually does correlate with ER protein in the tumour[86]. It was hypothesized that *ER* silencing via *ESR1* hypermethylation could indicate resistance to tamoxifen; but

unexpectedly, *ESR1* methylation was predictive of longer survival in tamoxifen-treated patients[87].

1.4 DNA METHYLATION AS A THERAPEUTIC TARGET

As many tumour suppressor genes are silenced via hypermethylation in breast cancer, then it may be possible to correct aberrant gene expression with epigenetic therapies[88,89]. Not only does this have the potential to re-activate tumour suppressor genes, it could also increase the efficacy of other treatments by reactivating important response mediators that were silenced by hypermethylation.

It is possible to prevent methylation from occurring by using nucleoside analogues for cytosine such as 5-azacytidine (azacytidine) and 5-aza-2'-deoxycytidine (decitabine)[90]. These compounds inhibit DNMTs and have been shown to decrease the overall methylation of cancer cells. At low doses, decitabine incorporates in the DNA and covalently binds to DNMTs. This prevents the downstream methylation of DNA, causes the degradation of the DNMT-DNA adduct which results in overall loss of DNMT activity in the cells, and leads to passive hypomethylation. At high doses, decitabine incorporation induces genotoxic stress and contributes to cell death[91]. There are several other nucleoside-based DNMT inhibitors, but decitabine and azacytidine are used most often in clinical practice[92].

Azacytidine and decitabine are approved to treat acute myeloid leukemia (AML) and myelodysplastic syndrome (MDS), but clinical trials in solid tumours have thus far shown little clinical benefit [93–96]. DNMT inhibitors might be better applied to breast cancer if patients could be classified based on their methylome profiles before beginning therapy.

1.5 BREAST CANCER STEM CELLS

Increasing evidence suggests that within a tumour there exist cancer cells with varying abilities to both initiate tumours and metastasize[97–104]. The most tumourigenic cancer cells— cancer stem cells (CSCs)— are a subpopulation of tumour cells hypothesized to be largely responsible for the heterogeneity that exists within tumours. CSCs have unlimited self-renewal potential and can also give rise to differentiated cancer cells. CSCs are functionally defined by a dramatically enhanced ability to form *in vivo* xenografts of tumours in immunodeficient mice[105]. While CSCs are highly tumourigenic, the relative resistance of CSCs to many standard chemotherapeutics and enhanced metastatic potential is of greatest concern[106–115]. Here, I will focus on what is currently known about the mechanisms of chemoresistance in breast CSCs, strategies to circumvent this resistance, and evidence for CSC-driven metastasis.

1.5.1 *IDENTIFICATION OF BREAST CANCER STEM CELLS BY INCREASED ALDEHYDE DEHYDROGENASE ACTIVITY*

Breast CSCs can be identified by several methods including fluorescence-activated cell sorting (FACS) analysis of progenitor-cell-specific surface protein markers (CD24-/CD44+), FACS analysis of the "side population" indicated by Hoechst dye exclusion, and by aldehyde dehydrogenase (ALDH) activity assays. High cytoplasmic ALDH activity is intrinsic to the CSCs of many cancers. Specifically, ALDH activity is measured employing a fluorescence-based enzymatic assay combined with FACS (the Aldefluor assay). The Aldefluor assay measures conversion of a membrane permeable ALDH substrate,

BODIPY aminoacetaldehyde, to a fluorescent, cytoplasmic-retained product, BODIPY aminoacetate. This assay was originally developed for isolation of viable hematopoietic stem cells from human umbilical cord blood[116]. However, following the publication of two seminal papers in 2007 that showed that Aldefluor+-isolated cancer cells of breast tumours and leukemias had CSC qualities (i.e. increased tumourigenicity and give rise to heterogeneous tumours)[104,117], the use of this assay was re-purposed for CSC identification, isolation and study. Aldefluor+-identified CSCs (ALDH+ cells) have been reported in many tumour types, including the cancers of liver, head and neck, lung, pancreas, cervix, thyroid, prostate, colon, bladder, and ovaries and breast[99,118,127–132,119–126].

ALDHs are a superfamily of enzymes that catalyze the oxidation of aldehydes to carboxylic acids and there are 19 genetically distinct isoforms expressed in humans[133,134]. The ALDH isoforms have distinct expression profiles in the body's tissues, substrate specificity, and function. In general, most ALDHs enzymes function in the removal of toxic aldehydes generated during metabolic processes. In addition, some isoforms have specialized functions, such as the homologous ALDH1A1, ALDH1A2 and ALDH1A3 isoforms, which oxidize the vitamin A metabolite retinal to retinoic acid (RA), a key cell signaling molecule[135].

1.5.2 *Specific Aldehyde Dehydrogenase Isoforms Associated with Cancer Stem Cells of Different Cancers*

When first used to study breast CSCs, the Aldefluor assay was believed to be specific for one ALDH isoform found in high abundance in hematopoietic stem cells, the ALDH1A1 isoform. However, while the 19 ALDH isoforms do have preferred substrate

specificity, they also have cross-reactivity, meaning the Aldefluor assay can detect the activity of multiple ALDH isoforms[136,137]. In agreement with this, a number of ALDH isoforms have been implicated as being responsible for the high Aldefluor/ALDH activity associated with CSCs, with certain isoforms being associated with specific cancers[138]. Van den Hoogen *et al*. used the Aldefluor assay to identify prostate CSCs, and reportedly found low expression of ALDH1A1, but higher expression of ALDH7A1 in prostate cancer cells and tissues[131]. This raises the possibility that for prostate cancer ALDH7A1 may be contributing to the Aldefluor activity of these cells. For colon cancer, it was reported that 98% of colon cancer samples were positive for ALDH1B1 expression, leading the authors to propose that ALDH1B1 may contribute to Aldefluor activity in colon cancer[139]. In another colon cancer study, murine xenograft tumours from colorectal cancer cell lines were investigated for ALDH gene expression, and ALDH3A1, ALDH5A1, and ALDH1A1 were expressed more in the tumourigenic populations than in non-tumourigenic cells[106]. However, of the three ALDH isoforms, the mRNA for ALDH1A1 was expressed at higher levels than the other two enzymes. In liver cancer cell lines, it was confirmed by both quantitative PCR and western blotting that expression of ALDH1A1 was increased in the population of CD133+-identified CSCs[127]. In ovarian cancer, ALDH1A1 expression has been clearly implicated in Aldefluor activity. Mice with xenograft ovarian tumours were treated with nanoliposomes that silenced ALDH1A1 expression, and Aldefluor analysis showed that silencing ALDH1A1 resulted in significantly lower Aldefluor activity[140]; importantly ALDH1A1 expression correlated with more aggressive disease in patients[141].

1.5.3 *ALDEHYDE DEHYDROGENASE 1A3*

A few studies suggest that ALDH1A3 expression may be at least as an important as ALDH1A1 in influencing the Aldefluor activity of cancer cells and CSCs. For breast cancer, gene expression and knockdown studies revealed that ALDH1A3 expression was the primary isoform contributing to Aldefluor activity of breast cancer patient tumours and cell lines[136]. Later, similar studies performed in melanoma implicated both ALDH1A1 and ALDH1A3 in determining Aldefluor activity in melanoma[142]. Furthermore, the authors conducted knockdown studies in melanoma cells and found that ALDH1A3 expression contributed to their tumourigenicity. More recently, it was demonstrated that for mesenchymal glioma and lung CSCs Aldefluor positivity was associated with enriched ALDH1A3 expression[143–145]. The associations of ALDH1A3 with aggressive phenotypes in multiple cancer types has made it a desirable target for novel therapies.

1.6 BREAST CANCER STEM CELLS ARE INTRINSICALLY RESISTANT TO THERAPY

CSCs are hypothesized to initiate cancer and give rise to heterogeneous tumours. Importantly, in terms of successful patient treatment, CSCs are also more resistant to commonly used chemotherapeutics and can repopulate a tumour after treatment (Figure 1.1). Multiple mechanisms have been identified for CSC-associated chemoresistance. These mechanisms include increased expression of ABC transporter efflux pumps, anti-apoptosis proteins, enhanced DNA repair mechanisms, increased activation of the embryonic signaling pathways (Notch, Wnt and Hedgehog), and the detoxification activity associated with the aforementioned ALDH enzymes. Identification of these mechanisms has led to development of specific strategies to circumvent CSC-associated

chemoresistance. Future clinical evidence will reveal if employing these adjuvant therapies will eradicate CSCs along with the bulk of the tumour and lead to improved patient outcomes with decreased cancer recurrence.

In treating all cancers, overcoming therapy resistance and recurrence after remission is a major challenge. Chemotherapeutic resistance can either be an innate characteristic of the primary tumour or developed later during recurrence (acquired resistance). Furthermore, chemoresistance is a complex problem as it is not usually isolated to one specific subclass of drug but tends to include multiple drug classes. Multidrug resistance (MDR) is a major hindrance to improving patient survival in all cancers. Perhaps an even greater concern, which current clinical strategies are only beginning to consider, is the intratumoural heterogeneity that exists within individuals and the potentially important role that this plays in dictating therapy resistance and recurrence[146]. Intratumoural diversity is at the genomic, epigenomic, transcript and proteomic level. Clonal evolution during the course of disease progression and treatment is only partially understood[143].

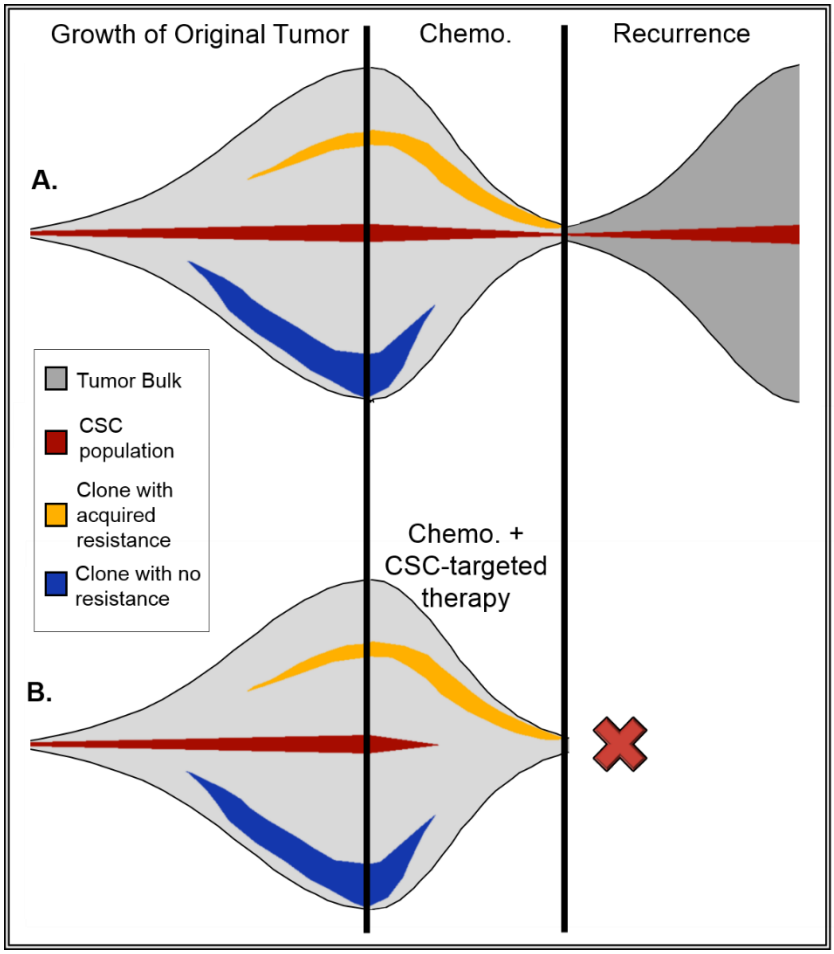

Figure 1.1: Model of cancer stem cell-associated chemotherapy resistance and recurrence. **A)** Expansion of original tumour based on the CSC population with development of multiple clones within the tumour. Chemotherapy reduces tumour bulk and eliminates chemosensitive clones but does not remove CSCs or chemoresistant clones; it is the CSC population that is then responsible for tumour recurrence. **B)** The addition of CSC-targeted therapy to the chemotherapeutic regime eliminates the CSC population, and though a drug-resistant clone persists through treatment, it is not able to induce tumour recurrence without CSCs.

As mentioned earlier, CSCs of various cancers can be identified via the exclusion of cellular stains such as Hoechst stain[147]. Relative to less tumourigenic non-CSCs, CSCs have decreased staining capacity with permeable dyes because of rapid efflux of these molecules. Like normal stem cells, CSCs have enhanced efflux mechanisms, which in

many cases is due to increased expression of ATP-binding cassette proteins or ABC transporters[148]. In particular, the efflux capacity of the SP has been attributed to increased expression of ABCB1, ABCC1, ABCG2, and ABCA3[109,149–153]. These transporters are also known to efflux chemotherapeutic drugs and are a common cause of chemotherapy resistance in breast cancer[154]. Therefore, increased expression of ABC transporters by CSCs is a primary mechanism of chemotherapeutic resistance, encompassing all cell-permeable drugs. Given the strong association between ABC transporter expression and CSCs, it is not surprising that their expression is sometimes used to identify CSCs[155,156].

1.6.1 *ABC TRANSPORTERS AND CHEMORESISTANCE*

ABC transporters are part of a large family of evolutionarily conserved proteins found in both prokaryotes and eukaryotes. In humans there are 48 known ABC transporters, divided into 7 subfamilies. These multisubunit, ATP-powered transmembrane proteins function in the transport of substrates across membranes and can either be classified as importers or exporters[157–159]. ABC importers (class 1 and 2) function in nutrient uptake, while ABC exporters efflux drugs (e.g. chemotherapeutics, antibiotics), peptides and toxins, and are involved in glycolipid flipping. Therefore, in addition to potentially causing problems in the effective treatment of cancer, these exporters also cause wide-spread anti-bacterial drug resistance. ABC exporters can efflux a wide array of chemotherapeutics, across multiple drug classes (e.g. colchicine, doxorubicin, etoposide, vinblastine, and paclitaxel) and are often responsible for MDR in cancer.

One well-studied ABC exporter, ABCB1 (also known as P-glycoprotein or MDR1) is often implicated in chemotherapy resistance in many cancers, including gastrointestinal

cancers and acute myeloid leukemia (AML)[160]. In 1989, Goldstein *et al*. performed a large-scale cross-cancer comparative study and classified tumours based on their MDR1 expression. They reported that intrinsically chemotherapy resistant colon, liver, kidney and pancreatic cancers, as well as some carcinoid tumours, chronic myeloid leukemia (CML), and non-small cell lung cancers expressed the highest levels of MDR1[161]. For breast cancer, MDR1 expression is varied. Meta-analyses suggest that MDR1 may be expressed in 40%, or as high as 66% of breast cancers[162,163]. Furthermore, some evidence suggests that chemotherapy treatment may increase expression of MDR1, which may explain why at least some acquired resistance in breast cancer correlates with increased MDR1 expression following neoadjuvant chemotherapy treatment[164]. Patients with high levels of MDR1 are three times more likely to be non-responsive to chemotherapy than MDR1 negative patients[162]. Finally, in direct proof of the role of MDR1 in chemotherapy resistance, inhibition of MDR1 expression sensitized breast cancer cells to chemotherapeutics[165].

There is increasing evidence linking the specific chemoresistance of CSCs specifically to MDR1 expression. Pancreatic CSCs identified in Panc-1, HPAC, and CFPAC-1 cells were resistant to gemcitabine and expressed high levels of MDR1[166,167]. CD133+-identified prostate CSCs were enriched in MDR1 expression[168]. Ovarian CSCs identified by cell surface markers CD44+CD117+CD133+ express high levels of MDR1[169]. A glioblastoma CSC cell line exhibited increased MDR1 expression and resistance to doxorubicin, etoposide, and carboplatin[170]. In CD34+CD38- AML CSCs, MDR1 expression was elevated and they were resistant to daunorubicin[171]. Breast cancer cell lines enriched for CSCs and spheroids had significantly higher MDR1 expression and

were resistant to multiple chemotherapeutics, including doxorubicin, cisplatin, and etoposide[172]. Therefore, in breast cancer and other malignancies, there is a strong association between expression of drug resistance-associated ABC transporters and CSCs.

1.6.2 *CHEMORESISTANCE OF CANCER STEM CELLS DUE TO ENHANCED DNA REPAIR, AVOIDANCE OF APOPTOSIS, AND STEM CELL PROGRAMS*

An important mechanism of resistance to DNA-damaging agents may be enhanced DNA repair. Cells deficient in elements of DNA repair are more sensitive to chemotherapeutic-induced double-strand breaks[173,174]. The DNA damage response in glioblastoma CSCs has been the most thoroughly investigated. Glioblastoma is often treated with temozolomide, an alkylating agent. Temozolomide alkylates guanine residues to O6-methylguanine (O6-MeG)[175]. This can be repaired by O-6-methylguanine-DNA methyltransferase (MGMT). If the lesion is not repaired, O6-MeG pairs with thymine during DNA replication and DNA mismatch repair machinery excises the mispaired thymine[176]. If the DNA lesion persists on the template strand, it causes repeated (and futile) cycles of mismatch repair. This ultimately results in collapse of the replication fork, triggering cell cycle arrest and apoptosis. Thus, low levels of MGMT and functional mismatch-repair machinery are essential for the response of these cells to temozolomide. In CD133+ glioma CSCs, higher levels of MGMT have been detected, conferring increased resistance to temozolomide therapy[177,178]. However, contradictory data has been presented where temozolomide selectively targets the CSC population of glioblastoma[179]. Further evidence will be required to definitively determine the contribution of CSCs to the chemoresistance of glioblastoma[180,181]

An important response of cancer cells to chemotherapeutics that target rapidly dividing cancer cells (such as paclitaxel and doxorubicin) is activation of apoptosis. Cancer cells demonstrate several mechanisms which interfere with drug induced apoptosis including manipulation of the B-cell CLL/lymphoma 2 (BCL-2) protein family. Under stress conditions, the cell fate decision to undergo apoptosis is governed by the interactions between different components of the BCL-2 family. The stress signal is carried by BAD and BIM, which interact with pro-survival BCL proteins (e.g. BCL-2, BCL-xL) and inhibit their repression of pro-apoptotic proteins BAX and BAK; which in turn activate apoptotic pathways and commit the cell to apoptosis[182]. Given the aggressive nature of CSCs and their high resistance to chemotherapy, several studies investigated the role of BCL-2 in mediating this resistance. In glioblastoma, CD133+-identified CSCs had greater BCL-2 expression and increased resistance to chemotherapeutics[177,183]. Additionally, CD133+ hepatocellular carcinoma CSCs were resistant to doxorubicin and 5-fluorouracil and overexpressed BCL-2[184].

Many aggressive cancers are associated with MDR, making effective cytotoxic therapy a difficult challenge. Embryonic signaling pathways such as wingless-related (Wnt), Notch, and Hedgehog have been implicated in this resistance in numerous cancer types[185–188]. For example, ovarian CSCs demonstrate resistance to cisplatin/paclitaxel which is c-Kit and Wnt dependent[189]. Silencing of Wnt2B or β-catenin enhances sensitivity of ovarian cancer cells to cisplatin or paclitaxel[190,191].

Evidence suggests that inhibiting Hedgehog signaling increases the response of cancer cells to multiple unrelated chemotherapies. Hedgehog contributes to chemoresistance by increasing drug efflux via ABC transporters. Hedgehog has been found

to regulate MDR1/ABCB1 and BCRP/ABCG2[192–194]. Pancreatic tumourspheres display resistance to gemcitabine; however, when treated with the Hedgehog inhibitor cyclopamine, this resistance was reversed[195,196]. Hedgehog signaling is also implicated in the chemoresistance of CSCs and other cancer types. These include paclitaxel-resistant breast cancer cells and putative prostate CSCs[197,198]; cisplatin-resistant ovarian CSCs[199]; and temozolomide-resistant CD133+-identified glioma CSCs[200].

Notch signaling has been implicated in the resistance of many cancers to various unrelated cytotoxic drugs. For example, the Notch1 receptor is highly expressed in cisplatin-resistant cells of head and neck squamous cell cancers, colorectal cancers, and ovarian carcinomas[201–203]. Interestingly, other Notch-dependent mechanisms have been indicated in the chemoresistance of pancreatic cancer[204,205]. Inhibition of Notch signaling is also able to counteract the chemoresistance of other cancer types including gliomas[200], osteosarcoma[206], and multiple myeloma[207]. There is also evidence of Notch-related chemoresistance specific to CSCs. For example, ovarian CSCs expressing increased Notch1 are more resistant to cisplatin and paclitaxel than their non-CSC counterparts[202].

1.6.3 *Function of Aldehyde Dehydrogenases in Detoxification*

ALDHs are a superfamily of enzymes that catalyze the oxidation of aldehydes to carboxylic acids. There are 19 genetically distinct isoforms expressed in humans[137]. In general, most ALDH enzymes function in the removal of toxic aldehydes generated during metabolic processes[137]. This detoxification activity implies a potential function in the resistance to certain chemotherapeutics. Aldehydes are naturally occurring compounds that are formed by the metabolism of carbohydrates, lipids, vitamins, amino acids, and steroids;

aldehydes will react with thiol and amino groups and lead to cellular damage. ALDHs oxidize and effectively detoxify many reactive aldehydes to protect cells. Furthermore, this detoxification activity extends beyond the reactive aldehydes generated from metabolic processes to aldehydes of exogenous origin, such as the metabolites of alcohol and chemotherapeutics.

Biotransformation of some anti-cancer drugs generates reactive aldehydes, which in addition to their primary mode of action contributes to their toxicity. One example is the commonly used chemotherapeutic cyclophosphamide. This alkylating agent and DNA synthesis inhibitor is used to treat many cancers, such as breast, lung, ovarian cancer, as well as AML, CML, neuroblastoma, sarcomas, and lymphoma[208–212]. Cyclophosphamide is a pro-drug that is converted to its main active metabolite, 4-hydroxycyclophosphamide, by liver enzymes. 4-hydroxycyclophosphamide exists in equilibrium with its tautomer, aldophosphamide, an aldehyde and ALDH substrate[213–216]. ALDHs oxidize aldophosphamide and generate the inactive metabolite carboxycyclophosphamide.

Prior to the association of ALDH activity with CSCs, ALDH enzymes were known to inactivate cyclophosphamide and this was seen as desirable activity since it limited the toxicity of the chemotherapeutic (i.e. ALDH expression is high in bone marrow stem cells, liver cells, and intestinal cells)[214–216]. At the time, the potential resistance of a sub-population of tumour cells (i.e. CSCs with high ALDH activity) was not a major concern. Studies on cyclophosphamide resistance mechanisms have identified the ALDH1A1 isoform, and the ALDH3A1 isoform to a lesser extent, as being primarily responsible for detoxifying cyclophosphamide[217–219]. When expression of ALDH1A1 was induced in L1210 leukemia cells, the cells became more resistant to cyclophosphamide[217].

ALDH1A1-deficiency in mice resulted in the hematopoietic cells having increased sensitivity to cyclophosphamide[220]. In breast cancer patient tumours, ALDH1A1 expression was predictive of tumour responsiveness to cyclophosphamide treatment[219]. Conversely, when ALDH1A1 and ALDH3A1 expression was reduced by RNA interference (RNAi), there was an increase in cyclophosphamide toxicity to lung adenocarcinoma cell line A549[218]. Together, these experiments suggest that ALDH1A1 and ALDH3A1 are involved in cyclophosphamide resistance in multiple cancer types. Therefore, which ALDH isoforms are expressed in and used to identify CSCs of various cancers becomes important when considering the potential role of ALDH in CSC chemotherapeutic resistance.

1.6.4 *Aldehyde Dehydrogenase Expression by Cancer Stem Cells is associated with Resistance to Multiple Chemotherapies*

There is evidence suggesting that ALDH+ CSCs are more resistant to cyclophosphamide. CSC enrichment was observed in colorectal cancer xenograft tumours after cyclophosphamide treatment, and this correlated with enhanced ALDH1A1 expression and Aldefluor activity[106]. In addition to the link between ALDH activity and cyclophosphamide resistance, there is also a general association of ALDH+ CSCs with resistance to other chemotherapeutics. Breast tumour samples with high levels of ALDH1A1 are associated with patient resistance to paclitaxel and epirubicin[113]. ALDH+ Ewing's sarcoma cells, from human cell lines and patient-derived xenografts had CSC properties and were resistant to doxorubicin[221]. ALDH+ subpopulations from lung cancer cells had increased resistance to multiple chemotherapeutic agents (cisplatin, gemcitabine,

vinorelbine, docetaxel, doxorubicin and daunorubicin) and lung cancer patients with high ALDH1A1 had worse outcomes[125]. ALDH1A1 expression confers gemcitabine resistance to pancreatic cancer cells[222]. Gastric CSCs with high ALDH activity exhibited increased resistance to 5-fluorouracil and cisplatin[223]. Similarly, ALDH activity attributed to ALDH1A1 protected a chemoresistant population of gastric cancer cells by reducing reactive oxygen species and consequently DNA damage and apoptosis[224]. There is also clinical evidence of ALDH imparting chemoprotectant properties. Patients with locally advanced breast cancer were treated with docetaxel and FEC 100 (an anthracycline-based drug); of the patients who did not have a complete response, if the remaining tumour cells were ALDH1A1 this was strongly predictive of worse overall survival[225].

Unlike the well-described mechanism with cyclophosphamide, it is unclear whether these other drugs are metabolized directly by ALDH enzymes or if ALDHs minimize their cellular toxicity by clearing reactive aldehydes generated during their primary mode of action. Alternatively, it is also possible that ALDH activity confers resistance by influencing cell signaling cascade such as the embryonic cell signaling pathways Notch and Hedgehog[223]. This is possible considering that three of the ALDH isoforms ALDH1A1, ALDH1A2 and ALDH1A3 are critical in the retinoic acid (RA) signaling pathway, and that two of these, ALDH1A1 and ALDH1A3 are expressed in the CSC populations of multiple cancers. The ALDH1A enzymes are the only enzymes that can generate RA from retinal[226,227]. Via their role in RA production, the ALDH1A enzymes can regulate expression of up to thousands of genes, influencing cell death, proliferation, and differentiation. Crosstalk between the RA cell signaling pathway and the embryonic cell signaling pathways is common. Therefore, evidence of ALDH-mediated

chemoresistance related to Notch or Hedgehog signaling may be connected to ALDH1A-mediated RA signaling.

1.7 THE IMPLICATION OF ALDH1A3 IN BREAST CANCER METASTASIS

1.7.1 *METASTASIS*

A relatively small portion of breast cancer patients present initially with existing metastasis (7%); however most breast cancer mortality is due to metastasis that occurs after the initial diagnosis[228,229]. This presents an important therapeutic window, where targeted interventions can prevent metastasis and lower breast cancer-associated mortality. Lowering the rate of metastasis (5-year rates of metastasis are ≈8%) is a desirable goal, and most efforts are focused on the relapse- and metastasis-prone TNBC subtype[230].

One strategy to reduce post-treatment metastasis is the addition of systemic adjuvant therapies to supplement surgery and radiation. These systemic cytotoxic agents (e.g. taxanes) are administered to eliminate residual tumour cells. Advances in systemic adjuvant therapies for breast cancer are reducing the incidence of metastasis to the bone, but have not reduced the risk of lethal lung, liver, or brain metastasis[231]. One reason for the lack of progress in lung or brain metastasis prevention is the tissue tropism and therapy resistance in TNBC. Triple-negative tumours have a tropism for the lung and brain, HER2 tumours seem to colonize the liver and brain, and ER/PR+ tumours had no identifiable tropism with overall low rates of metastasis[232].

The observation that tumour cells have preferred sites of metastasis corroborates the "seed and soil" hypothesis of metastasis first proposed 130 years ago[233]. This non-random establishment of secondary cancer sites is dependent on the interactions between the microenvironment of the metastatic site as well as the ability of the tumour cell to colonize that location. Metastasis involves the concerted evolution of cancer cells to permit their escape from the primary tumour and establish metastatic colonies at distant sites. This multistep process involves: initial escape from the primary tumour, intravasation to the lymphatic or circulatory system, travel throughout the body, adherence at secondary site, extravasation from circulation, colonizing a micrometastatic lesion, re-directing and creating a blood supply, and then growing into macrometastatic lesions[234]. Converting between a proliferative epithelial state to an invasive mesenchymal form to escape the primary tumour with subsequent reversion to an epithelial phenotype upon metastatic colonization may be essential. Based on pre-clinical evidence, ALDH+ CSCs from TNBC are poised to execute all these functions and are exceptionally adept at metastasizing[235]. Disrupting ALDH1A3-associated metastasis in TNBC could improve patient survival.

1.7.2 *BREAST CANCER STEM CELLS ARE METASTATIC*

The plasticity of breast CSCs is a major factor in their metastatic potential[236]. Epithelial-to-mesenchymal plasticity (EMP) is proposed as a major driver of metastasis, and breast CSCs seem to be able to convert between epithelial and mesenchymal phenotypes with ease[237]. ALDH+ breast CSCs are generally characterized as epithelial-like, while CD24-/CD44+ CSCs are more mesenchymal. Importantly, CSCs are not a rigid cell type and dynamically shift through these epithelial/mesenchymal phenotypes in

response to environmental cues. This hybrid epithelial/mesenchymal state has been observed in highly metastatic cells. In early stage breast cancer patients, analysis of blood samples revealed the presence of circulating tumour cells (CTCs). While different phenotypes were detected at equal rates- epithelial (28%), mesenchymal (24%), and hybrid (24%)—those patients with hybrid circulating tumour cells reminiscent of CSCs were at 7-fold increased risk of metastasis[238]. While the essential role of EMP in metastasis has been questioned, ALDH+ breast CSCs also have other qualities that prime these cells for metastatic colonization[239].

Many studies of metastasis focus on the initial stage metastasis: invasion through a basement membrane to access the lymphatic or circulatory system. Though this early step of metastasis is important, the latter stage of establishing a macrometastatic lesion is the rate-limiting stage of the metastatic cascade. An *in vivo* microscope tracking of metastatic cancer cells found that 90% of cancer cells are capable of escaping the primary tumour and extravasating into a metastatic niche. However, only ≈2% of cells could form micrometastases, and ≈0.02% of cells developed into macrometastases[240]. Based on experimental models, this 0.02% of successful cells is largely composed of CSCs which not only have the phenotypic plasticity to escape the primary tumour, but also have an enhanced ability to colonize metastatic lesions.

The true metastatic capacity of CSCs is revealed after the cells have already left the primary tumour site. Tumour cell clusters are more adept at establishing metastases than single cells[241]. After departing the primary tumour, pre-clinical models have characterized that breast CSCs travel in clusters with cancer-associated fibroblasts to improve their chances of establishing a metastatic colony[242]. Also aiding CSC-mediated metastasis is that

certain signals in metastatic environments seem to speak exclusively to CSCs. For example, MMTV-PyMT murine mammary carcinoma metastasis to the lung was reliant on lung stoma-based periostin signaling sustaining CSCs in the metastatic niche[243]. Thus, CSCs are informed by the metastatic niche.

The increased phenotypic plasticity and colonization ability observed in CSCs may explain their enhanced metastatic capacity in various models. Clinically, the majority of early disseminated cancer cells detected in the bone marrow of breast cancer patients have a putative breast cancer stem cell phenotype (CD24-/CD44+)[235]. In a thorough pre-clinical model using breast tumour samples from patients, CD24-/CD44+ sorted cells were GFP-labeled before being reunited with the RFP-labeled bulk tumour cell populations. This mixed-labelled population was orthotopically injected to form a mammary tumour, after a palpable tumour formed it was surgically resected to mimic typical treatment, and then latent metastasis was monitored. In this model, distant metastases in the lung, liver, or bones were exclusively formed by the GFP-labelled CSC population[244]. Less robust, but mirroring these findings are several experiments where ALDH+ or CD24-/CD44+ breast CSCs are injected intravenously and form significantly more metastatic lesions than their non-CSC counterparts[100]. Together, these data place ALDH1A3 and breast CSCs at the heart of breast cancer metastasis. Strategies to eliminate or hinder ALDH1A3-hi breast cancer cells are required.

1.8 THERAPIES TO ELIMINATE ALDH-HI BREAST CANCER CELLS

Conventional therapies have been mostly successful in reducing tumour bulk; however, recurrence is still a major concern for many cancer types. Approximately, 25%

of treated breast cancer patients eventually recur with metastases and succumb to the disease. It is hypothesized that targeting CSCs will reduce cancer recurrence and thus mortality. Based on some of the chemoresistance mechanisms discussed above, there are many potential avenues for overcoming CSC chemoresistance and effectively targeting these highly tumourigenic populations.

The embryonic signaling pathways, Wnt, Notch, and Hedgehog, are dysregulated in CSCs; with CSCs becoming dependent on these pathways. This presents many potential therapeutic targets that are already being heavily investigated. Herein, I will review other mechanisms of selectively targeting CSCs, such as ALDH inhibitors and ABC transport protein inhibitors.

1.8.1 *ABC TRANSPORTER INHIBITORS*

The association of increased ABC transporter expression and CSCs of various cancers has applications for identifying CSCs based on their increased efflux capacity and as a method for targeting them using ABC transporter inhibitors as adjuvant therapy. Regardless of the potential targeting of CSCs, using ABC transporter inhibitors as adjuvant therapies has the potential benefit of generally increasing the efficacy of chemotherapeutics, with the hope that it may allow lower dosages of chemotherapeutics.

Inhibitors of ABC transporters typically work by one of three ways: by specific proteins interaction, by interfering with cellular ATP levels required to power ABC transporters, or by influencing the cellular permeability to ions required for ABC transporter function[245]. These mechanisms illustrate the non-specificity of many ABC

transporter inhibitors. Verapamil, a calcium channel blocker, and cyclosporin A, an immunosuppressive drug, are early examples of ABCB1/MDR1 and ABCG2/BCRP inhibitors. These drugs have shown some efficacy in the treatment of many cancers, including breast cancer, AML, and non-small cell lung carcinoma[246–248]. However, the high toxicity associated with these drugs has limited their clinical applications in the treatment of cancer. Second-generation drugs with increased specificity and hopefully reduced side effects are under development. These included second-generation cyclosporine A analogue, valspodar; however, it too had limited clinical efficacy. For example, in a phase III study of ovarian or peritoneal cancer testing the effect of valspodar combined with paclitaxel and carboplatin versus paclitaxel and carboplatin alone, the inclusion of valspodar did not improve patient outcomes and valspodar-treated patients experienced greater treatment-related toxicity[249]. Third-generation ABC inhibitors with increased specificity are being developed and tested; however, these are also not showing significant promise. For example zosuquidar, a highly specific and potent inhibitor of MDR1/ABCB1, failed to improve outcomes of newly diagnosed AML patients[250].

While ABC inhibitors were originally positioned as broad-spectrum drugs that would increase the efficacy of chemotherapeutics on all the cells within a tumour, perhaps their greater utility will be in re-sensitization of a sub-population of tumour cells with pre-existing intrinsic resistance (i.e. CSCs)[251]. As proof of concept examples, verapamil can be used in conjunction with classic chemotherapies to target chemoresistant CSCs. Putative pancreatic CSCs were sensitized to gemcitabine[166], and $CD34^{+}CD38^{-}$-identified AML CSCs were sensitized to daunorubicin upon verapamil treatment[171]. Furthermore, verapamil sensitized ALDH+ Ewing's sarcoma CSCs to doxorubicin[221].

Other drugs include first-generation (imatinib) and second generation tyrosine kinase inhibitors (e.g. nilotinib, dasatinib, tandutinib, and erlotinib), which were originally used in the treatment of CML with increased BCR-ABL activity[252,253]. These inhibitors have also shown anti-ABC transporter activity, with some showing efficacy that extends to CSC populations by multiple mechanisms, including affecting transporter expression levels, acting as transporter substrates (competitive inhibitors), and influencing their ATPase activity. For example, nilotinib significantly enhanced the cytotoxicity of doxorubicin and mitoxantrone in $CD34^{+}CD38^{-}$-identified leukemia CSCs cells and reversed MDR in primary leukemic blasts overexpressing ABCB1/MDR1 and ABCG2/BCRP[254]. Similarly, tandutinib reversed ABCG2/BCRP-mediated drug resistance in the side population of lung cancer A549 cells[255]. Erlotinib, also showed MDR1/ABCB1 and BCRP/ABCG2 inhibition activity by down-regulating their expression and the modulating their ATPase activity. The potential of ABC transport inhibitors to sensitize ALDH+ CSCs to other therapeutics remains an option and the results of future clinical trials will determine the feasibility of this strategy.

1.8.2 *ALDEHYDE DEHYDROGENASE INHIBITORS*

As discussed earlier, increased ALDH activity is a common biomarker of CSCs and is involved in detoxifying certain chemotherapeutics. Furthermore, recent evidence suggests that ALDHs, in particular the ALDH1A3 isoform via inducing RA signaling, are active determinants of cancer progression[131,138,142,143]. These multiple roles in cancer make targeting ALDHs with specific inhibitors a promising avenue for novel anti-cancer and CSC therapy development. Known inhibitors of ALDHs include disulfiram, ampal,

benomyl, citral, chloral hydrate, chlorpropamide analogues, coprine, cyanamide, CVT-10216, benzimidazole-based analogues, daidzin, DEAB, gossypol, kynurenine tryptophan metabolites, molinate, pargyline, and nitroglycerin[256,257]. The specificity for specific ALDH isoforms was unknown for most of these inhibitors; however, some have reported differential inhibitory concentrations for ALDH1A1, ALDH3A1 and ALDH2 as reported in recent reviews[256,257].

Of these inhibitors, disulfiram is the most extensively studied and has generated the most recent interest with regards to potentially treating cancer and targeting CSCs. Disulfiram has been used in the clinic for decades to treat alcohol abuse. Also known as Antabuse or Antabus, disulfiram inhibits the breakdown of alcohol metabolite acetaldehyde by liver enzymes ALDH1A1 and ALDH2 (which are also known as acetaldehyde dehydrogenases) to acetic acid. The accumulation of acetaldehyde by disulfiram causes nausea and other symptoms which deters alcohol consumption. In addition to its use in the treatment of alcoholism, there is increasing indication that disulfiram has anti-cancer activity, by potentially multiple mechanisms. For breast cancer, it was reported that disulfiram reduced tumour growth in MDA-MB-231 breast cancer tumour xenografts[258]. However, the authors suggest that this anti-breast cancer activity is due to disulfiram complexing with copper (found endogenously in the tumour microenvironment), which results in proteasome inhibition[258]. The authors did not assess if inhibition of ALDH enzymes was a factor in the anti-breast cancer activity of disulfiram. Copper-complexed disulfiram also inhibited the growth of non-small cell lung cancer cells and sensitized them to cisplatin[259]. These authors noted that the combination disulfiram and copper treatment decreased expression of ALDH1 and other stemness markers in the

cancer cells. Furthermore, a high-throughput screen study identified disulfiram as an inhibitor of glioblastoma CSCs, which was potentiated when complexed with copper[260]. Other studies have shown that copper is not necessary for disulfiram-chemosensitization and targeting of CSCs. For example, disulfiram was shown to sensitize breast tumour xenografts to radiation treatment and tumour regression and coincided with a reduction in ALDH activity and other stemness markers[261]. Similarly, disulfiram chemosensitized a chemoresistant population of ALDH1A1-expressing gastric cancer cells[224].

The success of these studies has fuelled interest in the use of disulfiram clinically. Multiple clinical trials are being conducted to test the potential use of disulfiram as a cancer therapy by either complexing with copper and inhibiting proteasome activity or inhibiting ALDH1A1/CSC populations and sensitizing them to radiation and chemotherapeutics. These include phase I and phase II trials that are on either advanced or newly diagnosed glioblastoma multiforme and other solid tumours (NCT00571116, NCT01907165, NCT00742911, NCT00312819 and NCT01777919). In a small study of forty patients with stage IV non-small cell lung cancer, the addition of disulfiram to chemotherapy (cisplatin and vinorelbine) had an insignificant but promising clinical benefit. Two of the patients treated with disulfiram achieved long-term survival which is extremely rare among stage IV lung cancer patients treated with chemotherapy alone[262]. Pending the continued success of disulfiram in these trials, the clinical testing of other ALDH inhibitors will likely follow.

1.9 RESEARCH RATIONALE AND OBJECTIVES

The overarching goal of this work is to improve the survival of patients with breast cancer, especially those diagnosed with aggressive TNBC subtype. To do this, I will assess the potential of two distinct targets in the treatment of breast cancer: DNA methylation and ALDH1A3. Targetable DNA methylation was studied through the lens of DNA hypomethylating agent decitabine, and ALDH1A3 was investigated as a CSC-related pro-growth and metastasis protein.

Guiding Hypothesis 1:

Hypomethylating agent decitabine is not currently an effective breast cancer therapy. If there is a predictive gene expression or DNA methylation profile which defines decitabine sensitivity, then hypomethylating therapy could be applied specifically to patients with this sensitivity profile. Such a sensitivity profile may include: expression of decitabine processing enzymes, lack of multidrug resistance, or hypermethylation of key tumour suppressor genes. This will be tested by the following objectives:

1. Identify determinants of decitabine response in breast cancer cells
    - Characterize the sensitivity of a panel of breast cancer cells to decitabine treatment (Chapter 2)
    - Examine known or suspected mediators of decitabine response to identify key features of decitabine response (Chapter 2)
    - Functionally screen for hypermethylated tumour suppressor genes, that when resurrected by de-methylating therapy slow breast tumour growth. (Chapter 3)

- Functionally screen for other novel mediators which dictate decitabine response (Chapter 3)

Guiding Hypothesis 2:

Aldehyde dehydrogenase 1A3 is associated with the aggressive TNBC subtype, drug resistance, increased risk of metastasis, and cancer stem cells. If ALDH1A3 is important for TNBC tumour growth and is targetable, then inhibition of ALDH1A3 will suppress tumour growth. Currently, little is known about how ALDHs mechanistically contribute to metastasis. If ALDH1A3-hi TNBC cells have a distinct transcriptional or metabolomic profile from ALDH1A3-lo cells, then this could be used to explain the differences in metastatic potential. This will be tested by the following objectives:

2. Determine if ALDH1A3 is a potential target for breast cancer treatment
    - Develop an *in vivo* ALDH1A3 inhibition breast cancer model (Chapter 4)
    - Study the role of ALDH1A3 in breast cancer metastasis (Chapter 5)

CHAPTER 2: DECITABINE RESPONSE IN BREAST CANCER REQUIRES EFFICIENT DRUG PROCESSING AND IS NOT LIMITED BY MULTIDRUG RESISTANCE

Copyright statement

This chapter has been previously published as:

Dahn ML, BM Cruickshank, AJ Jackson, C Dean, RW Holloway, SR Hall, KM Coyle, H Maillet, DM Waisman, KB Goralski, CA Giacomantonio, ICG Weaver, P Marcato (2020). Decitabine response in breast cancer requires efficient drug processing and is not limited by multidrug resistance. Molecular Cancer Therapeutics. doi: 10.1158/1535-7163.MCT-19-0745

The text and figures appearing here have been edited for clarity and to include supplemental figures and tables.

Contribution statement

I wrote the manuscript and designed the experiments with the guidance of Dr. Paola Marcato. The manuscript was reviewed and edited by all authors. I performed experiments and collected data with assistance as follows:

BMC, generation of knockdown clones, cell viability assays, RT-qPCR, and assistance with *in vivo* decitabine treatment. AJJ, generation of knockdown clones, cell viability assays and RT-qPCR. CD, assistance with RT-qPCR. RWH and DMW, Western blots for DCK knockdowns. KMC, HM450 cell lines and MDA-MB-231 microarray. SRH and KBG, sourced taxol-resistant MDA-MB-231 cells. HM and ICGW, RUNX3 bisulfite pyrosequencing.

2.1 INTRODUCTION

DNA methylation is essential for gene regulation in normal cells[263]. In cancer, DNA methylation is largely dysregulated with global demethylation contributing to genomic instability and the hypermethylation of CpG islands in the promoters of tumour suppressor genes causing their aberrant silencing[263]. DNA methyltransferases (DNMTs) are required for both *de novo* methylation and maintenance of existing DNA methylation; DNMT upregulation is associated with both cancer and aberrant methylation. As such, DNMT inhibitors like decitabine and azacytidine are commonly used to treat hematological disorders [myelodysplastic syndrome (MDS) and some acute myeloid leukemias (AMLs)], where patients often share common epigenetic perturbations[264]. This has generated interest in using demethylating agents to treat solid tumours, including breast cancers[88].

Among breast cancers, triple-negative breast cancers (TNBCs) have poorer outcomes and represent the 15-20% of tumours that lack hormone receptors and targeted therapies[265,266]. The possibility of treating TNBCs with DNMT inhibitor decitabine is currently being investigated in clinical trials (i.e. NCT02957968, NCT03295552). Therefore, assessing the factors that determine the response to DNMT inhibitors in breast cancer, specifically TNBC, is both timely and critical if decitabine is to be used successfully. To date, there are few studies which examine breast cancer cells exclusively and profile response to decitabine across many cell lines.

A cytosine analog, decitabine is incorporated into DNA during synthesis, which imparts some specificity of the drug for rapidly dividing cells. DNMTs bind DNA-integrated decitabine leading to protein/DNA adduct formation, DNMT degradation, and subsequent reduction of DNA methylation. This inhibits tumour growth by a number of

potential mechanisms including demethylation and re-expression of aberrantly silenced tumour suppressor genes[267], induction of the DNA damage response by protein/DNA adduct formation[268], cytotoxicity induced by global demethylation[269], and demethylation of silenced tumour-associated antigens increasing anti-tumour immune responses[270,271]. Recently, a novel mechanism has been proposed as a key determinant for the response of decitabine: demethylation of endogenous retroviral elements resulting in dsRNA/anti-viral responses[272,273]. Additionally, decitabine's predominant mode of action is possibly dose-dependent: lower doses cause re-expression of silenced genes with minimal DNA damage, while higher doses cause more pronounced DNA damage responses and apoptosis[273,274]. In various cancer models, a number of potential treatment response biomarkers have been investigated including expression or mutation of nucleoside transporters, decitabine metabolism genes deoxycytidine kinase (*DCK*) and DNA methylation regulating enzymes such as DNMTs and tet methylcytosine dioxygenase 2 (*TET2*), the methylation of known tumour suppressor genes (e.g. *CDH2, BRCA1, RASSF1, RUNX3*), and global methylation levels[275–281]. It is unclear which mechanism of decitabine is most important for successful treatment of breast cancer patients or if the effects of decitabine differ in the breast cancers of different subtypes (i.e. TNBCs versus hormone expressing subtypes).

Herein, I performed transcriptome, methylome, *in vitro* growth assays, gene knockdown studies, tumour xenograft assays, and patient dataset analyses to assess the proposed potential anti-cancer mechanisms of decitabine in breast cancer. My analyses of a panel of 10 breast cancer cell lines revealed a range of sensitivity in breast cancer to decitabine, that was not based on hormone receptor status, genome-wide methylation, demethylation of tumour suppressor genes, or induction of viral mimicry responses.

Instead, my analyses demonstrated the requirement for expression of the decitabine-processing enzyme deoxycytidine kinase (DCK) and the induction of pathways of genes enriched in apoptosis, cell cycle, stress, and immune pathways. Finally, unlike the commonly used breast cancer drug paclitaxel, decitabine efficacy in breast cancer is not negatively impacted by increased expression of ATP-Binding cassette drug efflux transporter ABCB1, which is often seen as a mechanism of multi-drug resistance.

2.2 MATERIALS AND METHODS

2.2.1 *CELL CULTURE*

Cancer cell lines were obtained from ATCC, with the exception of SUM149 and SUM159 cells that were obtained from BioIVT (previously Asterand). MDA-MB-231, MDA-MB-468, MCF7, SKBR3, T47D, and HEK293T cells were grown in Dulbecco's Modified Eagle Medium (DMEM; Invitrogen) supplemented with 10% Fetal Bovine Serum (FBS; Invitrogen) and 1X antibiotic antimycotic (AA; 10,000 units/mL of penicillin, 10,000 µg/mL of streptomycin, and 25 µg/mL of Amphotericin B; Invitrogen). MDA-MB-436 cells were grown in Leibovitz's Medium (L-15; Invitrogen) supplemented with 10% FBS, 1X AA, 10 µg/mL human insulin (Sigma), and 16 µg/mL L-glutathione (Invitrogen); MDA-MB-453 cells were cultured in L-15 medium supplemented with 10% FBS and 1X AA; Hs578T cells were cultured in DMEM supplemented with 10% FBS, 1X AA, and 0.01 µg/mL human insulin. SUM149 and SUM159 cells were cultured in F-12 Ham's Nutrient Mix Medium supplemented with 5% FBS, 1X AA, 1µM 4-(2-Hydroxyethyl) piperazine-1-ethanesulfonic acid (HEPES; Invitrogen), 0.01 µg/mL human

insulin, 0.05 µg/mL hydrocortisone (Invitrogen). Cells were cultured in a humidified 37°C incubator with 5% CO_2, except for MDA-MB-436 and MDA-MB-453, which were cultured without the addition of CO_2.

2.2.2 *COLONY FORMING ASSAY*

Cells were seeded at low density and allowed to adhere for 24 hours in 24-well cell culture plates: MDA-MB-231 (30 cells/well), MDA-MB-468 (120 cells/well), MCF7 (60 cells/well), SKBR3 (60 cells/well), T47D (120 cells/well), MDA-MB-436 (200 cells/well), MDA-MB-453 (60 cells/well), Hs578T (60 cells/well), SUM149 (60 cells/well), and SUM159 (30 cells/well). Cells were treated with 0.122nM-2µM decitabine (5-aza-2′-deoxycytidine, DAC, Sigma) for 72 hours with media refreshed every 24 hours. Alternatively cells were treated with azacytidine (5-azacytidine, Sigma), Cells were then grown in appropriate media [lacking decitabine or azacytidine] for 7-10 days with media refreshed every other day. Colonies were then fixed in methanol for 10 minutes and stained using 0.05% crystal violet (Sigma); colonies were defined as >50 cells. An IC_{50} value for each cell line was determined using % colony forming efficiency (with no treatment wells representing 100% colony forming efficiency) and the Graphpad Prism equation: log(inhibitor) vs. normalized response Standard slope analysis ($Y = 100/(1 + 〚10〛 \hat{}(x - LogIC50)$)).

2.2.3 *ETHICS STATEMENT*

Animal investigations detailed in this manuscript have been conducted in accordance with the ethical standards and according to the Declaration of Helsinki and according to national and international guidelines. All experiments were conducted in accordance with the Canadian Council on Animal Care standards and a protocol approved by Dalhousie University Committee on Laboratory Animals (#13-010).

2.2.4 *TUMOUR GROWTH STUDIES*

Eight-week-old NOD/SCID female mice were injected with 2 x 10^6 MDA-MB-468 or MDA-MB-231 cells, or 3.5x10^6 SUM159 cells admixed 1:1 with Matrigel-HC (BD BioScience) into the mammary fat pad. Once palpable tumours formed, the mice were treated with 0.5 mg/kg decitabine (DAC) or vehicle control (phosphate buffered saline, PBS) by intraperitoneal injection for 3/5 day cycles as previously described[274]. This dose used in mice is approximately 10-fold lower than the 15 mg/m^2/day used to treat human hematopoietic malignancies (conversion based on Nair *et al.*, 2016)[282]. In humans, 15 mg/m^2/day achieves a maximum plasma concentration of 64.8 - 77.0 nM[283,284]. I used a sub-clinical dose to promote DNA hypomethylation over immediate cytotoxicity. Throughout the experiment, tumour volume was quantified (mm^3, length x width x depth / 2).

2.2.5 *KNOCKDOWN GENERATION*

Lentiviral shRNA knockdown clones of *ABCB1, DCK, DDX58* (RIGI), *IFIH1* (MDA5), *SLC28A1,* and *SLC29A1*, were generated using the pGipZ vector (Dharmacon)

packaged in HEK293T cells following standard protocols and listed in Table 2.1. Clones were selected by adding 1.5 µg/mL puromycin and subsequently maintained with 0.25 µg/mL puromycin media. For all knockdown clones created, a pGIPz vector control clone (containing a scrambled non-specific sequence in place of an shRNA) was generated simultaneously. Verification of knockdown was done through RT-qPCR and western blot (anti-DCK, Abcam, ab151966; anti-MDA5, Cell Signalling Technology, clone D74E4).

Table 2.1: shRNA clones

Gene		shRNA Used
ABCB1	shRNA1	V2LHS_131347
	shRNA2	V2LHS_131345
DCK	shRNA1	V2LHS_112524
	shRNA2	V2LHS_112523
DDX58	shRNA1	V3LHS_329694
	shRNA2	V3LHS_329693
SLC28A1	shRNA1	V2LHS_28638
	shRNA2	V3LHS_333611
SLC29A1	shRNA1	V3LHS_307348
	shRNA 2	V3LHS_307350

2.2.6 *REVERSE TRANSCRIPTASE QUANTITATIVE PCR (RT-QPCR)*

RNA was extracted from untreated and decitabine-treated cells (1μM decitabine for 72 hours with media refreshed daily). Cells were collected in Trizol (Invitrogen) and RNA was purified using a PureLink RNA kit (Invitrogen Thermo Fisher Scientific) following the manufacturer's instructions. Equal amounts of purified RNA were then reverse transcribed to cDNA using iScript (Bio-Rad) as per manufacturer's instructions. Diluted cDNA was used in RT-qPCR reactions with gene-specific primers (Table 2.2) and SsoAdvanced Universal SYBR Supermix (Bio-Rad) as per manufacturer's instructions with a CFX96 or CFX384 Touch Real-Time PCR Detection System (Bio-Rad). Standard curves were generated for each primer set and primer efficiencies were incorporated into the CFX Manager software (Bio-Rad). Relative expression for decitabine inducible genes was quantified using the ΔΔct method of the CFX Manager Software (Bio-Rad), where gene-of-interest quantification was normalized to reference genes RPL29 and TBP and then made relative to no-treatment control mRNA levels. For gene expression comparisons made between cell lines, the Δct expression method was used to quantify gene expression.

Table 2.2: RT-qPCR Primer Sequences

Gene	Forward Primer	Reverse Primer
Beta-2-microglobulin (B2M)	AGGCTATCCAGCGTACTCCA	CGGATGGATGAAACCCAGACA
Glyceraldehyde-3-phosphate dehydrogenase (GAPDH)	CCAGGTGGTCTCCTCTCGACTTC	GCTTGACAAAGTGGTCGTTGAG
Ribosomal protein L29 (RPL29)	ACATGCGCTTTGCCAAGAAG	GGCTTAACCTCCTTGGGCTT
TATA-box binding protein TBP	GGCACCACTCCACTGTATCC	GCTGCGGTACAATCCCAGAA
Solute carrier family 29 member 1 (SLC29A1)	ATGACAACCAGTCACCAGCC	GTTCCCAGACCCAGCATGAA
Solute carrier family 28 member 1 (SLC28A1)	AAGGGTGTTTGGAAAGGAGGT	CCCAGATGATGTGCCGAAGA
Multi-drug Resistance 1 (MDR1)	GAGAGATCCTCACCAAGCGG	ATCATTGGCGAGCCTGGTAG
Deoxycytidine kinase (DCK)	AGAAGCTGCCCGTCTTTCTC	GCAGCGATGTTCCCTTCGAT
Cytidine/uridine monophosphate kinase 1 (CMPK1)	TCTCCTCTGCTCTCCACGTC	GCAGAAAGGTGTGTGTAGCC
Nucleotide diphosphate kinase A (NME1)	ATCGTCTTTCAAGGCGAGGG	CCCCATCTGGTTTGATCGCA
Nucleotide diphosphate kinase B (NME2)	GACCGACCATTCTTCCCTGG	TTGGTCTCCCCAAGCATCAC
Cytidine aminase (CDA)	ATCGCCAGTGACATGCAAGA	GTACCATCCGGCTTGGTCAT
Proliferating cell nuclear antigen (PCNA)	AGGTGTTGGAGGCACTCAAG	CCAAAGAGACGTGGGACGAG
E3 ubiquitin-protein ligase (UHRF1)	GACAAGCAGCTCATGTCGATG	AGTACCACCTCGCTGGCATCAT
Tet methylcytosine dioxygenase 1 (TET1)	CCCTCCTCTCCACCTAACCA	TACCAGGCAATGTTGGCAGT
Tet methylcytosine dioxygenase 2 (TET2)	TTGGATACACCTGTCAAGACTCAAT	ACGCCATGTGTCTCAGTACATT
Tet methylcytosine dioxygenase 3 (TET3)	CCTCGGAGTTGGGACTCACT	GGACCTGCCAGGCCTTTATG
DNA methyltransferase 1 alpha (DNMT1A)	CGGCCTCGTCATAACTCTCC	TGAACCGCTTCACAGAGGAC
DNA methyltransferase 3 beta (DNMT3B)	TGTGGGGAAAGATCAAGGGC	ATGCCAGACATAGCCTGTCG
TNF receptor associated factor 6 (TRAF6)	GCGCACTGAACGAGCAAG	GCCACACAGCAGTCACTTTC
Ras association domain family member 1 (RASSF1A)	ACAAGGGCACGTGAAGTCAT	AAAGAGTGCAAACTTGCGGG
Runt related transcription factor 3 (RUNX3)	CTTTGGGGACCTGGAACGG	TTCCGAGGTGCCTTGGATTG

Gene	Forward Primer	Reverse Primer
BRCA1, DNA repair associated (BRCA1)	GGAAGAAACCACCAAGGTCCA	GACACCCTGTGGGCATGTT
Cadherin 2 (CDH2)	GGAGAGCGGTGGTCAAAGAG	AGTCCTGGTCCTCTTCTCCG
Interferon regulatory factor 7 (IRF7)	GTGGACTGAGGGCTTGTAG	TCAACACCTGTGACTTCATGT
2'-5'-oligoadenylate synthetase like (OASL)	GCAGAAATTTCCAGGACCAC	CCCATCACGGTCACCATTG
ISG15 ubiquitin-like modifier (ISG15)	GCCTCAGCTCTGACACC	CGAACTCATCTTTGCCAGTACA
retinoic acid- inducible gene 1 (RIG1)	CCAGCATTACTAGTCAGAAGGAA	CACAGTGCAATCTTGTCATCC
Interferon induced with helicase C domain 1 (IFIH1/MDA5)	CACTTCCTTCTGCCAAACTTG	GAGCAACTTCTTTCAACCACAG
Acidic repeat containing (ACRC)	TGGCTGCTACACCAAATCGT	ATGGCACCATGACCAGAGAC
C-C motif chemokine ligand 20 (CCL20)	ATTTATTGTGGGCTTCACACGG	GGATTTGCGCACACAGACAA
Maelstrom (MAEL)	TTTCACACCACTGAGGAGGC	GCCTCCAAGGAGAGCTTGAT
Tudor domain containing 1 (TDRD1)	CAACTGCAAAGTGGCCGAAA	AAATCAGAGCGTGGAGGCAA
Zinc finger protein 595 (ZNF595)	CCCCTGAAGAGTGGAAATGTCT	ACCAGGTCTGGGTTAGAGATCA
envE	ACTGGCCTTTTCCTAGGTGATAC	TACTATTAATGGCTGCACAAGCA
envFc1	GCTACACCACTCCTAACTCATCCT	TTGTAAGGGTGAAGTTACACCAGA
envRb	CACTAAGGGACACTTAAGCCAGAT	AGTATAGTATGTCGGCACTGTCCA
envT	AGGATTTGATGTTGGGACTATGTT	GGTGTTTCTGGAATATAGGGTCAC
envV2	TGTGTCTCTTCTAGGATAAAGCAATT	AGGGGGAGATGTGCTTATAGGT
ERVFRD1	CCTTCACTAGCAGCCTACCG	GCAATTGGTGGAGTAAGGGGA
ERVV	TTCCAGCAGGGTGGAAATCG	ATAGCCAGGAGGGGTACAGG
HERV-K-ORF1	TGGGCAACCATTGTCGGGAAAC	GGCTTATTCCCTGAAACACTTGGG
HERVK-5'UTR	CAGATGCTTGAAGGCAGCAT	ACGTTGGACAATACCTGGCT
HERV-K-ORF2	GGCTTATTCCCTGAAACACTTGGGA	TCATCAAGGCTGCAAGCAGCATAC
HERV-W	GTTGTCCTGGAGGACTTGGA	TATGGGTACGGAGGGTTTCA
LINE-2	CAGATCTCTCGGCAGAAACC	GCCTGGTGGTGACAAAATCT
LINE-1-ORF1	TCCTCGAGAAGAGCAACTCCA	GGGTTTCTGCCGAGAGATCC
LINE-1-ORF2	ATGGCCATACTGCCCAAGGT	TGGCTTAGGATTGACTTGGCA
LINE1-5'UTR	AAGGGGTGACGGTCGCACCTGGAA	AGCTGTGCTAGCAATCAGCGAGA
MLTA10	TCTCACAATCCTGGAGGCTG	GACCAAGAAGCAAGCCCTCA
MLT1B	TGCCTGTCTCCAAACACAGT	TACGGGCTGAGCTTGAGTTG
MER21C	GGAGCTTCCTGATTGGCAGA	ATGTAGGGTGGCAAGCACTG
ERVL	ATATCCTGCCTGGATGGGGT	GAGCTTCTTAGTCCTCCTGTGT
MLT1C49	TATTGCCGTACTGTGGGCTG	TGGAACAGAGCCCTTCCTTG
MLT1C627	TGTGTCCTCCCCCTTCTCTT	GCCTGTGGATGTGCCCTTAT
MER4D	CCCTAAAGAGGCAGGACACC	TCAAGCAATCGTCAACCAGA
MER57B1	CCTCCTGAGCCAGAGTAGGT	ACCAGTCTGGCTGTTTCTGT
MLT2B4	GGAGAAGCTGATGGTGCAGA	ACCAACCTTCCCAAGCAAGA

2.2.7 *PATIENT DATASET ANALYSIS*

Breast Cancer (METABRIC, Nature 2012 & Nat Commun 2016) (n=2509) and Breast Invasive Carcinoma (TCGA, Cell 2015) (n=817) clinical data (PAM50 subtype, hormone receptor status) and microarray z-score gene expression data were accessed via cBioportal[285,286]. Microarray-based gene expression of matched pre- and post- neoadjuvant chemotherapy biopsies from breast cancer patients was acquired from GSE28844[287]; histopathological response was based on Miller & Payne grading system.

2.2.8 *HUMAN METHYLATION 450K (HM450) ANALYSIS*

Genomic DNA was extracted from untreated and decitabine-treated cells (1μM DAC for 72 hours with media refreshed daily) using the PureLink DNA kit (Invitrogen). Methylation analyses using the HM450 bead chip array (Illumina) was performed by the Centre for Applied Genomics at the Hospital for Sick Children (Toronto, Ontario, Canada), including bisulfite conversion, hybridization, background subtraction, and normalization. β-values for each HM450 probe were calculated as the ratio of the methylated probe intensity to the overall intensity (the sum of the methylated and unmethylated probe intensities). Data is accessible from GSE78875[288]. Methylation β-value of probes from promoter-associated regions for *BRCA1*, *CDH2*, *RASSF1*, and *RUNX3* were extracted. CpGs from RUNX3 promoter-associated CpG island: cg19270505, cg11018723, cg13629563, cg22737001, cg26421310, cg26672794, and cg02970551.

2.2.9 *RUNX3 PROMOTER BISULFITE SEQUENCING:*

As previously described[56], DNA methylation was analyzed by sodium bisulfite pyrosequencing on a PyroMark Q24 Advanced pyrosequencer using the DNA EpiTect Fast

DNA Bisulfite Kit and PyroMark PCR Kit (Qiagen N.V., Venlo, the Netherlands), according to the manufacturer's instructions, beginning with 500 ng template DNA. A custom assay covering the RUNX3 gene promoter and 5'-untranslated regions was designed using PyroMark Assay Design software version 2.0 (Qiagen N.V.) and validated to amplify a single PCR product (243 nt). See Table 2.3 for the RUNX3 assay primers. PCR conditions were as follows: 95°C, 15 minutes (94°C, 30 seconds; 56°C, 30 seconds; 72°C, 30 seconds) 50 cycles; and 72°C, 10 minutes.

Table 2.3: Primer Sequences for RUNX3 promoter bisulfite pyrosequencing.

	Primer Sequence
Forward	GGGTTTTGGGTTGTGGTAT
Reverse	CCAAAACAAATCCTCCAAAATCAAAT

2.2.10 *GENE ARRAY ANALYSIS*

RNA purified from SUM159 cells that had been treated with 1μM DAC or vehicle for 72 hours (3n) was sent to The Centre for Applied Genomics at the Hospital for Sick Children (Toronto, Ontario, Canada) for sample preparation, amplification, hybridization to the Affymetrix HuGene 2.0 ST array, and data collection. The raw data for MDA-MB-231 and MDA-MB-468 is accessible from GSE103427[289], and the uploaded new data from GSE133987. The Transcriptome Analysis Console (TAC) software (ThermoFisher Scientific) was used to normalize the data and calculate fold changes in expression. Transcripts with confirmed gene annotations (not blank in the "Gene Symbol") category that were 1.5-fold up- or down-regulated significantly (based on ANOVA p-value <0.05) in at least one cell line were plotted based on the average fold-change across all three cell lines (1390 transcripts/1284 genes, Figure 2.15). Not all microarray gene expression "hits"

contained HM450 annotated CpG sites; unannotated transcripts were discarded. Only genes with 2 or more different regions annotated were plotted. All figures depict the mean methylation β-value of CpGs annotated for a given region (ex. TSS1500, TSS200, etc.).

2.2.11 *GENE SET ENRICHMENT ANALYSIS*

Using the HM450 and gene array data, I identified genes that were unmethylated in TSS1500 + TSS200 + Exon1 (≤0.5 β-value in all 3 regions) and for which decitabine up-regulated expression ≥1.5-fold (Table 2.4). Gene Set Enrichment Analysis (GSEA) was performed using online software (http://software.broadinstitute.org/gsea/index.jsp) to compute overlaps. The top 100 overlapping gene sets identified by GSEA for each cell line were identified. The # Genes in Overlap = k; # Genes in Gene Set = K; # Genes in Comparison = n; # Genes in Universe = N; Enrichment = $\frac{k/n}{K/N}$. Gene sets with similar functions were enriched across the three cell lines and were colour-coded for easier visualization.

Table 2.4: The number of upregulated and unmethylated genes in decitabine (DAC) treated breast cancer cells.

Cell Line	DAC Gene Expression Change	# of Transcripts >1.5-fold change in expression	# of Transcripts with Methylation Data	# of Up-Regulated + Unmethylated Genes
MDA-MB-231	Down-Regulated	238	168	
	Up-Regulated	604	426	81
MDA-MB-468	Down-Regulated	1232	895	
	Up-Regulated	1377	969	255
SUM159	Down-Regulated	1003	749	

Up-Regulated	1476	1121	172

2.2.12 *TAXANE-RESISTANT BREAST CANCER*

MDA-MB-231 cells with acquired ABCB1-mediated taxane resistance (Taxol-res) and the matched taxane sensitive cells (Control) were previously generated and characterized[290] and maintained in the same MDA-MB-231 growth conditions described above. Cells were treated with increasing doses of paclitaxel (Corporation Biolyse Pharma Corporation, St. Catherine's, ON, Canada) or decitabine +/- 10μM verapamil (verapamil hydrochloride; Sigma) and a colony forming IC_{50} was calculated.

2.3 RESULTS

2.3.1 *BREAST CANCER CELL LINES HAVE A BROAD RANGE OF SENSITIVITY TO DECITABINE, INDEPENDENT OF SUBTYPE*

To first explore the range of sensitivity to decitabine in breast cancer, I treated a panel of 10 cell lines representing ER+ breast cancers (MCF7, T47D), HER2+ (SKBR3), and TNBC (MDA-MB-231, MDA-MB-468, SUM149, SUM159, MDA-MB-436, MDA-MB-453, and Hs578T). Given the current clinical interest in treating TNBCs with decitabine (NCT02957968, NCT03295552), the panel has over-representation of TNBCs. In a subsequent colony-forming assay, the cell lines exhibited 50% inhibitory concentrations (IC_{50}s) ranging from 1 to 74 nM of decitabine (Figure 2.1A). The *in vitro* sensitivity to decitabine appeared to be independent of hormone receptor status (Figure 2.1A).

With the focus of ongoing clinical application in TNBCs, I also assessed the effect of decitabine on tumour growth of TNBC MDA-MB-468, MDA-MB-231 and SUM159

cells. Using the low-dose treatment protocol established by Tsai *et al.*[274], NOD/SCID mice bearing palpable tumours of the TNBC cell lines were treated intermittently with 0.5 mg/kg decitabine. This resulted in tumour growth suppression that mimicked the colony assay, with MDA-MB-468 tumours being the most sensitive and SUM159 tumours being the most resistant to decitabine (Figure 2.1B).

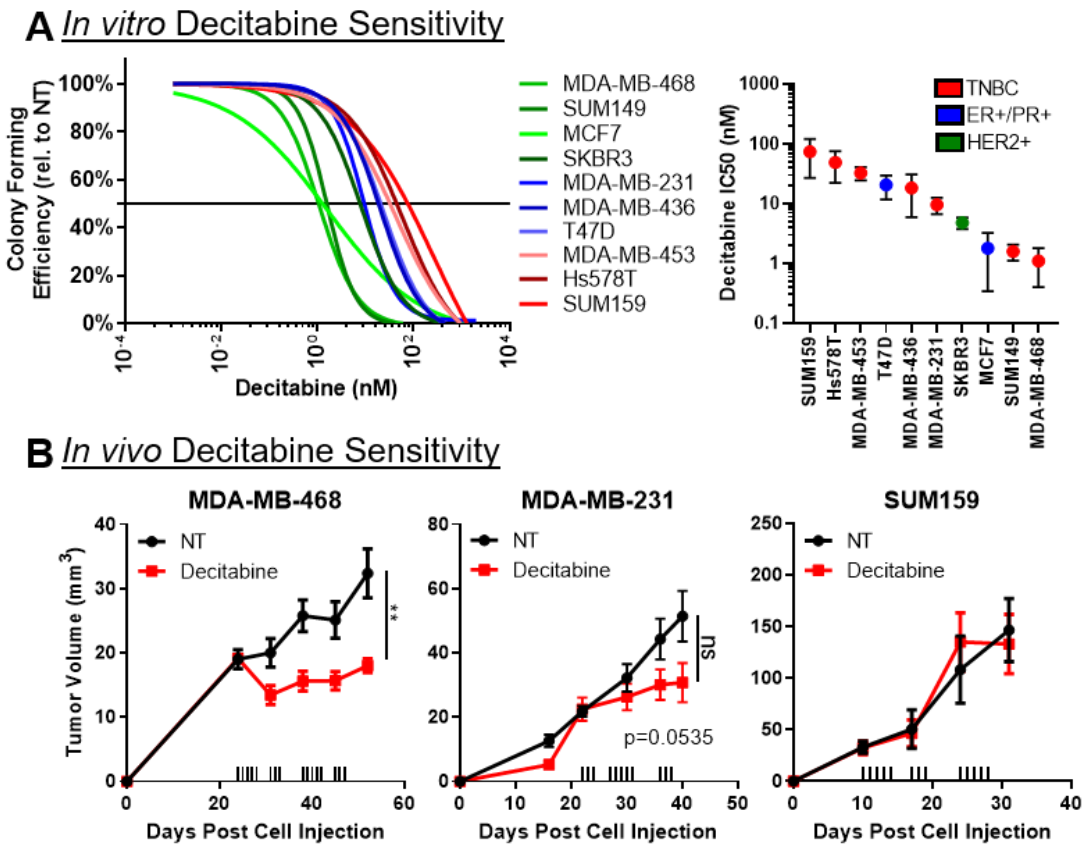

Figure 2.1: Sensitivity of breast cancer cell lines to decitabine treatment. A) Colony-forming assay to determine *in vitro* DAC IC_{50} for 10 breast cancer cell lines after 72 hour treatment. **B)** Xenograft determination of *in vivo* decitabine sensitivity. MDA-MB-468, MDA-231, and SUM159 xenografts treated with 0.5 mg/kg decitabine over 3-4 weeks; hatch marks on x-axis indicate when mice were injected; SEM error bars, one-way t-test, $p<0.05$*, $p<0.01$**, $p<0.001$***. BMC assisted with intraperitoneal decitabine injections.

2.3.2 *DCK IS REQUIRED FOR DECITABINE RESPONSE IN BREAST CANCER CELLS AND TUMOURS*

To assess the potential factors which may dictate breast cancer sensitivity to decitabine, I considered the cell-specific factors required for the cytosine analog's incorporation into DNA. Decitabine is imported into cells by sodium/nucleoside co-transporters solute carrier family 28 member 1 (SLC28A1) and SLC29A1[279,291]. Higher expression of either transporter was not associated with increased sensitivity (Figure 2.2A). Furthermore, knockdown of SLC28A1 in decitabine sensitive MDA-MB-468 cells did not alter the sensitivity of MDA-MB-468 cells to decitabine (Figure 2.2B). Knockdown of SLC29A1 in intermediately sensitive MDA-MB-231 (Figure 2.2C), which had high expression of the transporter (Figure 2.2A), also did not alter the sensitivity of the cells to decitabine. Together, this data suggests that assessing levels of the importers in patient tumours will not predict decitabine sensitivity or resistance in breast cancer.

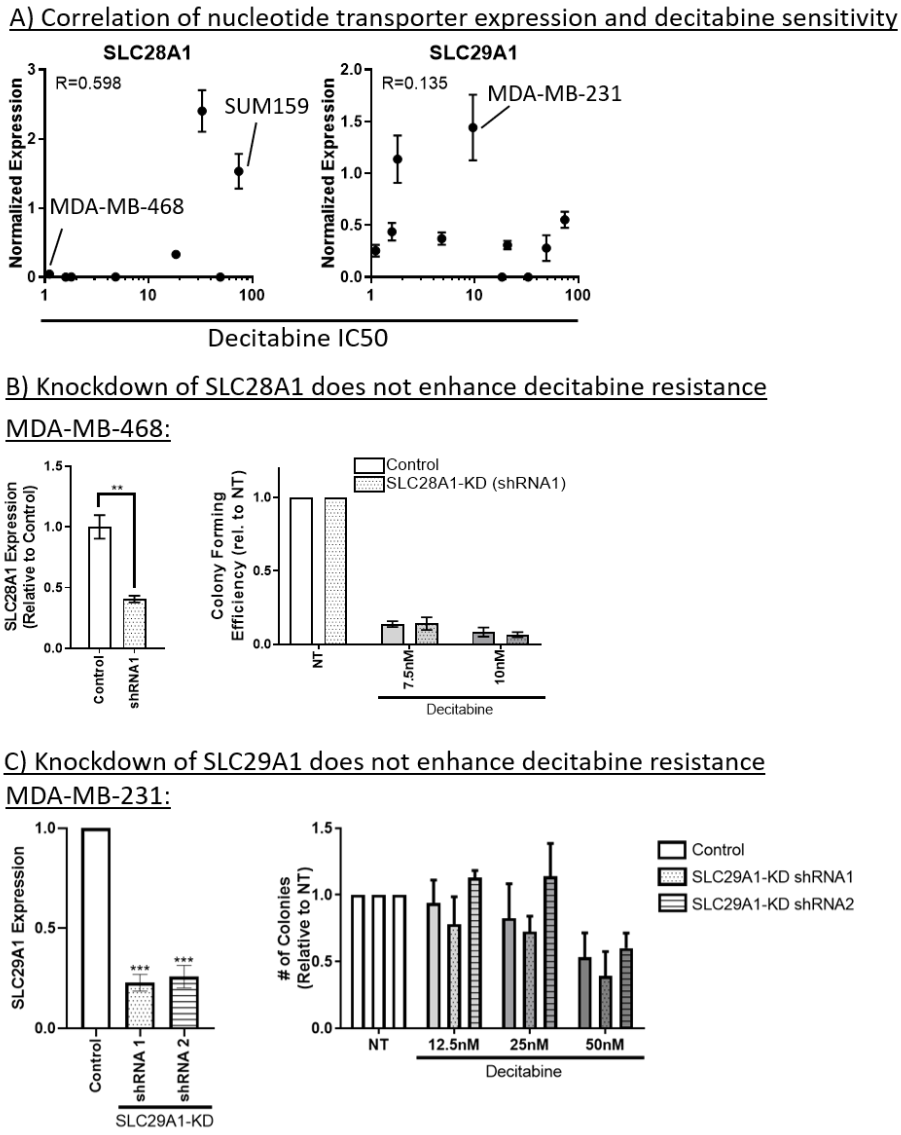

Figure 2.2: Increased levels of nucleoside transporters does not correlate with increased decitabine sensitivity in breast cancer cell lines. **A)** Expression of solute carrier family 28 member 1 (SLC28A1), and solute carrier family 29 member 1 (SLC29A1) was determined via RT-qPCR and normalized to reference genes B2M RPL29 across 10 breast cancer cell lines. Spearman correlation R. SD error bars (n=6). **B)** SLC28A1 knockdown in MDA-MB-468 breast cancer cells does not confer resistance to decitabine. SLC28A1 was knocked down via shRNA in MDA-MB-468 breast cancer cells (one sample t-test) and differential sensitivity to decitabine was assessed using a colony forming assay (one-way ANOVA). Error bars are standard deviation (n=4). **C)** SLC29A1 knockdown in MDA-MB-231 breast cancer cells does not confer resistance to decitabine**.** SLC29A1 was knocked down via shRNA in MDA-MB-231 breast cancer cells and differential sensitivity to decitabine was assessed using a colony forming assay. Error bars are standard deviation (n=4), one-way ANOVA; $p<0.01$, $p<0.001$***. BMC assisted with colony-forming assay; CD assisted with RT-qPCR.

Once imported, decitabine is sequentially phosphorylated by DCK, cytidine/uridine monophosphate kinase 1 (CMPK1), and finally nucleoside diphosphate kinases 1 and 2 (NME1, NME2)[91]. DCK is a rate-limiting step for the incorporation of decitabine in MDS and AML[91,292] and could possibly be a rate-limiting step for decitabine response in breast cancer. Consistent with its requirement for decitabine processing, knockdown of DCK significantly decreased the sensitivity of both the decitabine-sensitive MDA-MB-468 cells and decitabine-resistant SUM159 cells (Figure 2.3). This was also observed *in vivo*, where MDA-MB-468 tumours with DCK knockdown were comparably resistant to decitabine (Figure 2.4A). The reduction in DCK levels also hampered expression of decitabine-inducible genes (Figure 2.4B) that were identified as up-regulated by decitabine in the gene array. It is noteworthy that MDA-MB-468 cells with DCK knockdown remained sensitive to the ribonucleoside analog and DNMT inhibitor azacytidine (Figure 2.4C), which does not require DCK for DNA incorporation and activity[292].

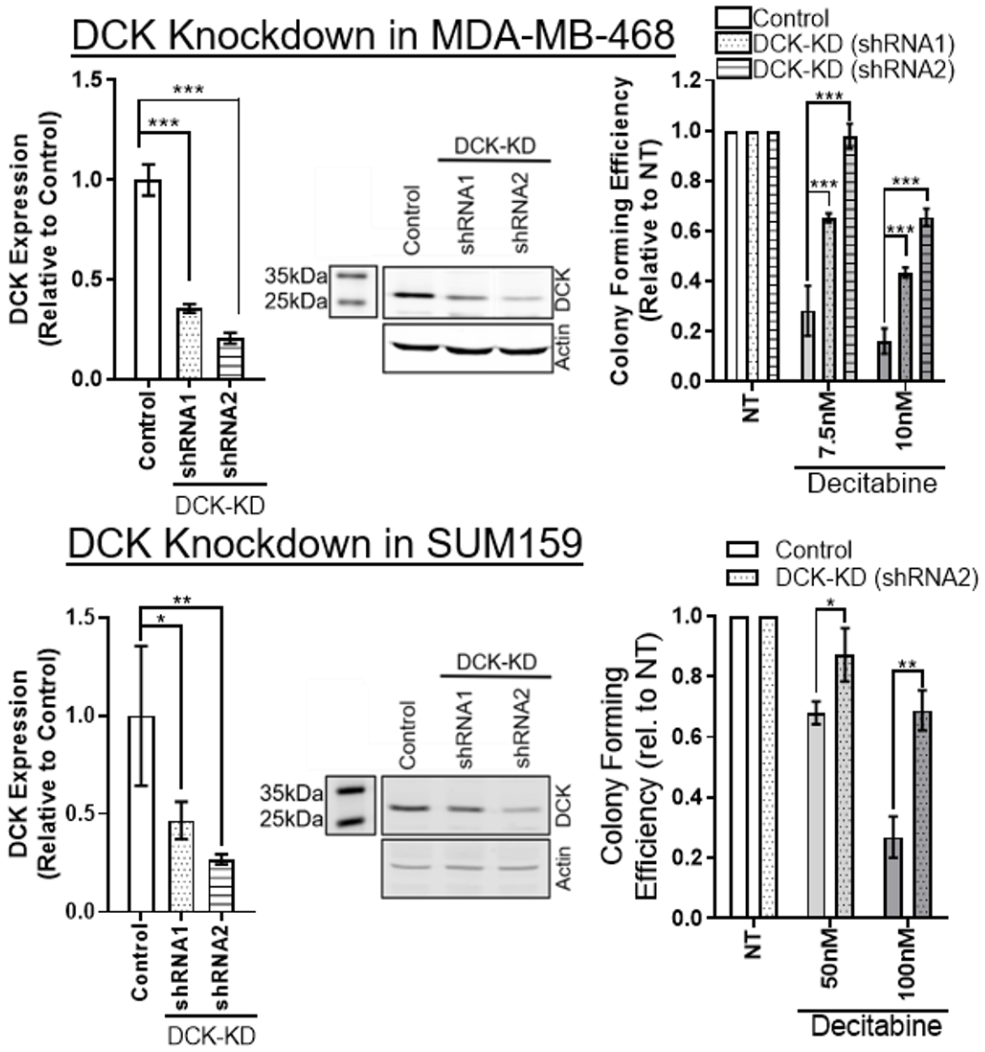

Figure 2.3: Deoxycytidine kinase (DCK) is an important mediator of *in vitro* decitabine response. Efficient shRNA-mediated knockdown of DCK conferred *in vitro* resistance to DAC in MDA-MB-468 and SUM159 cells. Knockdowns validated at mRNA level by RT-qPCR and protein level by Western blot. *In vitro* sensitivity determined by colony forming assay. SD error bars, ANOVA with Dunnett's post-hoc test. $p<0.05$*, $p<0.01$**, $p<0.001$***. BMC assisted with colony forming assay, RWH generated Western blots.

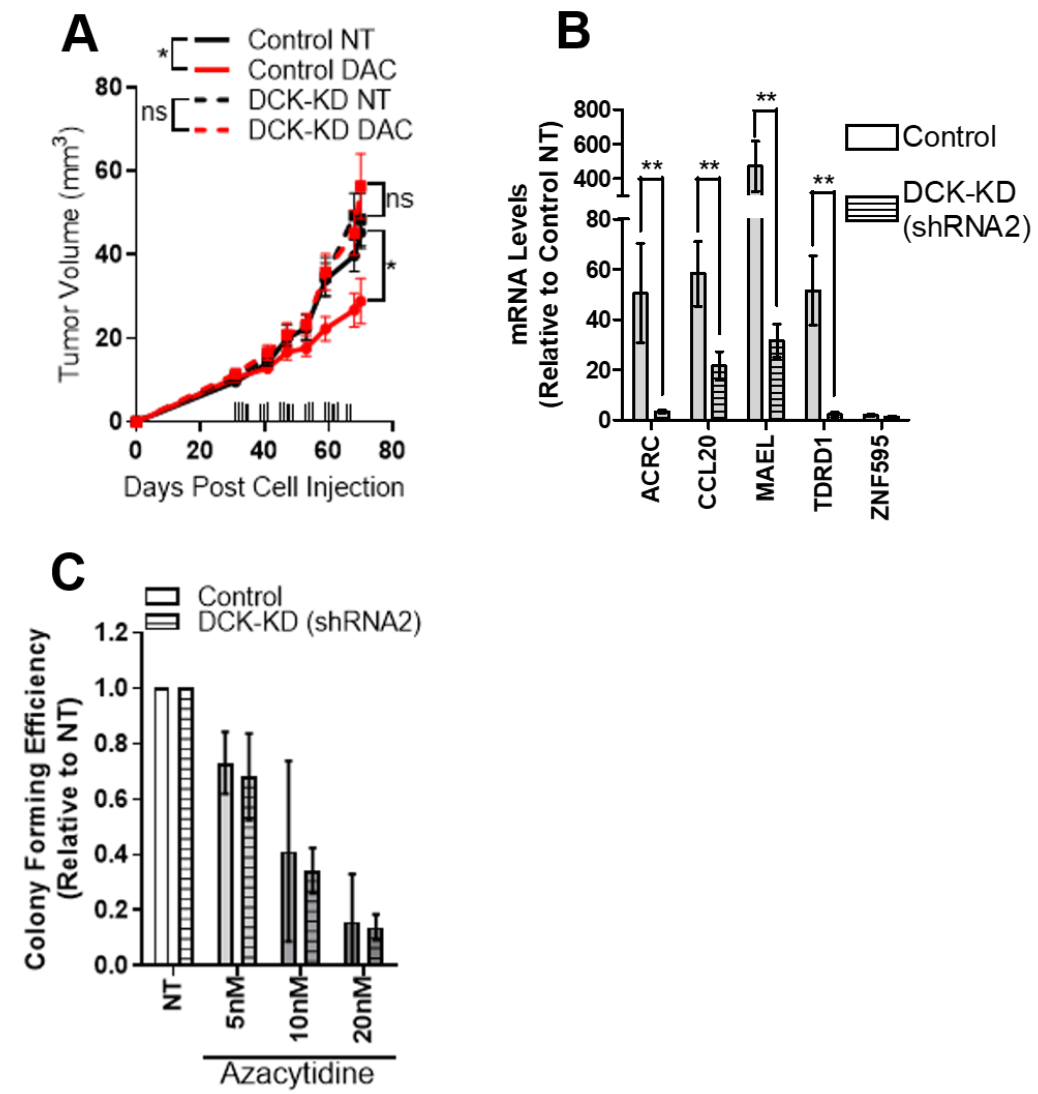

Figure 2.4: Deoxycytidine kinase (DCK) is an important mediator of decitabine but not azacytidine response. A) shRNA-mediated knockdown of DCK conferred *in vivo* resistance to DAC to MDA-MB-468 treated tumours (Control NT n=10, Control DAC n=10, DCK-KD NT n=10, DCK-KD DAC n=12), one-way ANOVA. **B)** DCK Knockdown in MDA-MB-468 cells dampens decitabine-induced gene expression**.** Genes identified as induced by decitabine in the breast cancer cells by the gene array include acidic repeat containing (ACRC), C-C motif chemokine ligand 20 (CCL20), maelstrom (MAEL), tudor domain containing 1 (TDRD1), and zinc finger protein 595 (ZNF595). Expression of these genes in MDA-MB-468 cells was assessed by RT-qPCR upon DCK knockdown (shRNA2) and 72h treatment with 1µM decitabine (n=3). Unpaired, one-tailed t-test with Welch's correction compared decitabine-treated control to decitabine-treated DCK-KD cells, SD error bars. **C)** DCK knockdown in MDA-MB-468 cells does not confer resistance to azacytidine. (n=3) SD error bars, one-way ANOVA. $p<0.05$*, $p<0.01$**. BMC assisted with intraperitoneal decitabine injections.

I assessed expression levels of DCK and the other nucleotide kinases involved in processing deoxynucleotides/decitabine in the 10 breast cancer cell lines and noted similar levels of DCK, CMPK1, NME1 and NME2 across the cell lines (Figure 2.5). The lack of a correlation between DCK expression and decitabine IC_{50} of the cell lines was likely due to the small range of differences in DCK levels between the cell lines (Figure 2.5). However, given the importance of DCK in mediating decitabine response in breast cancer as demonstrated by my knockdown experiments (Figures 2.3A, 2.3B, 2.4), I assessed the expression of the DCK in two breast cancer patient cohorts (METABRIC, Figure 2.6A and TCGA Cell 2015, Figure 2.6B). DCK mRNA levels in the breast cancer patient tumours followed a normal distribution and was overall more abundant in the luminal B, basal-like (which consists predominately of TNBCs), and TNBC subtypes. This suggests that for most patients (and in the TNBC patients that are currently being treated by decitabine in clinical trials), limited DCK expression will not be a barrier to successful decitabine therapy. Since the patients that will be treated with decitabine will likely have had anthracycline and/or taxane chemotherapy prior to enrollment in a clinical trial, it is important to determine if DCK levels are altered post-treatment with standard chemotherapy drugs. Microarray-based gene expression from 56 matched pre- and post-chemotherapy breast tumour samples showed that DCK expression was elevated after chemotherapy in patients who did not show a histopathological response to treatment (Figure 2.6C). This suggests that these patients would be good candidates for decitabine treatment, at least with respect to the essential decitabine processing enzyme DCK.

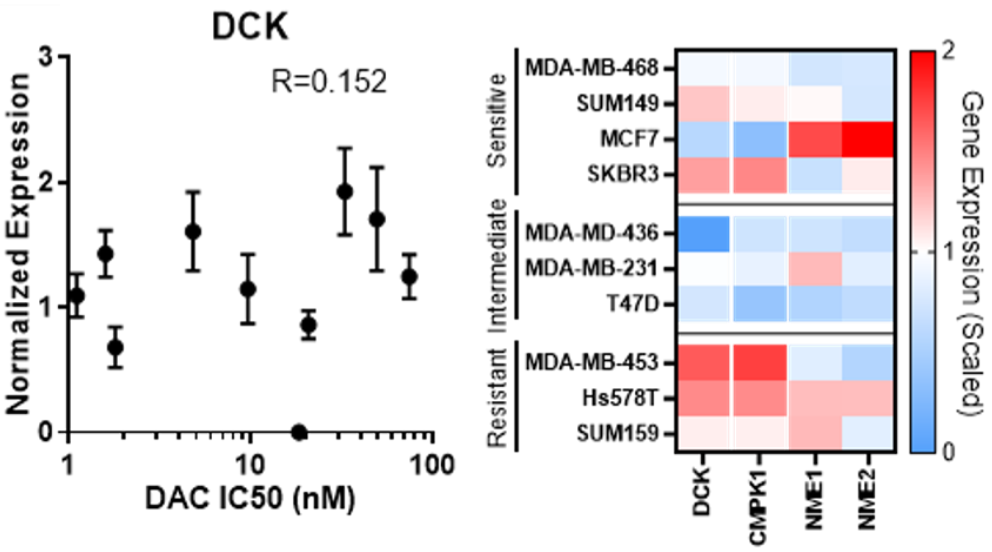

Figure 2.5: Nucleotide kinase expression is not associated with decitabine response. RT-qPCR of nucleotide kinases (DCK, CMPK1, NME1, NME2) across breast cancer cell lines, SD error bars. Spearman correlation R. CD assisted with RT-qPCR.

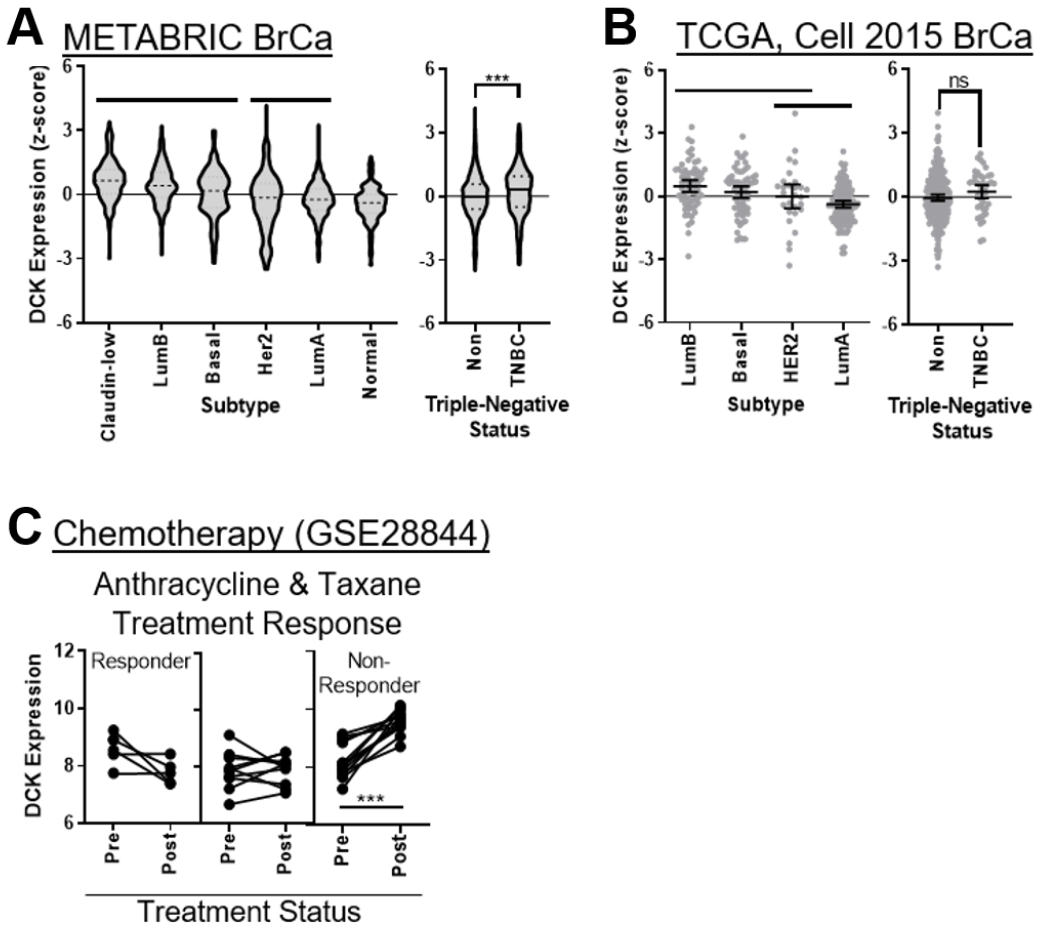

Figure 2.6: Expression of DCK is higher in TNBC and basal-like subtypes and is increased after treatment with chemotherapy. **A)** Expression of DCK via microarray based on PAM50 subtype and triple-negative receptor status in METABRIC and **B)** TCGA Cell, 2015 breast cancer patient cohorts. Straight lines note groups that are not significantly different, ANOVA with (Tukey's post-hoc test). **C)** DCK expression via microarray in the GSE28844 dataset of breast cancer patients pre- and post-anthracycline/taxane treatment.; paired two-tailed t-test; $p<0.001$***.

2.3.3 *GENOME-WIDE AND REGION-SPECIFIC METHYLATION OF BREAST CANCER CELLS IS NOT PREDICTIVE OF DECITABINE RESPONSE*

Genome-wide hypomethylation with concurrent hypermethylation of promoter regions is observed in cancer cells[293]; therefore, I wondered if any correlations with genome-wide or region-specific methylation could predict response to decitabine in breast cancer. For this purpose, I performed HM450 and gene expression analysis of decitabine treated cells. The colony assay (Figure 2.1) is a long term two-week plus assay and hence results in an enhanced decitabine sensitivity in the nM range in IC_{50s}. While informative for determining relative sensitivities, this assay is insufficient for harvesting cell samples for HM450 and RNA analysis, which required >300,000 cells. Therefore, I determined a concentration of decitabine that when applied to sub-confluent monolayers of >300,000 cells seeded in 6 well plates would result in approximate 50% growth inhibition of cells after 72 hours (0.6μM-9μM; Figure 2.7). A dose of 1μM decitabine (which represents a median IC_{50} in the cell line panel) was applied to sub-confluent monolayers for 72 hours (Figure 2.7). Furthermore, this dose causes minimal apoptosis after 72 hours of treatment (day 4 post seeding), but in subsequent days (decitabine treatment has ceased but cell culture continued) causes dramatic cell death and growth inhibition (Figure 2.8). This is further evidence of the long-term effects of decitabine which are also captured by the ultra-sensitive colony assay (Figure 2.1).

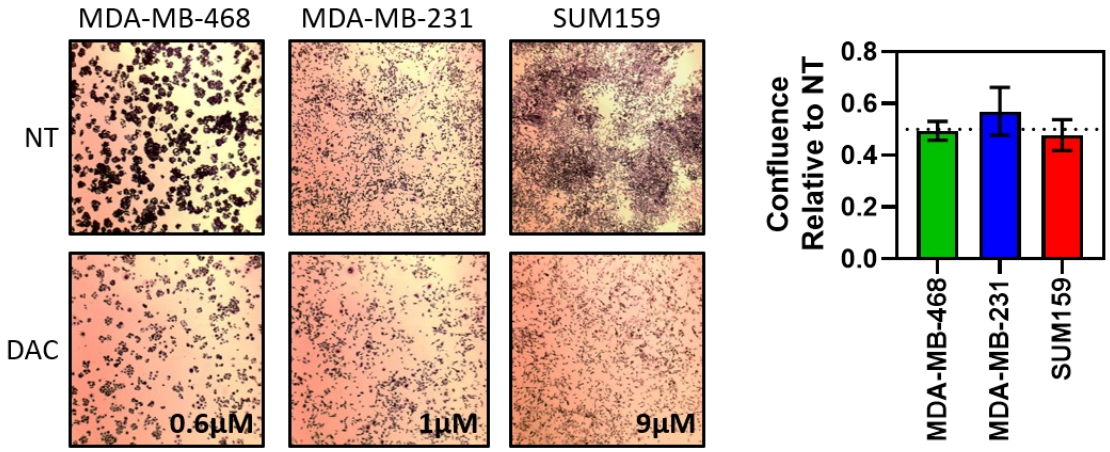

Figure 2.7: Cell confluency half maximal inhibitory concentration (IC_{50}) of decitabine in MDA-MB-468, MDA-MB-231, and SUM159 cells. The cells were seeded in 6 well plates and cultured as sub-confluent monolayers with indicated concentrations of decitabine (DAC) for 72 hours. Light microscopy images of crystal violet stained cells after 72 hours treatment with decitabine (left). Confluence of relative to no treatment (NT) cells was determined by quantifying total cell area coverage across 4 images/well using Image J. n=3. SD error bars.

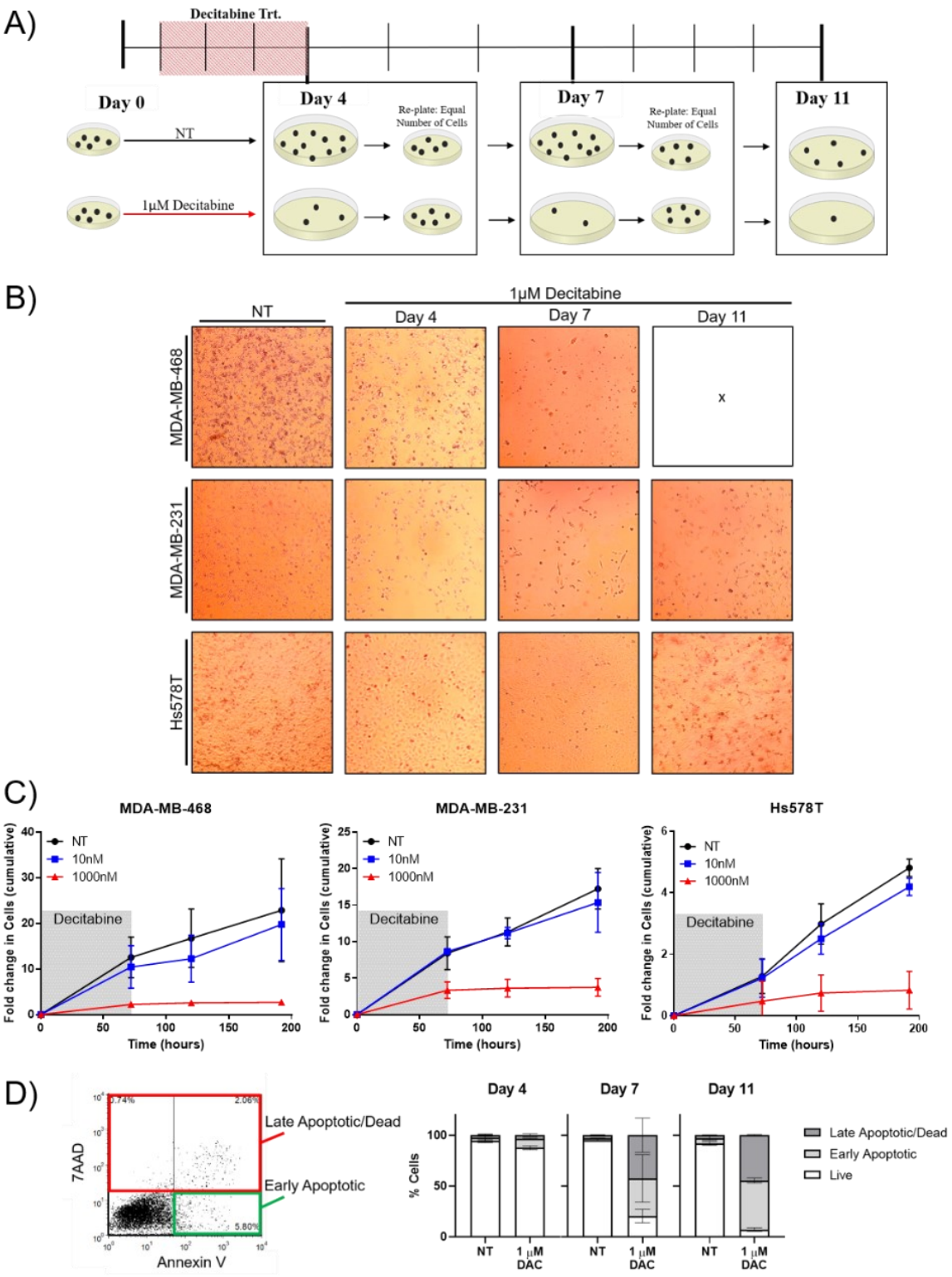
A)
Decitabine Trt.
Day 0
Day 4
Day 7
Day 11
NT
1μM Decitabine
Re-plate: Equal Number of Cells
Re-plate: Equal Number of Cells
B)
NT
1μM Decitabine
Day 4
Day 7
Day 11
MDA-MB-468
MDA-MB-231
Hs578T
x
C)
MDA-MB-468
MDA-MB-231
Hs578T
NT
10nM
1000nM
Decitabine
Fold change in Cells (cumulative)
Time (hours)
D)
7AAD
Annexin V
0.74%
2.06%
5.80%
Late Apoptotic/Dead
Early Apoptotic
Day 4
Day 7
Day 11
% Cells
NT
1 μM DAC
Late Apoptotic/Dead
Early Apoptotic
Live

Figure 2.8: Long-term response of sub-confluent monolayers of TNBC cell lines treated for 72 hours with 1μM decitabine. A) Schematic of the treatment time course. Cells were treated with decitabine for 72 hours and then re-plated and allowed to grow in regular media for an additional 7 days. **B)** Light microscopy 40X images of decitabine sensitive MDA-MB-468, intermediately sensitive MDA-MB-231 and decitabine resistant Hs578T cells show that 72 hours of 1μM decitabine is sufficient to slow long-term growth of all cell lines; NT images taken at day 4. **C)** At day 4 post seeding (immediately after 72h treatment) a differential response is observed with MDA-MB-468 cells being significantly depleted by the treatment and the Hs578T cells with no significant effect on cell abundance. **D)** Annexin V/7-AAD staining and quantification by flow cytometry of MDA-MB-231 cells treated with 1μM decitabine (DAC) for 72 hours (Day 4). Initial cell death is low; however, the percentage of apoptotic cells reaches ≈95% a week after treatment is removed. n=3. SD error bars. BMC assisted with long-term cell culturing and flow cytometry.

I analyzed HM450 data from 10 breast cancer cell lines (not treated with decitabine) and found that total genome-wide DNA methylation was not associated with response to decitabine and was overall similar among the cell lines (Figure 2.9). In agreement with this, the levels of DNMT1A, DNMT3B, and Tet methylcytosine dioxygenase 1, 2 and 3 (which act in the demethylation of DNA)[294], were also similar across the cell lines, consistent with the overall similar genome-wide methylation (Figure 2.10).

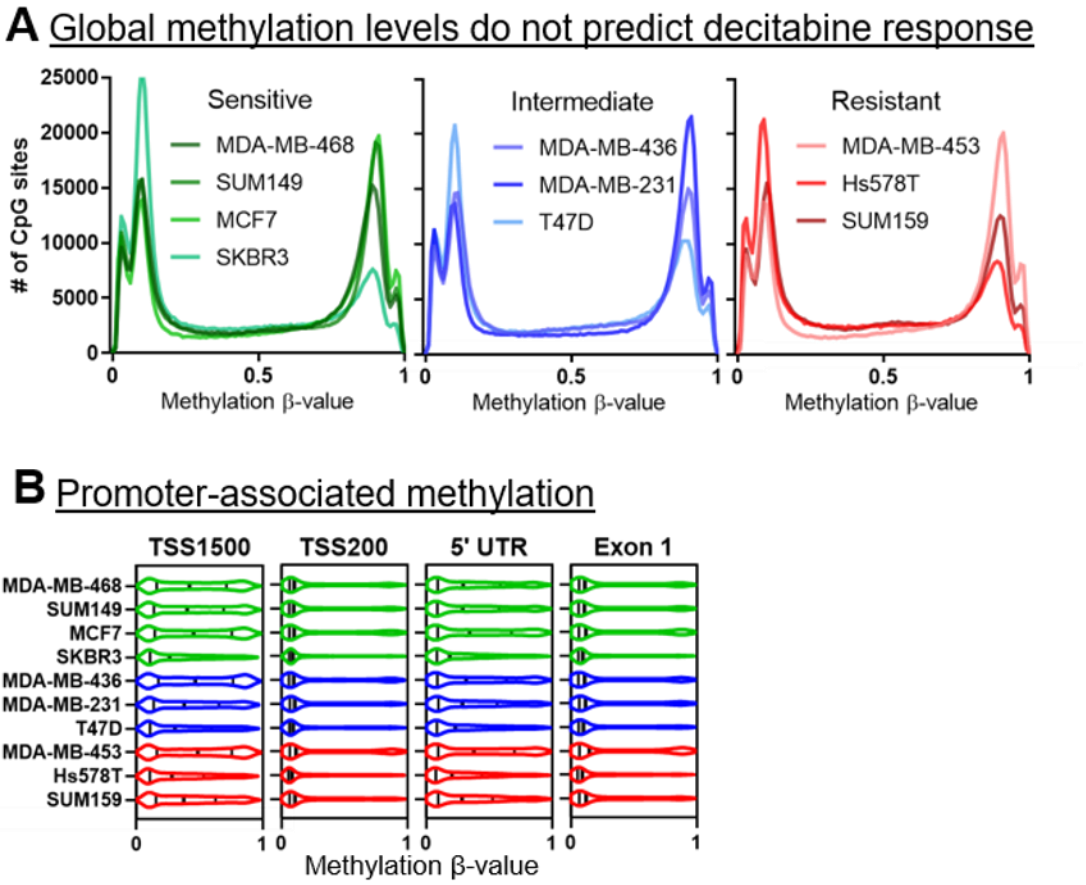

Figure 2.9: Breast cancer sensitivity to decitabine (DAC) is not associated with global methylation or promoter methylation. A) DNA Methylation as determined via HM450 array among breast cancer cell lines as a frequency distribution of CpG sites with a given methylation β-value. **B)** Distribution of HM450 Methylation β-values for promoter-associated regions TSS1500, TSS200, 5'UTR, and Exon 1 among the 10 breast cancer cell lines. KMC submitted cell line DNA for HM450 analysis.

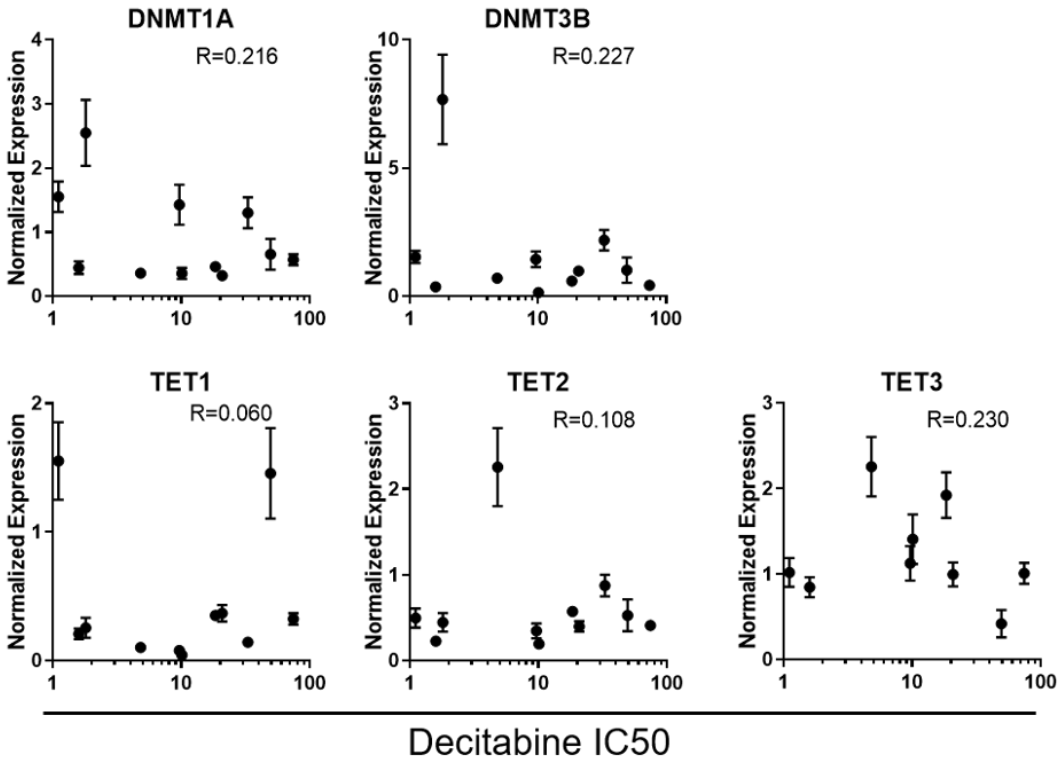

Figure 2.10: Expression of DNA methylation and demethylation-associated genes does not correlate with decitabine response in breast cancer cells. mRNA of DNA methyltransferase 1 (DNMT1), DNA methyltransferase 3 beta (DNMT3B), methylcytosine dioxygenase 1 (TET1), ten-eleven translocation methylcytosine dioxygenase 2 (TET2), and ten-eleven translocation methylcytosine dioxygenase 3 (TET3) determined via RT-qPCR and normalized to reference genes B2M RPL29, and plotted versus the decitabine IC_{50} of the 10 breast cancer cell lines (from Figure 2.1). Standard deviation error bars (n=6), Spearman correlation R. CD assisted with RT-qPCR.

To determine if promoter methylation was predictive of decitabine sensitivity, CpGs identified within 1500bp or 200bp of the transcription start site (TSS1500 and TSS200 respectively), within the 5'UTR, or within the first exon were evaluated with the HM450 assay. Overall, promoter DNA methylation was absent in most genes across all cell lines (Figure 2.9) and little differential methylation between decitabine-response groups was observed (Figure 2.11A). I noted that 434 genes had z-score > 1 for at least 1 promoter-associated CpG, with the majority of those hypermethylated promoter genes occurring in the decitabine resistant MDA-MB-453 cell line (Figure 2.11B). However, there are only a few genes that are consistently methylated across the 3 decitabine-resistant cell lines, and in patient tumours the genes are consistently unmethylated across all patient samples. (Figure 2.12A). This suggests that the existence of specific CpG sites that can stratify breast cancers for decitabine response based on hypermethylation likely do not exist. I also performed a principal component analysis (PCA) of TSS200 and gene body CpGs in the 10 cell lines which shows that the cell lines do not separate according to sensitivity (Figure 2.12B).

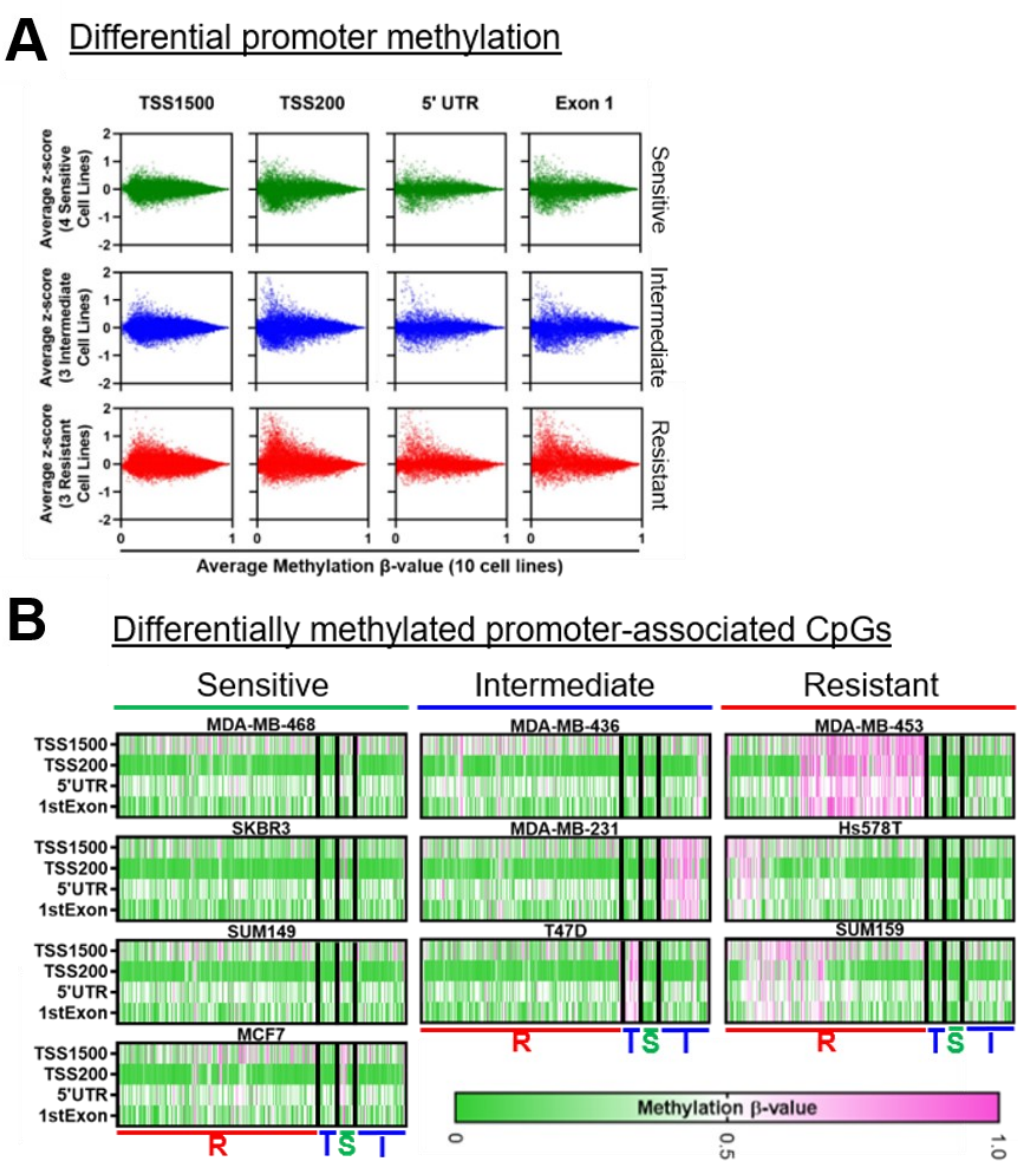

Figure 2.11: Breast cancer sensitivity to decitabine (DAC) is not associated with a specific pattern of methylation. A) The average methylation β-values for promoter-associated regions TSS1500, TSS200, 5UTR, and Exon 1 among the 10 cell lines are plotted against the decitabine-treatment relative change in methylation of those promoter regions (Methylation z-score) based on decitabine responsiveness. Sites located in upper left zone of dot plot represent sites that are hypermethylated in (e.g. resistant) cell lines compared to the rest of the cell lines. **B)** The hypermethylated regions identified in **A)** are represented by the methylation β-value in each cell line. KMC submitted cell line DNA for HM450 analysis.

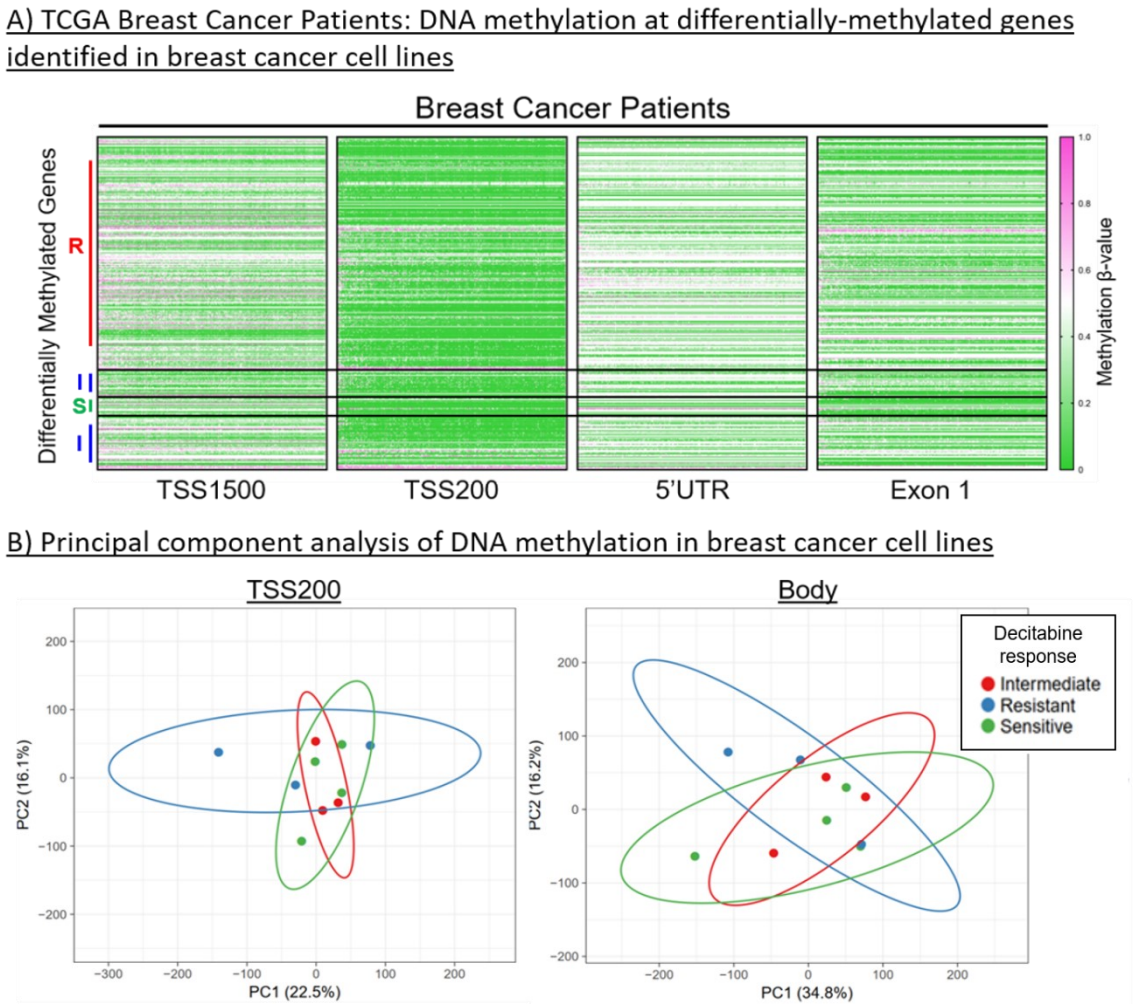

Figure 2.12: Primary breast tumours and breast cancer cell lines cannot be defined as decitabine-sensitive or -resistant based on differentially methylated CpGs in cell lines. A) TCGA, Cell 2015 HM450 Methylation β-values for 434 genes identified as differentially methylated in the cell lines (n=741). Patients with highest methylation of genes identified as methylated in decitabine-resistant cell lines are leftmost in the heatmaps. Data accessed by cBioportal[285,286] and TCGA Methylation Wanderer[295]. **B)** Principal Component Analysis (PCA) of DNA methylation status of CpGs within 200 nt of the transcription start site (TSS200) and CpGs in gene bodies in 10 breast cancer cell lines.

2.3.4 *GENOME-WIDE AND GENE-SPECIFIC DEMETHYLATION OF TUMOUR SUPPRESSOR GENES BY DECITABINE IN BREAST CANCER CELLS IS NOT CORRELATED WITH DECITABINE RESPONSE*

Although baseline methylation did not reveal any putative biomarkers, I hypothesized that genomic demethylation in the presence of decitabine may correlate with decitabine response. I analyzed HM450 data from six TNBC cell lines treated with 1μM decitabine for 72 hours. This revealed that decitabine induced a range of demethylation in the cells; however, the extent of demethylation was not reflective of the decitabine sensitivity in the cell lines. For example, SUM149 cells are generally highly sensitive (Figure 2.1), but on a genome-wide scale had comparatively little demethylation (Figure 2.13A), while SUM159 are resistant, and yet comparatively lost their methylation. Hence, although demethylation is associated with decitabine treatment in breast cancer cells, it is not correlative of IC_{50}s determined by the colony assay (Figures 2.1 and 2.13A).

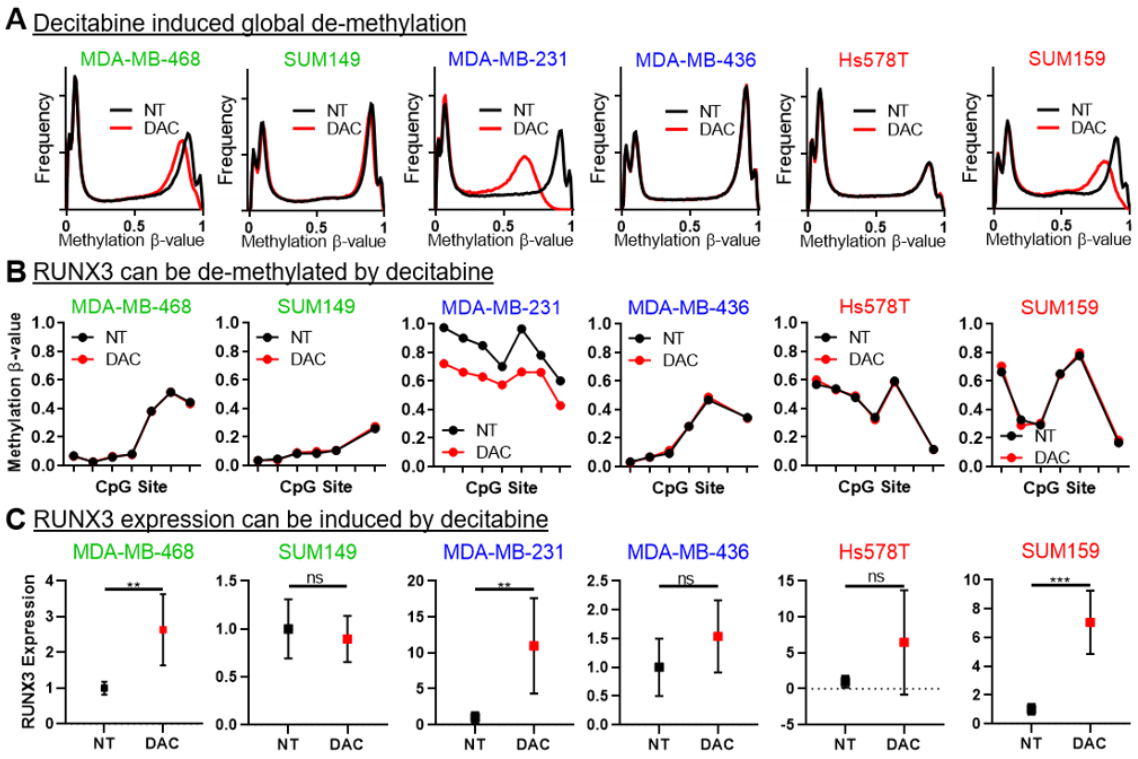

Figure 2.13: Breast cancer sensitivity to decitabine (DAC) is not associated DAC-induced demethylation or by induction of common hypermethylated tumour suppressor genes (e.g. RUNX3). DNA Methylation as determined via HM450 array among breast cancer cell lines **A)** after treatment with 1μM DAC for 72 hours. **B)** Methylation via HM450 of a promoter-associated CpG island in RUNX3 after treatment with 1μM DAC for 72 hours and **C)** RUNX3 mRNA levels via RT-qPCR after DAC treatment; SD error bars, one-way t-test, $p<0.01$**, $p<0.001$***. KMC submitted cell line DNA for HM450 analysis, CD assisted with RT-qPCR.

The extent of genome-wide demethylation was reflective of gene-specific demethylation of promoter regions and of known tumour suppressors *RUNX3* (Figure 2.13B), *BRCA1, CDH2,* and *RASSF1* (Figure 2.14), but not associated with response (Figure 2.1). Intriguingly, increased expression of *RUNX3* (Figure 2.13C) and *CDH2* (Figure 2.14) in many cases was not paired with promoter demethylation (Figure 2.13B, Figure 2.14), suggesting that induced expression of these well-characterized hypermethylated tumour suppressor genes[296–298] by decitabine is not necessarily due to promoter demethylation and may be a result of other effects of decitabine treatment. In validation of the HM40 data, we performed bisulfite pyrosequencing of 32 CpGs in the promoter region of *RUNX3* (Figure 2.15). The sequencing data generally agrees with the HM450 data and demonstrated that the SUM159 promoter is hemimethylated and is overall minimally demethylated by decitabine treatment, while the more methylated MDA-MB-231 *RUNX3* promoter contains a cluster of CpG sites around the start codon that are demethylated upon decitabine treatment (CpG site 11 to 17, Figure 2.15).

A) BRCA1

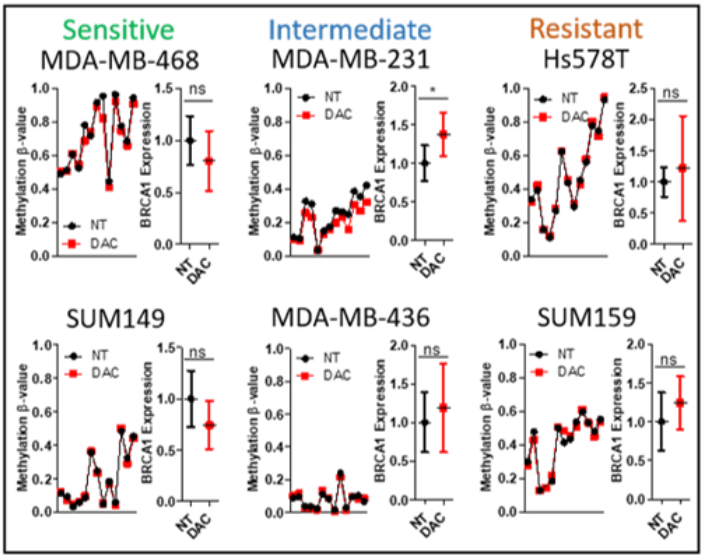

B) CDH2

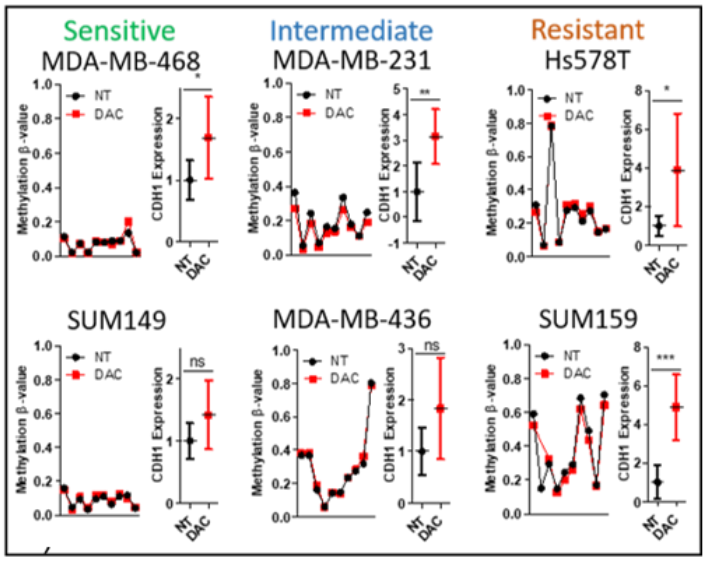

C) RASSF1A

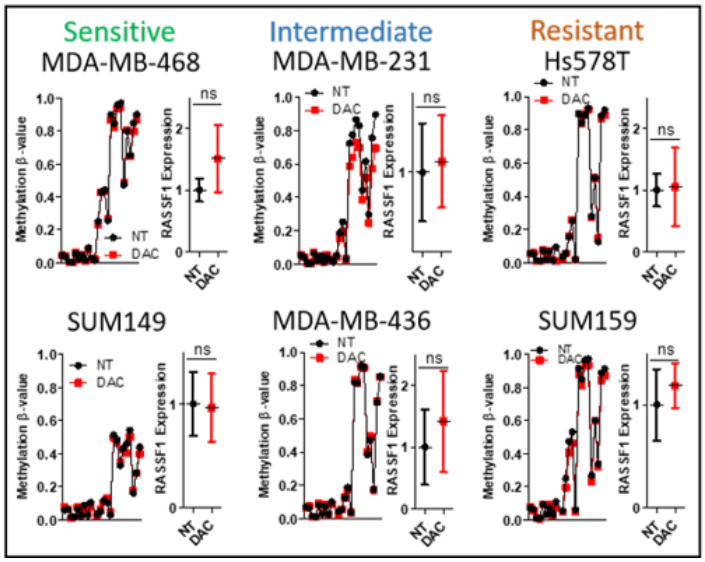

Figure 2.14: BRCA1 (A), CDH2 (B), and RASSF1 (C) promoter methylation and gene expression after decitabine treatment. The decitabine-sensitive MDA-MB-468 and SUM149, decitabine-intermediately sensitive MDA-MB-231 and MDA-MB-436, and decitabine-resistant Hs578T and SUM159 breast cancer cell lines were treated with 1µM decitabine for 72 hours. Decitabine-induced (DAC) changes in methylation of CpG sites associated with a CpG island on the promoter region of BRCA1 was determined via HM450K Illumina BeadChip Array; each dot represent a CpG site (n=1). Expression of BRCA1 **(A)**, CDH2 **(B)** or RASSF1 **(C)** after decitabine treatment (DAC) was determined via RT-qPCR (n=6); SD error bars; one-sample t-test; $p<0.05$ *. KMC submitted cell line DNA for HM450 analysis, CD assisted with RT-qPCR.

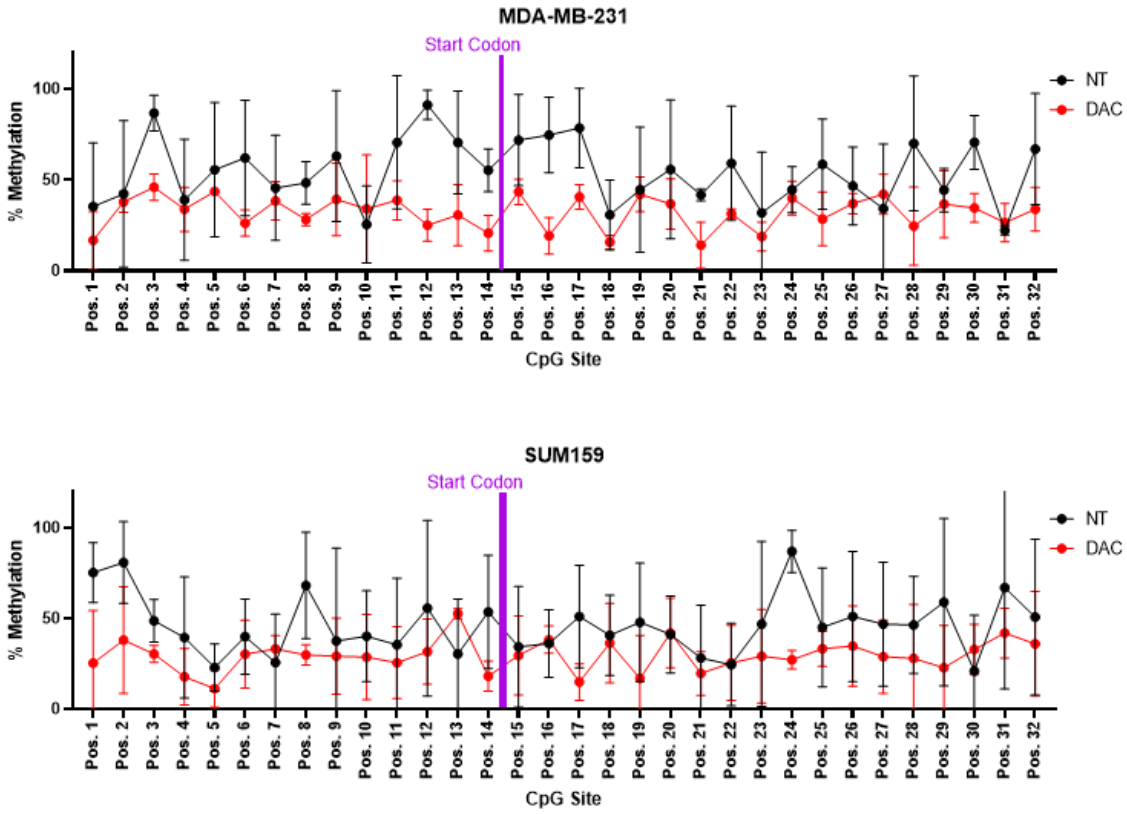

Figure 2.15: Bisulfite Pyrosequencing of CpGs in the RUNX3 promoter region in MDA-MB-231 and SUM159 breast cancer cells treated for 72 hours with 1µM decitabine. The start codon is located between CpGs 14 and 15. n=3, SD error bars. HM and ICGW performed bisulfite pyrosequencing.

2.3.5 *DECITABINE UPREGULATES GENE EXPRESSION VIA DEMETHYLATION OF PROMOTERS AND INDUCES TRANSCRIPTIONAL PROGRAMS FOR STRESS, CELL CYCLE ARREST, APOPTOSIS, AND IMMUNE RESPONSE*

Since my analyses of gene-specific demethylation of tumour suppressor genes failed to identify correlations with expression and decitabine sensitivity (Figure 2.13-2.15) I extended my gene expression analyses genome-wide. Three cell lines spanning the range of decitabine sensitivity were assessed for expression changes in the presence of decitabine by microarray. Extensive upregulation of gene expression was observed across all three cell lines while concurrently many genes were downregulated (Figure 2.16 and 2.17). Interestingly, though the magnitude of induction was variable, there was significant overlap in which transcripts were upregulated between the cell lines, with few differentially regulated genes (Figure 2.16A). Independent GSEA of the up-regulated vs. down-regulated transcripts showed that there is significant overlap of the breast cancer decitabine up- or down-regulated transcripts with existing azanucleoside-mediated gene expression datasets. The gene set Kim_Response_to_TSA_and_decitabine is from 4 glioma cell lines treated with combination decitabine and trichostatin A (histone deacetylase inhibitor)[299], dataset Zhong_response_to_azactidine_and_TSA is from 4 non small cell lung cancer cell lines treated with a combination of azacytidine and trichostatin A[300], and dataset Heller_HDAC_targets_silenced_by_methylation is from 3 multiple myeloma cell lines treated with a combination of azacytidine and trichostatin A[301]. If these up-regulated transcripts are hypermethylated tumour suppressor genes then I would expect the more decitabine-sensitive cell lines to have stronger induction of these gene sets, but this is not the case as SUM159 (decitabine-resistant) has the most extensive gene upregulation.

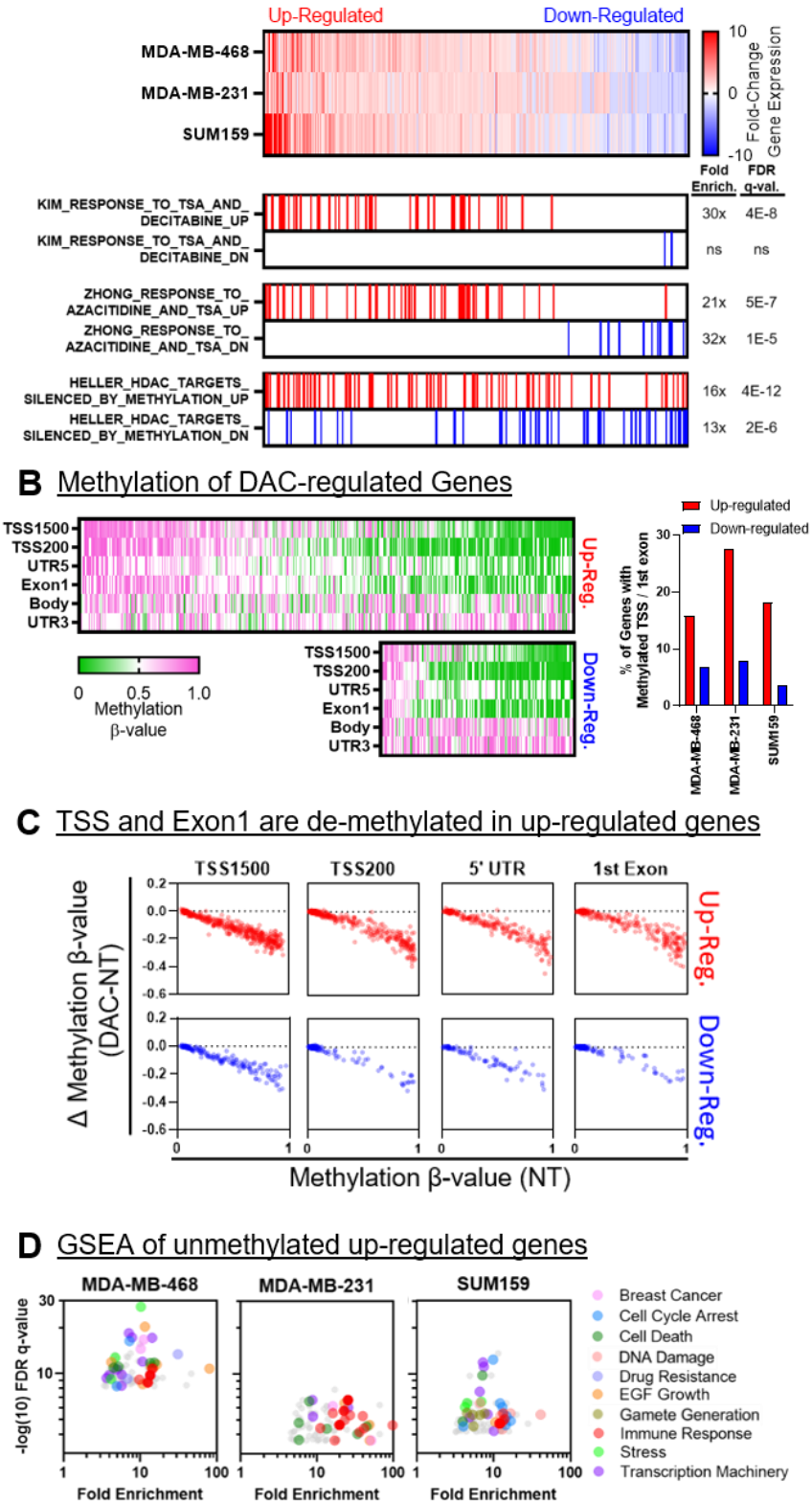
A DAC Consistently Alters Gene Expression
Up-Regulated
Down-Regulated
MDA-MB-468
MDA-MB-231
SUM159
10
0
-10
Fold-Change Gene Expression
Fold Enrich.
FDR q-val.
KIM_RESPONSE_TO_TSA_AND_DECITABINE_UP
KIM_RESPONSE_TO_TSA_AND_DECITABINE_DN
30x 4E-8
ns ns
ZHONG_RESPONSE_TO_AZACITIDINE_AND_TSA_UP
ZHONG_RESPONSE_TO_AZACITIDINE_AND_TSA_DN
21x 5E-7
32x 1E-5
HELLER_HDAC_TARGETS_SILENCED_BY_METHYLATION_UP
HELLER_HDAC_TARGETS_SILENCED_BY_METHYLATION_DN
16x 4E-12
13x 2E-6
B Methylation of DAC-regulated Genes
TSS1500
TSS200
UTR5
Exon1
Body
UTR3
Up-Reg.
Down-Reg.
0 0.5 1.0
Methylation β-value
Up-regulated
Down-regulated
% of Genes with Methylated TSS / 1st exon
MDA-MB-468
MDA-MB-231
SUM159
C TSS and Exon1 are de-methylated in up-regulated genes
TSS1500
TSS200
5' UTR
1st Exon
Δ Methylation β-value (DAC-NT)
Up-Reg.
Down-Reg.
Methylation β-value (NT)
D GSEA of unmethylated up-regulated genes
MDA-MB-468
MDA-MB-231
SUM159
-log(10) FDR q-value
Fold Enrichment
Breast Cancer
Cell Cycle Arrest
Cell Death
DNA Damage
Drug Resistance
EGF Growth
Gamete Generation
Immune Response
Stress
Transcription Machinery

Figure 2.16: Decitabine induces expression of methylated genes, drug response pathways, and immune response pathways genes regardless of DAC sensitivity. A) Gene expression microarray of cell lines treated with 1μM DAC for 72 hours showing genes significantly up- or down-regulated (1.5-fold) in any cell line; GSEA showing genes from independent datasets of azanucleoside-treated cancer cells. **B)** Left: HM450 methylation values of genes for which expression was affected by decitabine treatment in MDA-MB-231 cells significantly up- (426 genes) or down-regulated (168 genes). Right: Proportion of genes with methylated TSS (transcription start site) or exon 1 that are up- or down-regulated in expression after DAC treatment. **C)** HM450 methylation on genes for which decitabine affects expression in MDA-MB-231; change in methylation after 72 hours decitabine treatment (DAC-NT) versus pre-decitabine methylation (NT). **D)** Top 100 enriched gene sets in the un-methylated (TSS/Exon1) DAC up-regulated genes based on GSEA; gene included in each pathway indicated by color. KMC submitted cell line DNA for HM450 analysis. KMC submitted MDA-MB-468 and MDA-MB-231 RNA for Affymetrix Human Gene 2.0 ST microarray.

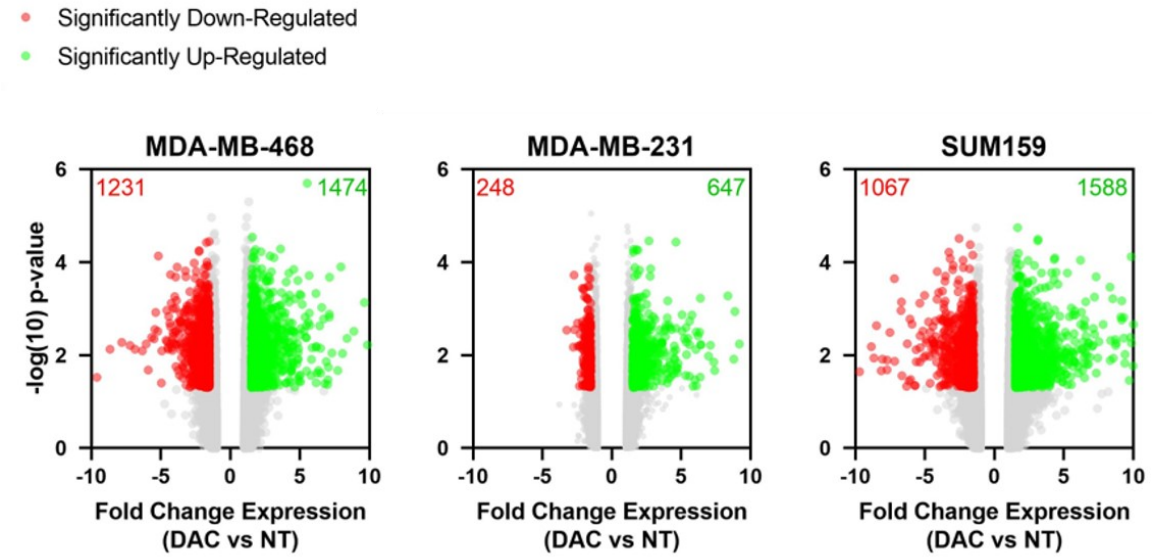

Figure 2.17: Genome-wide expression changes induced by decitabine treatment in breast cancer cells. Gene expression changes induced by decitabine are quantified in MDA-MB-468, MDA-MB-231 and SUM159 cells using the Affymetrix Human Gene 2.0 ST microarray platform (n=3). The log2-fold change in expression is plotted versus the –log10 (ANOVA p-value). Only probes with a >1.50-fold expression change and a p-value of <0.05 are indicated as colored dots. KMC submitted MDA-MB-468 and MDA-MB-231 RNA for Affymetrix Human Gene 2.0 ST microarray.

To determine if there is direct upregulation of gene expression via demethylation of promoter regions, HM450 Methylation β-values from the genes that were up or downregulated by decitabine in all three cell lines were examined. More often, the TSS1500, TSS200, 5'UTR, and Exon1 regions were methylated in upregulated genes compared to downregulated genes in MDA-MB-231 (Figure 2.16B), MDA-MB-468 (Figure 2.18A) and SUM159 cells (Figure 2.18B). As expected, there was general demethylation of these regions in upregulated genes after decitabine treatment in MDA-MB-231 (Figure 2.16C), MDA-MB-468 and SUM159 cells (Figure 2.19). Intragenic (especially gene body) DNA methylation may serve as a positive regulator of transcription, where loss of methylation inhibits gene expression[302]. This may explain why downregulated genes were more likely to have methylation of the 3'UTR and gene body compared to upregulated genes (Figure 2.20).

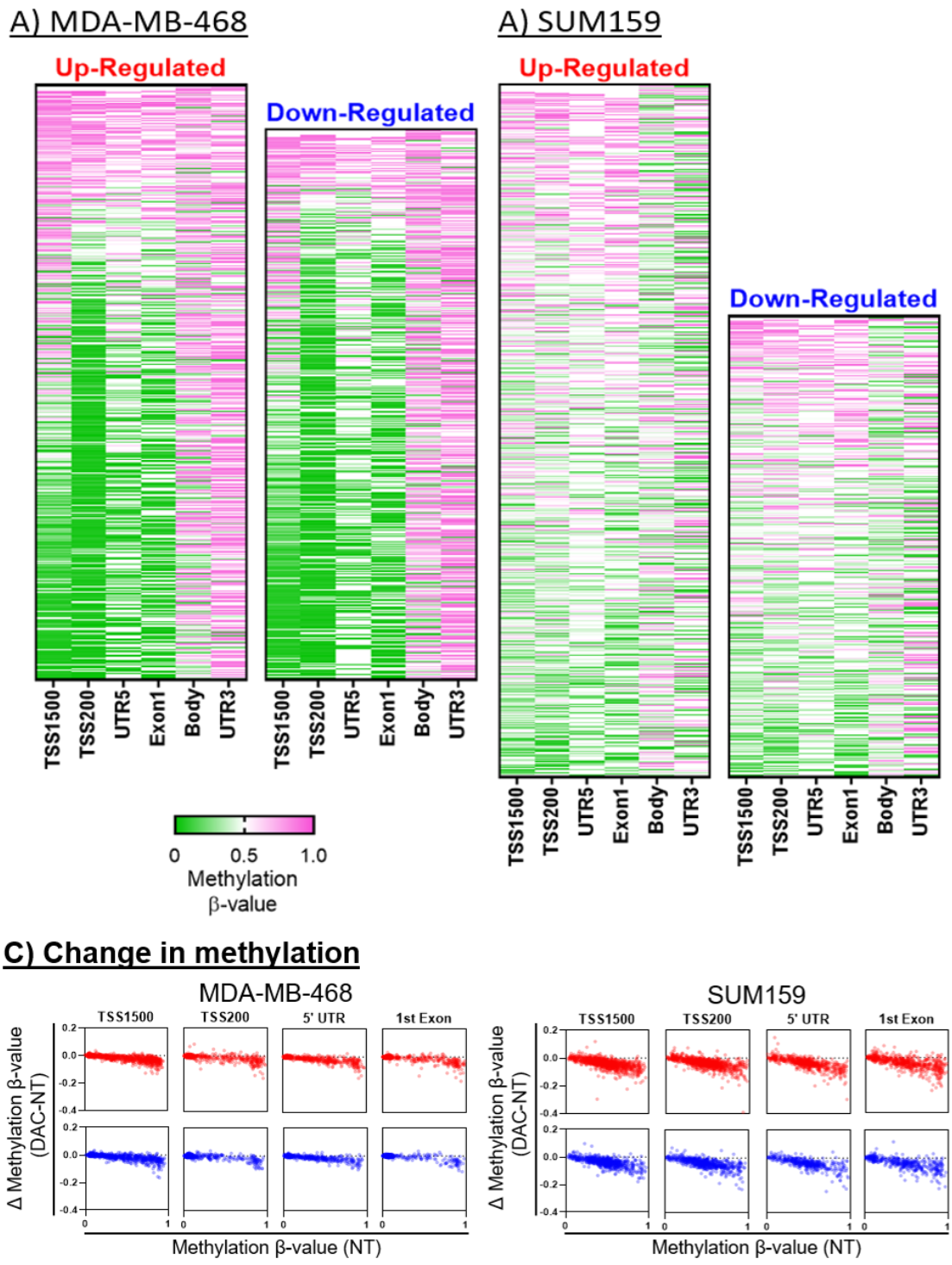

Figure 2.18: Clustering of the decitabine up- and downregulated genes based on HM450 methylation values of gene regions in **A)** MDA-MB-468 and **B)** SUM159 cells. **C)** Methylation changes in TSS1500/TSSS200/5UTR/Exon1 of genes up- or down-regulated by decitabine. KMC submitted cell line DNA for HM450 analysis and MDA-MB-468 RNA for Affymetrix Human Gene 2.0 ST microarray.

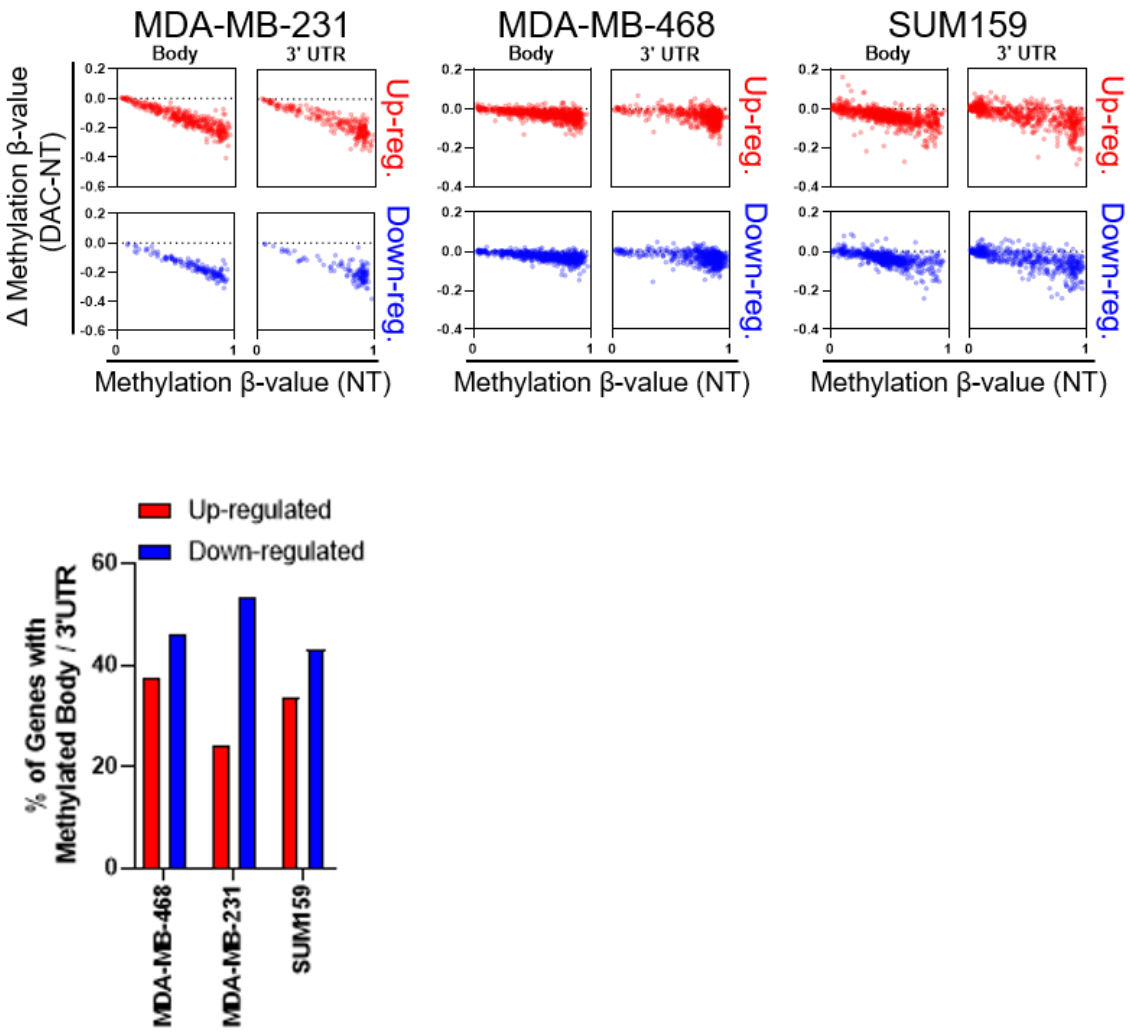

Figure 2.19: Methylation changes in Gene Body/3UTR of genes up- or down-regulated by decitabine. KMC submitted cell line DNA for HM450 analysis and MDA-MB-468 RNA for Affymetrix Human Gene 2.0 ST microarray.

Genes that were confirmed to have hypermethylated promoter regions only constituted 16-28% of total decitabine-upregulated genes (Figure 2.16B), leaving the majority of upregulated genes without a clear cause for upregulation. Direct gene expression changes induced by demethylation are well-characterized outcomes of decitabine treatment; however, the indirect gene expression changes that are not readily explained by methylation changes are not as well understood. These indirect changes may be due to the demethylation of transcription factors or the epigenetic resurrection of other upstream signalling pathways. In a GSEA of the decitabine-upregulated genes with unmethylated TSS and Exon1 in each cell line, all three cell lines showed upregulation of genes associated with cell cycle arrest, cell death, DNA damage, stress, immune response, and transcriptional machinery (Figure 2.19D).

2.3.6 *DECITABINE INDUCES VIRAL MIMICRY RESPONSE IN BREAST CANCER CELLS, BUT dsRNA SENSORS ARE NOT REQUIRED FOR IN VITRO SENSITIVITY*

Among the most consistently upregulated pathways by decitabine in the cell lines were immune-related pathways (Figure 2.19D). Consistent with this, interferon-inducible 2'-5'-oligoadenylate synthetase-like (OASL) was up-regulated in MDA-MB-231 cells upon decitabine treatment. Recent reports have highlighted the requirement for the viral mimicry response (interferon-induced OASL is part of this response) for decitabine sensitivity for *in vitro* and *in vivo* growth inhibition of colorectal and ovarian cancer cells[272,273]. In those studies, demethylation by decitabine leads to re-expression of epigenetically silenced endogenous retroviral elements (ERVs), leading to a cascade of events that results in induction of the interferon response (Figure 2.20A). I assessed the level of induction of

previously described mediators of the decitabine-induced viral mimicry response in the breast cancer cell lines. I assessed expression of the ERVs in my cell lines using a panel of previously described and newly designed primers (Table 2.5). I was unable to detect expression of many of these transcripts in the 10 breast cancer cell lines (pooled cDNA sample of all cell lines no treatment and decitabine treated, Table 2.5). Decitabine-induced expression of *ERVs MLT1C49* or *MLT2B4* was observed in some of the cell lines (e.g. SKRBR3, MDA-MB-436) treated with 1μM decitabine for 72 hours; however, induction was inconsistent and did not correlate with sensitivity (Figure 2.20B). I further explored the induction of ERVs *EnvE, ERVFRD1*, and the 5'UTR region of *HERV-K* in decitabine sensitive MDA-MB-468 cells, intermediately sensitive MDA-MB-231 cells and resistant SUM159 cells treated with their cell confluency IC_{50}s of decitabine. This again resulted in limited induction of these ERVs, which did not correlate with decitabine sensitivities (Figure 2.21A). Of note these ERVs were also not induced in the MDA-MB-468 tumours that had been treated with decitabine (Figure 2.1, Figure 2.21B).

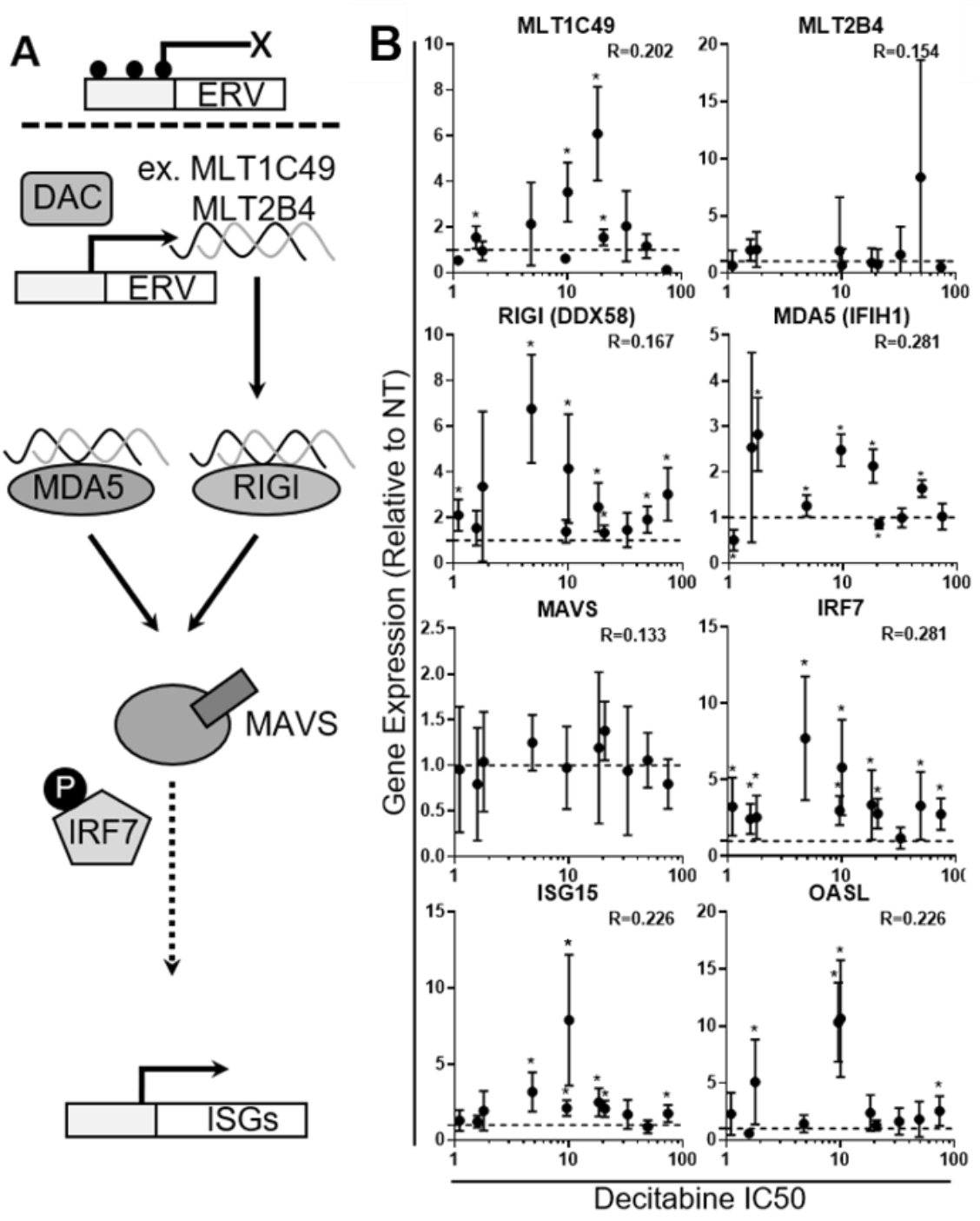

Figure 2.20: Decitabine induces expression of the dsRNA pathway but it is not essential for DAC sensitivity. A) dsRNA "viral mimicry" pathway components **B)** show increased gene expression via RT-qPCR in breast cancer cell lines after 1μM DAC treatment for 72 hours; SD error bars, one-sample t-test, Spearman correlation R. CD assisted with RT-qPCR.

Table 2.5: Endogenous Retroviral Element RT-qPCR primers quality control summary[272,273,303].

ERV	Source	Primer Efficiency	Other Issues
envE	(Chiappinelli *et al*., 2015; Strissel *et al*., 2012)	138.7	Requires double RNA conc.
envFc1	(Chiappinelli *et al*., 2015; Strissel *et al*., 2012)	336.4	
envRb	(Chiappinelli *et al*., 2015; Strissel *et al*., 2012)	234.3	
envT	(Chiappinelli *et al*., 2015; Strissel *et al*., 2012)	74	Wide melt curve
envV2	(Chiappinelli *et al*., 2015; Strissel *et al*., 2012)	-	No amplification
ERVFRD1	Meg Dahn	97	
ERVV	Meg Dahn	593	
HK5-orf1	Meg Dahn	273.6	
HK5-utr	Meg Dahn	115	
HK-orf-2	Meg Dahn	-	No amplification
HW1	Meg Dahn	627.5	
L-2	Meg Dahn	286.9	2 melt curves
L-orf1	Meg Dahn	362.5	2 melt curves
L-orf2	Meg Dahn	257.6	2 melt curves
L-utr	Meg Dahn	166	2 melt curves
MLTA10	(Roulois *et al*., 2015)	-	No amplification
MLT1B	(Roulois *et al*., 2015)	-	No amplification
MER21C	(Roulois *et al*., 2015)	-	No amplification
ERVL	(Roulois *et al*., 2015)	-	No amplification
MLT1C49	(Roulois *et al*., 2015)	87	
MLT1C627	(Roulois *et al*., 2015)	-	No amplification
MER4D	(Roulois *et al*., 2015)	-	No amplification
MER57B1	(Roulois *et al*., 2015)	-	No amplification
MLT2B4	(Roulois *et al*., 2015)	111	

N.B. **Bolded** ERVs are ones that were quantified by RT-qPCR in this manuscript.

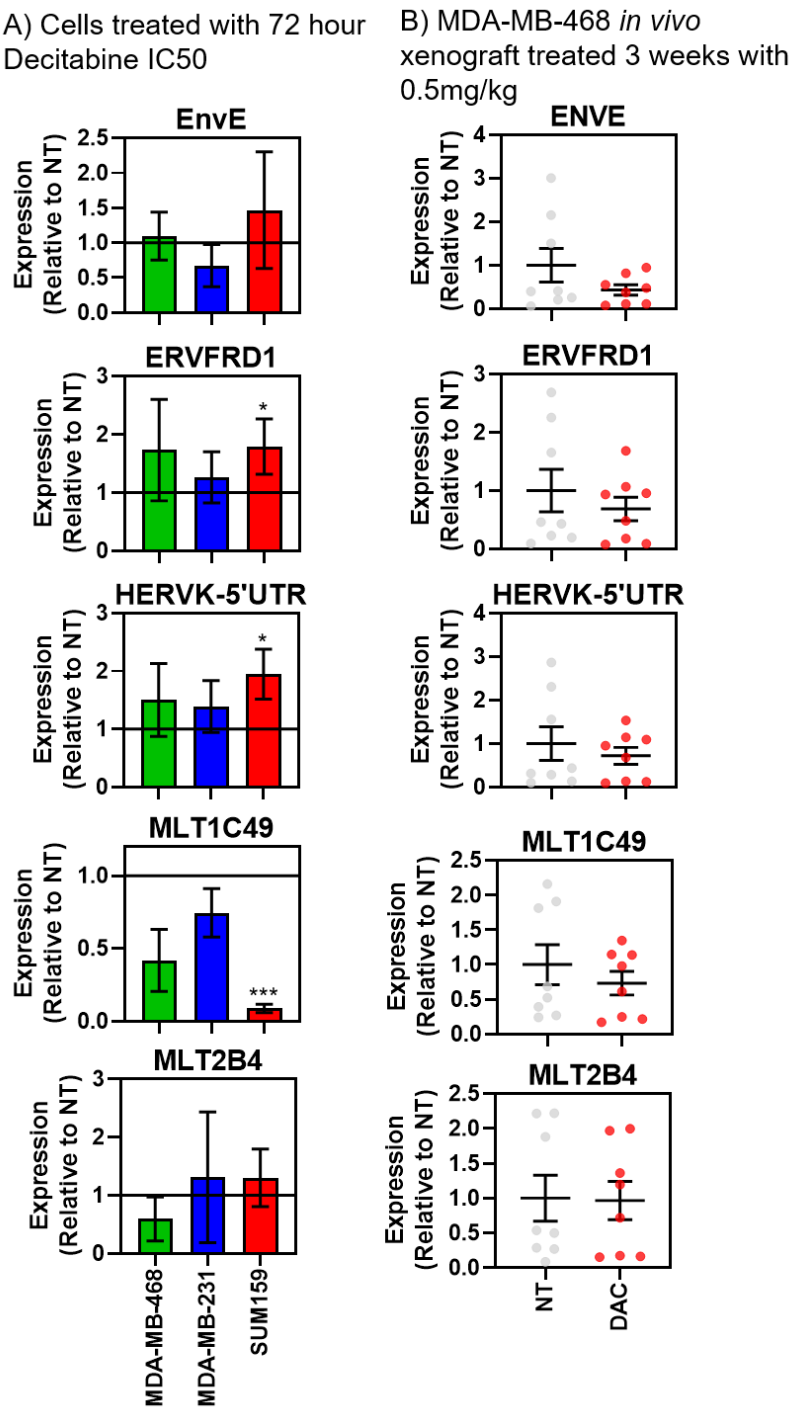

Figure 2.21: RT-qPCR of Endogenous Retroviral Elements ERVs in decitabine treated breast cancer cells. A) MDA-MB-468, MDA-MB-231 and SUM159 breast cancer cells treated with their respective cell confluency 72 hour decitabine IC_{50}s (0.6uM, 1uM, and 9uM), n=4; SD error bars; one sample t-test. **B)** MDA-MB-468 xenograft tumours treated with 0.5 mg/kg decitabine for 3 weeks (tumour growth in Figure 2.1B); 2-tailed t-test (NT n=8; DAC n=8). SEM error bars. $p<0.05$*, $p<0.001$***.

The general response to ERVs is better detected by assessing levels of double stranded (ds)RNA recognition pattern receptors melanoma differentiation-associated protein (MDA5, encoded by *IFIH1*) and retinoic acid-inducible gene I (RIG-I, encoded by *DDX58*) after decitabine treatment. RIG-I and/or MDA5 were induced by decitabine in most of the cell lines (Figure 2.20B). Downstream effectors such as mitochondrial anti-viral signaling protein (*MAVS*), transcriptional activator of interferon, interferon regulatory factor 7 (*IRF7*), anti-viral *OASL*, and interferon response mediator interferon-stimulated gene 15 (*ISG15*) were also generally induced in the cell lines, but did not correlate with sensitivity (Figure 2.20B). I also used our gene expression microarray data to evaluate a larger panel of reported interferon stimulated genes (Table 2.6) in decitabine treated MDA-MB-468, MDA-MB-231 and SUM159 cells (Figure 2.22A). These analyses suggest two points; 1) that strong induction of interferon-stimulated genes is not associated with increased sensitivity to decitabine, and 2) that decitabine-induced expression of IFN stimulated genes is not due a direct de-methylation of the promoter regions of these genes. Please note that the HM450 methylation data revealed that the most strongly induced genes (*DDX58, HPSE, IFI6, IFIT1, IFIT3, OAS3,* and *ZC3HAV1*) have an unmethylated promoter region (TSS200/1500, Figure 2.22B); therefore it is unlikely that the increased expression in a result of decitabine directly demethylating these genes. Regardless, the induction of some of these genes is consistent with a viral mimicry response being induced through increased MDA5/RIG-I in the breast cancer cells.

Table 2.6: Interferon-stimulated genes [304]. The fold changes in gene expression upon decitabine treatment is taken from our microarray data, ANOVA p-value <0.05*; p<0.01**; p<0.001***.

Interferon-Induced Gene	MDA-MB-468	MDA-MB-231	SUM159
ADAR	-1.01	1.02	-1.32
BST2	1.57	-1.14	1.01
CD74	-1.44	-1.11	1.08*
DDIT4	-3.26	-2.69	-8.48
DDX58	1.46*	1.44*	1.35*
DDX60	-1.07	1.29	-1.04
EIF2AK2	1.1*	-1.09	-1.18
GBP1	-1.04	-1.07	1.55**
GBP2	-2.48	1	-1.04
HPSE	1.68*	2.01*	3.51**
IFI44L	-1.42	1.25	1.37
IFI6	2.07	1.74**	2.32*
IFIT1	1.71	1.64**	2.26*
IFIT2	1.54*	1.87*	1.15
IFIT3	2.14***	1.48*	1.77
IFIT5	1.54*	-1.16	-1.08
IFITM1	1.1	1.18*	-1.08
IFITM2	-1.1	1.04	1.23
IFITM3	-1.01	1.13**	1.2*
IRF1	1.48*	1.1	-1.16
IRF7	1.53*	1.39	1.01
ISG15	1.08	1.43*	1.37
ISG20	-1.13	1.58*	-1.01
MAP3K14	1.68*	1.1	1.07
MB21D1	3.83**	1.14*	1.36
MOV10	-1.17	1.11*	1.06
MS4A4A	-1.08	1.05	-1.21
MX1	1.05	1.17	1.1**
MX2	1.02	1.04	1.41
NAMPT	1.14*	1.11**	-1.45
OAS1	-1.89	1.04	-1.15
OAS2	1.11	1.59*	1.04
OAS3	1.12	1.24*	1.31
OASL	-1.07	1.9*	1.26
P2RY6	-1.14	1.05	-1.21
PML	1	-1.11	1.08
RSAD2	1.21	2.11*	1.01
RTP4	1.15	1.1	-1.22
SLC15A3	1.41	1.11	1.15
SLC25A28	1	-1.12	-1.22
SSBP3	-1.46	1.12	1.56
SUN2	-1.28	1.06	-1.46
TREX1	-1.17	-1.07	-1.14
TRIM25	-1.08	-1.08	-2.27
TRIM5	-1.51	-1.1	1.06
ZC3HAV1	-1.08	1.41*	3.88**

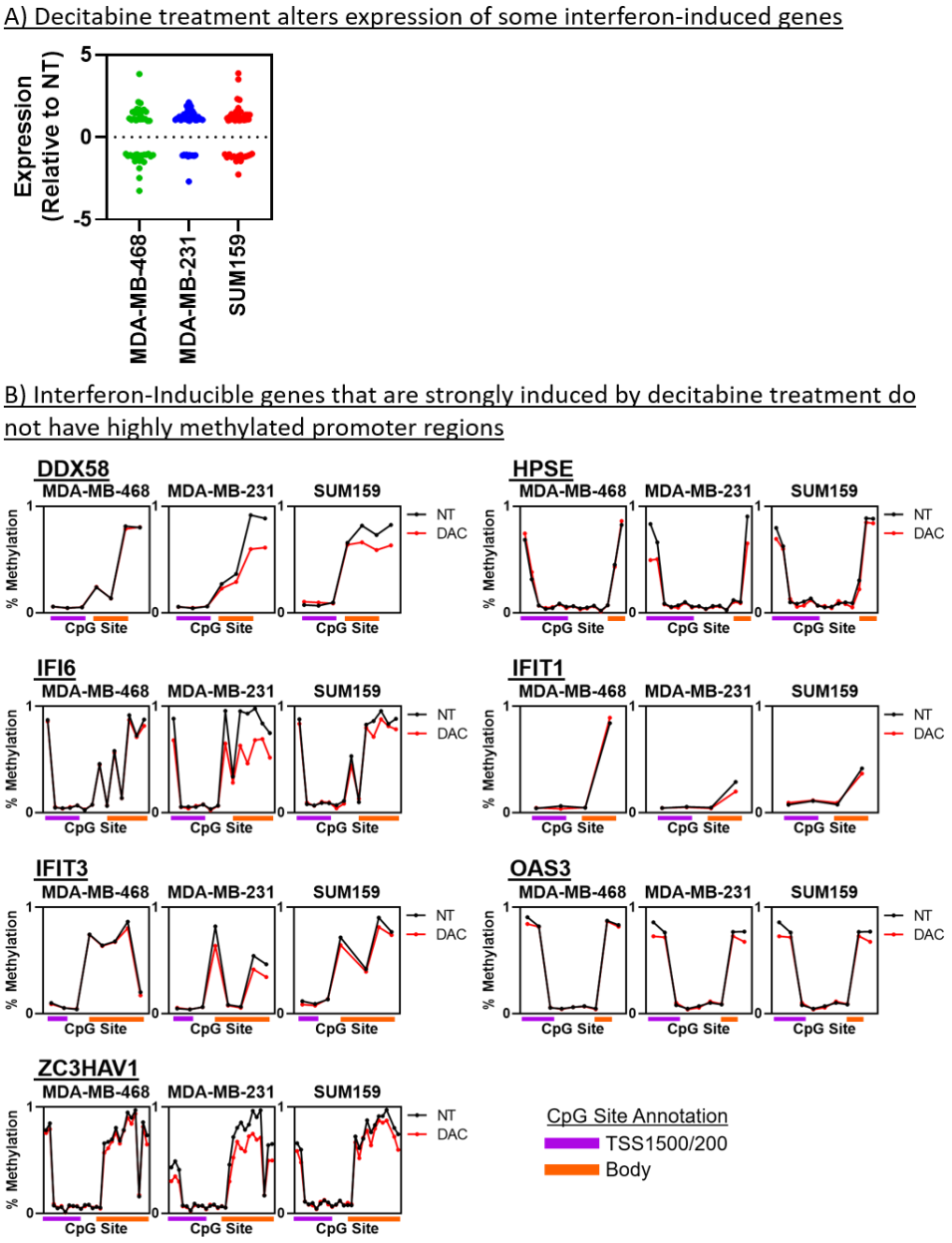

Figure 2.22: Decitabine treatment alters expression of some interferon-induced genes, but strength of induction is not associated with decitabine sensitivity. **A)** MDA-MB-468 (sensitive), MDA-MB-231 (intermediate), and SUM159 (resistant) cells were treated for 72 hours with 1μM decitabine and expression of the 46 genes noted in Table 2.6 were assessed via microarray and depicted as dots. **B)** Interferon-inducible genes that are strongly induced by decitabine treatment do not have strongly methylated promoter regions in MDA-MB-468, MDA-MB-231, and SUM159 breast cancer cells. HM450 analysis of 7 interferon-inducible genes that were strongly upregulated after 72 hours of 1μM decitabine. Generally, the promoter region (TSS1500/200) is unmethylated and the gene body is methylated which suggests that DNA methylation is not silencing these genes in any of these breast cancer cell lines.

Via knockdown, MDA5 has been shown to be an essential mediator of the viral mimicry response induced by decitabine in colorectal cancer[273]. I therefore knocked down MDA5 in the most decitabine sensitive MDA-MB-468 cells (Figure 2.23A) to determine, if like DCK knockdown, this would render the cells less sensitive to decitabine. However, in contrast to my results with DCK (Figure 2.3, knockdown of MDA5 did not make MDA-MB-468 cells resistant to decitabine (Figure 2.23A). Similarly, RIG-I knockdown did not make the cells more resistant to decitabine (Figure 2.23B). Together these data suggest that while the viral mimicry response is generally induced in breast cancer cells, it does not appear to be the key determinant of decitabine sensitivity in the cells *in vitro*.

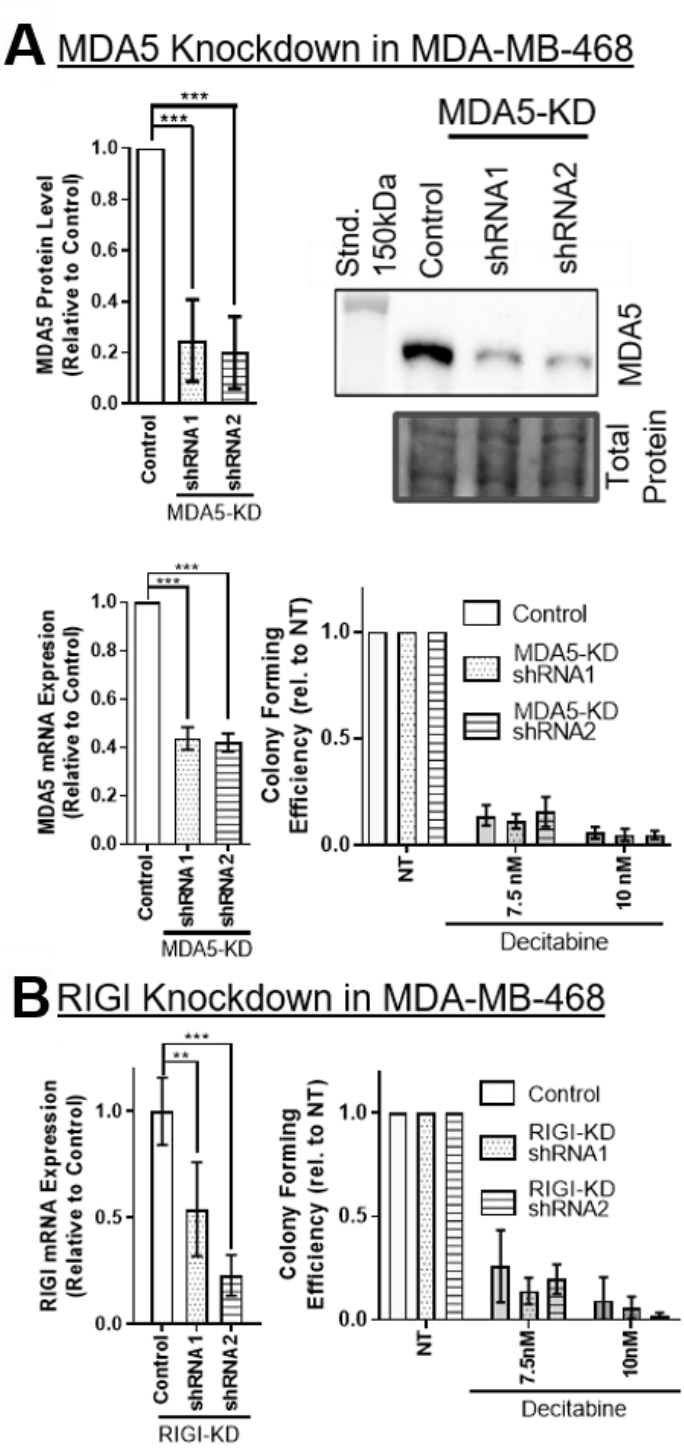

Figure 2.23: RIGI and MDA5 are not essential for decitabine sensitivity. shRNA-mediated knockdown of **A)** MDA5 (IFIH1) or **B)** RIGI (DDX58) in MDA-MB-468 cells does not affect *in vitro* DAC sensitivity in colony forming assay. SD error bars, ANOVA with Dunnett's post-hoc test; $p<0.01$**, $p<0.001$***. AJJ assisted with MDA5-KD colony-forming assay and generated Western blot.

2.3.7 *HIGH LEVELS OF EXPORTER ABCB1 DOES NOT LIMIT DECITABINE RESPONSE IN BREAST CANCER CELLS*

A consideration for the TNBC patients receiving decitabine in clinical settings is the potential presence of multidrug resistance acquired during initial chemotherapy treatment. Increased expression of exporter multidrug resistance gene ABCB1, is a common resistance mechanism for many drugs[162,305]. Gene expression from 56 matched breast tumour samples pre- and post- chemotherapy treatment showed that *ABCB1* expression was elevated post-chemotherapy in patients with at least partial response to treatment (Figure 2.24A). This suggest that the effect of ABCB1 expression in breast cancer needs to be assessed for its impact on decitabine response.

I assessed expression of *ABCB1* across the ten breast cancer cell lines and noted increased expression in decitabine resistant SUM159 and Hs578T cells, but also decitabine sensitive MDA-MB-468 cells (Figure 2.24B). This may suggest that increased ABCB1 is a potential mechanism of decitabine resistance in breast cancer; however, knockdown of ABCB1 in decitabine sensitive MDA-MB-468 cells had minimal impact on decitabine sensitivity (Figure 2.24C).

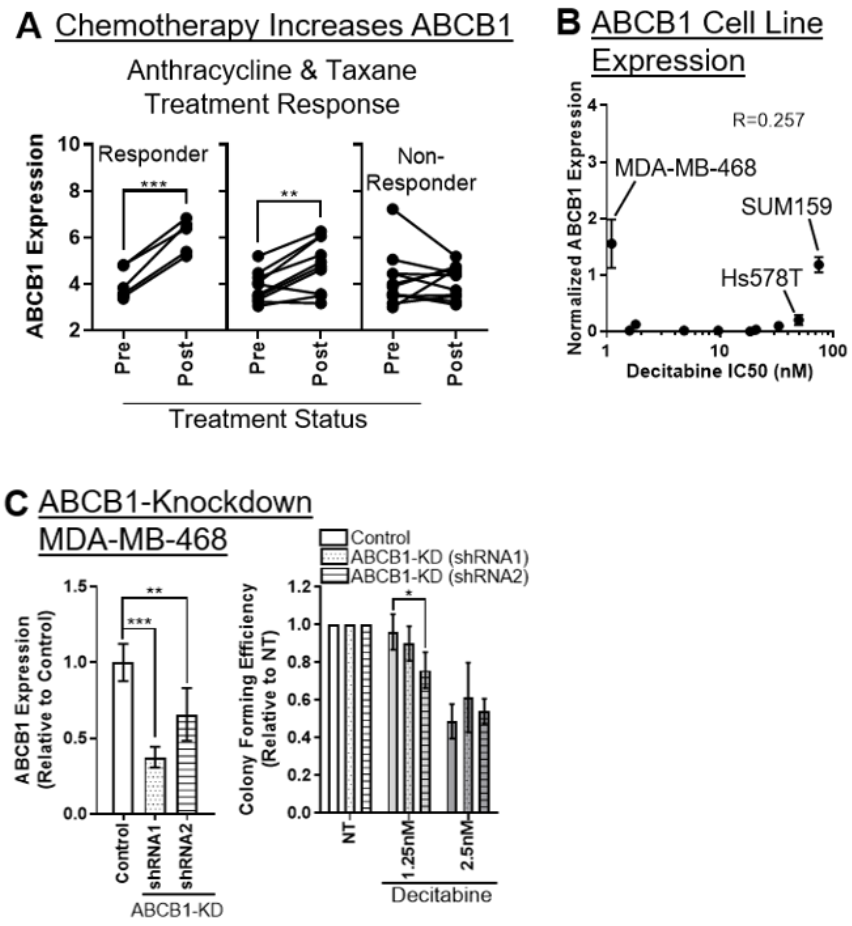

Figure 2.24: ABCB1 increases with taxane treatment but has minimal effects on decitabine sensitivity. A) ABCB1 expression via microarray in GSE28844 dataset of breast cancer patients treated with anthracyclines and taxanes (paired two-tailed t-test). **B)** Expression of ABCB1 across breast cancer cell lines by RT-qPCR. **C)** shRNA mediated ABCB1 knockdown and *in vitro* decitabine sensitivity; ANOVA with Dunnett's post-hoc test. $p<0.05$*, $p<0.01$**, $p<0.001$***. CD assisted with RT-qPCR.

To further assess how multidrug resistance impacts decitabine response, I used a variant of the MDA-MB-231 cell line with acquired taxol- and anthracycline-resistance and ABCB1-overexpression[290]. I confirmed the resistant cell line had increased ABCB1 expression, was significantly more resistant to paclitaxel than the control cell line, and that paclitaxel resistance in the cells could be reduced by the addition of the ABCB1 inhibitor

verapamil (Figure 2.25A). Importantly, the taxol-resistant MDA-MB-231 cells were not resistant to decitabine and ABCB1 inhibition did not further sensitize cells to decitabine, implying that ABCB1 does not play a major role in decitabine response (Figure 2.25B). Therefore, increased expression of ABCB1 in the tumours of breast cancer patients that will receive decitabine after having received chemotherapy will not be a significant barrier to decitabine response.

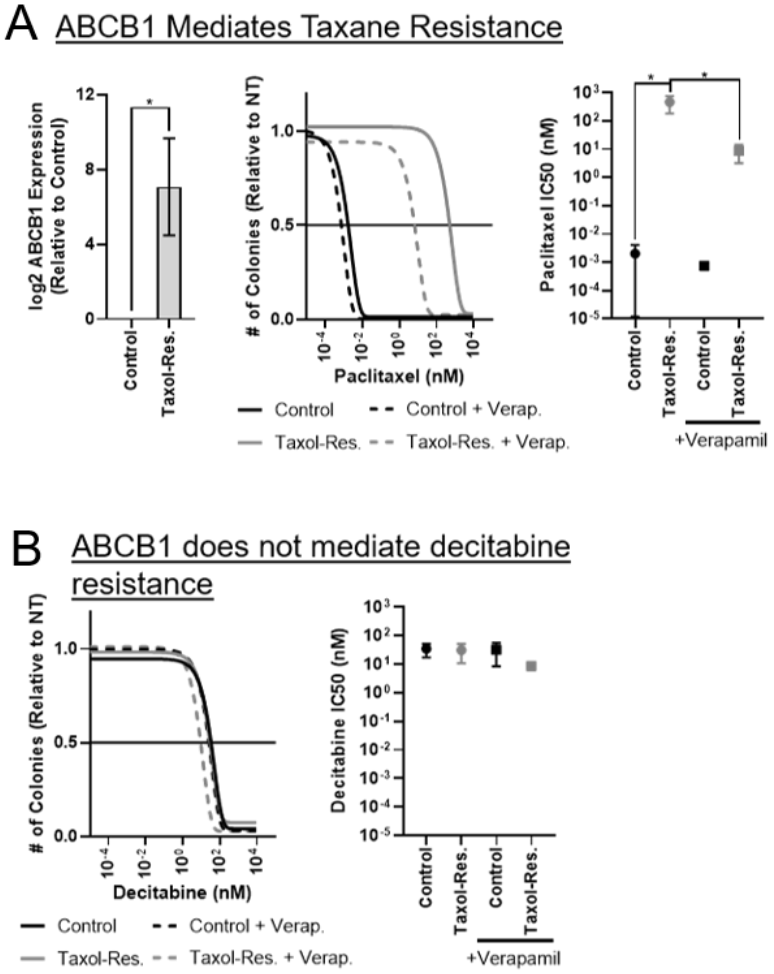

Figure 2.25: ABCB1 causes resistance to taxanes but has minimal effects on decitabine sensitivity A) ABCB1 expression via RT-qPCR in taxol-resistant MDA-MB-231 cells; one-tailed t-test. Colony forming IC_{50} assay in taxol-resistant MDA-MB-231 treated with ABCB1 inhibitor verapamil and paclitaxel or **B)** decitabine. ANOVA with Tukey's post-hoc; $p<0.05$*, $p<0.01$**, $p<0.001$***. SRH and KBG supplied taxol-resistant MDA-MB-231 cell lines.

2.4 DISCUSSION

My comprehensive analysis of decitabine response in breast cancer cells screened many of the potential mechanisms of decitabine to determine if essential factors and/or predictors of sensitivity could be identified that may impact the success of ongoing clinical trials in TNBCs. Together, this study revealed a range of responses to decitabine in breast cancer that could not be predicted based on commonly proposed mechanisms (e.g. demethylation of tumour suppressor genes, viral mimicry response). My transcriptome and methylome analyses also demonstrated that while decitabine induces genome-wide expression changes and demethylation, these effects are not necessarily paired and do not correlate with sensitivity. Instead, it became apparent that the many gene expression changes induced by decitabine are either an indirect result of its demethylation and/or a consequence of cell death, DNA damage, and immune responses being induced. Notably, I describe a requirement for DCK, the decitabine processing enzyme, for decitabine-induced growth suppression and gene expression changes. DCK is comparatively abundant in TNBC and is increased post-chemotherapy in non-responding patients. This combined with my demonstration that multidrug-resistant/ABCB1-overexpressing breast cancer cells remain sensitive to decitabine, suggests that decitabine may be useful as part of a second-line therapy regimen for TNBC patients.

The initial enthusiasm for hypomethylating agents (e.g. decitabine and azacytidine) to treat MDS has been tempered by years of clinical use which indicate that fewer than half of patients maintain a response to the therapy[306]. This is also true for chronic monomyelocytic leukemia (CMML, for which azacytidine and decitabine are the only approved drugs), where overall response rates hover at 40% and complete response at

<20% [307]. As an AML therapy, overall response to decitabine is also ≈40%, though there is some encouraging data to suggest a precision medicine approach could work for treating older AML patients with decitabine. For example, *DNMT3A* mutations, *TET2* mutations and *IDH1/2* mutations have all been associated with favorable outcomes in AML (and some MDS cases)[308–310]. However, similar stratification strategies are unlikely to work in breast cancer and other solid tumours; since mutations in epigenetic machinery genes are far less common[285,286]. Regardless, even for these blood malignancies/disorders there are many other clinical factors such as age, cytogenetics, prior treatment regimen, global or gene-specific methylation, and gene expression patterns that influence response to decitabine[311]. While there is compelling evidence for each of these factors individually, most recent studies cannot form a cohesive molecular profile of favorable decitabine response for AML, MDS, or CMML. As such, my gene-specific and genome-wide transcription and methylation results in breast cancer are unsurprising and suggest that predicting decitabine response will be multi-factorial and decitabine will likely be used in combination with other drugs.

Potential rational combinations include using DNA hypomethylating agents followed by immunotherapeutics such as checkpoint inhibitors. This strategy should increase the immunogenicity of tumours by inducing expression of hypermethylated cancer testis antigens (and HERVs) with decitabine, and concomitantly inhibit the downregulation of elicited anti-tumour cytotoxic T cell responses by blocking PD1-PDL1 or CTLA4-CD80/86 interactions. This is the intended strategy for an ongoing clinical trial for TNBC (NCT02957968), where patients are treated sequentially with decitabine plus checkpoint inhibitor pembrolizumab (anti-PD1), followed by standard chemotherapy.

In these immunotherapeutic-based combination approaches, it is also important to consider how decitabine affects PDL1 expression, and in this regard the data is somewhat contradictory. In murine solid tumour studies, decitabine reduced PDL1 levels on tumour cells and subsequently improved infiltration of cytotoxic CD8+ T-cells and enhanced anti-PD1 immunotherapy [312–315]. In another study examining DNA methylation and PDL1 expression patterns in melanoma cell lines and TCGA melanoma patient data, decitabine induced expression of PDL1 in cells, and in hypomethylated treatment-naïve patient tumours, there was strong expression of "viral mimicry" HERVs and higher PDL-1[316]. However, decitabine treatment also increased PDL1 levels in MDS, CMML, and AML patients [317]. Importantly, MDS patients with the most elevated PDL1 post-decitabine were also the most resistant to decitabine therapy. Together, these studies underlie the importance of determining how decitabine effects immunogenicity in the clinic versus in pre-clinical animal studies, and that these effects may also be cancer-type-specific.

Based on the mixed results of these well-established immunogenic pathways, we should be hopeful but cautious when interpreting any viral mimicry responses induced by decitabine. I see a clear induction of the viral mimicry response genes (e.g. *OASL* and *ISG15*) in breast cancer cells; however, this was not paired with a favorable decitabine response. The direct cytotoxicity of MDA5-mediated viral mimicry that was observed in colorectal cancer cells[273] was not replicated in my MDA5 knockdown breast cancer cells. Importantly, I did not assess the immunogenicity of decitabine treatment; hence, it is possible that while induction of this pathway is not directly cytotoxic in breast cancer cells, may be important for inducing anti-tumour effects in immunocompetent models and patients.

CHAPTER 3: AN UNBIASED GENOME-WIDE SCREEN IDENTIFIES MTHFD2 AS A MEDIATOR OF DECITABINE RESPONSE IN BREAST CANCER

Contribution statement

I wrote the manuscript and designed the experiments with the guidance of Dr. Paola Marcato. I performed experiments and collected data with assistance as follows:

Dr. Paola Marcato: generation of MDA-MB-231 Decode shRNA library cell line and assistance with orthotopic injection of MDA-MB-231 cells. Philip Parsons: standard curve for RT-qPCR primers. Dejan Vidovic and Thomas Hyunh: generation of several lentiviral products. Dr. Krysta Mila Coyle: HM450 DNA methylation array. Brianne Marie Cruickshank: assistance with intraperitoneal decitabine injections. Mona Challa: RT-qPCR of tumours. Dr. Kerry Goralski and Dr. Steven Robert Hall: acquisition of taxane-resistant MDA-MB-231 cells. Dr. J Patrick Murphy, Michael Anthony Giacomantonio, Dr. Alejandro Cohen, and Hayley Walsh: mass spectrometry sample preparation, data collection and normalization. Dr. Ian Weaver: LINE1 and CCL20 bisulfite pyrosequencing.

3.1 INTRODUCTION

Cancer is a generally thought of as a mutation-driven disease; however, in addition to mutations, epigenetic modifications such as DNA methylation play a role in the progression of cancer[88]. Hypermethylation of CpG sites at the promoter region of a gene can effectively silence expression of that gene; and in cancer, hypermethylation often silences tumour suppressor genes (TSGs)[61,318]. DNA methylation and other epigenetic modifications (e.g. histone acetylation) are complicit in all of the cancer hallmarks defined by Hanahan and Weinberg[22] as aberrant epigenetic marks have been shown to regulate expression of many hallmark pathways. As such, DNA methylation, especially hypermethylation and silencing of key growth regulatory genes, has been presumed to be a potential target of epigenetic therapy for solid tumours.

DNA methyltransferases (DNMTs) are a group of enzymes required for DNA methylation, and inhibitors of these proteins have the potential to reduce hypermethylation of TSGs and may be effective cancer therapies[268]. Once such DNMT inhibitor, decitabine (5-aza-2'-deoxycytidine), is currently approved by the FDA to treat myelodysplastic syndromes and is in clinical trials to treat solid malignancies (NCT01799083, NCT03875287, NCT01799083, etc.).

DNMT inhibitors are promising chemotherapeutics for treating many cancers because a) most cancers present with aberrant DNA methylation, b) this methylation evolves with tumour progression, c) these modifications are far more plastic than mutations and therefore may be more "druggable"[61,318]. However, like in most solid tumours, the plasticity and abundance of promoter DNA hypermethylation in breast cancer makes it difficult to determine which CpG sites are most important in the establishment and

maintenance of a tumour. In general, two approaches have been taken to elucidate the essential DNA methylation changes for breast cancer: 1) determining methylation status of known tumour suppressor genes and 2) identifying cancer-specific methylation changes by comparing the cancer epigenome to the normal tissue epigenome[74,80,85,319–324].

While previous studies have revealed an important prognostic and mechanistic role of DNA methylation in cancer, there is only occasional overlap of the gene lists generated by these studies. This highlights a key issue in the study of cancer DNA methylation: it is difficult to isolate the key "driver" events from the many "passenger" events. Most epigenome-wide studies depend on correlative evidence and identify 10,000s of potential gene hits, while methylation analysis of known TSGs excludes all TSGs that have not yet been identified. Furthermore, it is unknown if these hits contribute to the susceptibility of a cancer cell to a de-methylating agent. Determining the key "driver" DNA methylation events in breast cancer with a novel approach will add to our understanding of the role of DNA methylation in breast cancer and will reveal a cohort of patients whose tumours may respond to demethylating agents such as decitabine.

To overcome the limitations of previous attempts to generate a phenotypically relevant DNA methylation profile in breast cancer and to also identify biomarkers that predict response to decitabine, I performed a knockdown screen. My approach to identify driver DNA methylation events is simultaneously functional and genome-wide. An *in vivo* genome-wide knockdown screen was performed using the ThermoFisher Decode lentiviral knockdown library in the MDA-MB-231 cell line. These shRNA library MDA-MB-231 cells were orthotopically implanted in female NOD/SCID mice and the mice were divided into no treatment and decitabine treatment groups. Decitabine treatment resulted in smaller

tumours—however cells that harboured the shRNA knockdown of a hypermethylated tumour suppressor gene, or a gene required for decitabine sensitivity would have a growth advantage.

It should be noted that decitabine's mode of action is not limited to resurrection of tumour suppressor genes, and that growth suppression in decitabine-treated cells has been linked to other potential mechanisms such as induction of the DNA damage response, cytotoxicity induced by global demethylation, and induction of the dsRNA response[325–327]. It is unclear which consequence of decitabine is essential for the successful treatment of patients. There is evidence that the main mode-of-action for de-methylation therapies is dependent on the tissue of origin (e.g. ovarian and colorectal tumours have a strong dsRNA response) and a suggestion that some tumours are more epigenetically "primed" to respond to de-methylating therapy than others (i.e. a tumour with more hypermethylated promoters may be more inclined to respond). Defining biomarkers of response to de-methylation therapy is a step towards the effective use of decitabine since it will allow patient stratification.

The genome-wide knockdown screen led to the identification of several putative hypermethylated TSGs; however only knockdown of methylenetetrahydrofolate dehydrogenase 2 (MTHFD2) bestowed relative resistance to MDA-MB-231 tumours treated with decitabine. Most striking was how knockdown of MTHFD2 restricted the growth of MDA-MB-231 tumours; this is likely because MTHFD2 is vital for nucleotide biosynthesis in cancer cells and reduced nucleotide pools slow tumour growth[328,329]. The only synergistic result of combined MTHFD2-KD and decitabine treatment came in the

form of increased chemokine (C-C motif) ligand 20 (CCL20) expression which is known to promote breast cancer resistance to chemotherapies.

This genome-wide screen did not reveal the hypothesized panel of functional hypermethylated tumour suppressor genes, instead I have found that MTHFD2 is a key metabolic enzyme which supports breast tumour growth. MTHFD2 is consistently up-regulated in many cancer types, and its expression significantly correlates with poor clinical outcome in breast cancer, pancreatic carcinomas, renal cell carcinoma, leukemia and in a particularly aggressive metabolic subtype of hepatocellular carcinoma[330–337]. MTHFD2 is a potential target for cancer therapy in its own right, and high MTHFD2 expression may be a marker for breast cancer patients with aggressive disease that may be suitable for nucleotide-based therapies like decitabine.

3.2 MATERIALS AND METHODS

3.2.1 *CELL CULTURE*

Cancer cell lines were obtained from ATCC (American Type Culture Collection). MDA-MB-231, MCF7, SKBR3, T47D, and HEK293T cells were grown in Dulbecco's Modified Eagle Medium (DMEM; Invitrogen) supplemented with 10% fetal bovine serum (FBS; Invitrogen) and 1X antibiotic antimycotic (AA; Invitrogen). MDA-MB-436 cells were grown in Leibovitz's Medium (L-15; Invitrogen) supplemented with 10% FBS, 1X AA, 10 µg/mL human insulin (Sigma), and 16 µg/mL L-glutathione (Invitrogen). Cells

were cultured in a humidified 37°C incubator with 5% CO_2, except for MDA-MB-436 which were cultured without the addition of CO_2.

MDA-MB-231 cells with acquired ABCB1-mediated taxane resistance (Taxol-res) and the matched taxane sensitive cells (Control) were previously generated and characterized[290] and maintained in the same MDA-MB-231 growth conditions described above.

3.2.2 *GENERATION OF SHRNA LIBRARY IN MDA-MB-231 CELLS*

Three Decode lentiviral shRNA pools containing 10,000 shRNAs per pool (30,000 total), targeting 15,221 RefSeq mRNA accession numbers corresponding to 11,954 human genes with well categorized biological functions or processes were purchased from Thermo Scientific (catalogue # RHS5339). The titre of the shRNA pools was determined using HEK293T cells at $\geq 5 \times 10^8$ transfection units (TU)/mL. Using the pGipZ scramble shRNA control (catalogue # RHS4348), we determined the relative TU/mL for MDA-MB-231 compared to HEK293T cells (HEK293T: 4.53×10^8 TU/mL; MDA-MB-231: 1.09×10^8 TU/mL). The relative transduction efficiency of MDA-MB-231 was thus calculated as 0.24.

Following the manufacturer's instructions, we generated MDA-MB-231 shRNA pools with 100-fold representation of the shRNA library. Each pool was transduced into MDA-MB-231 using DMEM with 10% FBS and 8 µg/mL sequabrene (Sigma). To achieve 100-fold representation of each shRNA pool, the cells were infected at a multiplicity of infection (MOI) of 0.3. 4×10^6 MDA-MB-231 cells (cultured in 150 mm dishes) were

transduced with 1.2 x 10^6 TU of each pool (11.0 µL). Lentivirus was left for 6 h before replacement with complete media (DMEM with 10% FBS and 1x AA).

Two days post-transduction, the expanded cells harbouring the shRNA sequences were selected with 1.5 µg/mL puromycin, maintained in 0.25 µg/mL, and immediately frozen to minimize changes in shRNA representation (> 2 x 10^6 cells per vial).

3.2.3 *MDA-MB-231 IN VIVO DECITABINE-TREATED SHRNA SCREEN*

All animal studies have been conducted in accordance with the ethical standards and according to the Declaration of Helsinki and the Canadian Council on Animal Care (CCAC) standards, and performed under protocol numbers 13-010, 15-013, 17-011, and 19-013. Tumour volume was quantified as (mm^3, length x width x height / 2).

MDA-MB-231 shRNA screen cells admixed 1:1 with high concentration phenol red-free Matrigel (BD Bioscience) and 2x10^6 cells were orthotopically injected into lower mammary fat pad of 8-9 week-old female NOD/SCID mice (n=18; each pool n=6). After development of palpable tumours (day 24) mice were divided into treatment or no treatment groups. Treatment group (n=9) received intraperitoneal injections daily for 8 days of 0.5 mg/kg decitabine; no treatment received PBS (phosphate buffered saline; n=9). On day 32 post-cell injection, mice were sacrificed. This experiment was independently repeated a second time so that n=6 for relative shRNA abundance analysis.

3.2.4 *Analysis of relative knockdown abundance in decitabine-treated in vivo shRNA screen*

Tumour tissue was minced and homogenized into 1-2mm^3 pieces and digested for 14 hours in the PureLink® Genomic Digestion Buffer and Proteinase K (Invitrogen) at 55°C. Genomic DNA was isolated from tumours using the PureLink® DNA purification kit as per manufacturer's specifications. Molecular barcodes unique to each shRNA were then amplified from genomic DNA using Phusion Hot Start II DNA Polymerase (Thermo Fisher Scientific) and the negative selection primers included with the Decode screen (RHS5339) as per manufacturer's instructions. PCR products were run on a 2% agarose ethidium bromide gel alongside 1kb Plus DNA ladder (Invitrogen), and the resulting 250-350bp sequence was purified with the PureLink® PCR Purification kit (Invitrogen) as per manufacturer's specifications. 1 µg of DNA from each pool was combined, for a total of 3 µg per sample.

Samples were labeled, hybridized, scanned, and normalized by Ambry Genetics (California, USA) following instruction in the Decode Array kit. DNA quality and concentration were determined on a NanoDrop spectrophotometer (ThermoFisher). Labeling reactions were prepared using Thermo scientific Decode RNAi Pooled Lentiviral shRNA screening libraries protocols and the SureTag complete DNA labeling protocol for aCGH (version 7.1) with 1 µg DNA input. The protocol consists of two parts: labeling of the RNA and hybridization.

First, 1ug of decitabine-treated samples were labeled with Cyanine 5-dUTP (Cy5) and no treatment samples with Cyanine 3-dUTP (Cy3) using Exo-Klenow fragment. Labeled DNA was then purified using Millipore Amicon Ultracel-30 filters and the

labeling efficiency determined by the Nanodrop spectrophotometer. Next, the labeled DNA was prepared for hybridization with Human Cot-1 DNA and placed on the decode array and hybridised at 65°C for ~17-20 hours. Finally, the arrays were washed and scanned at 5µm resolution on an Agilent G2565CA High Resolution Scanner

Data was processed through Agilent's Feature Extraction software version 11.5.1.1. All runs passed the recommended quality control metrics set forth by Agilent. Quartile normalization was applied to each sample. Fold changes for each sample were calculated and shRNAs which were overrepresented (enriched) and underrepresented (depleted) in the experimental sample (MDA-MB-231 with decitabine treatment) were identified.

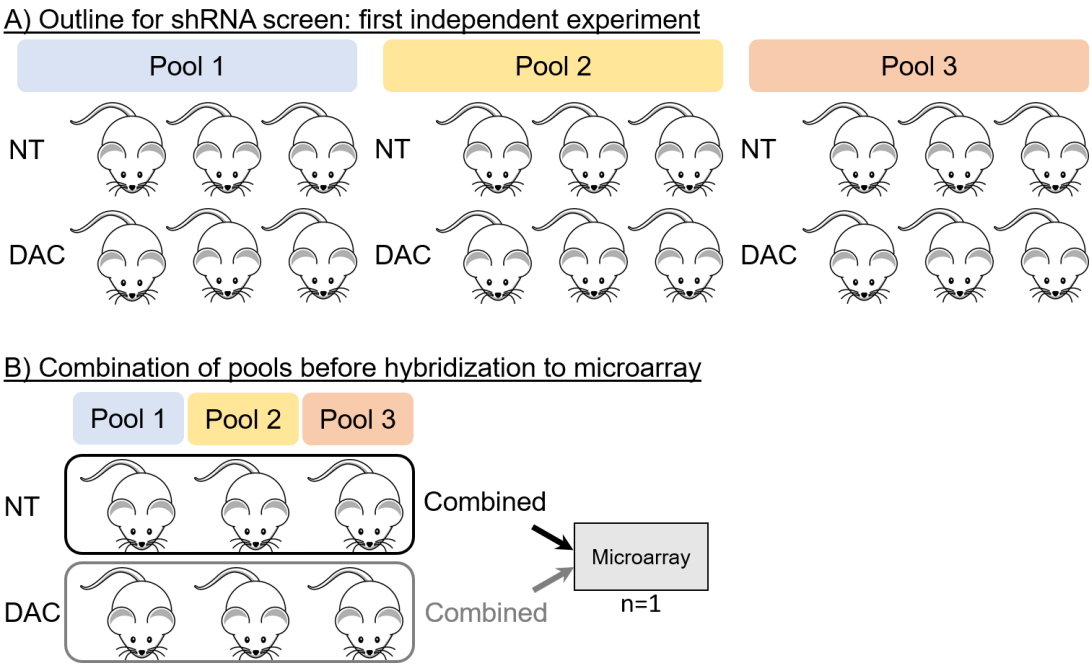

Figure 3.1: Schematic for combining the three Decode shRNA pools to obtain relative shRNA abundance. **A)** Each shRNA pool was injected into 6 mice, 3 of which were treated with decitabine. **B)** To obtain 1n of relative abundance for every shRNA in the screen, DNA from 1 tumour for each pool was pooled together, NT pooled DNA was labeled with Cy3 and DAC pooled DNA was labeled with Cy5 prior to hybridization to custom Decode microarray.

3.2.5 *Analytic Technique for Assessment of RNAi by Similarity (ATARiS)*

ATARiS was hosted on GenePattern servers and accessed through the integrative analysis platform GenomeSpace[338–340]. Instead of focusing on the effects of individual shRNAs, this GenePattern module assessed patterns of shRNA representation from the genome-wide screen to generate a per-gene value of the phenotypic effect of gene suppression. ATARiS generated so-called gene "solutions" which contained ≥2 shRNAs which exerted similar effects in the screen. Additionally, a consistency score (c-score) was quantified for each solution which represented the confidence that the observed effect of the shRNA was due to on-target gene suppression (e.g. an shRNA which is consistently enriched (5n/6n) in the decitabine samples would have a high c-score).

3.2.6 *Generation of individual knockdown clones*

Lentiviral shRNA knockdown clones (Table 3.1) were generated using the pGipZ vector (Dharmacon). Briefly, lentivirus was assembled in HEK293T cells using a second-generation packaging system (pMD2.G, pSPAX2). Lentiviral supernatants were collected and filtered (0.45 μm) prior to being applied to MDA-MB-231 cells. Clones were selected by administering 1.5 μg/mL puromycin and subsequently maintained in 0.25 μg/mL puromycin media. For all knockdown clones created, a GIPz vector control clone (containing a scrambled non-specific sequence in place of an shRNA) was generated simultaneously. Verification of knockdown was done through RT-qPCR.

Table 3.1: pGIPz IDs for shRNA knockdowns generated in MDA-MB-231 cells

Gene	pGIPZ Oligo ID
AGBL2	V2LHS_157785
APOD	V2LHS_132618
CD82	V2LHS_133578
CD83	V2LHS_28332
COL16A1	V2LHS_150774
CROCC	V2LHS_256714
DNAH5	V2LHS_113470
ERN1	V2LHS_19871
HIST1H2BA	V2LHS_100002
KLHL3	V2LHS_154277
MTHFD2	V2LHS_90966
	V2LHS_90968
NSMCE2	V2LHS_179144
OGT	V2LHS_28023
RRN3	V2LHS_175550
SLITRK4	V2LHS_234490
SNAI2	V2LHS_153128
TMBIM4	V2LHS_97338
TRPC4	V2LHS_97884
UBE2J1	V2LHS_233446
XRCC4	V2LHS_202124

3.2.7 *Reverse transcriptase quantitative PCR (RT-qPCR)*

RNA was extracted from untreated and decitabine-treated cells (1μM decitabine for 72 hours with media refreshed daily as previously described in Chapter 2). Cells were collected in Trizol (Invitrogen) and RNA was purified using a PureLink RNA kit (Invitrogen Thermo Fisher Scientific) following the manufacturer's instructions. For tumour RNA, 50 mg of minced tumour tissue was homogenized in Trizol and RNA was purified using the PureLink RNA kit. Equal amounts of purified RNA were then reverse transcribed to cDNA using iScript (Bio-Rad) as per manufacturer's instructions. Diluted cDNA was used in RT-qPCR reactions with gene-specific primers (Table 3.2) and SsoAdvanced Universal SYBR Supermix (Bio-Rad) as per manufacturer's instructions

with a CFX96 or CFX384 Touch Real-Time PCR Detection System (Bio-Rad). Standard curves were generated for each primer set and primer efficiencies were incorporated into the CFX Manager software (Bio-Rad). Relative expression for decitabine inducible genes was quantified using the ΔΔct method of the CFX Manager Software (Bio-Rad), where gene-of-interest quantification was normalized to reference genes GAPDH and B2M and then made relative to no-treatment control mRNA.

Table 3.2: RT-qPCR primer sequences

Gene	Forward Primer	Reverse Primer
ACRC	TGGCTGCTACACCAAATCGT	ATGGCACCATGACCAGAGAC
AGBL2	TCACGTTGCAAGGACCAGAA	AGGTCAGTTCGCAAGGTGAG
APOD	AAGCCACCCCAGTTAACCTC	TACGGTGCCGATGGCATAAA
B2M	AGGCTATCCAGCGTACTCCA	CGGATGGATGAAACCCAGACA
CCL20	ATTTATTGTGGGCTTCACACGG	GGATTTGCGCACACAGACAA
CD82	ACTGGACAGACAACGCTGAG	TGTCCTCTTCCCCCTTGACT
CD83	CTGCTGCTGGCTCTGGTTAT	GGGAAGATACTCTGTAGCCGTG
COL16A1	CCAGGTGAAAAAGGACCACGA	CCATCCAAAGTCCCGGAGC
CROCC	TTATCCAGACACTGGAGAGCAG	CGGGTGACAATCTCCCTGATAA
DNAH5	TGGAAGCATAGCGTCACTCG	TCAGGTCCAAACAGGAAGCC
ERN1	AAAACTACGCCTCCCCTGTG	GTCAGATAGCGCAGGGTCTC
GAPDH	GGAGTCAACGGATTTGGTCGTA	TTCTCCATGGTGGTGAAGAC
HIST1H2BA	TTGAGCGTATAGCGAGCGAG	AGCGCACTGCTGTCTGAAT
KLHL3	TTGGAGTGCTTAGCGGACAG	CTGCCACTTGCTTCCAGGTA
MAEL	TTTCACACCACTGAGGAGGC	GCCTCCAAGGAGAGCTTGAT
MTHFD2	TTCTGGAAGGAAACTGGCCC	GCCAACCAGGATCACACTCA
NSMCE2	AGAGCCCGCTCTCACTTTTC	GGTAGTCCAAGCTGTCTCCG
OGT	GTTCCGGCCCATGTTGTTTC	GGCTTCAAACCCTGGGAACT
RRN3	CTGTGACAGAAGTCTTGCTGAAG	CGGAATTCTAGCAGCCAGTTG
SLITRK4	CCGGCAGTGATTTTGACGTG	TGTGACCATTGGGAGTGGTG
SNAI2	AGACCCCCATGCCATTGAAG	GGCCAGCCCAGAAAAAGTTG
TDRD1	CAACTGCAAAGTGGCCGAAA	AAATCAGAGCGTGGAGGCAA
TMBIM4	CTGTTTGCCCTCGGATCTCT	AACTGCCACAGTCAGAGCTT
TRPC4	GCATGGCATGAAACATGGCT	TCCTTAGAGGGATGCGGTCT
UBE2J1	AACATTCCAGGGTGCTACGG	TCGAGGGCTCATGGAGGTAT
XRCC4	ATTCAGCATGGACTGGGACAG	GGTCCTGCTCCTGACAACAAT
ZNF595	CCCCTGAAGAGTGGAAATGTCT	ACCAGGTCTGGGTTAGAGATCA

3.2.8 *HUMAN METHYLATION 450K (HM450) ANALYSIS*

Genomic DNA was extracted from untreated and decitabine-treated MDA-MB-231 cells (1μM DAC for 72 hours with media refreshed daily) using the PureLink DNA kit (Invitrogen). Methylation analyses using the HM450 bead chip array (Illumina) was performed by the Centre for Applied Genomics at the Hospital for Sick Children (Toronto, Ontario, Canada), including bisulfite conversion, hybridization, background subtraction, and normalization.

3.2.9 *BREAST CANCER PATIENT GENE EXPRESSION AND METHYLATION ANALYSIS*

DNA methylation (HM450) and matched gene expression (RNA Seq; log2 RSEM+1) data for n=720 breast tumour samples and n=80 normal breast tissue samples (from reduction mammoplasties) from the TCGA Cell, 2015 dataset was accessed through TCGA Wanderer[295].

3.2.10 *IN VIVO DECITABINE TREATMENT*

MDA-MB-231 control, APOD-KD, or MTHFD2-KD cells were admixed 1:1 with high concentration phenol red-free matrigel (BD Bioscience) and $2x10^6$ cells were orthotopically injected into lower mammary fat pad of 8-9 week-old female NOD/SCID mice. Once palpable tumours formed, the mice were treated with 0.5 mg/kg decitabine (DAC) or vehicle control (phosphate buffered saline, PBS) by intraperitoneal injection for 3/5 day cycles as previously described[274]. Throughout the experiment, tumour volume was quantified (mm^3, length x width x depth / 2). Tumours were excised and weighed before being processed for metabolomics, RNA extraction (for gene expression), or DNA extraction (for DNA methylation analysis).

3.2.11 *HIGH PERFORMANCE LIQUID CHROMATOGRAPHY/MASS SPECTROMETRY (HPLC-MS) METABOLOMICS*

Metabolites were extracted from tumour samples by crushing 50 mg of minced tumour tissue into ice-cold 80% methanol. To eliminate large cellular debris, samples were centrifuged at 500 x g for 5 minutes and the supernatant was decanted to a new tube. Samples were centrifuged at 13,000 x g for 5 min. A 25 µL aliquot of supernatant was

added to 225 µL of hydrophilic interaction liquid chromatography (HILIC) loading buffer containing 95% acetonitrile, 2 mM ammonium hydroxide, and 2 mM ammonium acetate. Samples were centrifuged again at 13,000 x g for 5 min. Next, 50 µL injections of the supernatant were loaded on an Acquity UPLC BEH Amide, 1.7 µm particle size, 2.1 x 100 mm column (Waters #186004801). Multiple reaction monitoring (MRM) was performed using a Sciex 5500 QTRAP mass spectrometer (MS) using a previously described acquisition method[341]. This hybrid dual quadrupole linear ion trap mass spectrometer (MS) was used for quantitative profiling of endogenous polar metabolites, both positive and negative modes, from an *in vivo* source. Peak heights for individual metabolites were extracted using Multiquant Software (Sciex). From a single MS analysis, Q1/Q3 MRM transition mass spectra in both ionization modes were normalized independently. EigenMS normalization was performed through the NOREVA (NORmalization and EVAluation of Metabolomics Data) platform[342]. Unsupervised hierarchical clustering and principal component analysis (PCA) of normalized metabolite abundances was performed using the MetaboAnalyst platform[343].

3.2.12 *SERINE- AND GLYCINE-DEPENDENT GROWTH ASSAY*

MDA-MB-231 control and MTHFD2-KD clones were cultured in Minimum Essential Medium (MEM; Invitrogen) containing 10% FBS, 1x Anti-Anti, 0.25 µg/mL puromycin, and 1x MEM Non-Essential Amino Acids Solution (NEAA; Invitrogen). Cells were seeded at a density of 50,000 cells/well in 12-well cell culture plates (Corning) in MEM growth media. After 24 hours, growth media was replaced with MEM containing 10% dialyzed FBS (Gibco), 1 x AA, 0.25 µg/mL puromycin, and supplemented with

appropriate non-essential amino acids (10mM; glycine, L-serine, L-alanine, L-asparagine, L-aspartic acid, L-glutamic acid [ReagentPlus] and L-proline; Sigma) for 72 hours with media refreshed daily. After 72 hours, cells were trypsinized and counted using a haemocytometer.

3.2.13 *LINE1 AND CCL20 BISULFITE PYROSEQUENCING*

As previously described[56], DNA methylation was analyzed by sodium bisulfite pyrosequencing on a PyroMark Q24 Advanced pyrosequencer using the DNA EpiTect Fast DNA Bisulfite Kit and PyroMark PCR Kit (Qiagen N.V., Venlo, the Netherlands), according to the manufacturer's instructions, beginning with 500 ng template DNA. Assays covering the L1PA2 (a major subfamily of LINE1 retrotransposon) sequence and CCL20 gene promoter were designed using PyroMark Assay Design software version 2.0 (Qiagen N.V.) and validated to amplify a single PCR product (L1PA2 400 nt; CCL20 381 nt). See Table 3.3 for the L1PA2 and CCL20 assay primers. PCR conditions were as follows: 95°C, 15 minutes (94°C, 30 seconds; 56°C, 30 seconds; 72°C, 30 seconds) 50 cycles; and 72°C, 10 minutes.

Table 3.3: Bisulfite pyrosequencing primer sequences

Target	Primer	Sequence
L1PA2 (LINE1)	Forward Primer	AGGGAGAGTTAGATAGTG
	Reverse Primer	(biotin)AACTATAATAAACTCCACCC
	Sequencing Primer	GGAGAGTTAGATAGTGG
CCL20 promoter	Forward Primer	ATGAGGAAAAAGTAGGAAGTT
	Reverse Primer	(biotin)CCTTAAAAACCCCCAATTAAACTC
	Sequencing Primer	AGGAAAAAGTAGGAAGTTT

3.2.14 *STATISTICAL ANALYSES*

All statistical analyses were performed in GraphPad Prism 8 unless indicated otherwise. Statistical tests and significance are indicated in all figure captions.

3.3 RESULTS

3.3.1 *GENOME-WIDE shRNA SCREEN IDENTIFIES shRNAs ENRICHED OR DEPLETED BY DECITABINE TREATMENT*

The MDA-MB-231 breast cancer cell line was chosen as an appropriate decitabine response model in which to establish the shRNA library because this cell line is intermediately sensitive to decitabine treatment (Chapter 2 Figure 2.1). This moderate response to decitabine could be attributed to re-expression of tumour suppressor genes or other modalities (as described in Chapter 2).

The shRNA library MDA-MB-231 cells were orthotopically implanted in female NOD/SCID mice and the mice were divided into no treatment and decitabine treatment group (total n=6). Decitabine treatment resulted in smaller tumours (Figure 3.2A)—however, in theory cells that harboured an shRNA knockdown of a gene required for decitabine sensitivity or knockdown of a hypermethylated tumour suppressor gene had a growth advantage. Due to the growth advantage of specific knockdowns, when the tumour-wide DNA is analyzed, there is enrichment of the shRNA sequences associated with decitabine sensitivity genes. In contrast, shRNA sequences that knockdown genes important for resistance to decitabine would be depleted.

As expected, most shRNAs were not enriched or depleted in the decitabine-treated tumours and had a median DAC/NT shRNA abundance of ≈0 (Figure 3.2B). shRNAs that were either enriched or depleted 2-fold in 5 out of 6 n were prioritized for further study (Figure 3.2C & 3.2D). It was noted that there was inconsistent enrichment/depletion of multiple shRNAs per gene among the genes prioritized based on 2-fold and 5/6n criteria (e.g. TMBIM4, OGT, DNAJB9, and TXNRD1; Figures 3.2C & 3.2D).

A) *In vivo* genome-wide shRNA screen

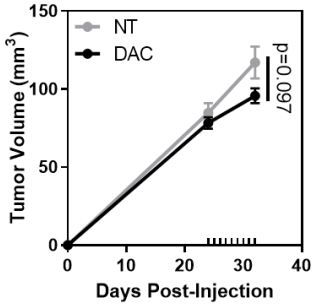

B) Distribution of shRNA abundance

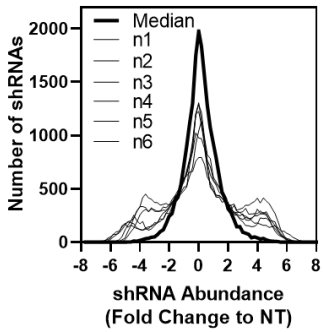

C) Enriched shRNAs

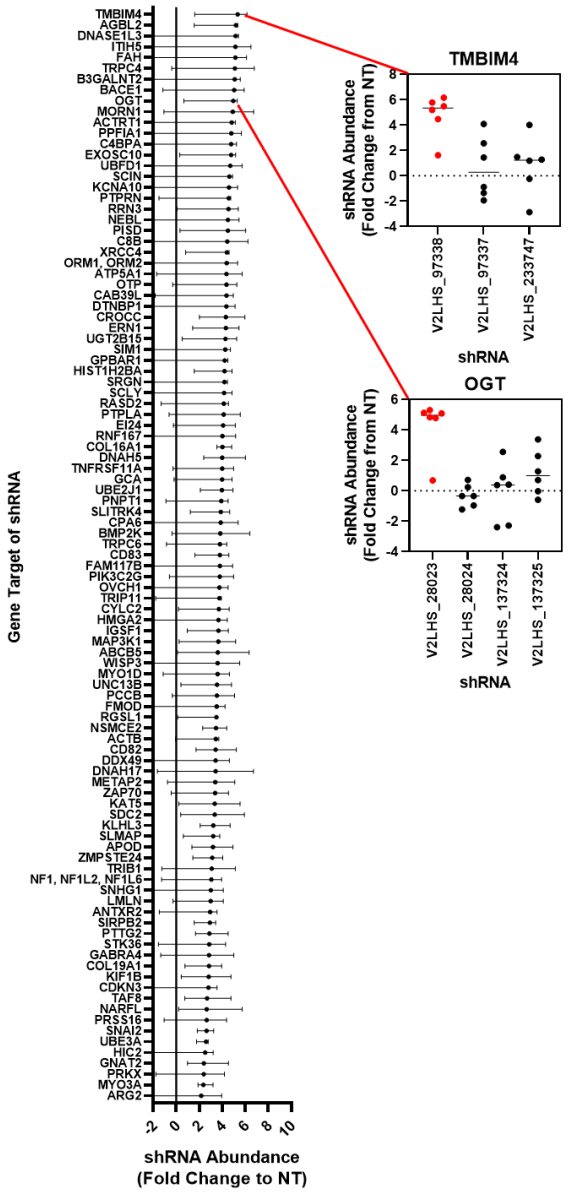

D) Depleted shRNAs

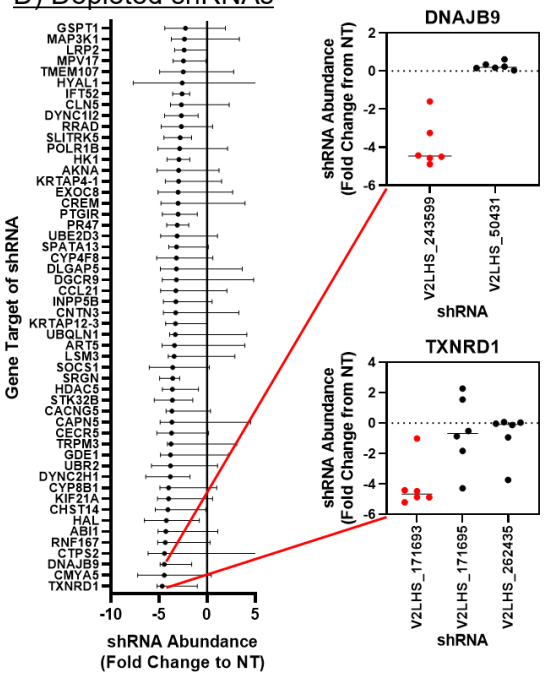

Figure 3.2: Genome-wide shRNA screen in decitabine-treated MDA-MB-231 tumours reveals consistently enriched and depleted shRNAs. A) Independent replicate #1: tumour growth of MDA-MB-231 shRNA library tumours treated with 0.5 mg/kg intraperitoneally injected decitabine (DAC) for 8 days (hatch marks on x-axis; n=9 mice per group; mean with SEM error bars and unpaired one-tailed test for tumour volume significance. **B)** Frequency distribution of shRNA fold-change abundance between DAC and NT tumours for each n (1-6) and the median of the pooled 6n. **C)** shRNAs ≥2-fold enriched or **D)** ≥2-fold depleted in 5 out of 6n; median with SD error bars. Two highly enriched shRNAs (corresponding to genes TMBIM4 and OGT) and two strongly depleted shRNAs (corresponding to genes DNAJB9 and TXNRD1) genes are represented in red. The enrichment/depletion of any additional shRNAs for each exemplar gene are shown in black. PM generated MDA-MB-231 Decode shRNA library cell line.

3.3.2 *ENRICHED SHRNAS KNOCKDOWN PUTATIVE HYPERMETHYLATED TUMOUR SUPPRESSOR GENES*

The goal of this project is to validate an innovative approach (*in vivo* genome-wide knockdown screen) of isolating the key "driver" DNA methylation events in breast cancer from the thousands of "passenger" events. Not only will this add to our basic understanding of DNA methylation in breast cancer growth and progression, but will potentially lead to a gene signature that may be applied in the clinic to identify patients who will respond well to DNMT inhibitors like decitabine.

Before functionally characterizing gene hits from an shRNA-based screen, it is essential to confirm that the depleted/enriched shRNA targets the intended gene. Poor knockdown efficiency is a known downside to shRNA-based screens. To address this pitfall, RT-qPCR validation of individual MDA-MB-231 knockdown clones was performed for the 19 most consistently enriched shRNAs from the screen (Figure 3.3A). Of these, 4 shRNAs could not be validated as the knockdown clone did not exhibit reduced expression of the supposed gene target (TMBIM4, TRPC4, XRCC4, and KLHL3).

If the enriched shRNAs from the screen are indeed knocking down hypermethylated tumour suppressor genes (TSGs) in the MDA-MB-231 cells, then treating MDA-MB-231 cells with decitabine should induce the expression of these genes via de-methylation. After 72 hours treatment with 1μM decitabine, there was elevated expression of 5/15 remaining gene candidates (COL16A1, CROCC, HIST1H2BA, CD83, and APOD; Figure 3.3B), and promoter or CpG island-associated DNA methylation was significantly reduced in 4/5 remaining gene candidates (COL16A1, CROCC, HIST1H2BA, and APOD; Figure 3.4). CD83 molecule (CD83) contains an initially unmethylated promoter in MDA-

MB-231 cells, thus decitabine treatment does not de-methylate this gene and it is removed from contention as a hypermethylated TSG.

It was confirmed in a cohort of primary breast tumours (TCGA, Cell 2015; n=720) that the 4 remaining candidate genes have elevated methylation of promoter-associated and CpG island-associated CpGs compared to normal breast tissue samples (n=80; Figure 3.5A). Additionally, gene expression negatively correlated with methylation at promoter-associated CpGs in apolipoprotein D (APOD; r= -0.3206, -0.336, -0.3458, and -0.4029) and collagen type XVI alpha 1 chain (COL16A1; -0.1995, -0.2818, -0.2088, -0.2134, -0.2076, -0.2019) (Figure 3.5B) suggesting that methylation partially dictates gene expression for these genes. Ciliary rootlet coiled-coil, rootletin (CROCC) does not have any promoter-annotated CpGs annotated in the HM450 assay, and methylation of its intragenic CpG island does not significantly correlate with expression. Expression of histone H2B type 1-A (HIST1H2BA) was absent from 713/720 breast cancer samples and from all normal breast tissue samples; therefore, no association between methylation and expression was found. This leaves COL16A1 and APOD as the strongest candidate hypermethylated TSGs identified by the Decode screen.

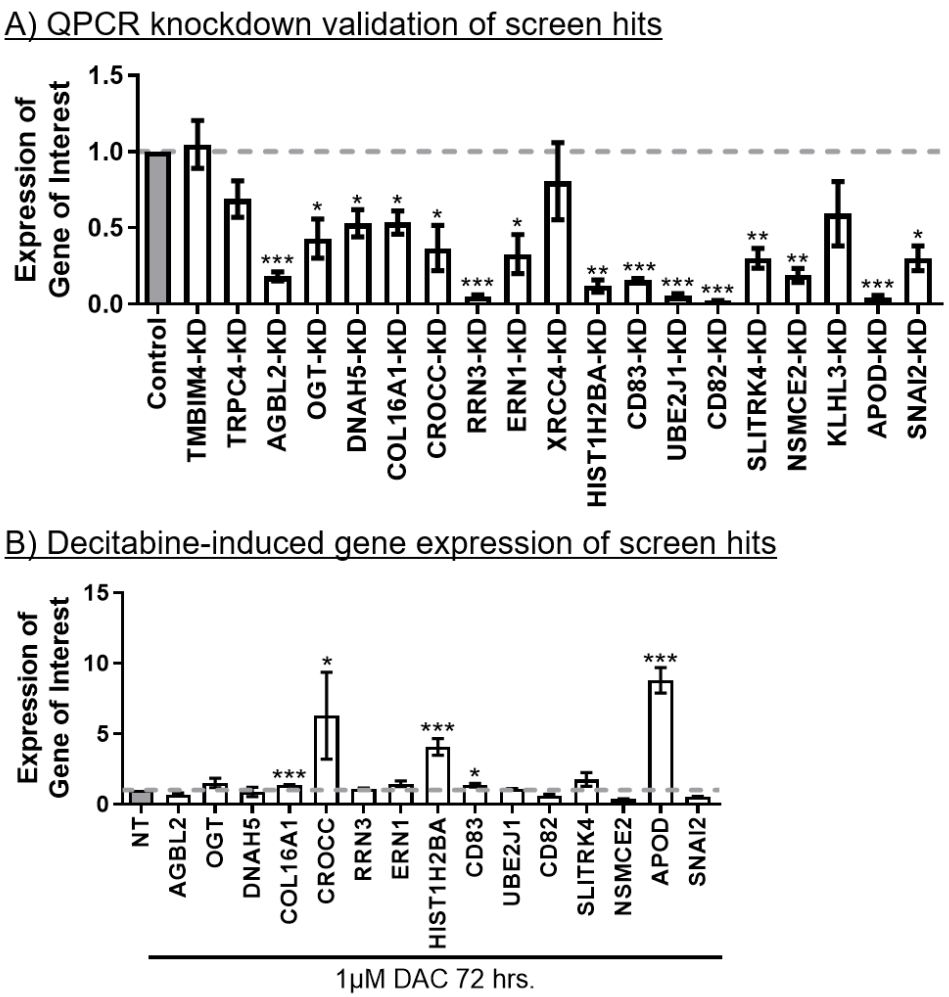

Figure 3.3: Enriched shRNAs efficiently knockdown the intended gene targets and expression of the target gene is induced by decitabine treatment. **A)** RT-qPCR validation of knockdown efficiency in individual MDA-MB-231 knockdown clones; n=4, mean with SD error bars, one-sample t-test. **B)** RT-qPCR expression of genes targeted by enriched shRNAs in MDA-MB-231 cells treated with 1μM decitabine for 72 hours; n=4, mean and SD error bars, one-sample t-test. $p<0.05$*; $p<0.01$**; $p<0.001$***. PP assisted with RT-qPCR.

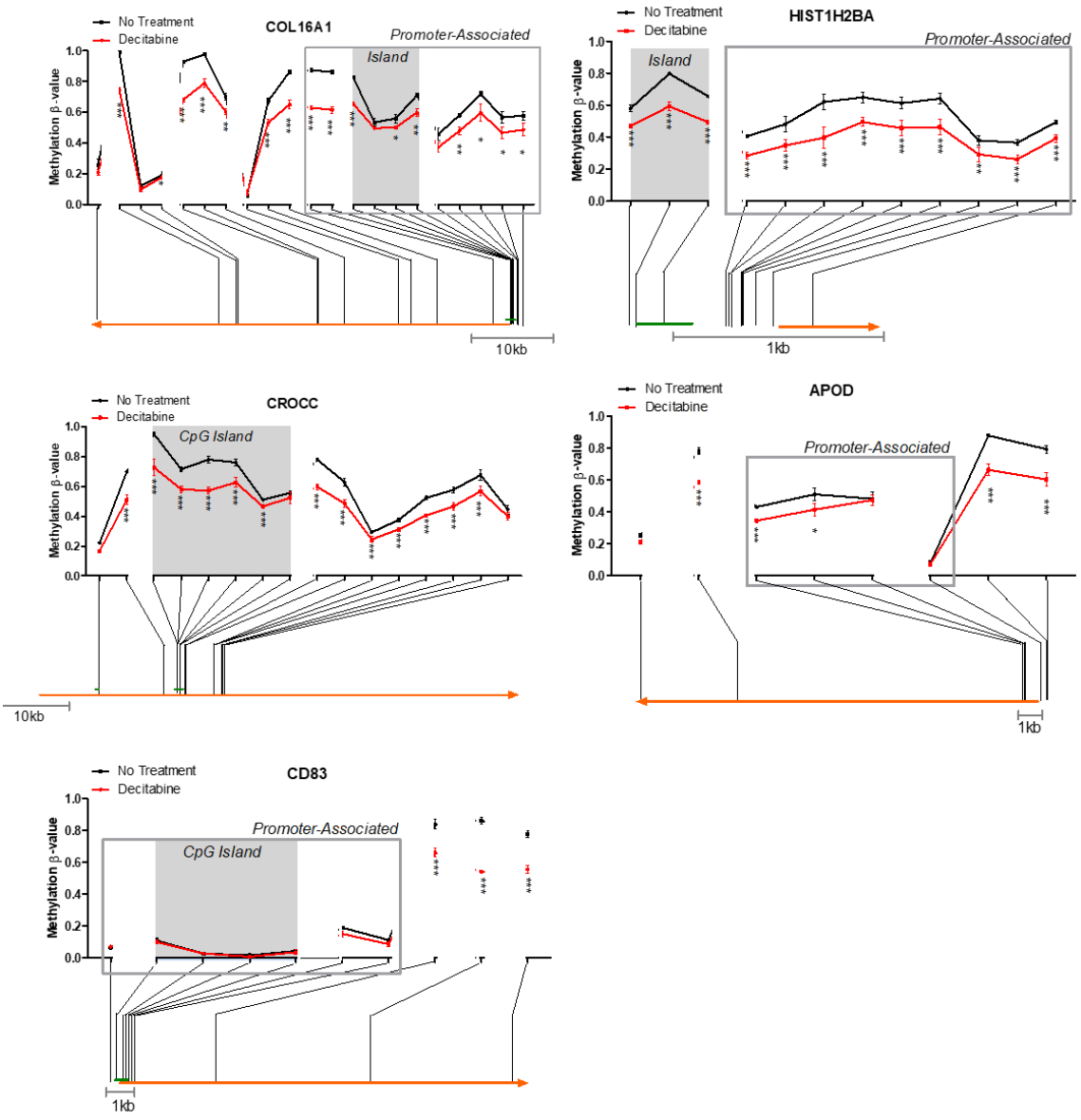

Figure 3.4: Putative hypermethylated tumour suppressor genes are de-methylated by *in vitro* decitabine treatment. DNA methylation of potential hypermethylated tumour suppressor genes determined by HM450 bead chip array in MDA-MB-231 cells treated with 1 µM decitabine for 72 hours. Each CpG is mapped to its location on the gene of interest, CpG islands and promoter-associated CpGs are indicated; n=3 per group decitabine- and untreated; mean with SD error bars; paired one-tailed t-test; $p<0.05$*; $p<0.01$**; $p<0.001$***. KMC submitted MDA-MB-231 DNA for HM450 analysis.

A) Methylation of putative hypermethylated TSGs in normal vs malignant breast tissue

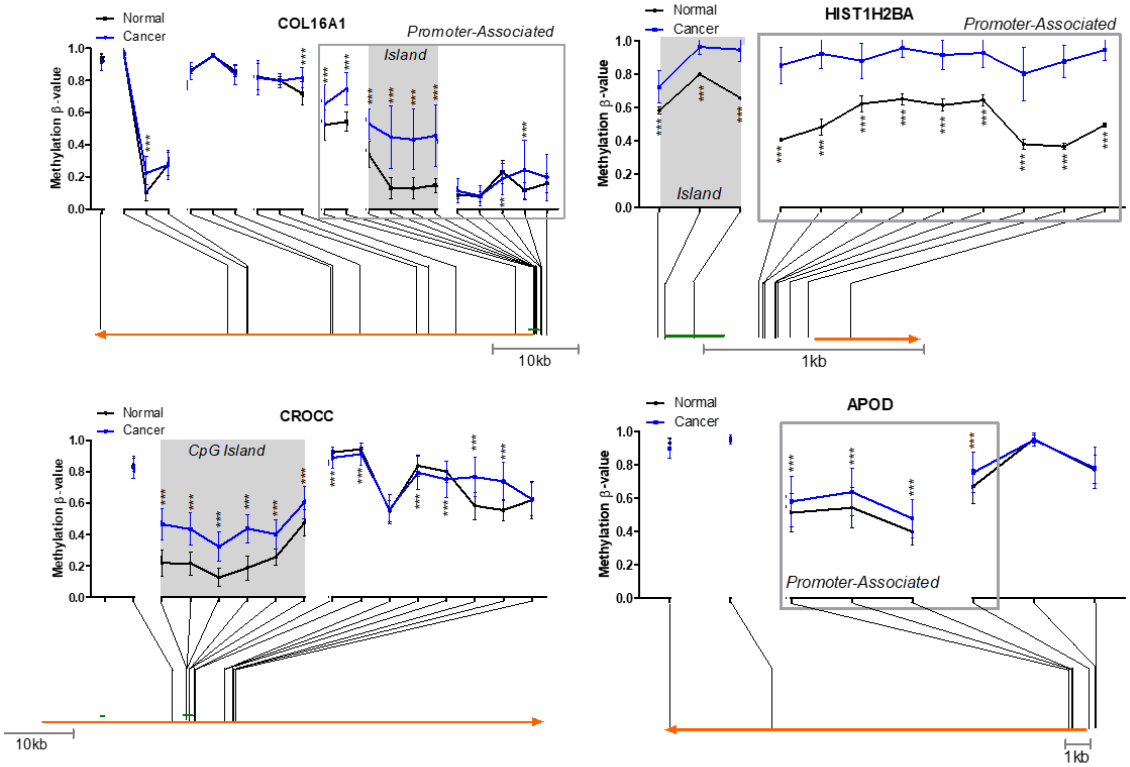

B) Breast cancer patients: correlation of promoter methylation and gene expression

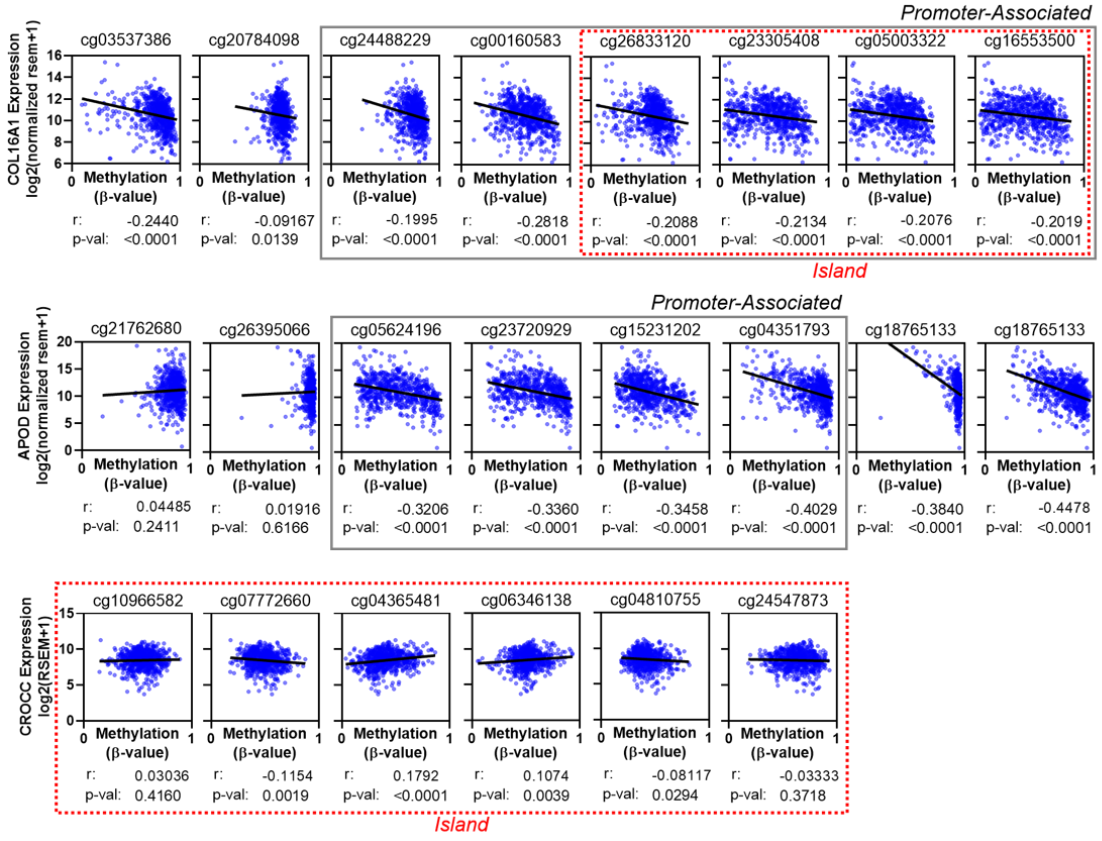

Figure 3.5: Putative hypermethylated tumour suppressor genes are more methylated in breast cancer compared to normal breast tissue. **A)** DNA methylation of putative hypermethylated TSGs determined by HM450 bead chip array in 720 primary breast tumours and 80 normal breast tissue samples. Each CpG is mapped to its location on the gene of interest, CpG islands and promoter-associated CpGs are indicated; mean with SD error bars; paired one-tailed t-test. **B)** Methylation of promoter-associated CpGs In APOD and COL16A1 are negatively correlated with expression. HM450 bead chip array for DNA methylation and RNA-Seq log2(RSEM+1) expression; Spearman correlation r- and p-values. $p<0.001$***.

3.3.3 *APOLIPOPROTEIN D MAY BE A WEAK HYPERMETHYLATED TUMOUR SUPPRESSOR GENE BUT IS NOT PART OF A HYPERMETHYLATED TSG PROFILE*

Among the candidate genes remaining, APOD had the most potential as a hypermethylated tumour suppressor gene. APOD showed the greatest gene expression induction after decitabine treatment (Figure 3.3B), the APOD shRNA identified in the screen was more efficient than the shRNAs for other gene candidates (Figure 3.3A), and there is evidence that elevated APOD contributes to growth arrest or differentiation in breast cancer cells[344]. If APOD is a potent hypermethylated tumour suppressor gene, then decitabine should not inhibit growth of the APOD-KD tumours because although the tumour suppressor gene (APOD) is released from methylation-based silencing, it is still suppressed via knockdown. However, growth of the APOD-KD tumours was still slowed by decitabine treatment (Figure 3.6A). Possibly, APOD is not a true gene hit from the shRNA screen, as the other two shRNAs targeting APOD in the screen were not enriched (Figure 3.6B).

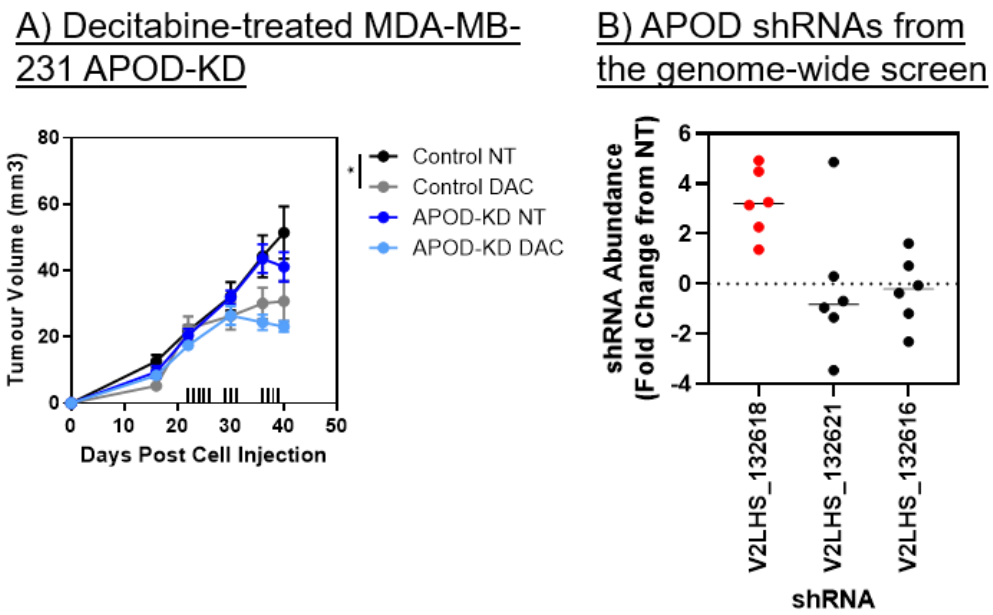

Figure 3.6: Knockdown of APOD does not confer decitabine resistance. A) NOD/SCID mice harbouring MDA-MB-231 Control or APOD-KD tumours were intraperitoneally injected with 0.5 mg/kg decitabine (DAC) or PBS vehicle (NT) (Control NT n=7; Control DAC n=9; APOD NT n=5; APOD DAC n=9; mean with SEM error bars; one-way ANOVA with Tukey's post-hoc test; $p<0.05$* **B)** Relative abundance of the APOD-targeted shRNAs from the screen. The APOD-targeted shRNA identified as >2-fold enriched in 5 out of 6n (V2LHS_132618) is represented in red, with the other two APOD-targeted shRNAs in black. BMC assisted with intraperitoneal injections.

It is also possible that suppression of single hypermethylated tumour suppressor gene (APOD-KD) is insufficient in the context of this individual knockdown clone model and that resurrection of multiple hypermethylated TSGs is necessary for decitabine-mediated growth suppression. If this is the case, then breast cancer cell lines that are most sensitive to decitabine should have hypermethylation of the top two putative TSGs identified in the screen (APOD and COL16A1). The promoter methylation status of APOD and COL16A1 was assessed using the HM450 DNA methylation array for ten breast cancer cell lines with known decitabine response (Chapter 2). Unsupervised clustering suggests

that the response to decitabine was not correlated to APOD/COL16A1 methylation (Figure 3.7). This is best illustrated in the MDA-MB-453 cell line which based on APOD/COL16A1 hypermethylation is primed to be sensitive to de-methylating therapy; yet MDA-MB-453 is one of the most decitabine-resistant cell lines. At this point, the evidence is unconvincing that the genome-wide screen has identified potent and common hypermethylated TSGs in breast cancer cells.

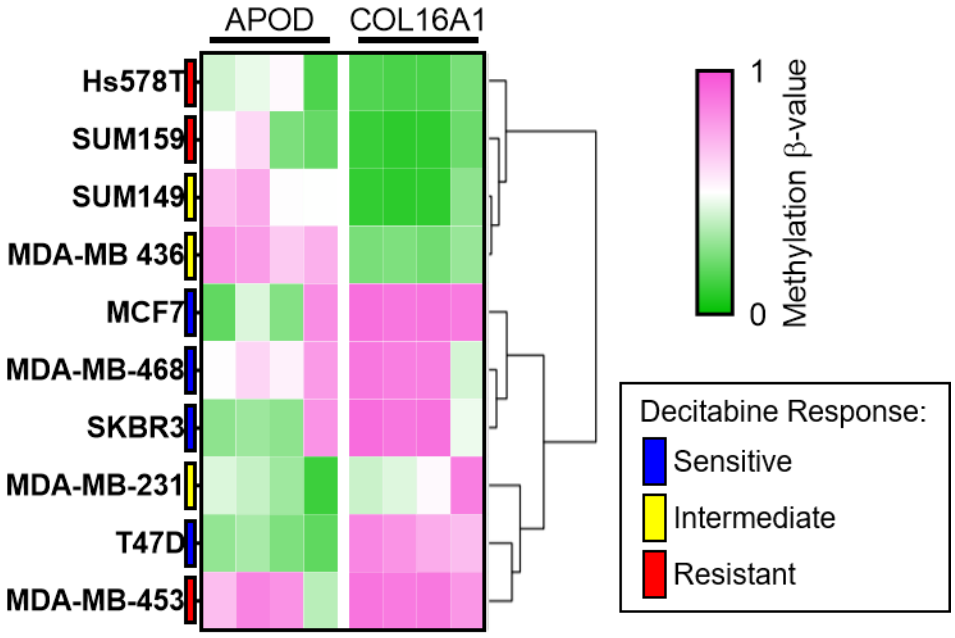

Figure 3.7: Promoter-associated methylation of APOD and COL16A1 in breast cancer cell lines does not associate with decitabine sensitivity. DNA methylation is determined by HM450 for 4 promoter-associated CpGs each in APOD and COL16A1. Decitabine response was previously determine by colony forming IC_{50} (Chapter 2). KMC submitted cell line DNA for HM450 analysis.

3.3.4 *NEITHER NUCLEOTIDE PROCESSING, IMPORT/EXPORT, DNA METHYLATION/DEMETHYLATION, NOR VIRAL MIMICRY ARE IMPLICATED IN DECITABINE RESPONSE IN THE GENOME-WIDE SCREEN*

In Chapter 2, I identified deoxycytidine kinase (DCK) as a key mediator of both *in vitro* and *in vivo* decitabine response in breast cancer cells. DCK is an essential mediator of decitabine response as it is required to phosphorylate decitabine prior to DNA integration and is upstream of all DNA methylation or gene expression changes. It was therefore problematic that DCK was not an enriched shRNA target in the screen. The likely explanation is that the pooled shRNA library did not contain a highly efficient DCK shRNA.

In my previous experiment showing that breast cancer cells with DCK-KD are resistant to decitabine *in vivo* (Chapter 2, Figure 2.3), I used the highly efficient DCK knockdown V2LHS_112523; and only included the less efficient V2LHS_112524 clone for *in vitro* experiments. This less efficient DCK-KD clone was significantly less resistant to decitabine than the more efficient clone (Chapter 2 Figure 2.3). Unfortunately, the Decode screen contains only this less efficient (and less phenotypically impactful) V2LHS_112524 sequence as well as the V2LHS_112519 sequence of unknown knockdown efficiency (shown as shRNA #1 and #2 respectively in Figure 3.8). This provides a plausible reason as to why DCK was not a top hit of the decitabine-response screen.

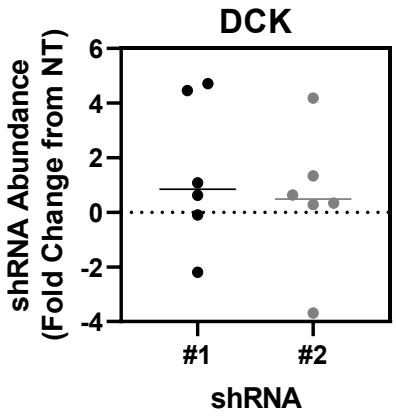

Figure 3.8: Relative abundance of shRNAs targeting DCK in decitabine-treated MDA-MB-231 shRNA library tumours. shRNA abundance >0 implies that knockdown confers resistance.

The other decitabine response pathways investigated in Chapter 2 (nucleotide import/export, DNA methylation/de-methylation machinery, and viral mimicry) were similarly of no consequence to decitabine response in the Decode screen (Figure 3.9A-C). Importantly, knockdown of ATP binding cassette subfamily B member 1 (ABCB1) which mediates resistance to several breast cancer therapies, does not also confer resistance to decitabine and consistently, its knockdown was not of consequence in the screen (Figure 3.9A)[160]. Knockdown of the enzymes which facilitate DNA methylation (DNA methyltransferases: DNMT1, DNMT3A, and DNMT3B) as well as the proteins that mediate removal of methyl groups from DNA (ten-eleven translocation methylcytosine dioxygenases 1 & 2: TET1 and TET2) did not alter sensitivity to decitabine in the screen (Figure 3.9C). Possibly, the dsRNA viral mimicry response is occurring within the decitabine-treated tumours, but as shown before (Chapter 2 Figure 2.23) knockdown of the key viral mimicry mediator DEAD-Box Helicase 5 (DDX58) does not impart decitabine

sensitivity (Figure 3.9C). An shRNA targeting melanoma differentiation-associated protein 5 (MDA5) which is the other dsRNA viral mimicry mediator, was not contained in the shRNA library. The Decode screen was designed to capture protein-coding genes, so no endogenous retroviral elements (which only create double stranded RNAs) were targeted by the shRNA library.

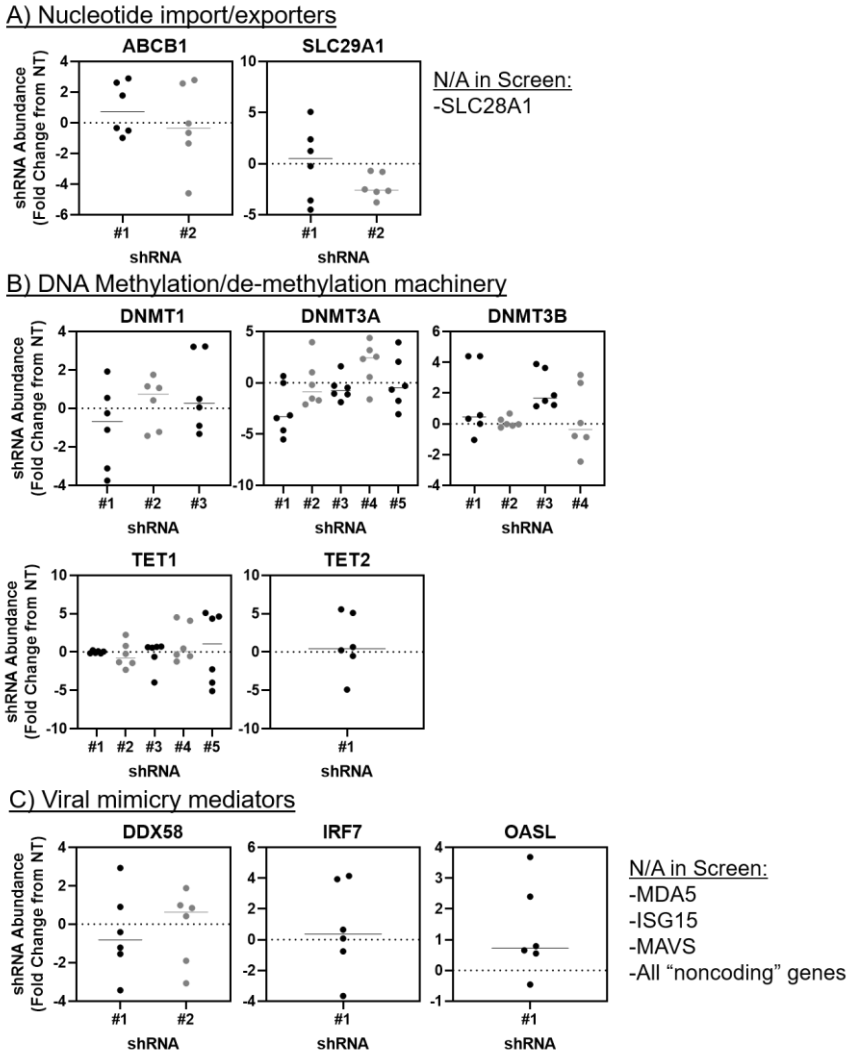

Figure 3.9: Relative abundance of shRNAs targeting nucleotide import/export, DNA methylation, and viral mimicry genes in decitabine-treated MDA-MB-231 shRNA library tumours. shRNA abundance >0 implies that knockdown confers resistance.

3.3.5 *IDENTIFICATION OF MTHFD2 THROUGH ATARIS*

The initial strategy of identifying the most enriched or depleted shRNAs from the decitabine-treated Decode screen resulted in a lack of functional targets that validated for decitabine sensitivity. Scanning the shRNAs with known or suspected decitabine-related functions (nucleotide import, DNA methylation machinery, and viral mimicry) also resulted in a lack of functional targets. A new strategy for prioritizing gene hits from the screen is called for.

The Decode screen might be better approached with gene-centric hit prioritization instead of an shRNA-centric strategy. If a gene plays a vital role in decitabine response, then I would expect multiple shRNAs to exhibit the same effect (whether enriched or depleted), while allowing for different knockdown efficiencies to present as different magnitudes of effect on the phenotype.

One gene-centric method for identifying RNAi screen hits is Analytic Technique for Assessment of RNAi by Similarity (ATARiS). This platform prioritizes gene hits based on several shRNAs for the same gene exerting the same effect on phenotype. I applied the decitabine Decode screen shRNA abundances to this analysis pipeline. The 3504 genes that are targeted by a single shRNA are exempt from this analysis (Figure 3.10A), of the remaining 17378 eligible shRNAs, 1558 ATARiS gene solutions were generated. These solutions represent gene hits from the screen and contain between 2-5 shRNAs for a given gene solution. Each ATARiS solution is given a median abundance score for the contained shRNAs, significance p-value pertaining to whether the solution is significantly enriched or depleted (median shRNA abundance $\neq 0$), and consistency c-score which is higher in solutions where there is less variance between replicates for each shRNA (Table 3.4).

The most significant and enriched gene solution is for methylenetetrahydrofolate dehydrogenase (NADP+ dependent) 2 (MTHFD2) (Figure 3.10B) containing 3 MTHFD2-targeted shRNAs (Figure 3.10C). 3 shRNAs targeted towards MTHFD2 were contained in the MTHFD2 gene solution, though V2LHS_90968 (MTHFD2-KD shRNA 66) and V2LHS_90968 (MTHFD2-KD shRNA 68) have a greater magnitude of enrichment than V2LHS_90967. Together, this reveals that knockdown of MTHFD2 confers a significant and consistent level of resistance to decitabine treatment in the Decode screen.

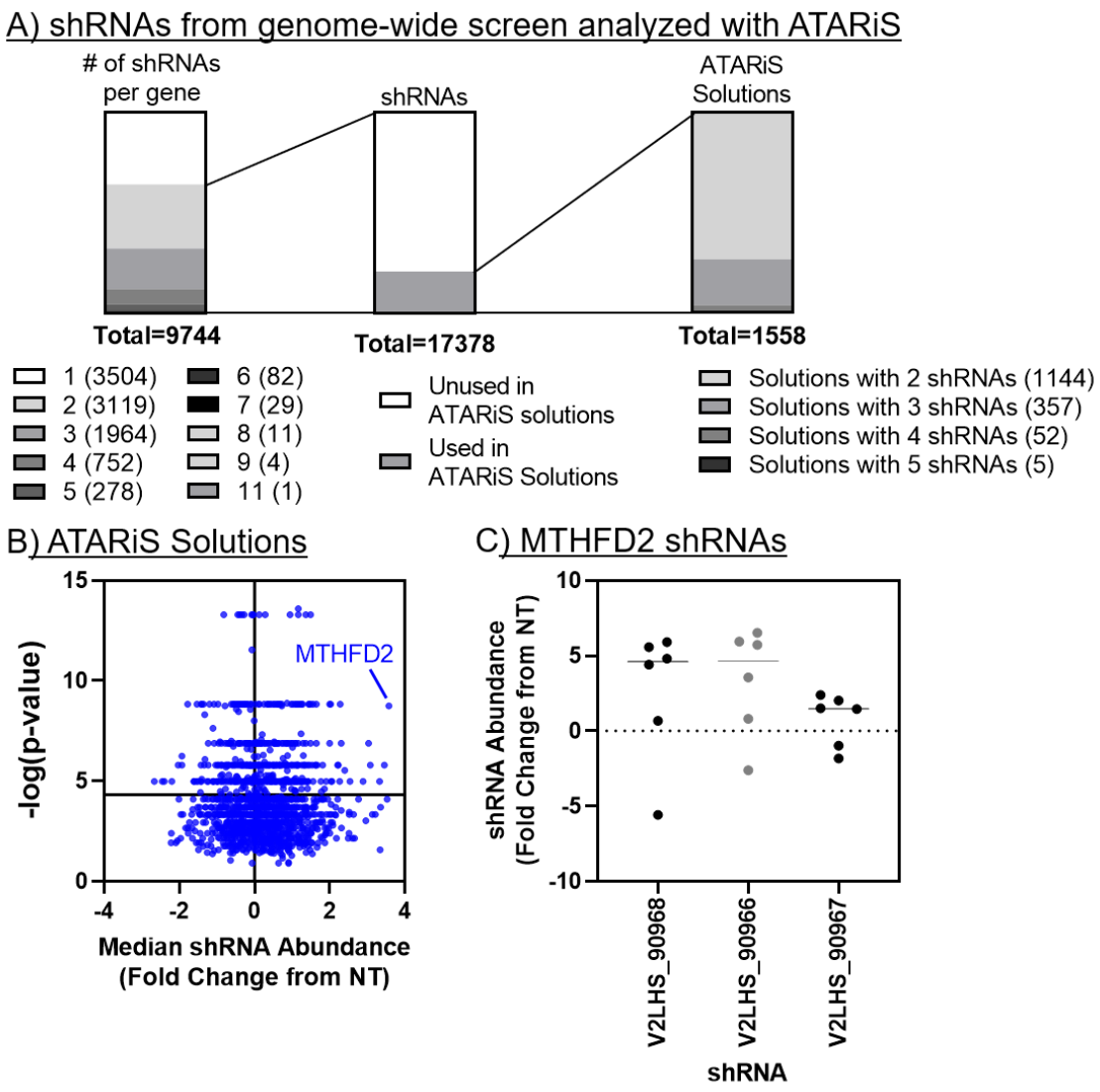

Figure 3.10: MTHFD2 is the most enriched ATARiS gene solution from the decitabine Decode screen. A) Genes that are targeted by more than one shRNA are eligible to be used in ATARiS solutions. This generated 1558 total gene solutions most of which contain 2 or 3 shRNAs. **B)** Significance and median shRNA abundance for the 1558 gene solutions. **C)** Abundance of three shRNAs targeting MTHFD2 in the decitabine-treated shRNA library tumours. All three shRNAs are contained in the MTHFD2 ATARiS gene solution.

Table 3.4: ATARiS gene solutions for shRNAs that were enriched in decitabine-treated MDA-MB-231 Decode shRNA library tumours

Gene	shRNAs in Solution	Median shRNA Abundance (Fold Change to NT)	p-value	c-score
Methylenetetrahydrofolate dehydrogenase (NADP+ dependent) 2 (MTHFD2)	V2LHS_90966 V2LHS_90967 V2LHS_90968	3.572	0.002	2.703
Very low density lipoprotein receptor (VLDLR)	V2LHS_171963 V2LHS_218476	3.448	0.018	1.740
Claudin 10 (CLND10)	V2LHS_95077 V2LHS_230865	3.326	0.032	1.500
Caspase 10 (CASP10)	V2LHS_188943 V2LHS_194005	3.075	0.018	1.740
Homeodomain interacting protein kinase 1 (HIPK1)	V2LHS_140675 V2LHS_202529	3.031	0.008	2.070
Pituitary tumour-transforming 2 (PTTG2)	V2LHS_12576 V2LHS_198047	2.882	0.032	1.500
Sodium voltage-gated channel alpha subunit 1 (SCN1A)	V2LHS_94851 V2LHS_94854	2.536	0.032	1.500
Ras and Rab interactor 2 (RIN2)	V2LHS_50920 V2LHS_50849 V2LHS_50850	2.394	0.022	1.670
UDP glucuronosyltransferase family 2 member B15 (UGT2B15)	V2LHS_231652 V2LHS_94115	2.306	0.008	2.070
Estrogen receptor binding site associated antigen 9 (EBAG9)	V2LHS_240649 V2LHS_242967	2.274	0.002	2.660
Keratin 72 (KRT72)	V2LHS_64837 V2LHS_64839	2.261	0.032	1.500
Nedd4 family interacting protein 2 (NDFIP2)	V2LHS_77838 V2LHS_77909	2.222	0.018	1.740
Sperm associated antigen 7 (SPAG7)	V2LHS_67448 V2LHS_67453	2.208	0.018	1.740
Myelin expression factor 2 (MYEF2)	V2LHS_188303 V2LHS_194759	2.058	0.032	1.500
Catechol-O-methyltransferase (COMT)	V2LHS_112401 V2LHS_265760	2.039	0.032	1.500
Leptin receptor overlapping transcript like 1 (LEPROTL1)	V2LHS_261525 V2LHS_74463	1.998	0.008	2.070

Gene	shRNAs in Solution	Median shRNA Abundance (Fold Change to NT)	p-value	c-score
F-box protein 28 (FBXO28)	V2LHS_254655 V2LHS_254695	1.994	0.002	2.660
Transcriptional adaptor 2A (TADA2L)	V2LHS_131910 V2LHS_236711	1.902	0.032	1.500
Leucine carboxyl methyltransferase 1 (LCMT1)	V2LHS_268706 V2LHS_97118 V2LHS_97119	1.857	0.041	1.387
UDP-glucose pyrophos-phorylase 2 (UGP2)	V2LHS_84682 V2LHS_84686	1.808	0.018	1.740
Mitogen-activated protein kinase 1 (MAP3K1)	V2LHS_100862 V2LHS_203111 V2LHS_263235	1.775	0.045	1.851
ATPase H+ transporting V1 subunit F (ATP6V1F)	V2LHS_242716 V2LHS_28381	1.762	0.032	1.500
Interleukin 36 receptor antagonist (IL1F5)	V2LHS_18953 V2LHS_18954	1.661	0.018	1.740
Ring finger protein 213 (RNF213)	V2LHS_130529 V2LHS_21660	1.642	0.008	2.070
RUN domain containing 3B (RUNDC3B)	V2LHS_41859 V2LHS_41860	1.642	0.002	2.660
Synaptoporin (SYNPR)	V2LHS_18163 V2LHS_18164	1.622	0.018	1.740
Sperm associated antigen 6 (SPAG6)	V2LHS_43508 V2LHS_43511	1.621	0.018	1.740
Thymine DNA glycosylase (TDG)	V2LHS_153856 V2LHS_153860	1.555	0.002	2.660
Homeostatic iron regulator (HFE)	V2LHS_192666 V2LHS_269842	1.554	0.032	1.500
Transmembrane protein 132D (TMEM132D)	V2LHS_204101 V2LHS_82061	1.535	0.018	1.740

3.3.6 *KNOCKDOWN OF MTHFD2 IMPAIRS MDA-MB-231 TUMOUR GROWTH AND CONFERS RELATIVE RESISTANCE TO DECITABINE*

All shRNA screens have a degree of stochasticity, so although the ATARiS gene solution identification strongly suggests that MTHFD2 knockdown imparts MDA-MB-231 cells with decitabine resistance, generating individual knockdown clones of MTHFD2 is the only way to confirm this. The knockdown clones for V2LHS_90968 (MTHFD2-KD shRNA 66) and V2LHS_90968 (MTHFD2-KD shRNA 68) were therefore created in the MDA-MB-231 cell line. Both MDA-MB-231 MTHFD2-KD clones show significant reduction in MTHFD2 mRNA (shRNA 66 = 68% efficient; shRNA 68 = 95% efficient) (Figure 3.11A). An individual knockdown clone was not generated for third shRNA of the MTHFD2 gene solution (V2LHS_90967), because compared to the other two shRNAs it had a small magnitude of effect in the Decode screen (Figure 3.10C).

To confirm that MTHFD2-KD does impart resistance to decitabine in MDA-MB-231 tumours as the screen suggests, both MTHFD2-KD clones and a control vector clone were orthotopically injected into NOD/SCID mice which were subsequently treated with 0.5 mg/kg decitabine. Strikingly, knockdown of MTHFD2 dramatically impaired MDA-MB-231 tumour growth reflected in both tumour volume and final mass (Figure 3.11B). Both MTHFD2-KD shRNAs produced tumours that were significantly smaller than control tumours regardless of decitabine treatment. As before (Chapter 2), this decitabine treatment regimen resulted in a moderate reduction of MDA-MB-231 tumour growth; however, growth of MDA-MB-231 MTHFD2-KD tumours was not impacted by decitabine treatment. Relative to MDA-MB-231 control tumours, MTHFD2-KD tumours are resistant to decitabine treatment. Now that the decitabine resistance of MTHFD2-KD has been

confirmed, I investigate mechanisms by which MTHFD2-KD may imbue MDA-MB-231 cells with decitabine resistance.

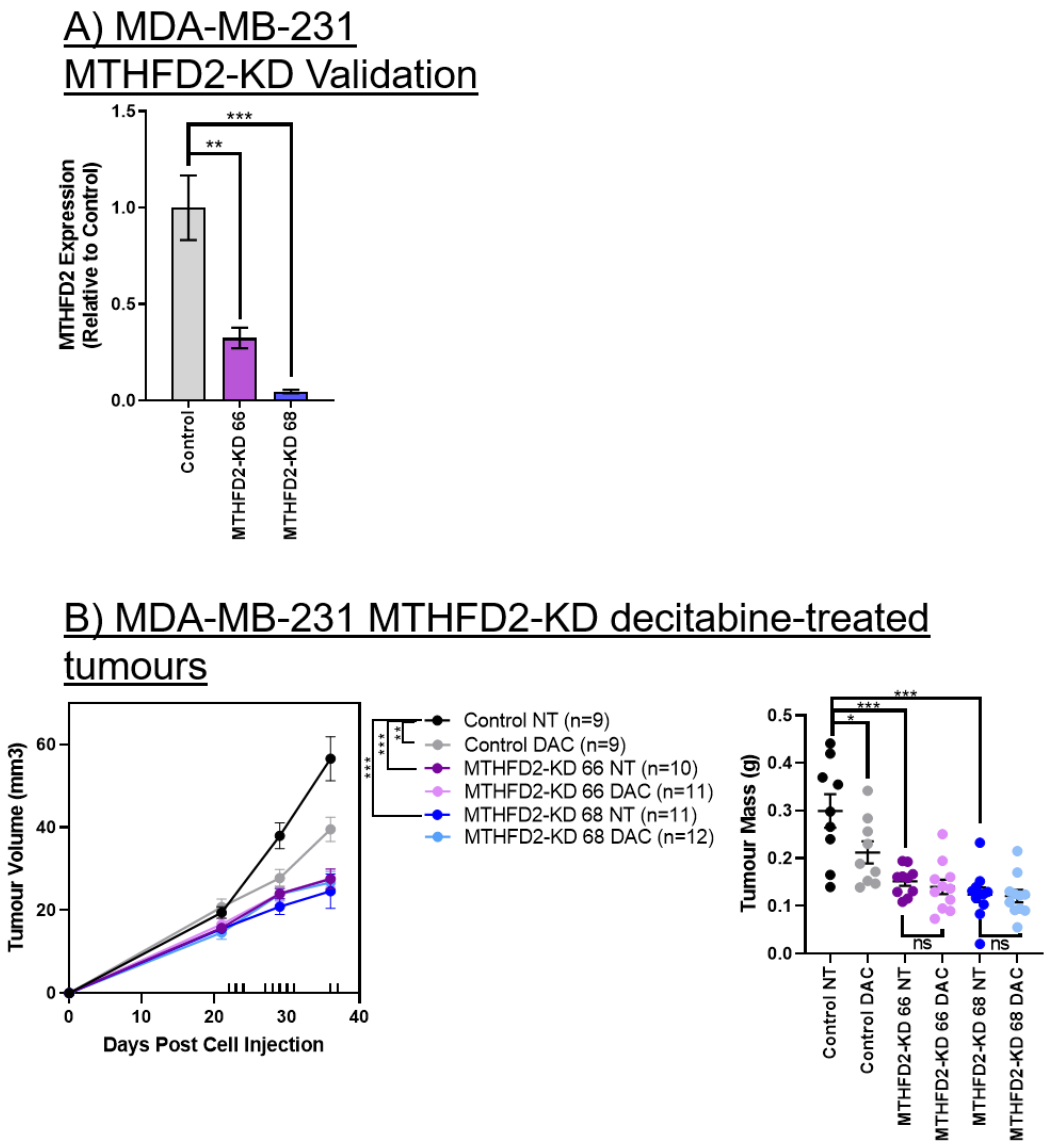

Figure 3.11: MDA-MB-231 MTHFD2-KD tumours are smaller are more resistant to decitabine treatment. A) RT-qPCR validation of MTHFD2-KD in MDA-MB-231 cells (n=4; one-way ANOVA with Dunnett's post-hoc test). **B)** NOD/SCID mice harbouring MDA-MB-231 Control or MTHFD2-KD (shRNA 66 or 68) tumours were intraperitoneally injected with 0.5 mg/kg decitabine (DAC) or PBS vehicle (NT) (Control NT n=9; Control DAC n=9; MTHFD2-KD [shRNA 66] NT n=10, MTHFD2-KD [shRNA 66] DAC n=11, MTHFD2-KD [shRNA 68] NT n=11, MTHFD2-KD [shRNA 68] DAC n=12). Tumour volume (mm^3, length x width x height / 2) and mass (g), mean with SEM error bars, one-way ANOVA with Tukey's post-hoc test. $p<0.05$*, $p<0.01$**, $p<0.001$***.

3.3.7 *CHEMOTHERAPY RESISTANCE GENE CHEMOKINE (C-C MOTIF) LIGAND 20 IS UP-REGULATED BY COMBINATION MTHFD2-KD AND DECITABINE TREATMENT*

Though the intent was to identify tumour suppressor genes, knockdown of MTHFD2 actually impaired MDA-MB-231 tumour growth and high expression of MTHFD2 is associated with aggressive disease and poor prognosis in many solid tumour types[330–337]. Based on the evidence that MTHFD2 is almost certainly not a tumour suppressor, alternate explanations for why this gene was identified in the screen need to be pursued.

Induction of gene expression modules associated with DNA damage and cell cycle arrest is observed in decitabine-treated cancer cells (Chapter 2, Figure 2.16D). These pathways are similarly up-regulated upon treatment with other cytotoxic chemotherapies (e.g. taxanes) and are thought to represent a shared cellular response to DNA damaging agents. One possible explanation for MTHFD2-KD conferring resistance to decitabine, is that decitabine-inducible expression of drug-response genes is modified in the MTHFD2-KD tumours.

As a component of chemoresistance in solid tumours, chemokine (C-C motif) ligand 20 (CCL20) expression changes are indicative of a coordinated drug response in breast cancer cells[345,346]. The expression of the chemoresistance gene CCL20 was strongly induced (7-fold) by decitabine in MDA-MB-231 cells *in vitro* (Affymetrix HuGene 2.0 ST array; GSE103427; Chapter 2). CCL20 expression was assessed in the MDA-MB-231 MTHFD2-KD decitabine-treated tumours by RT-qPCR and was found to be upregulated by decitabine treatment. This induction was enhanced by MTHFD2-KD (Figure 3.12A).

To determine whether increased CCL20 expression was due to de-methylation of the CCL20 promoter, bisulfite pyrosequencing was performed for 6 CpGs in the CCL20 promoter region (Figure 3.12B). Decitabine-induced CCL20 expression is likely not attributable to de-methylation of the CCL20 promoter because all 6 assayed CpGs are relatively unmethylated (7-20% methylated) to begin with (Control NT) and are not further de-methylated by either decitabine treatment or MTHFD2-KD. Increased CCL20 could therefore be a result of a more generalized response to a cytotoxic agent and may not be specific to de-methylation therapy.

To support the idea that CCL20 is involved in drug resistance, CCL20 expression is higher in the taxol-resistant MDA-MB-231 cells (Figure 3.12C). Interestingly, with elevated CCL20, there is loss of MTHFD2 in the taxol-resistant MDA-MB-231 cells. Currently, we have no clear mechanism to offer for why there is enhanced CCL20 expression in the MTHFD2-KD tumours, but it is a potential reason for the resistance of the MTHFD2 KD tumours to decitabine.

A) CCL20 expression in decitabine-treated MTHFD2-KD tumours

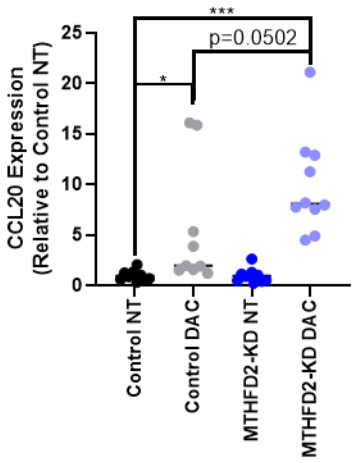

B) CCL20 methylation bisulfite pyrosequencing

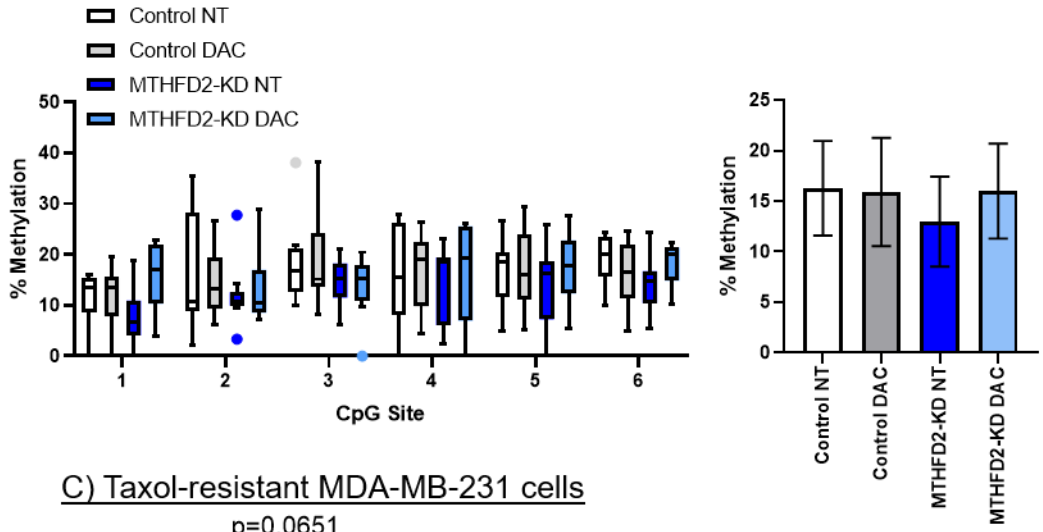

C) Taxol-resistant MDA-MB-231 cells

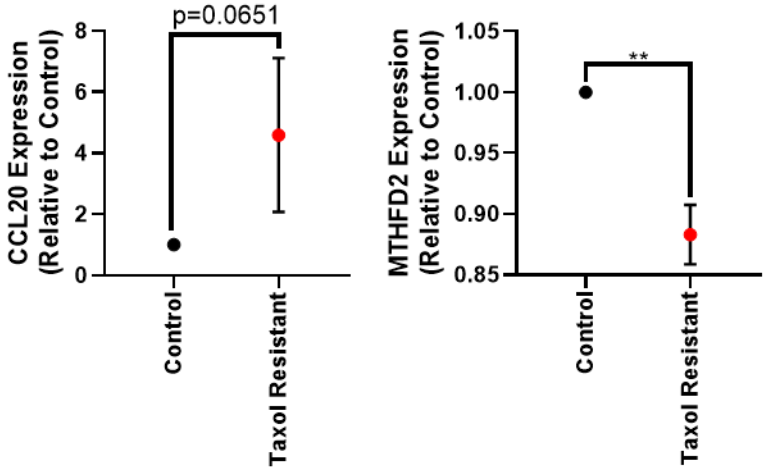

Figure 3.12: Chemotherapy-response gene CCL20 is up-regulated by decitabine in decitabine-treated tumours independent of its promoter methylation status. A) RT-qPCR mean gene expression of CCL20 from decitabine-treated MDA-MB-231 MTHFD2-KD tumours (Control NT n=10, Control DAC n=9, MTHFD2-KD [shRNA 66] NT n=11, MTHFD2-KD [shRNA 66] DAC n=10; one-way ANOVA with multiple comparisons). **B)** CCL20 promoter region CpG methylation quantified with bisulfite pyrosequencing for individual CpGs (median with Tukey bars) and the average of the 6 assessed CpGs (mean with SD error bars). **C)** RT-qPCR expression of CCL20 and MTHFD2 in taxol-resistant MDA-MB-231cells compared to control cells; n=4; mean with SD error bars; one sample t-test; $p<0.05$*; $p<0.01$**; $p<0.001$***. MC assisted with RT-qPCR of MTHFD2-KD tumour, ICGW performed CCL20 bisulfite pyrosequencing, SRH and KBG supplied taxol-resistant MDA-MB-231 cells.

3.3.8 *METABOLOMICS OF DECITABINE-TREATED MTHFD2-KD TUMOURS REVEALS DYSREGULATED FOLATE METABOLISM*

While gene expression changes (like CCL20) are an important element of decitabine response, the loss of DNMT activity and subsequent loss of DNA methylation are also substantial outcomes of decitabine treatment. DNA methylation relies on one-carbon metabolism to replenish the supply of the universal methyl donor S-adenosylmethionine (SAM); disruption of the SAM supply can result in loss of methylation[347]. Disruption of one-carbon metabolism can also reduce DNA methylation by virtue of limiting the available SAM[348]. Therefore, as an enzyme that is integral to mitochondrial one-carbon metabolism in breast cancer cells[334,349,350], MTHFD2 may impact response to de-methylating therapy via its role in one-carbon metabolism.

HPLC-MS metabolomics was performed to gain a preliminary characterization of the one-carbon metabolism state of MDA-MB-231 MTHFD2-KD (shRNA 68) tumours treated with decitabine. The tumour categories (Control NT, Control DAC, MTHFD2-KD NT, or MTHFD2-KD DAC) had distinct metabolite profiles, illustrated in principal component analysis (PCA; Figure 3.13). Decitabine treatment elicits an extensive shift of metabolites in the control tumours shown by the large discrepancy between Control NT

and Control DAC tumour samples in PCA. MTHFD2-KD NT and MTHFD2-KD DAC tumours were not as distinct, indicative perhaps of the lesser impact decitabine had on the MTHFD2-KD tumours. In unsupervised clustering of metabolites (Figure 3.14), the tumour categories generally cluster together, and portray the extent to which of metabolites are changed by decitabine treatment and/or MTHFD2-KD.

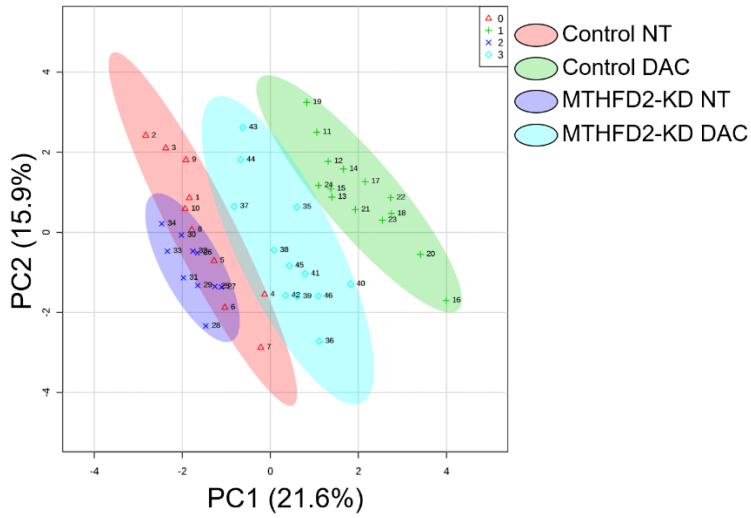

Figure 3.13: Principle Component Analysis (PCA) of metabolite abundances in MDA-MB-231 MTHFD2-KD decitabine-treated tumours reveals they have distinct metabolite profiles. (Control NT n=10; Control DAC n=14, MTHFD2-KD [shRNA 68] NT n=10, MTHFD2-KD [shRNA 68] DAC n=12). JPM, MAG, AC, and HW developed targeted metabolomics method, ran the mass spectrometer, and assisted in data analysis.

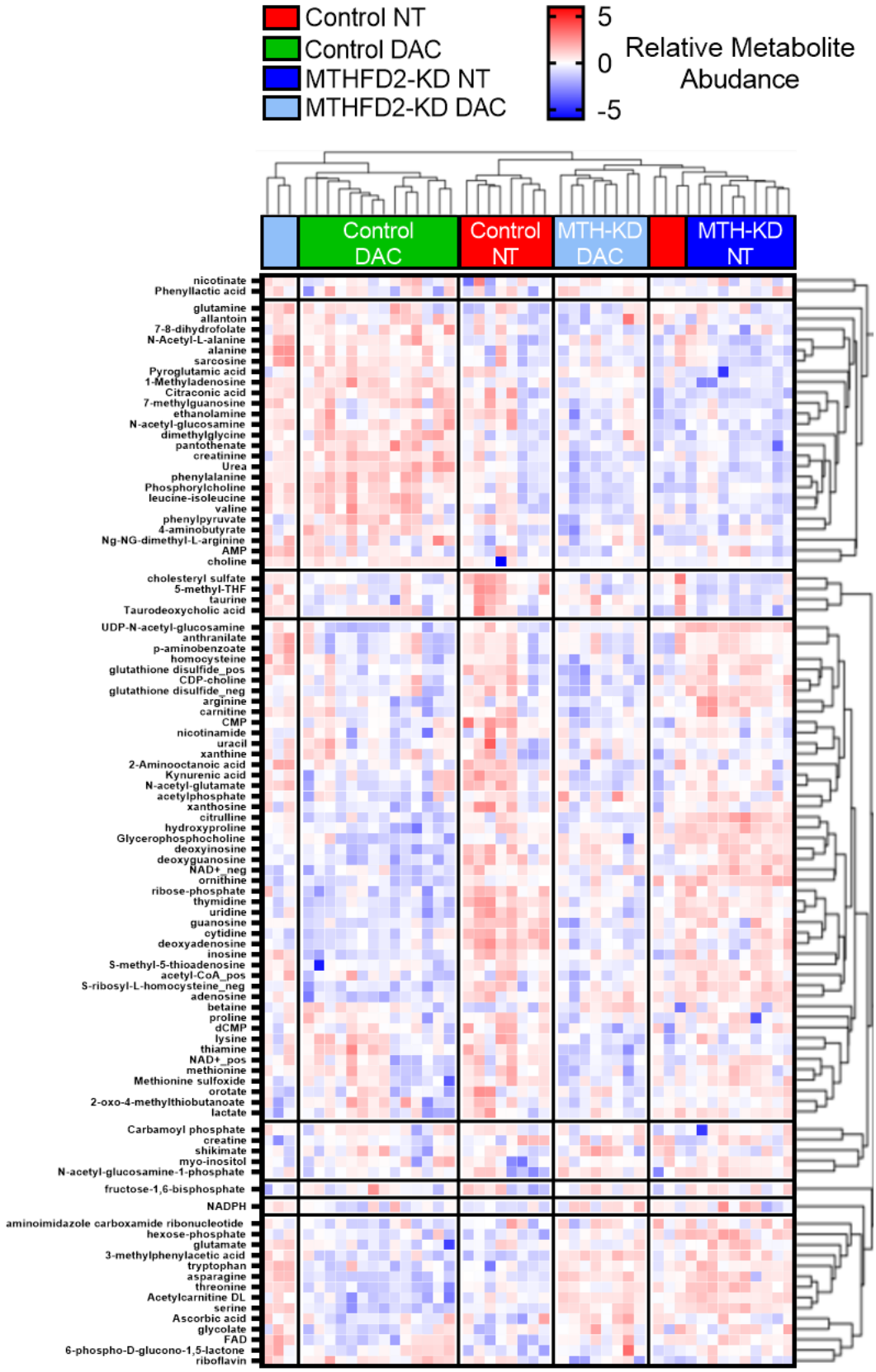
Control NT
Control DAC
MTHFD2-KD NT
MTHFD2-KD DAC
5
0
-5
Relative Metabolite Abudance
Control DAC
Control NT
MTH-KD DAC
MTH-KD NT
nicotinate
Phenyllactic acid
glutamine
allantoin
7-8-dihydrofolate
N-Acetyl-L-alanine
alanine
sarcosine
Pyroglutamic acid
1-Methyladenosine
Citraconic acid
7-methylguanosine
ethanolamine
N-acetyl-glucosamine
dimethylglycine
pantothenate
creatinine
Urea
phenylalanine
Phosphorylcholine
leucine-isoleucine
valine
phenylpyruvate
4-aminobutyrate
Ng-NG-dimethyl-L-arginine
AMP
choline
cholesteryl sulfate
5-methyl-THF
taurine
Taurodeoxycholic acid
UDP-N-acetyl-glucosamine
anthranilate
p-aminobenzoate
homocysteine
glutathione disulfide_pos
CDP-choline
glutathione disulfide_neg
arginine
carnitine
CMP
nicotinamide
uracil
xanthine
2-Aminooctanoic acid
Kynurenic acid
N-acetyl-glutamate
acetylphosphate
xanthosine
citrulline
hydroxyproline
Glycerophosphocholine
deoxyinosine
deoxyguanosine
NAD+_neg
ornithine
ribose-phosphate
thymidine
uridine
guanosine
cytidine
deoxyadenosine
inosine
S-methyl-5-thioadenosine
acetyl-CoA_pos
S-ribosyl-L-homocysteine_neg
adenosine
betaine
proline
dCMP
lysine
thiamine
NAD+_pos
methionine
Methionine sulfoxide
orotate
2-oxo-4-methylthiobutanoate
lactate
Carbamoyl phosphate
creatine
shikimate
myo-inositol
N-acetyl-glucosamine-1-phosphate
fructose-1,6-bisphosphate
NADPH
aminoimidazole carboxamide ribonucleotide
hexose-phosphate
glutamate
3-methylphenylacetic acid
tryptophan
asparagine
threonine
Acetylcarnitine DL
serine
Ascorbic acid
glycolate
FAD
6-phospho-D-glucono-1,5-lactone
riboflavin

Figure 3.14: Metabolite abundance heatmap for HPLC-MS metabolomics of MDA-MB-231 MTHFD2-KD decitabine-treated tumours. Unsupervised hierarchical clustering based on Euclidean distances was performed on EigenMS normalized metabolite abundances and is portrayed here as row-centered (z-score) relative metabolite abundances (Control NT n=10; Control DAC n=14, MTHFD2-KD [shRNA 68] NT n=10, MTHFD2-KD [shRNA 68] DAC n=12). JPM, MAG, AC, and HW developed targeted metabolomics method, ran the mass spectrometer, and assisted in data analysis.

MTHFD2 is key regulator of one-carbon metabolism in cancer cells; it is a mitochondrial enzyme which converts 5,10-methylenetetrahydrofolate (5,10-mTHF) to formyltetrahydrofolate (fTHF) (Figure 3.15A). Formate then passively diffuses out of the mitochondria to feed into nucleotide biosynthesis, ATP biosynthesis, and the methylation cycle. It has not been fully elucidated why cancer cells flux folate metabolism through the mitochondrial instead of through the essentially identical cytosolic pathway. MTHFD2's functional equivalent in the cytosol is methylenetetrahydrofolate dehydrogenase/cyclohydrolase and formyltetrahydrofolate synthetase 1 (MTHFD1), yet MTHFD1 does not seem to be able to fully compensate for loss of MTHFD2 and in cancer models where MTHFD2 is inhibited, growth suppression is observed[332,351–353].

Given MTHFD2's role as a moderator of folate metabolism in cancer cells, it was expected that MTHFD2-KD tumours would exhibit impaired folate metabolism. Knockdown of MTHFD2 resulted in reduced 5-methyl-THF (mTHF) and concurrent increased serine (Ser) abundance (Figure 3.15C). This is likely due to the loss of MTHFD2 causing the reversal of the THF/5,10-mTHF reaction resulting in subsequent gain of serine (Figure 3.15B)[350]. If glycine is removed from the media, then this reaction can no longer be reversed and 5,10-mTHF can no longer be converted to THF. This manifests as impaired growth of MTHFD2-KD cells in glycine depleted media but not in replete conditions

(Figure 3.16). THF but not 5,10-mTHF can be exported from the mitochondria, so in the absence of both glycine and MTHFD2 5,10-mTHF is trapped within the mitochondria, folate metabolism in breast cancer cells is hobbled and this results in a growth disadvantage.

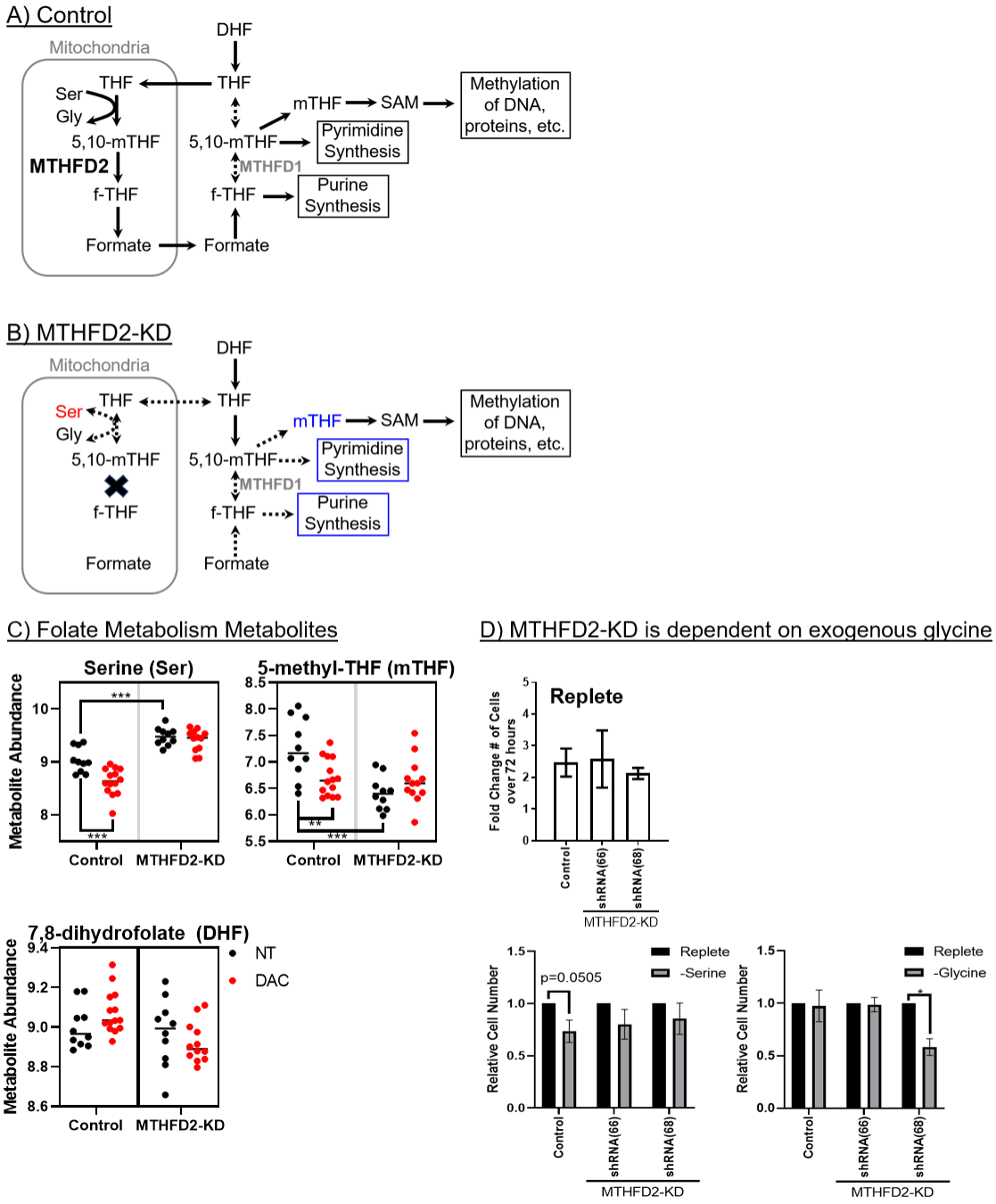

Figure 3.15: Disrupted folate metabolism of MTHFD2-KD MDA-MB-231 tumours. Schematic for how folate metabolism, methylation, and nucleotide synthesis interconnect in **A)** control cells with native high MTHFD2 activity and in **B)** MTHFD2-KD cells with mitochondrial folate metabolism inhibition. 7,8-dihydrofolate (DHF), THF (Tetrahydrofolate), 5,10-mTHF (5,10-methylenetetrahydrofolate), mTHF (5-methyl-tetrahydrofolate), fTHF (10-formyltetrahydrofolate), SAM (S-adenosylmethionine), Ser (serine), Gly (glycine). **C)** Mean abundance of metabolites within the folate cycle is altered in MTHFD2-KD and decitabine-treated MDA-MB-231 tumours. (Control NT n=10; Control DAC n=14, MTHFD2-KD [shRNA 68] NT n=10, MTHFD2-KD [shRNA 68] DAC n=12) One-way ANOVA with Tukey's post-hoc test; $p<0.01$**; $p<0.001$***. JPM, MAG, AC, and HW developed targeted metabolomics method, ran the mass spectrometer, and assisted in data analysis.

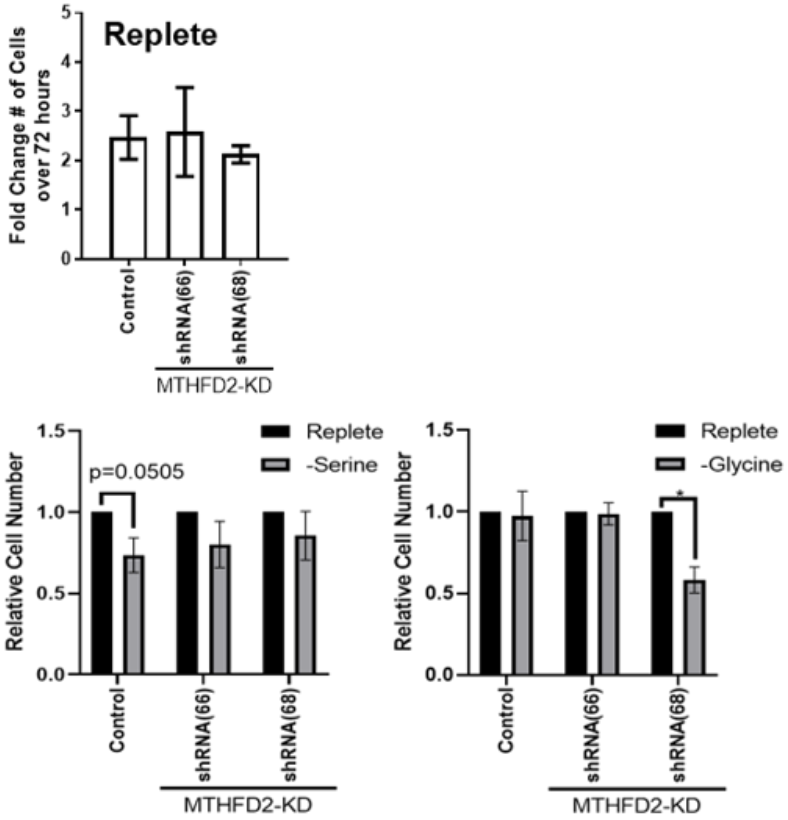

Figure 3.16: MDA-MB-231 MTHFD2-KD (shRNA 68) cells are dependent on exogenous glycine *in vitro*. Relative growth rate of MDA-MB-231 control or MTHFD2-KD cells grown for 72 hours in 10% dialyzed FBS media supplemented with non-essential amino acids +/- serine or glycine. Top graph is fold change of cell number over 72 hours growth period, with bottom graphs made relative to each clone's own growth rate in replete conditions. n=4, mean, SD error bars

3.3.9 *DECITABINE TREATMENT AND MTHFD2-KD IN MDA-MB-231 TUMOURS DEPLETE NUCLEOTIDE LEVELS BUT DO NOT ALTER LINE1 METHYLATION*

A major product of MTHFD2 one-carbon metabolism is adenosine for ATP as well as nucleotide biosynthesis. It is unclear how loss of MTHFD2 would impact DNA methylation. Trapping 5,10-mTHF in the mitochondria may slow the production of SAM and hinder DNA methylation; conversely, THF could be re-assigned to the cytosolic production of SAM resulting in increased DNA methylation capacity. The observed reduction of m-THF (Figure 3.15C) generally implies reduced SAM production. The consequence of impaired folate metabolism in MTHFD2-KD cells may include reduced nucleotide pools and/or aberrant DNA methylation.

Decitabine treatment is also known to interfere with DNA synthesis; therefore, both MTHFD2-KD and decitabine might reduce nucleotide levels in the tumour samples[337,354]. Tumours with MTHFD2 knockdown had reduced abundance of almost all nucleotides and precursors that were quantified by our HPLC-MS method (Figure 3.17A). More dramatic however was the loss of nucleotides in the decitabine-treated samples from both control and MTHFD2-KD tumours. The decitabine-associated loss of nucleotides was most pronounced in the control tumours which were relatively more sensitive to decitabine than MTHFD2-KD tumours.

Aside from nucleotide pre-cursors, one-carbon metabolism is essential for generation of the universal methyl donor S-adenosylmethione (SAM). SAM is the methyl donor for DNA methylation, and depletion of SAM can lead to reduced DNA methylation[348]. If MTHFD2 activity partially dictates SAM levels, then MTHFD2-KD tumours could have global DNA hyper/hypomethylation. To test this, methylation of long

interspersed nuclear elements (LINE1)—which comprise ≈17% of the genome and are an appropriate proxy for measuring genome-wide methylation— was assessed via bisulfite pyrosequencing in the decitabine-treated MTHFD2-KD tumours. Methylation was quantified at 27 CpGs within the class 1 Long Interspersed Nuclear Element, and there was no significant difference in methylation at any CpG site or average methylation across all 27 CpG sites (Figures 3.17A & 3.17B). Neither decitabine nor knockdown of MTHFD2 hypomethylated this class 1 LINE.

Together, this suggests that my decitabine treatment regimen (0.5 mg/kg 3/5-day cycles) is having a major impact on nucleotide abundance and may not result in global hypomethylation of DNA. Knockdown of MTHFD2 could impair growth of MDA-MB-231 tumours through a mechanism similar to decitabine by limiting the nucleotide pool. As for how MTHFD2 confers resistance to decitabine: MTHFD2-KD tumours are likely resistant to decitabine by virtue of their slow growth rate. Decitabine is a cell cycle dependent cytidine analog which is only incorporated during S-phase. MTHFD2-KD tumours are growth impaired (perhaps by weakened nucleotide biosynthesis) and therefore undergo fewer cell divisions during the treatment cycle than control tumours, incorporating less decitabine and appearing relatively resistant to its effects.

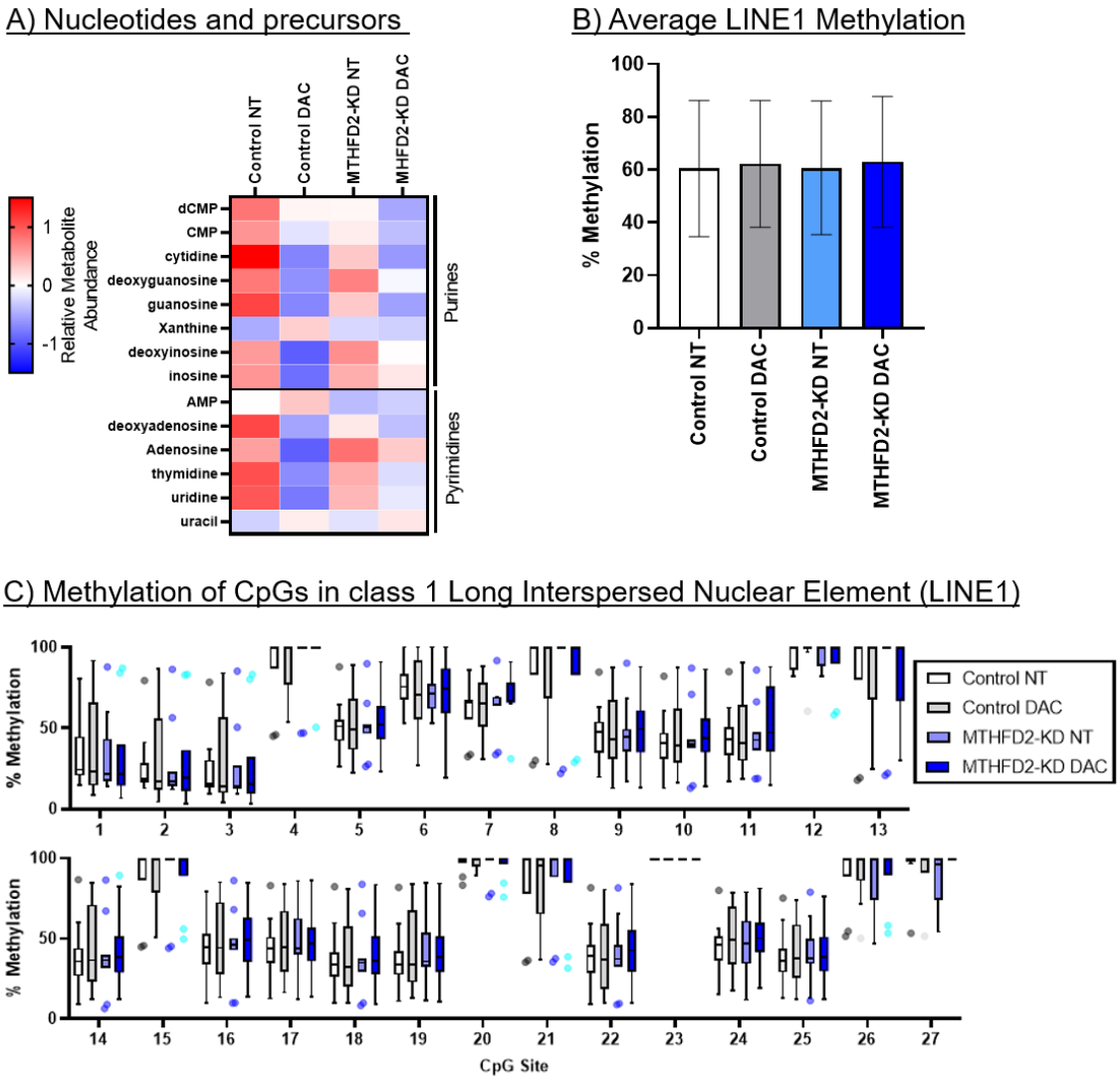

Figure 3.17: Methylation of class 1 long interspersed nuclear element (LINE1) in decitabine-treated MDA-MB-231 MTHFD2-KD (shRNA 66) tumours. A) Abundance of nucleotides or nucleotide pre-cursors is reduced in decitabine-treated and MTHFD2-KD tumours. (Control NT n=10; Control DAC n=14, MTHFD2-KD [shRNA 68] NT n=10, MTHFD2-KD [shRNA 68] DAC n=12) **B)** Methylation of individual CpG sites within LINE1 (median with quartiles and Tukey bars) and **C)** average methylation of all 27 CpG sites (mean with SD error bars). Control NT n=10, Control DAC n=9, MTHFD2-KD (shRNA 66) NT n=11, MTHFD2-KD (shRNA 66) DAC n=10. JPM, MAG, AC, and HW developed targeted metabolomics method, ran the mass spectrometer, and assisted in data analysis; ICGW performed bisulfite pyrosequencing of LINE1.

3.4 DISCUSSION

The intent of this genome-wide screen was to parse out functionally relevant "driver" hypermethylated tumour suppressor genes from the thousands of "passenger" genes which do not contribute to breast tumour growth. Another classification of genes that was likely to be revealed alongside the hypermethylated TSGs were genes that mediate response to decitabine treatment such as cytidine kinases (DCK; Chapter 2). Unexpectedly, I have instead identified a potent oncogene—MTHFD2, as a mediator of sensitivity to decitabine.

A major assumption of my approach was that there are hypermethylated tumour suppressor genes that are potent enough individually to affect growth of breast cancer cells. This has never been proven before, as most investigations towards hypermethylated TSGs follow a similar paradigm: 1) known tumour suppressor is hypermethylated in tumour cells compared to normal tissue, 2) treatment with a DNMT inhibitor de-methylates the tumour suppressor and resurrects expression, 3) reduced growth of tumour cells treated with the DNMT inhibitor is attributed to the now active tumour suppressor gene. These approaches downplay the other effects of de-methylating treatment such as the genome instability that accompanies global loss of DNA methylation as well as the differential expression of hundreds of genes in addition to the assayed hypermethylated TSG.

We do not know if DNA methylation is causative in breast cancer or is a symptom of other metabolic/genomic perturbations. Unlike leukemias which commonly harbour mutations to epigenetic machinery[264,308,355], breast cancers rarely have mutations to epigenetic modulators. Aberrant DNA methylation in breast cancer is often given a causative role in tumourigenesis and progression: common DNA methylation patterns in

breast cancer are attributed to the selective advantage that silencing a tumour suppressor gene would afford a cancer cell. Rapidly proliferating breast cancer cells would therefore accumulate an advantageous methylome that would evolve over time. My data here suggests that a single hypermethylated gene (e.g. APOD) does not impart a significant growth advantage to MDA-MB-231 breast cancer cells. Instead, aberrant DNA methylation in breast cancer is perhaps poised more as a symptom of dysregulated mitochondrial one-carbon metabolism.

Overexpression of MTHFD2 is an early event in oncogenic transformation, and contributes to the rapid proliferation of breast cancer cells by facilitating nucleotide production[351,356,357]. Cancer cells are "nucleotide factories", supported by consistent up-regulation of nucleotide synthesis enzymes in almost all tumours[358]. Other one-carbon metabolism modules have a high degree of intratumoural and interpatient variability in their expression, including those enzymes responsible for DNA methylation[359]. The preoccupation with nucleotide synthesis (driven by MTHFD2) may come at the expense of replenishing SAM pools and may contribute to the global loss of DNA methylation that is seen in almost all tumours. Though I did not observe a gain of LINE1 methylation in the MTHFD2-KD tumours, it would be interesting to see what a more inclusive DNA methylation profile (i.e. the HM450 array) would reveal. Global hypomethylation with concurrent hypermethylation of promoter regions may yet be due to an imbalance of one-carbon metabolism. Perhaps there is still an important interaction between MTHFD2 mitochondrial one-carbon metabolism and the establishment/maintenance of DNA methylation patterns. Alternatively— and more likely— MTHFD2-KD disrupts nucleotide

biosynthesis, reducing proliferation, and thus reducing the effect of S-phase dependent decitabine.

Since MTHFD2-KD tumours are impaired in their proliferative ability, they would not incorporate decitabine to the same extent as their control cell counterparts- imparting MTHFD2-KD cells with a sort of artificial decitabine resistance. This study should be repeated with a third generation non-nucleoside DNMT inhibitor which would be independent of cell proliferation[360–362]. An additional quality metric that should be included prior to de-convoluting the shRNA abundances in the tumours, is ensuring that the de-methylating therapy was able to significantly hypomethylate tumour DNA. I did not confirm efficient decitabine-induced hypomethylation here, and the LINE1 methylation results would suggest that global loss of methylation did not occur in the decitabine treated tumours. My treatment regimen of 0.5 mg/kg systemic decitabine was based on landmark papers which established that this dosing schedule exerts durable DNA hypomethylation in xenografted breast cancer cell lines[274,363]. A 10x higher dose of decitabine (5 mg/kg) has been previously used to treat MDA-MB-231 xenografts, but was seen to cause more DNA damage-related effects[364]. Toxicity was a limiting factor for my 0.5 mg/kg decitabine dosing schedule, so increasing the number of treatments to induce hypomethylation is impractical. Recreating the study using a non-nucleoside DNMT inhibitor is an important step to establishing an interaction between MTHFD2 and decitabine treatment[360,361].

Other improvements could be made to the shRNA screen itself. More recent shRNA-based screens contain far more shRNAs per gene. More shRNAs per gene aids the prioritization of screen hits because multiple shRNAs for a gene which exert a similar effect strongly imply that gene has a role in the phenotype. In our ThermoFisher Decode

screen, 3504 genes had to be excluded from ATARiS gene prioritization because only one shRNA was targeted to those genes. Using an expanded shRNA library in tandem with a non-nucleoside DNMT inhibitor would be technical improvements over my methodology.

Realistically, first generation DNMT inhibitors like decitabine are not going to be applied as single agents in the treatment of solid tumours. Clinical trials have been too disappointing, and there is not enough evidence to support that these agents can effectively de-methylate tumour DNA[326,365,366]. The future of epigenetic therapy for breast cancer patients may include non-nucleoside based DNMT inhibitors in tandem with other chemotherapies or immunotherapies. MTHFD2 inhibitors are also being developed and will enter clinical trials for the treatment of multiple malignancies soon[367,368]. If there is a relationship between MTHFD2 and DNA methylation, as this screen may suggest, then there may be some predictive signature for DNMT inhibitor response that involves MTHFD2 (i.e. tumours with high MTHFD2 may be more sensitive to decitabine treatment). If this is the case, we can better apply epigenetic therapy and MTHFD2 inhibitors.

CHAPTER 4: INHIBITION OF ALDH1A3 REDUCES BREAST TUMOUR GROWTH AND INHIBITS RETINOIC ACID-ASSOCIATED GENE EXPRESSION

Copyright statement

This chapter has been previously published as:

Thomas ML, R De Antueno, KM Coyle, M Sultan, BM Cruickshank, MA Giacomantonio, R Duncan CA Giacomantonio, P Marcato (2016). Citral reduces breast tumour growth by inhibiting cancer stem cell marker ALDH1A3. Molecular Oncology doi: 10.1016/j.molonc.2016.08.004

The text and figures appearing here have been edited for clarity and to include supplemental figures and tables.

Contribution statement

I wrote the manuscript and designed the experiments with the guidance of Dr. Paola Marcato. The manuscript was reviewed and edited by all authors. I performed experiments and collected data with assistance as follows:

RDA & RD: optimization and preparation of citral nanoparticles. KMC: Western blots and RT-qPCR. MS and MAG: RT-qPCR. BMC: nanoparticle preparation. PM: tail vein injection of nanoparticles.

4.1 INTRODUCTION

First described in leukemia[98], and later in solid tumours, cancer stem cells (CSCs) are a highly tumourigenic subpopulation present within the heterogeneous tumours of many cancers including breast cancer[97]. These cells share certain characteristics with normal stem cells including the ability to self-renew and to differentiate. CSCs also demonstrate a highly malignant phenotype, being able to initiate tumours, and promote epithelial-to-mesenchymal transition and metastasis[97,100,237]. Most concerning in terms of effective patient treatment and mitigating the risk of recurrence is the resistance of CSCs to common chemotherapies and radiotherapy[369,370]. These characteristics suggest that CSCs must be eliminated during treatment to avoid risk of relapse, and that this subpopulation of cells is poised to avoid elimination. Thus, therapies that target CSC activities may improve cancer treatment efficacy and patient outcomes.

CSC-associated enzymes and signaling pathways may provide novel avenues of therapeutic intervention, since these pathways (e.g. Notch, Wnt, and Hedgehog[371]) and enzymes (e.g. aldehyde dehydrogenases; ALDHs) are also mediators of tumourigenicity, metastasis, and therapy resistance. A common biomarker for CSC identification is high Aldefluor fluorescence associated with increased ALDH activity[104]. ALDHs are a superfamily of enzymes present in all three taxonomic domains with 19 isoforms expressed in humans[134]. ALDHs convert aldehydes to carboxylic acids; metabolic processes generate toxic aldehydes and ALDHs are required to maintain cellular homeostasis. Furthermore, individual ALDH isoforms have varied substrate specificity and more specialized functions. Members of the ALDH1A family (ALDH1A1, ALDH1A2, ALDH1A3) oxidize

the vitamin A metabolite, retinal, to retinoic acid (RA), a developmental cell signalling and gene expression induction molecule that also plays an important role in cancer[226].

Both ALDH1A1 and ALDH1A3, as well as other isoforms (e.g. ALDH1A2, ALDH2 and ALDH7A1), have been implicated as contributors to CSC-associated Aldefluor fluorescence, with specific isoforms playing a more predominant role in different cancers[136,144,372–375]. In particular, expression of the ALDH1A3 isoform is of primary importance for the Aldefluor fluorescence of breast cancer, lung cancer, melanoma, malignant pleural mesothelioma, and head and neck cancer[136,138,142,144,376]. In addition to being associated with CSCs, expression of ALDH1A1 and ALDH1A3 often correlates with poor prognosis in cancers such as breast, prostate and lung, kidney, esophageal, and head and neck[100,104,372,377–380]. ALDH1A3 has also been directly implicated in tumour progression and therapy resistance. For breast cancer, ALDH1A3 been shown to promote tumour growth and metastasis though production of retinoic acid (RA) and expression of RA-inducible genes[138]. ALDH1A3 also promotes the growth of lung tumours, glioblastoma, and melanoma[143,144,381]. Furthermore, it is associated with the chemoresistant population of mesothelioma[376] and is a causative agent in the radioresistant population of head and neck cancer[20]. Together, these results suggest that targeting CSC-associated ALDH1A enzymes, in particular ALDH1A3, may be an effective adjuvant cancer therapy[142,380].

Due to their promise as an anti-CSC agent, several ALDH inhibitors have been explored for anti-cancer activity. Pan-ALDH inhibitor DEAB reduces growth of melanoma xenografts and the number of residual melanoma cells[381]. However, DEAB has a very short duration of efficacy *in vivo* and probably requires modification or encapsulation to have

therapeutic value[382]. Another ALDH inhibitor of considerable interest is disulfiram, which can inhibit TGF-β induced "stem like" features of MDA-MB-231 breast cancer cells[383], increase chemosensitivity[224], and also reduce mammosphere formation[384]. However, the ability of disulfiram to directly inhibit ALDH in breast cancer cells was not confirmed, and though mammospheres had increased expression of ALDH1A3, disulfiram did not reduce mammosphere-associated ALDH1A3 mRNA. Thus, the effect of specifically inhibiting ALDH1A3 has not been explored yet, nor is the specificity of disulfiram for ALDH1A3 known.

A panel of compounds known to inhibit at least one ALDH isoform and with unknown ALDH1A3 inhibitory activity were investigated for their potential as ALDH1A3 inhibitors in breast cancer. Citral was identified as a strong inhibitor of ALDH1A3 and reduced ALDH1A3-dependent colony formation, gene expression, and tumour growth. To my knowledge, this is the first study to characterize inhibitors of ALDH1A3 specifically and is the first to show that inhibiting ALDH1A3 can slow breast tumour growth.

4.2 MATERIALS AND METHODS

4.2.1 *ALDH INHIBITORS AND CELL LINES*

All ALDH inhibitors were acquired from Sigma and dissolved in the indicated vehicle (Table 4.1). MDA-MB-231, MDA-MB-468, or SKBR3 cells were challenged with dissolved drug or vehicle alone at the indicated final concentration. The cells were obtained from American Type Culture Collection and the same ALDH isoform overexpression or knockdown clones generated and validated in our prior publications (ALDH1A1 shRNA 1, ALDH1A3 shRNA 3 and ALDH2 shRNA2; Table 4.2; Figures 4.1-4.4) were used[136,138]. All cells were cultured in Dulbecco's Modified Eagle Medium (Invitrogen) supplemented with 10% fetal bovine serum (Invitrogen), 1X antibiotic-antimycotic (Invitrogen), and 0.25 µg/mL puromycin (Sigma) in a 37°C humidified chamber with 5% CO_2.

Table 4.1: ALDH inhibitors used in current study. Compounds were dissolved in the indicated vehicle at the given stock concentration based on manufacturer specifications. All compounds were obtained from Sigma.

Compound	Cat. Number	Vehicle	Stock concentration
3-Hydroxy-dl-kynurenine	H1771	Hydrochloric acid	100mM
Benomyl	45339	Chloroform	100mM
Chloral Hydrate	C8383	Water	100mM
Citral	C83007	Dimethyl sulfoxide	100mM
Cyanamide	187364	Water	100mM
Daidzin	30408	Dimethyl sulfoxide	50mM
DEAB	D86256	Dimethyl sulfoxide	100mM
Disulfiram	86720	Dimethyl sulfoxide	20mM
Gossypol	G8761	Methanol	5mM
Kynurenic Acid	K3375	Dimethyl sulfoxide	25mM
Molinate	36171	Water	2mM
Pargyline	P8013	Water	100mM

Table 4.2: shRNA knockdown sequences (from Marcato, 2011) used to generate ALDH1A1, ALDH1A3, and ALDH2 knockdowns[136].

Target	shRNA	Sequence
ALDH1A3	shRNA1	TGCTGTTGACAGTGAGCGCGCATAGCAAATCCTAGGATAA TAGTGAAGCCACAGATGTATTATCCTAGGATTTGCTATGCT TGCCTACTGCCTCGGA
	shRNA2	TGCTGTTGACAGTGAGCGCGCTGTAATTCACTTTAACAAAT AGTGAAGCCACAGATGTATTTGTTAAAGTGCCTTACAGATT GCCTACTGCCTCGGA
ALDH1A1	shRNA1	TGATGTTGACAGTGAGCGCCCACGTGGACTCTTTAATAAAT AGTGAAGCCACAGATGTATTTATTAAAGATGCCACGTGGA TGCCTACTGCCTCGGA
	shRNA2	TGATGTTGACAGTGAGCGCGGAGTGTTTACCAAAGACATTT AGTGAAGCCACAGATGTAAATGTCTTTCCTAAACACTCCTT TGCCTACTGCCTCGGA
ALDH2	shRNA1	TGCTGTTGACAGTGAGCCGAGCTGATAAGTACCACGGGAA ATAGTGAAGCCACAGATGTATTTCCCGTGGTACTGCCTCGG A
	shRNA2	TGATGTTGACAGTGAGCGCGCAGGCATACACTGAAGTGAA TAGTGAAGCCACAGATGTATTCACTTCAGTGTATGCCTGCA TGCCTACTGCCTGGA

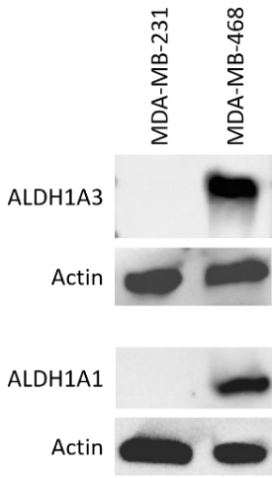

Figure 4.1: Protein expression of ALDH1A1 and ALDH1A3 in MDA-MB-231 and MDA-MB-468 cells. Endogenous ALDH1A1 and ALDH1A3 protein levels are detected by western blot in the cell lines. KMC generated Western blot.

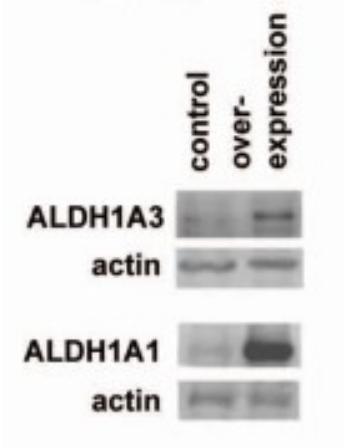

Figure 4.2: Overexpression of ALDH1A3 and ALDH1A1 increases the ALDH protein levels in MDA-MB-231 cells. ALDH1A3 and ALDH1A1 protein levels are detected by western blot in the cell lines (vector control or overexpression clones). Taken from Supplementary Figure 1 Marcato, 2015[1].

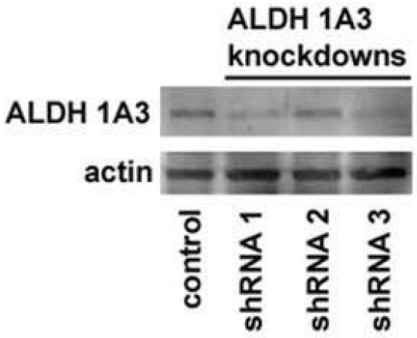

Figure 4.3: Knockdown of ALDH1A3 reduces ALDH1A3 protein levels in MDA-MB-468 cells. ALDH1A3 protein levels are detected by western blot in the cell lines (vector control or knockdown clones); shRNA 3 used in the current study. Taken from Figure 5 Marcato, 2011[2].

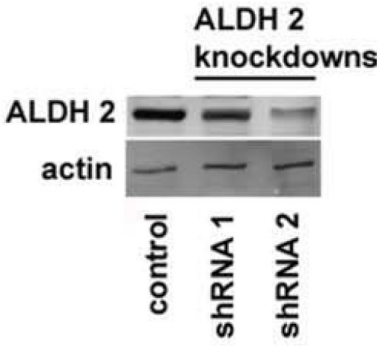

Figure 4.4: Knockdown of ALDH2 reduces ALDH2 protein levels in SKBR3 cells. ALDH2 protein levels are detected by western blot in the cell lines (vector control or knockdown clones); shRNA 2 used in the current study. Taken from Figure 5 Marcato, 2011[2].

4.2.2 *Western Blot determination of ALDH1A1 and ALDH1A3 protein levels*

Western blotting of cell lysates performed using anti-human ALDH1A1 (mouse monoclonal; BD Bioscience or ALDH1A3 (mouse monoclonal clone 4EB; Origene) followed by secondary species-specific horseradish peroxidase (HRP)-conjugated goat anti-mouse IgG (Jackson Immunoresearch) were used to detect ALDH isoforms protein levels. β-actin was detected using specific mouse monoclonal antibody (Santa Cruz Biotechnologies). Immuno-reactive proteins were detected by chemiluminescence (using Clarity ECL blotting substrate (Bio-Rad)) and visualized with images captured with a ChemiDoc Imager (Bio-Rad).

4.2.3 *Aldefluor Assay on Patient-Derived Xenograft and Cell Lines*

A patient-derived xenograft (PDX) previously established in female NOD/SCID mice[136] was harvested to generate cell suspensions. Red blood cells were lysed, and remaining cells were washed with PBS and Aldefluor assay performed as per the manufacturer's instructions (Stemcell Technologies), with or without the addition of one of the panel of drugs (Table 4.1). To eliminate dead cells and non-cancer cells of mouse origin, cells were stained with viability stain 7-AAD (Biolegend) and anti-H2Kd (mouse histocompatibility class I) conjugated to Alexafluor 647 nm (Biolegend), respectively. Cell populations were identified using a FACSCalibur flow cytometer (Becton Dickinson). Distinct Aldefluor-positive and Aldefluor-negative populations in the PDX were revealed after excluding debris, mouse, and dead cells. For cell line assays anti-H2Kd stain was not used and Aldefluor levels were quantified via mean fluorescence intensity.

4.2.4 *Flow cytometry analysis of CD24 and CD44 expression upon citral treatment*

MDA-MB-231 control and ALDH1A3-OE cells were seeded at 400,000 cells/well in a 6-well plate and treated for 24 hours with 100 μM citral or plain media. Cells were trypsinized and washed with PBS before CD24/CD44 staining using CD24 (Biolegend) conjugated to Alexafluor 519nm; and CD44 (eBioscience) conjugated to Alexafluor 575nm. To eliminate dead cells, cells were stained with viability stain 7-AAD (Biolegend). Cell populations were identified using a FACSCalibur flow cytometer (Becton Dickinson).

4.2.5 *Quantifying live cells*

Cells quantified for percentage of early and late apoptotic cells via Alexa Fluor 488 conjugated- Annexin V (Invitrogen) and 7-AAD (Biolegend) staining following the manufacturer's protocol and analyzed with a FACSCalibur.

4.2.6 *Generation of Citral Nanoparticles (Citral-NP)*

Nanoparticle encapsulated citral (citral-NP) and empty nanoparticles (vehicle control) were generated based on Zeng *et al.,* 2015 protocols with few modifications[385]. Briefly, 1 mL of a 0.5 mM polyethylene glycol-block-polycaprolactone (Polymer Source, Quebec, CAN; PEG-b-PCL; MW PEG: 10,000; MW PCL: 5,000) solution was made in HPLC-grade acetone (ThermoFisher Scientific). Citral (16 mg/mL), followed by 1 mL of PBS added while vortexing to form nanoparticles. Rotary evaporation and nitrogen gas flushing removed acetone. Samples were reconstituted and centrifuged at 8,000 x g for 5 minutes for the separation of two distinct layers: an upper waxy layer containing polymer

aggregates and excess unencapsulated citral, and a lower more fluid layer containing nanoparticles. The lower layer was collected and unencapsulated citral and nanoparticles >220 nm were removed by filtering (0.22 µm nylon syringe filter, Fisher Scientific).

4.2.7 *HPLC DETERMINATION OF CITRAL-NP CONCENTRATION*

High performance liquid chromatography (HPLC) was used to measure the concentration of nanoparticle encapsulated citral. A known dilution of citral-NP was injected into a 18C 3.9x150 mm Symmetry column (Waters) and eluted at room temperature with isocratic 40% water and 60% acetonitrile (both, with 0.1% trifluoroacetic acid) for 10 minutes at a rate of 0.5 mL/minute using a Waters 2695 separations module and a Waters 2487 dual λ absorbance detector set at 254nm. No peaks were detected for PEG-b-PCL at this wavelength, whereas acetone eluted at ≈2.55 minutes (Figure 4.5).

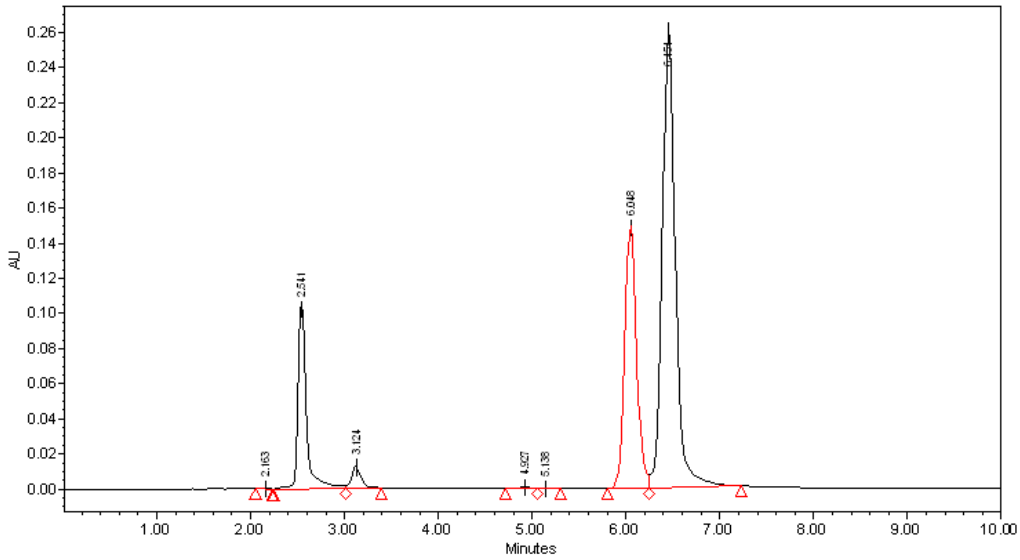

Figure 4.5: Representative HPLC chromatogram showing contamination of citral nanoparticles with acetone used to solubilize the PEG-b-PCL polymer. Acetone elutes at 2.5 minutes; the two citral isomers neral and geranial elute at 6 minutes and 6.4 minutes, respectively. Citral-NP sample with residual acetone was obtained by excluding the nitrogen gas flushing step from the nanoparticle preparation protocol. RDA and RD assisted with nanoparticle optimization and generation.

4.2.8 *CALCULATING THE LOADING EFFICIENCY OF CITRAL-NP MICELLES*

Example calculation: 64 mg citral added per 1 mL citral-NP preparation. Average of 8.05 mg citral in final nanoparticle encapsulated citral samples as determined through HPLC analysis. This value is post-evaporation, post-phase separation, and post-filtration. On average, 0.12 mg of final sample is unencapsulated "free" citral. This value was determined by HPLC analysis of sample prepared with identical protocol as citral-NP except no polymer was added.

8.05 mg - 0.12 mg = 7.93 mg nanoparticle encapsulated citral

7.93 mg / 64 mg = **12.4%** of 64 mg initial citral is successfully encapsulated

4.2.9 *TUMOUR GROWTH INHIBITION STUDY WITH UNENCAPSULATED CITRAL*

Eight week old NOD/SCID female mice were orthotopically injected in the mammary fat pad four with 2 x 10^6 vector control or ALDH1A3 overexpression MDA-MB-231 cells, admixed in 1:1 ratio with phenol red-free high concentration matrigel (Fisher Scientific). Subsequently, the mice were randomly divided into vehicle (dimethyl sulfoxide; DMSO) or citral treatment groups and were injected intraperitoneally for three consecutive days then one day no injection for 56 total days with 20 µL of vehicle or citral (0.1 mg per dose) (n=6 mice per group). Resulting tumour growth was quantified (mm^3, length x width x height / 2) for the duration of the experiment.

4.2.10 *IN VIVO CITRAL-NP TREATMENT*

Eight-week-old NOD/SCID female mice were orthotopically injected with 2 x 10^6 MDA-MB-231 vector control or ALDH1A3 overexpression cells, admixed in 1:1 ratio

with phenol red-free high concentration matrigel (Fisher Scientific). Subsequently, the mice were randomly divided into empty-NP (NT) or citral-NP treatment groups (n=6 per group) and were injected via tail vein every 3 or 4 days (alternating) with 100 µL of citral-NP (0.4 mg/kg) or saline. Resulting tumour growth was quantified (length x width x height / 2) and on day 38 the tumours were harvested and weighed from euthanized mice.

4.2.11 *IN VITRO GROWTH RATE ANALYSIS*

Seeded cells were treated with 100 µM citral or vehicle control and collected and counted 24 or 72 hours later. Growth rate = number of cells at a time point / number of cells pre-treatment, normalized to the vehicle control, no treatment (NT) growth rate.

4.2.12 *COLONY FORMING ASSAY*

Seeded cells were treated with 100 µM citral or vehicle for 24 hours prior to re-seeding at very low confluency for single cell generation of colonies (20 cells/cm^2 for MDA-MB-231 cells, 50 cells/cm^2 for MDA-MB-468 cells) and cultured for 13 days with media change every other day. Resulting colonies were visualized by methanol fixation and 0.05% crystal violet staining. Colonies >50 cells were counted, and colony forming efficiency = number of colonies / number of seeded cells.

4.2.13 *REVERSE TRANSCRIPTASE QUANTITATIVE PCR (RT-QPCR)*

After treatment with the ALDH inhibitors for 24 hours, RNA from the cells was extracted using Trizol (Invitrogen) and the Purelink RNA kit (Invitrogen), and reverse

transcribed with iScript™ cDNA Synthesis Kit (Bio-Rad) as per manufacturer's instructions. Reverse transcriptase quantitative PCR (RT-qPCR) used SsoAdvanced Universal SYBR supermix (Bio-Rad) with gene-specific primers (Table 4.3) was performed as per manufacturer's instructions using a 96CFX Touch Real-Time PCR Detection System (Bio-Rad). Standard curves were generated to incorporate primer efficiencies and relative levels of mRNA were calculated utilizing internal reference gene B2M.

Table 4.3: RT-qPCR primer sequences

	Gene		Sequence
Housekeeping Gene	**B2M**	Forward	AGGCTATCCAGCGTACTCCA
		Reverse	CGGATGGATGAAACCCAGACA
RA-Inducible Gene	**RARRES1**	Forward	ACGGCTCATCGAGAAAAAGA
		Reverse	GAAAGCCAAATCCCAGATGA
	RARβ	Forward	GGTTTCACTGGCTTGACCAT
		Reverse	GGCAAAGGTGAACACAAGGT
	ELF3	Forward	CCAGCGATGGTTTTCGTGAC
		Reverse	GATGTCCCGGATGAACTCCC
CSC-Associated Gene	**ITGA6**	Forward	TCAGCCAAAGATACTAGTGCCA
		Reverse	TTGAGGATCACCTACATAGAGCG
	CD44	Forward	CCCATTCGACAACAGGGACA
		Reverse	AGCTGAGGTCACTGGGATGA
	ALDH1A1	Forward	TGTTAGCTGATGCCGACTTG
		Reverse	TTCTTAGCCCGCTCAACACT
Pluripotency Gene	**SOX2**	Forward	AACCAGCGCATGGACAGTTA
		Reverse	GACTTGACCACCGAACCCAT
	POU5F1	Forward	TGATCCTCGGACCTGGCTAA
		Reverse	CCCCACAGAACTCATACGGC
	NANOG	Forward	CCTGTGATTTGTGGGCCTGA
		Reverse	GGGCTGTCCTGAATAAGCAGA

4.2.14 *STATISTICAL ANALYSIS*

GraphPad Prism Version 4 was used to perform one-way ANOVAs and post-hoc tests, or paired t-tests as indicated in the figure legends. Significance is indicated as follows $p<0.05$*, $p<0.01$**, $p<0.001$***.

4.3 RESULTS

4.3.1 *CITRAL, DEAB, AND BENOMYL ELIMINATE THE ALDEFLUOR-POSITIVE POPULATION OF A BREAST CANCER PATIENT DERIVED-XENOGRAFT TUMOUR*

To identify a compound that would inhibit ALDH1A3 activity specifically and ALDH1A3-mediated breast tumour growth, I compiled a group of previously described ALDH inhibitors, some of which had been tested for cytotoxic effects, tumour growth inhibition potential, and anti-CSC activity[256]. As a first assessment of the ALDH inhibition capacity of the compounds, I tested their ability to reduce Aldefluor fluorescence associated with CSCs[104,136]. Using a PDX previously demonstrated to contain Aldefluor-positive tumour initiating cells and high ALDH1A3 expression[136], I quantified and compared the efficiency of the 12 compounds[256] to eliminate the Aldefluor-positive population from the PDX tumour *ex vivo*. PDX cells from serial passages were incubated with the Aldefluor substrate with increasing concentrations of ALDH inhibitor. The mean percentage Aldefluor-positive cells in this PDX was 4.56%. Of the 12 inhibitors tested, citral, DEAB and benomyl significantly reduced the Aldefluor-positive population (Figure 4.6). Interestingly, disulfiram, which has previously been used as an ALDH inhibitor in cancer models[224], only partially eliminated the Aldefluor-positive population (Figure 4/6B, not significant). This suggests that at least for this PDX, citral, DEAB and benomyl have superior activity against the Aldefluor-positive tumour population.

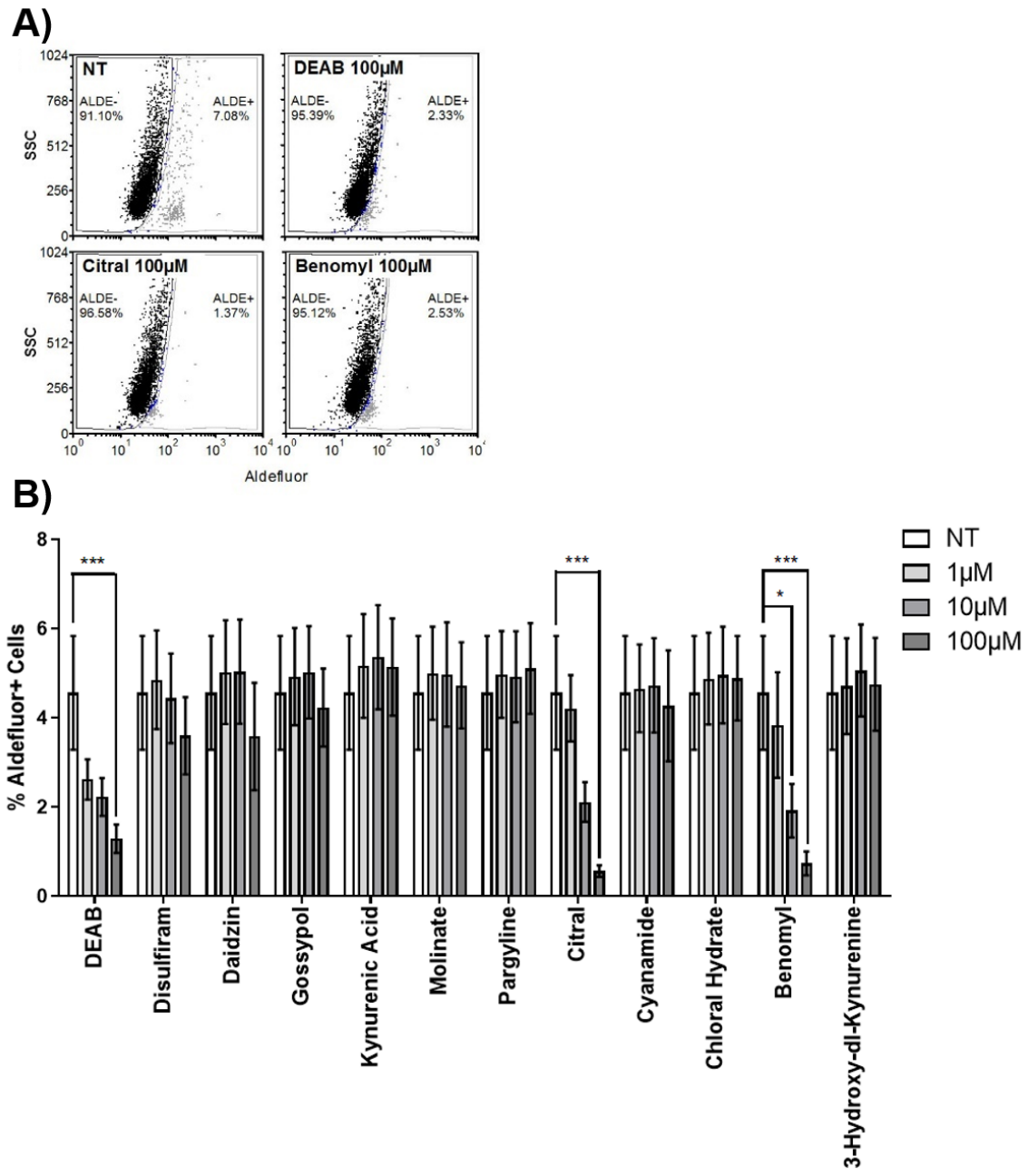

Figure 4.6: Citral, benomyl, and DEAB eliminate the Aldefluor+ population in a patient-derived xenograft (PDX) *ex vivo*. A) Representative dot plots. **B)** Indicated drugs were added to harvested tumour cells of a PDX and Aldefluor assay performed. Significance determined by one-way ANOVA with Tukey post-hoc test.

4.3.2 *CITRAL IS MOST EFFECTIVE AT INHIBITING ALDEFLUOR FLUORESCENCE INDUCED BY ALDH1A3*

Multiple ALDH isoforms can contribute to the Aldefluor fluorescence observed in breast cancer cells, with ALDH1A3, as well as ALDH1A1 and ALDH2 to a lesser degree, being the most important[136]. Therefore, cell lines with defined ALDH isoform expression were used to compare the specificity of the compounds for inhibiting the production of Aldefluor fluorescence by a specific isoform. For this purpose, I used MDA-MB-231, MDA-MB-468 and SKBR3 breast cancer cells.

MDA-MB-231 cells have very low endogenous Aldefluor fluorescence[136], and therefore served as a good model system to introduce isoform-specific Aldefluor fluorescence by overexpressing individual ALDH isoforms. The low protein expression of ALDH1A1 and ALDH1A3 in MDA-MB-231 cells in comparison to MDA-MB-468 cells was previously reported via quantitative proteomics[386] and is visualized here by western blotting in Figure 4.1. Overexpression of ALDH1A1 or ALDH1A3 to a greater degree, significantly increased mean Aldefluor fluorescence compared to that of cells with vector control (Figure 4.8A and 4.7A, respectively). Expression of the ALDH isoforms was previously shown[138], and illustrated here in Figure 4.2. ALDH1A3-specific Aldefluor fluorescence can also be modeled with MDA-MB-468 breast cancer cells that have endogenously high Aldefluor fluorescence dependent upon ALDH1A3 expression[136]. Knockdown ALDH1A3 cells showed significantly reduced mean Aldefluor fluorescence compared to scramble control (Figure 4.7B). Similarly, ALDH2-associated Aldefluor fluorescence can be modeled with SKBR3 breast cancer cells with high endogenous levels of ALDH2 activity[136]. Knockdown ALDH2 cells showed significantly lower mean Aldefluor fluorescence compared to cells with scramble control (Figure 4.8B). The

reduction of ALDH1A3 and ALDH2 protein levels in the knockdown cell lines was shown previously[136], and illustrated here in Figures 4.3 and 4.4.

To assess the effect of the 12 compounds on Aldefluor fluorescence induced by ALDH1A1, MDA-MB-231 cells overexpressing ALDH1A1 (ALDH1A1-OE) were incubated with Aldefluor substrate in the presence of increasing drug concentrations. Only DEAB significantly reduced the mean Aldefluor fluorescence of MDA-MB-231 ALDH1A1 cells (Figure 4.8A), suggesting the other drugs were ineffective ALDH1A1 inhibitors under the experimental conditions.

Similarly, to assess the effect of the inhibitors on Aldefluor fluorescence mediated by ALDH1A3, increasing concentrations of the compounds were added to MDA-MB-231 cells with or without overexpression of ALDH1A3 (ALDH1A3-OE), and to MDA-MB-468 cells with high endogenous ALDH1A3-dependent Aldefluor fluorescence. Of the 12 inhibitors tested, citral, DEAB and benomyl significantly reduced ALDH1A3-mediated Aldefluor fluorescence production in the breast cancer cells (Figure 4.7); however, citral was the most effective, significantly inhibiting ALDH1A3 at the lowest concentration of 1 μM.

Finally, ALDH2-dependent Aldefluor fluorescence production was challenged with increasing concentrations of the compounds applied to SKBR3 cells with predominately ALDH2-dependent Aldefluor fluorescence. Citral, DEAB and benomyl significantly reduced Aldefluor fluorescence of SKBR3 cells to a similar extent, suggesting that all three compounds effectively inhibit ALDH2 (Figure 4.8B). Therefore, in terms of reducing Aldefluor fluorescence specifically associated with ALDH1A3 or ALDH2, citral was the most effective inhibitor, while DEAB was the most effective pan ALDH inhibitor.

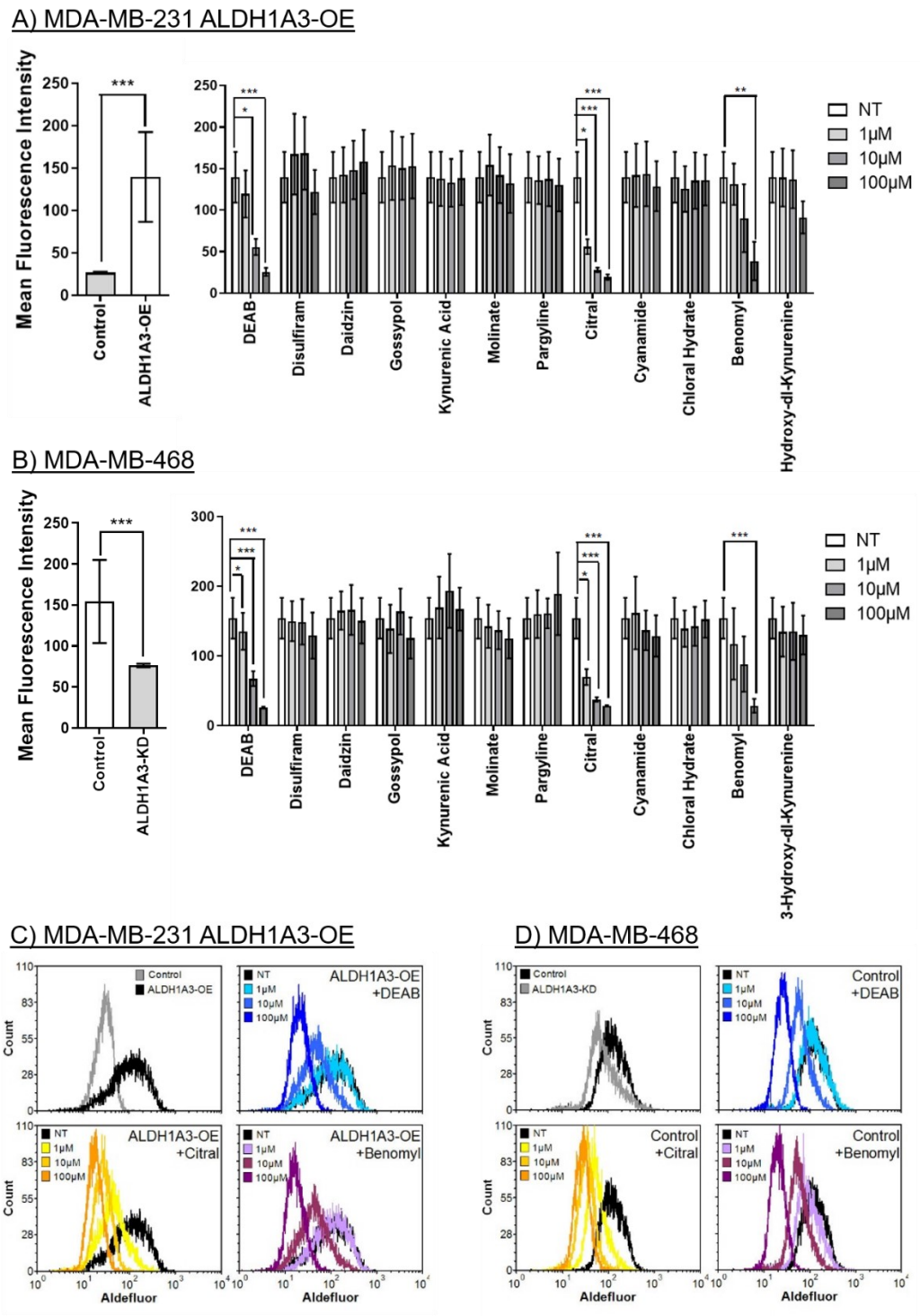

Figure 4.7: Citral is the best inhibitor of ALDH1A3-mediated Aldefluor positivity quantified by mean fluorescence intensity. The effect of overexpression or knockdown of ALDH1A3 in Aldefluor positivity (relative mean fluorescence intensity, MFI). The effect of indicated drugs on Aldefluor positivity mediated by ALDH1A3 in MDA-MB-231 ALDH1A3-OE cells (**A, C)** and in MDA-MB-468 cells with intrinsic high ALDH1A3 (**B, D)** Significance determined by one-way ANOVA with Tukey's post-hoc test.

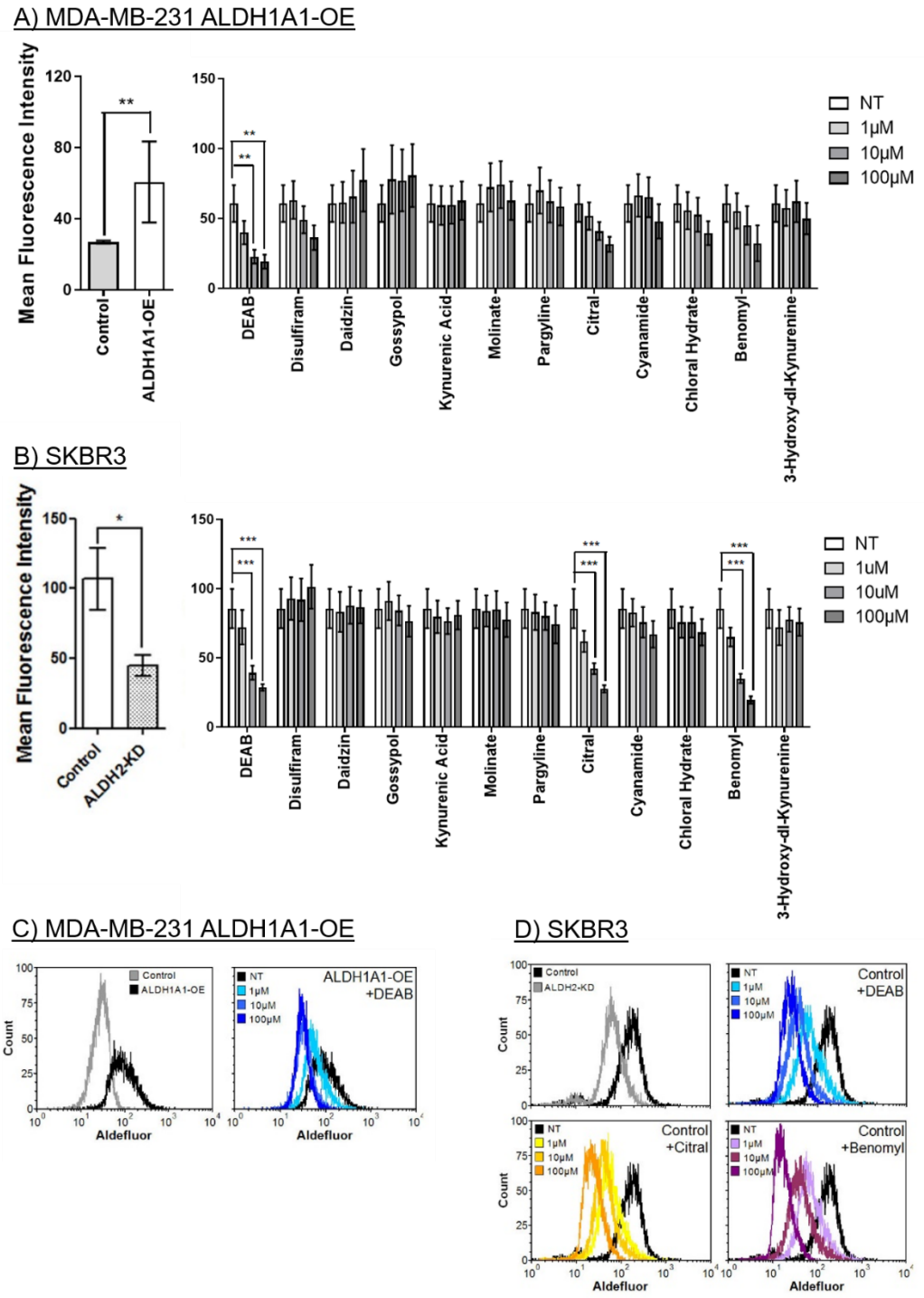

Figure 4.8: Citral is not the best inhibitor of ALDH1A1/ALDH2-mediated Aldefluor positivity quantified by mean fluorescence intensity. The effect of overexpression of ALDH1A1 or ALDH2 knockdown in Aldefluor positivity (relative mean fluorescence intensity, MFI). The effect of indicated drugs on Aldefluor positivity mediated by ALDH1A1 in MDA-MB-231 ALDH1A1-OE cells (**A, C)** and in SKBR3 cells with intrinsic high ALDH2 (**B, D)** Significance determined by one-way ANOVA with Tukey's post-hoc test.

4.3.3 *DISULFIRAM, GOSSYPOL, AND CITRAL INDUCE APOPTOSIS IN MDA-MB-231 CELLS*

To compare the effect of the inhibitors on apoptosis and also to test if ALDH1A3 expression has an effect on the sensitivity of cells to apoptosis, I next assessed the ability of the panel of inhibitors to induce apoptosis in MDA-MB-231, with or without overexpression of ALDH1A3. Of all the drugs, disulfiram most strongly induced apoptosis, which was magnified in the ALDH1A3-OE cells (Figure 4.9). Gossypol also induced apoptosis in the cells, regardless of ALDH1A3 expression. At the highest concentration tested (100 μM), citral induced a low level of cell death in MDA-MB-231 ALDH1A3-OE cells after 24 hours but did not appear to induce morphological changes (Figures 4.9 & 4.10). Citral was shown to induce apoptosis and cell cycle arrest in other cancer cell lines, although this is the first indication that its effects on cell viability may be minimally related to ALDH activity[387,388].

Taking into consideration all four assays (i.e. elimination of Aldefluor-positive population in a PDX, reduction of ALDH1A3-specific Aldefluor fluorescence in breast cancer cells, and apoptosis induction which was associated with ALDH1A3), citral stood out among the ALDH inhibitor panel as a potentially effective ALDH1A3/Aldefluor fluorescence inhibitor. Therefore, I focused the remainder of my studies on the ability of citral to inhibit ALDH1A3-mediated tumour growth.

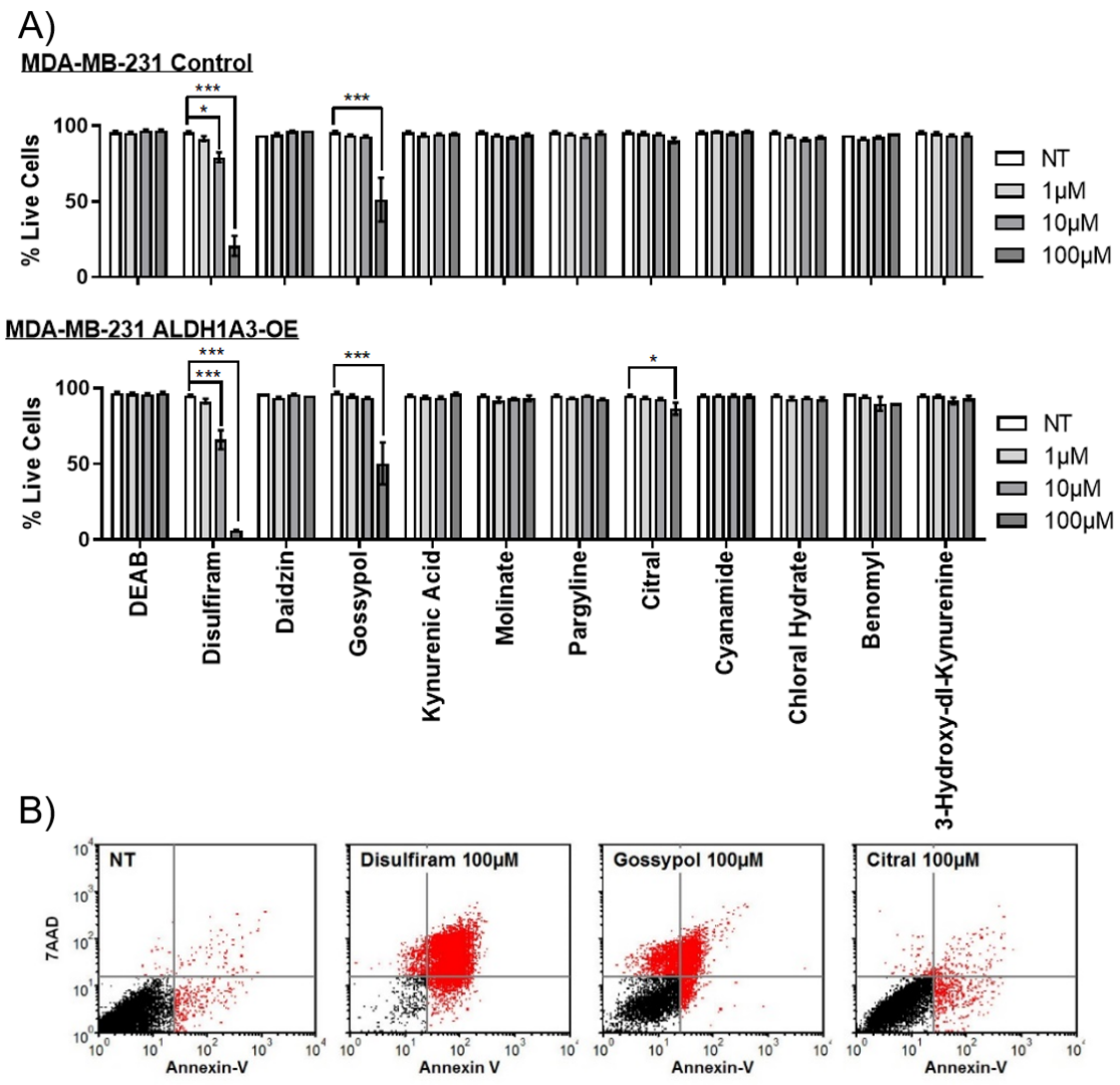

Figure 4.9: Disulfiram, gossypol, or citral induce apoptosis in MDA-MB-231 cells. A) MDA-MB-231 vector control and ALDH1A3-OE cells were treated with indicated drugs for 24 hours and assessed for live cells (percentage annexin-V-negative and 7-AAD-negative) by FACS analysis of annexin-V-Alexafluor 488 and 7-AAD stained cells. Significance determined by one-way ANOVA with Tukey's post-hoc test. **B)** Representative dot plots.

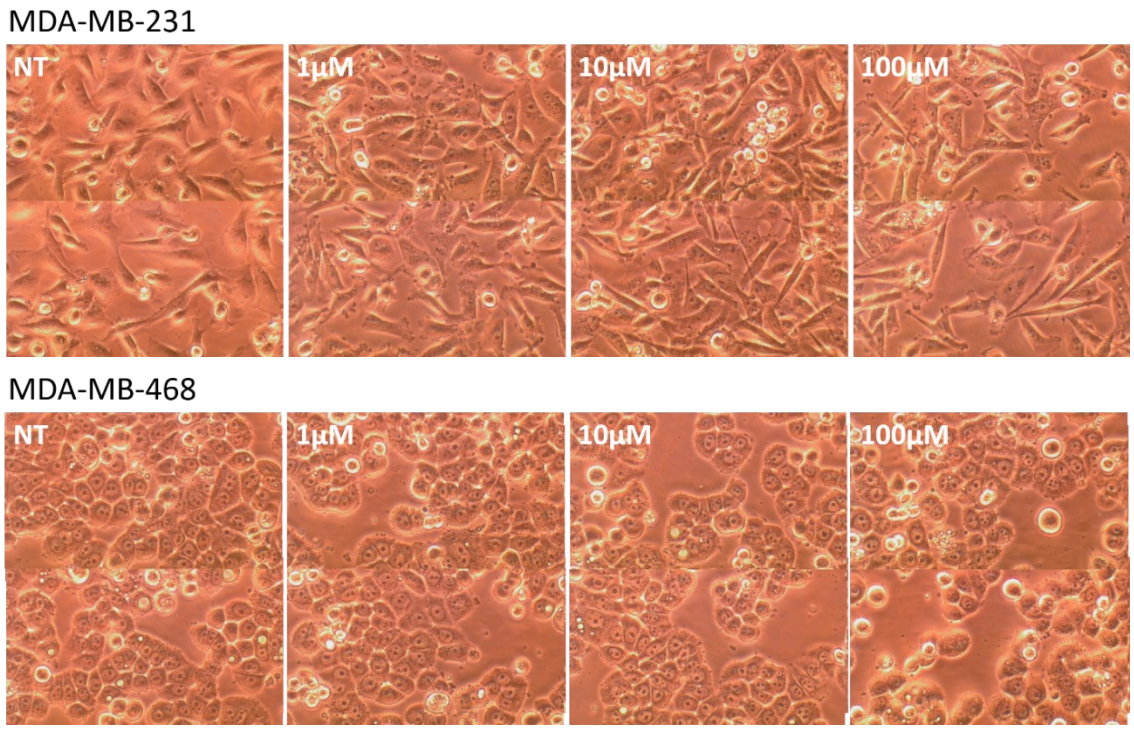

Figure 4.10: MDA-MB-231 and MDA-MB-468 cells treated for 24 hours with citral and aside from some cell death at higher concentrations, morphological changes are not detected. Images captured with a bright field microscope.

4.3.4 *NANOPARTICLE-ENCAPSULATED CITRAL REDUCES ALDH1A3-MEDIATED TUMOUR GROWTH OF MDA-MB-231 CELLS*

Citral is a common component of fragrances and flavor additives and is known to degrade at acidic pH and under oxidative stress[389], suggesting it likely requires stabilization or encapsulation to enhance *in vivo* bioavailability. Zeng *et al* reported a PEG-b-PCL micelle-encapsulation method for citral (referred to as nanoparticle-encapsulated NP)[385]. These authors also demonstrated that citral-NP inhibited the tumour growth of murine mammary 4T1 tumour cells implanted in the BALB/C mice[385]. In the present study I found that intraperitoneal administration of free citral was ineffective at reducing tumour growth of MDA-MB-231 cells, regardless of ALDH1A3 expression (Figure 4.11). Therefore, I adapted the encapsulation strategy devised by Zeng *et al*., to generate nanoparticle

encapsulated citral (citral-NP) and an empty nanoparticle control using PEG-b-PCL. HPLC confirmed that citral is composed of two E and Z isomers in a 2:1 ratio, as reported by Zeng *et al.* (Figure 4.12A). HPLC was used to quantify free citral and citral-NP, and equivalent doses based on the HPLC quantification had similar effects on Aldefluor fluorescence, indicating citral-NP was as bioactive as free citral (Figure 4.12B). The loading efficiency of this citral-NP preparation was estimated to be 12.4%. The mean citral concentration for an individual preparation of citral-NP was 8.05 mg/mL. Subsequently, the nanoparticle preparations were administered to mice bearing MDA-MB-231 ALDH1A3-OE or vector control tumours via tail vein injections. As I previously reported, overexpression of ALDH1A3 increased tumour growth of MDA-MB-231 cells[138] (Figure 4.12C). Citral-NP significantly reduced tumour volume and tumour weight of MDA-MB-231 ALDH1A3-OE cells but not MDA-MB-231 vector control cells (Figure 4.12C and 4.12D). This suggests that the tumour growth inhibitory effect of citral is related to its anti-ALDH activity, and in the case of ALDH1A3 expressing breast tumour cells, its specific inhibition of ALDH1A3.

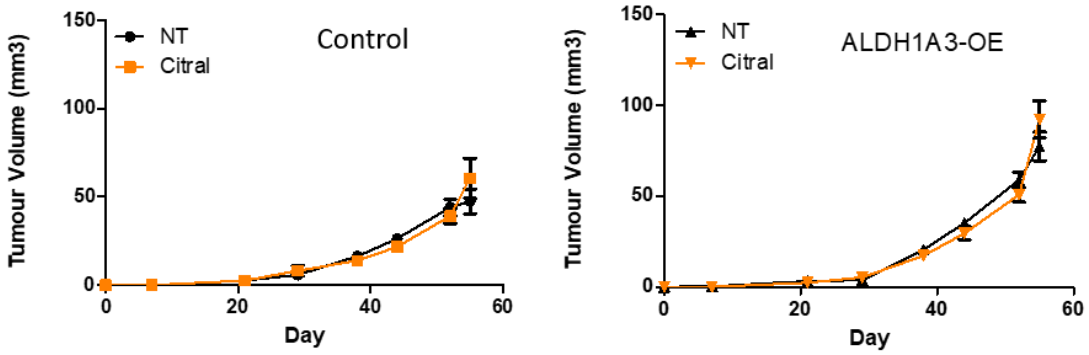

Figure 4.11: Unencapsulated citral fails to inhibit MDA-MB-231 tumour growth regardless of ALDH1A3 expression. **A)** vector control MDA-MB-231 tumour growth is not affected by citral treatment. **B)** ALDH1A3-overexpression MDA-MB-231 tumour growth is not affected by citral treatment.

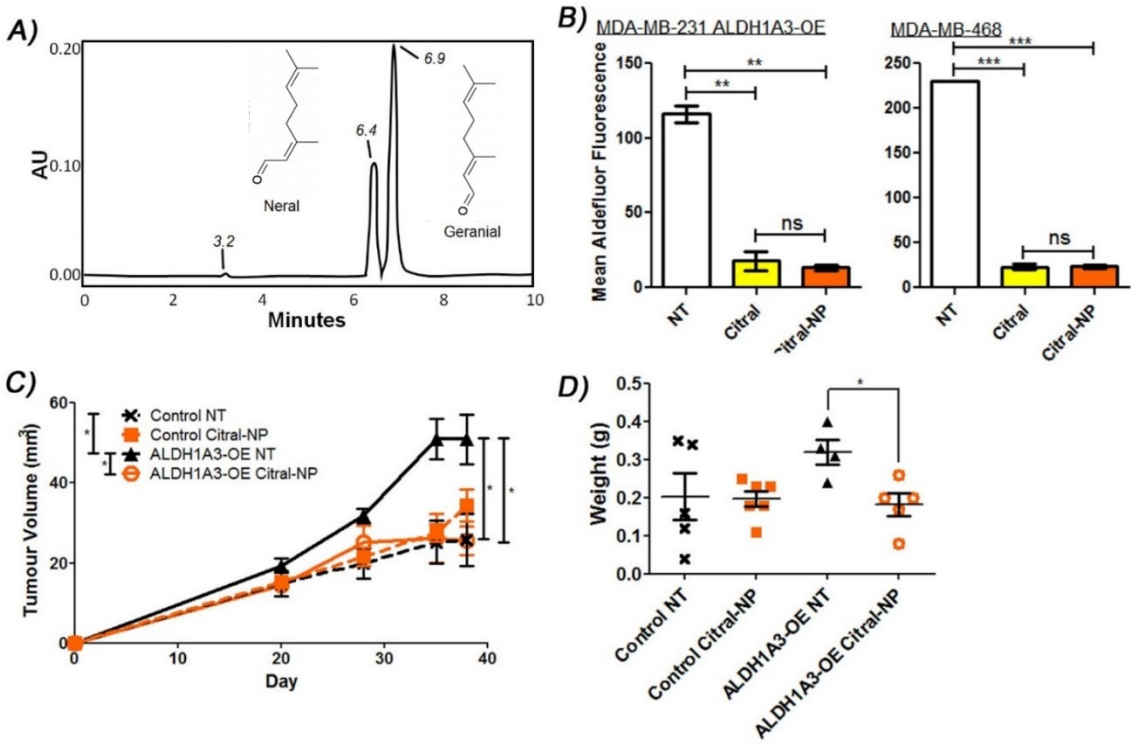

Figure 4.12: Nanoparticle encapsulated citral reduces ALDH1A3-mediated MDA-MB-231 tumour growth. A) Nanoparticle encapsulated citral (citral-NP) quantification via HPLC illustrated the two isomers present in citral and estimated the citral concentration. Three peaks present on the HPLC chromatogram represent the "non-citral" products in the Sigma citral (elute 3.2 minutes), the neral or E isomer (elute 6.4 minutes), and the geranial or Z isomer (elute 6.9 minutes). **B)** The effect of 100µM citral-NP and unencapsulated citral in the Aldefluor assay performed on MDA-MB-468 cells and MDA-MB-231 ALDH1A3-OE cells. **C)** Tumour measurements in mice injected with MDA-MB-231 vector control or ALDH1A3-OE cells, with or without citral-NP treatment. **D)** The resulting tumour weights. **B, C, D)** Significance determined by one-way ANOVA with Tukey's post-hoc test. RDA and RD assisted with nanoparticle optimization and generation; PM assisted with tail vein injection.

4.3.5 *CITRAL REDUCES ALDH1A3-MEDIATED COLONY FORMATION*

To further study the effect of citral on cancer cells, the potential mechanisms for the ALDH1A3-specific tumour growth reduction caused by this compound were investigated. The minor apoptotic effects observed in Figure 4.9 upon treatment of cells

with 100 μM of citral are probably insufficient to explain the observed tumour growth inhibition effects, since citral inhibits ALDH1A3 activity at much lower concentrations (i.e. 1μM decreases Aldefluor fluorescence). Furthermore, the effect of citral on cancer cell proliferation over 72 hours was not ALDH1A3-dependent (Figure 4.13A). Therefore, I assessed the effects of citral on other cellular growth and signalling assays that may be specific to ALDH1A3 activity and related to the enhanced tumour growth mediated by the enzyme. Notably, the colony formation assay (clonogenic assay) quantifies the ability of a single cell to grow into a colony, and has been utilized to illustrate CSC phenotype since it measures the ability of the cells to undergo "unlimited" division[390]. In both MDA-MB-231 and MDA-MB-468 cells, higher ALDH1A3 expression was associated with increased colony formation. Most importantly, citral reduced colony formation only in those cell lines with high ALDH1A3 expression (Figure 4.13B and 4.13C). The results from the colony formation assay mirror the tumour growth assay results (Figure 4.13C and 4.13D) and suggest citral may be inhibiting the enhanced ability of ALDH1A3 expressing MDA-MB-231 cells to form tumours.

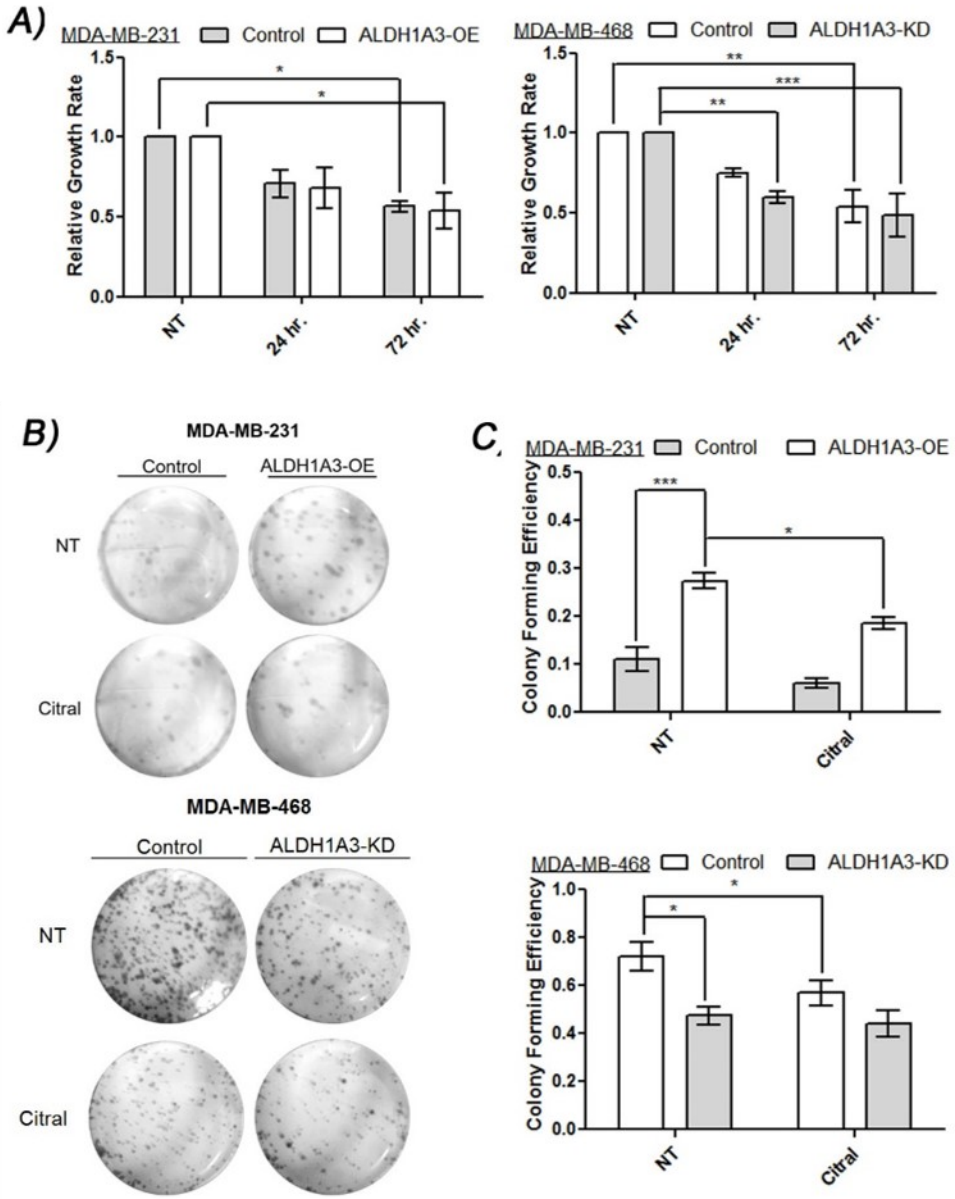

Figure 4.13: Citral reduces cell growth and ALDH1A3-mediated colony formation. **A)** MDA-MB-231 cells with or without ALDH1A3-OE and MDA-MB-468 cells with or without knockdown of ALDH1A3 were treated with citral for 72 hours and their growth rate normalized to no treatment. **B, C)** MDA-MB-231 cells with or without ALDH1A3-OE and MDA-MB-468 cells with or without knockdown of ALDH1A3 were pre-treated with 100μM citral or vehicle for 24 hours prior to colony formation assay. **B)** Representative images of colonies. **A, C)** Significance determined by one-way ANOVA with Tukey's post-hoc test.

4.3.6 *CITRAL INHIBITS ALDH1A3-MEDIATED GENE EXPRESSION*

To investigate the mechanism by which citral exerts its anti-tumourigenic and anti-growth effects, I evaluated expression of genes inducible by retinoic acid, or pluripotency and markers associated with breast CSCs upon ALDH1A3 modulation and citral treatment. The effects of ALDH1A3 on MDA-MB-231 breast tumour growth and metastasis is dependent upon its induction of RA signaling via expression of RA-inducible genes[138]. Furthermore, expression of RA-inducible genes in breast cancer is specifically dependent upon expression ALDH1A3[138]. Therefore, I evaluated the effect of citral on ALDH1A3-induced expression of RARβ, RARRES1, and ELF3, all of which are RA-inducible and contain retinoic acid response elements (RAREs)[138]. Overexpression of ALDH1A3 in MDA-MB-231 cells increased expression of RARβ, RARRES1, and ELF3 (Figure 4.14A), while knockdown of ALDH1A3 in MDA-MB-468 cells reduced expression of RARβ, RARRES1, and ELF3 (Figure 4.14B). Citral significantly reduced ALDH1A3-dependent expression of RARβ, RARRES1, and ELF3 in MDA-MB-231 cells (Figure 4.14A), and reduced expression of RARβ and RARRES1 in MDA-MB-468 cells (Figure 4.14B).

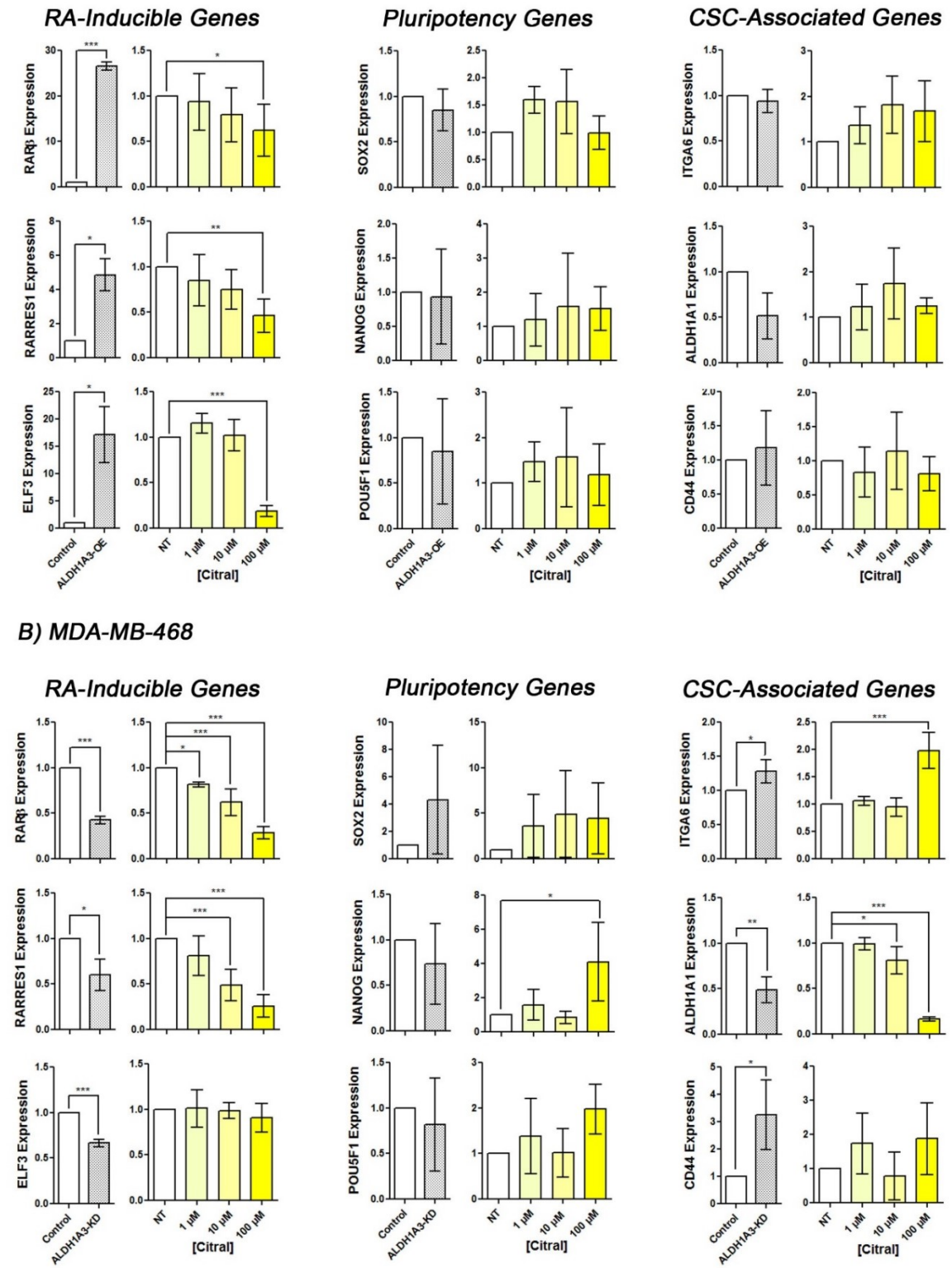
A) MDA-MB-231 ALDH1A3-OE
RA-Inducible Genes
Pluripotency Genes
CSC-Associated Genes
RARβ Expression
RARRES1 Expression
ELF3 Expression
SOX2 Expression
NANOG Expression
POU5F1 Expression
ITGA6 Expression
ALDH1A1 Expression
CD44 Expression
Control
ALDH1A3-OE
NT
1 μM
10 μM
100 μM
[Citral]
B) MDA-MB-468
RA-Inducible Genes
Pluripotency Genes
CSC-Associated Genes
RARβ Expression
RARRES1 Expression
ELF3 Expression
SOX2 Expression
NANOG Expression
POU5F1 Expression
ITGA6 Expression
ALDH1A1 Expression
CD44 Expression
Control
ALDH1A3-KD
NT
1 μM
10 μM
100 μM
[Citral]

Figure 4.14: Citral reduces ALDH1A3-mediated expression of retinoic acid-inducible genes. Relative mRNA expression levels of retinoic acid-inducible genes RARβ, RARRES1, and ELF3, pluripotency genes SOX2, NANOG, and POU5F1/Oct4, and CSC-associated genes ITAG6, ALDH1A1, and CD44 was quantified by RT-qPCR, normalized to control and B2M levels in MDA-MB-231 ALDH1A3-OE cells (**A)** and MDA-MB-468 cells (**B)** with increasing citral treatment for 24 hours compared to vehicle no treatment control. Significance of ALDH1A3-OE compared to control MDA-MB-231 cells (**A)** and ALDH1A3 knockdown compared to control MDA-MB-468 cells **(B)** was determined by t-test. **A, B)** Significance of citral treatments compared to vehicle no treatment determined by one-way ANOVA with Dunnett's post-hoc test. MS and MAG assisted with RT-qPCR.

In contrast, the expression of pluripotency and markers associated with breast CSC- was not consistently altered by ALDH1A3 expression or citral treatment MDA-MB-231 and MDA-MB-468 cells (Figure 4.14A and 4.14B)[391]. While ALDH1A3-KD and citral treatment increased ITGA6 expression in MDA-MB-468 cells, no change in expression was observed in MDA-MB-231 cells. An opposite effect was seen for ALDH1A1 expression where ALDH1A3-KD and citral treatment reduced ALDH1A1 expression in MDA-MB-468, though no change was observed in MDA-MB-231 cells. Gene expression of CSC-associated/marker CD44 was also not consistently altered by ALDH1A3 expression or citral treatment. This result mirrors my cell surface expression analysis of breast CSC markers CD24 and CD44; neither ALDH1A3 expression nor citral treatment altered the percentage CD24-/CD44+ cells in MDA-MB-231 cells (Figure 4.15). Together, the gene expression analysis strengthens the possibility that citral's inhibition of ALDH1A3-mediated tumour growth are related to inhibition of ALDH1A3-induced retinoic acid signaling.

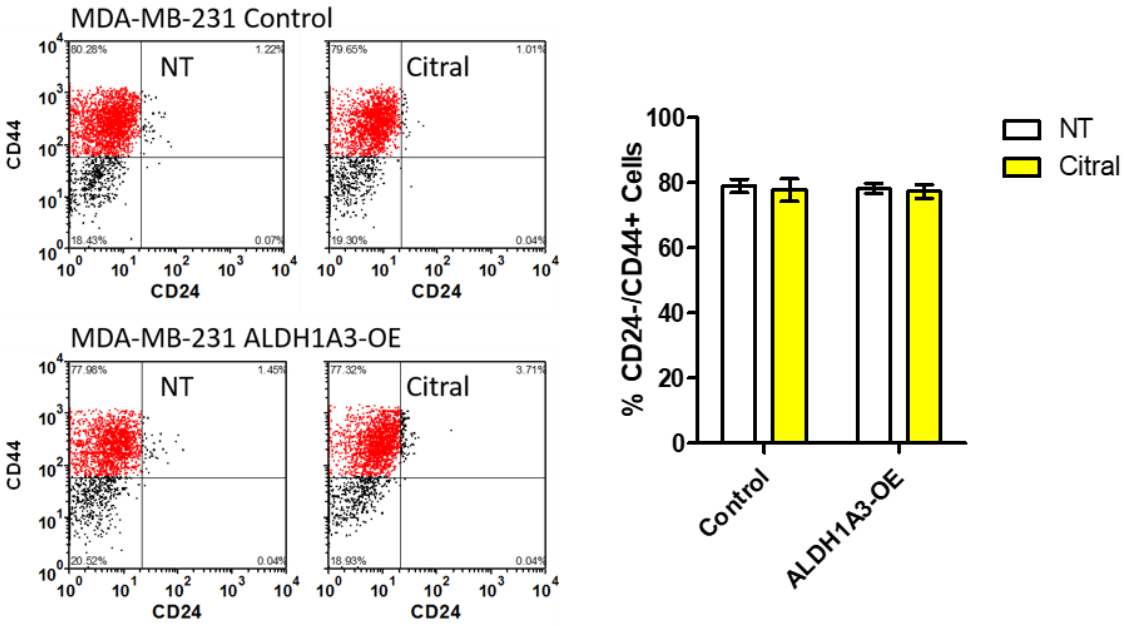

Figure 4.15: Treating MDA-MB-231 control or ALDH1A3-OE cells with 100 µM citral for 24 hours does not alter the number of CD24-/CD44+ cells. A majority of MDA-MB-231 cells are CD24-/CD44+ (≈80%), overexpression of ALDH1A3 does not alter this value, nor does citral treatment.

4.4 DISCUSSION

Breast CSCs are highly tumourigenic and resistant to conventional therapies[97,100,237,369,370]; therefore, the presence of a residual population of CSCs after treatment may increase a patient's risk for relapse and justifies a search for compounds that target CSC-associated activity. High ALDH activity is used as a biomarker for many types of CSCs, and more recently it has been shown that ALDH1A3 has a functional role in breast cancer, lung cancer, melanoma, malignant pleural mesothelioma, and head and neck cancer[136,138,142,144,376] . To date, the inhibition of ALDH1A3 as a breast cancer therapy has not been explored.

I evaluated 12 compounds with known inhibitory activity for other ALDH isoforms (with unknown ALDH1A3 activity)[256], and found that citral effectively inhibited ALDH1A3. To my knowledge, this is the first time that these compounds have been comparatively investigated for ALDH inhibitory activity in live cells using the Aldefluor assay. Previous cell-free enzymatic and/or *in vivo* assays implied that chloral hydrate, citral, cyanamide, daidzin, DEAB, disulfiram, gossypol, molinate, and pargyline inhibit ALDH1A1 or ALDH2 (reviewed in Koppaka *et al*., 2012)[256]. Of the compounds I tested, only DEAB, citral, and benomyl significantly inhibited ALDH1A3, ALDH1A1, or ALDH2-mediated Aldefluor fluorescence in breast cancer cells. The lack of positive results with the other compounds could be attributed to the fact that the previous studies reporting inhibition of ALDH isoforms were performed using cell-free enzymatic assays or animal models. Several of these compounds potentially require *in vivo* processing, as in the case of cyanamide, which requires the action of catalase to inhibit ALDH2, or pargyline which is activated in liver microsomes. Furthermore, the efficiency by which these compounds

can enter (and remain within) the cell is unknown and could contribute to their lack of effects in the present study.

Our 12 drug panel included disulfiram, a long-used drug in the deterrence of alcohol abuse, which has also been extensively tested previously for its anti-cancer properties. The most commonly reported anti-cancer mechanism of disulfiram is the inhibition of the proteasome-mediated degradation pathway[258]. Specifically, when bound to copper, the disulfiram/copper complex is a potent proteasome inhibitor, thereby inducing apoptosis of cancer cells. In cancers with clearly elevated copper levels such as glioblastoma multiforme, disulfiram treatment induces apoptosis and re-sensitizes the tumours to temozolomide therapy[392,393]. However, as illustrated by my findings here, it is possible that the apoptotic effects of disulfiram are not only attributable to its effects on proteasome-inhibition but may also be related to its ALDH enzyme inhibition activity.

Another drug tested here, gossypol, induced notable apoptosis in MDA-MB-231 cells. This is consistent with the previously described pro-apoptotic activity of gossypol on breast cancer[394]. Interest in gossypol as a breast cancer treatment stalled after a Phase I/II clinical trial determined the compound has negligible antitumour effects on refractory metastatic breast cancer[395]. Furthermore, the lack of ALDH1A3-specific apoptotic effects induced by gossypol decreased its relevance as a potential ALDH1A3-specific inhibitor in this study

Importantly, in addition to inhibiting Aldefluor fluorescence, citral treatment resulted in direct inhibition of ALDH1A3-mediated breast tumour growth. It is probable that citral inhibits general tumour growth by several mechanisms such as autophagy or apoptosis[385,388], but this is the first report of ALDH1A3-specific inhibition resulting in

decreased tumour growth. Since ALDH1A3 can mediate breast cancer growth through upregulating RA signaling[138], and citral can inhibit ALDH1A3-mediated expression of RA-inducible genes, this is a likely mechanism for citral-mediated tumour growth inhibition. The ideal cancer therapy would reduce tumour mass as well as CSCs while sparing normal cells. Notably, citral is reported to be less cytotoxic towards normal mammary epithelial cells (MCF10A) than breast cancer cell lines MCF7 and MDA-MB-231, suggesting a cancer-specific effect[396]. A recent report demonstrated that citral reduced tumour growth in the 4T1 syngeneic tumour model; this growth inhibition was not associated with CSC targeting[385]. In the present study I report that citral reduced tumour growth driven by the CSC marker ALDH1A3 as well as ALDH1A3-mediated colony formation. Finally, while free citral was ineffective *in vivo*, nanoparticle encapsulated citral reduced ALDH1A3-mediated tumour growth, illustrating the beneficial effects of encapsulation in the *in vivo* delivery of drugs in the treatment of cancer. Nanoparticle encapsulation for the delivery of anti-cancer drugs has several advantages: particles are too large for renal clearance or penetration of the endothelial junctions of normal blood vessels, yet the particles are small enough to extravasate the "leaky" vessels surrounding tumours[397]. These characteristics define the enhanced-permeability and retention effect and are likely responsible for the improved efficacy of citral-NP relative to free citral observed in this study.

In conclusion this study conceptualizes the use of ALDH1A3-specific inhibitors in the treatment of cancer and illustrates the proof of principle that this enzyme may be targeted to reduce tumour growth associated with ALDH1A3. It would be worthwhile to investigate whether the anti-cancer activity of citral that is observed in endometrial cancer,

ovarian cancer, cervical cancer, B-lymphoma, and glioblastoma, can be partially attributed to ALDH1A3 inhibition. Having illustrated the proof of principle with citral, small molecule library screening may identify ALDH1A3 inhibitors which are effective at nM concentrations, and therefore would likely be superior novel drug candidates. Future studies with citral and other ALDH1A3-specific inhibitors will determine if the tumour-initiating potential and therapy resistance of Aldefluor-positive identified CSCs can be abrogated with such inhibitors. This could lead to the adjuvant application of ALDH1A3-specific inhibition in the treatment of certain cancers where ALDH1A3 plays a functional role in tumour growth, metastasis, and chemo- or radio-resistance.

CHAPTER 5: TRANSCRIPTOMICS AND METABOLOMICS IDENTIFY PUTATIVE ROLE FOR PLASMINOGEN ACTIVATION AND GABA METABOLISM IN ALDH1A3-MEDIATED BREAST CANCER METASTASIS

Contribution Statement

Dr. Paola Marcato: generation of MDA-MB-231 ALDH1A3-OE and MDA-MB-468 ALDH1A3-KD cell lines, all-trans retinoic acid pellet implantation. Cheryl Dean: lung and brain histology, lung RT-qPCR metastasis assay. Dr. Dharini Bharadwaj: plasminogen activation assay. Dr. J Patrick Murphy, Michael Anthony Giacomantonio, Dr. Alejandro Cohen, and Hayley Walsh: mass spectrometry sample preparation, data collection and normalization. Hayley Walsh: systemic GABA administration. Dr. Krysta Mila Coyle: MDA-MB-231 ALDH1A3-OE microarray

5.1 INTRODUCTION

The survival rate of breast cancer has improved dramatically over time largely due to the development of hormone receptor targeted therapies[1]. However, there remains a population of patients with aggressive disease who do not benefit from these targeted therapies as their tumours do not express the necessary cell surface hormone receptors (estrogen receptor [ER], progesterone receptor [PR], or epidermal growth factor receptor [HER2]). These triple negative breast cancer (TNBC) patients have an intrinsically more aggressive disease and worse prognosis which is exacerbated by the lack of effective therapies. Although initial response to chemotherapy may be profound, relapse and metastasis occurs frequently and early in TNBC patients[8]. Developing therapies that can benefit this population of TNBC patients is essential.

One hypothesis for why TNBC is such an aggressive disease is that high aldehyde dehydrogenase 1A3 (ALDH1A3) is driving tumour growth and metastasis. High ALDH activity (due to ALDH1A3 isoform activity) is a defining feature of breast cancer stem cell (CSC) populations, these CSCs are abundant in TNBC primary tumours relative to non-TNBC, and ALDH1A3 has been shown to accelerate tumour growth and metastasis in the MDA-MB-231 TNBC model[138,398,399]. While ALDH1A3 inhibitors are under development, understanding how ALDH1A3 contributes to growth and metastasis could reveal novel avenues for targeting aggressive TNBC and CSCs[400].

As a retinaldehyde dehydrogenase, ALDH1A3's main function is the synthesis of retinoic acid[135]. High ALDH1A3 activity leads to an abundance of retinoic acid and subsequent retinoic acid-inducible gene expression. As a potent transcription factor, retinoic acid mediates the expression of hundreds of genes, and the transcriptional overlap

of ALDH1A3-overexpression and exogenous retinoic acid treatment has been exhaustively documented[288,289]. Herein, I examine pro-metastasis and cancer progression mechanisms of ALDH1A3 in both the gene expression changes induced by ALDH1A3 and in potential mechanisms beyond its function in gene expression regulation (e.g. metabolomics). These analyses revealed roles for plasminogen activation, prostaglandin synthesis and the GABAergic system in ALDH1A3-hi breast cancer cells.

Breast CSCs with high ALDH1A3 activity (ALDH+ cells) have enormous metastatic potential. To determine whether the mechanisms governing ALDH+ and ALDH1A3-OE metastasis may be similar, gene set enrichment analysis was performed on genes up-regulated in both types of ALDH-hi breast cancer cell. Unsurprisingly, retinoid biosynthesis was enhanced in both cell types. Prostaglandin E2 synthesis, which accelerates growth of *in vitro* cancer stem cell mammospheres, and enhances metastasis *in vivo*[401], was commonly up-regulated in ALDH-hi cells.

Plasminogen activation is an established means by which tumours cells can invade through the basement membrane in the initial phase of metastasis. This occurs through the ability of activated plasminogen (plasmin) to degrade extracellular matrix proteins (similar to fibrinolysis), liberate growth factors that had been sequestered in the ECM, and activate several matrix metalloproteases[402]. Here, in MDA-MB-231 and MDA-MB-436 TNBC cells, high ALDH1A3 activity leads to enhanced plasminogen activation and plasminogen-based cellular invasion.

The product of all gene expression regulation, translational regulation, and environmental context is the metabolome. HPLC-MS metabolomics revealed a loss of γ-aminobutyric acid (GABA) and its intermediates N-acetylputrescine and glutamate in

MDA-MB-231 ALDH1A3-OE tumours/cells. Aside from its main role as an inhibitory neurotransmitter, GABA has been shown to moonlight as a pro-growth and pro-metastasis molecule. In TNBC cells with aberrant GABA metabolism, there is an enhanced ability to metastasize to the brain[403]. To test the overall effect of GABA on MDA-MB-231 cells, mice harbouring MDA-MB-231 ALDH1A3-OE or control tumours were administered with systemic GABA. Abundant GABA increased MDA-MB-231 metastasis, and this is supported by clinical data that breast tumours with low expression of γ-aminobutyrate transaminase (ABAT; which degrades GABA) are at a greater risk for brain and lung metastasis.

This novel connection between GABA signaling/metabolism and ALDH1A3 needs further study as it may have significant clinical connotations. Currently, patients receiving taxane-based chemotherapy can be prescribed GABA agonists like gabapentin to alleviate peripheral nerve pain[404]. Many of these patients have TNBC with significant ALDH1A3 activity. If GABA signaling and ALDH1A3 interact, then giving these patients a GABA agonist may unwittingly create a permissive environment for lung or brain metastasis.

5.2 MATERIALS AND METHODS

5.2.1 *CELL CULTURE*

Cancer cell lines were obtained from ATCC. MDA-MB-231, MDA-MB-468, and HEK293T cells were grown in Dulbecco's Modified Eagle Medium (DMEM; Invitrogen)

supplemented with 10% Fetal Bovine Serum (FBS; Invitrogen) and 1X antibiotic antimycotic (AA; Invitrogen). MDA-MB-436 cells were grown in Leibovitz's Medium (L-15; Invitrogen) supplemented with 10% FBS, 1X AA, 10 µg/mL human insulin (Sigma), and 16 µg/mL L-glutathione (Invitrogen). ALDH1A3-OE and ALDH1A3-KD cells and their associated vector control cell lines were maintained in media supplemented with 0.25 µg/mL puromycin (Sigma). Cells were cultured in a humidified 37°C incubator with 5% CO_2, except for MDA-MB-436 which were cultured without the addition of CO_2.

5.2.2 *GENERATION OF ALDH1A3-KD IN MDA-MB-436 CELLS*

To generate ALDH isoform knockdowns, retroviral vector pSMP (Open Biosystems, Huntsville, AL) with either the shRNAmir scramble sequence or shRNAmir sequences specific to each ALDH isoform (Table 5.1) were transfected into Phoenix cells following standard procedures. The retroviral supernatants were applied to cultured MDA-MB-436, and stable transfectants were selected with puromycin (Sigma). The same ALDH1A3 overexpression MDA-MB-231 clone as in our prior publication was used[136,138].

Table 5.1: shRNA Sequences for ALDH1A3-KDs

Target	shRNA	Sequence
ALDH1A3	shRNA1	TGCTGTTGACAGTGAGCGCGCATAGCAAATCCTAGGATA ATAGTGAAGCCACAGATGTATTATCCTAGGATTTGCTATG CTTGCCTACTGCCTCGGA
	shRNA2	TGCTGTTGACAGTGAGCGCGCTGTAATTCACTTTAACAAA TAGTGAAGCCACAGATGTATTTGTTAAAGTGCCTTACAGA TTGCCTACTGCCTCGGA

5.2.3 *REVERSE-TRANSCRIPTASE QUANTITATIVE PCR*

MDA-MB-436 control and ALDH1A3-KD cells were collected in Trizol (Invitrogen) and RNA was purified using a PureLink RNA kit (Invitrogen Thermo Fisher Scientific) following the manufacturer's instructions. Equal amounts of purified RNA were then reverse transcribed to cDNA using iScript (Bio-Rad) as per manufacturer's instructions. Diluted cDNA was used in RT-qPCR reactions with gene-specific primers (Table 5.2) and SsoAdvanced Universal SYBR Supermix (Bio-Rad) as per manufacturer's instructions with a CFX96 or CFX384 Touch Real-Time PCR Detection System (Bio-Rad). Standard curves were generated for each primer set and primer efficiencies were incorporated into the CFX Manager software (Bio-Rad). Relative expression for plasminogen activation and RA-inducible genes in ALDH1A3-KD cells was quantified using the ΔΔct method of the CFX Manager Software (Bio-Rad), where gene-of-interest quantification was normalized to reference genes TBP and RPL29 and then made relative control cells mRNA levels.

Table 5.2: RT-qPCR Primer sequences

Gene	Forward Primer	Reverse Primer
TBP	GGCACCACTCCACTGTATCC	GCTGCGGTACAATCCCAGAA
RPL29	ACACACAACCAGTCCCGAAA	TCTTGGCAAAGCGCATGTTC
ALDH1A3	TCTCGACAAAGCCCTGAAGT	TATTCGGCCAAAGCGTATTC
PLAT	TGTGTGGAGCAGTCTTCGTT	TCGCTGCAACCTTGGTAAGA
PLAU	GTCACCTACGTGTGTGGAGG	AGTTAAGCCTTGAGCGACCC
PLAUR	CCTCGCGACATGGGTCAC	GGCAATCCCCGTTGGTCTTA
SERPINE1	TTGGTGAAGGGTCTGCTGTG	GGGTGAGAAAACCACGTTGC
SERPINB2	GCAGTTACCCCCATGACTCC	GTGCCTGCAAAATCGCATCA
DHRS3	TCTGTGATGTGGGCAACCG	ATGGTGATGTCACCCACCTTC
RARβ	GGTTTCACTGGCTTGACCAT	GGCAAAGGTGAACACAAGGT
RARRES1	ACGGCTCATCGAGAAAAAGA	GAAAGCCAAATCCCAGATGA
GAPDH (human)	CAAGGCTGAGAACGGGAAG	CGCCCCACTTGATTTTGGAG
GAPDH (mouse)	GCGAGACCCCACTAACATCA	GGCGGAGATGATGACCCTTT

5.2.4 *ALDEFLUOR ASSAY*

MDA-MB-436 control or ALDH1A3-KD cells were washed with PBS and Aldefluor assay performed as per the manufacturer's instructions (Stemcell Technologies). To eliminate dead cells, cells were stained with viability stain 7-AAD (Biolegend). Cell populations were identified using a FACSCalibur flow cytometer (Becton Dickinson). After excluding debris and dead cells, Aldefluor levels were quantified via mean fluorescence intensity.

5.2.5 *BREAST CANCER CELL LINE XENOGRAFTS*

Animal investigations detailed in this manuscript have been conducted in accordance with the ethical standards and according to the Declaration of Helsinki and

according to national and international guidelines. All experiments were conducted in accordance with the Canadian Council on Animal Care standards and a protocol approved by Dalhousie University Committee on Laboratory Animals (#19-013b).

For the *in vivo* all-trans retinoic acid (ATRA) treatment, a subcutaneous slow-release ATRA pellet (5 mg / 60 days; Innovative Research of America) was implanted into mice one day prior to cancer cell injection[288]. Eight week old NOD/SCID female mice were orthotopically injected with MDA-MB-436 (5 x 10^6 /mouse), MDA-MB-436 vector control or MDA-MB-436 ALDH1A3 knockdown cells (5 x 10^6/mouse), MDA-MB-231 (2 x 10^6/mouse), MDA-MB-231 vector control or ALDH1A3-OE (2 x 10^6/mouse) admixed in 1:1 ratio with phenol red-free high concentration matrigel (BD Bioscience). Resulting tumour growth was quantified (mm^3; length x width x height / 2).

5.2.6 *PLASMINOGEN ACTIVATION ASSAY*

MDA-MB-231 control/ALDH1A3-OE or MDA-MB-436 control/ALDH1A3-KD cells were seeded at a density of 30,000 cells/well in cell culture grade 96-well plates (Corning) overnight and washed three times with incubation buffer (Hanks balanced salt solution containing 3 mM $CaCl_2$ and 1 mM $MgCl_2$; Invitrogen). Cells were then incubated with 0.5 μM glu-plasminogen (Molecular innovations (Michigan, USA), for 25 minutes before the addition of 500 μM plasmin chromogenic substrate, S2251 (Chromogenix, Diapharma Group). Plasmin activity was measured spectrophotometrically (405 nm) taking readings every 2 minutes for 2 hours. Time course data were analyzed according to the equation describing the rate of *p*-nitroanilide (*p*-NA) production $A405\ nm = B + Kt2$, where K is the rate constant for the acceleration of *p*-NA generation and B is the y-intercept.

Under our experimental conditions, *K* is proportional to the initial rate of plasmin formation from plasminogen.

5.2.7 *TRANSWELL INVASION ASSAY*

Plasminogen was stripped from regular FBS by passing the FBS through a lysine Sepharose column, which allows plasminogen to bind to the column. The flow-through from the lysine Sepharose column which is free of plasminogen was collected and filter sterilized using 0.2µm filters (Fisher Scientific).

Cells (2.5 x 10^4) were seeded in 0% FBS media into the upper well of either a Matrigel-coated invasion chamber (Corning) or an uncoated migration chamber (Corning) with 8 µm pore size. The bottom chamber contained 10% plasminogen-stripped FBS as a chemoattractant +/- 0.25µM plasminogen (Molecular innovations, Michigan, USA). In the case of MDA-MB-436 ALDH1A3-KD cells, 10% replete FBS was used with no supplemented plasminogen. After 24 hours, migrated or invaded cells which had crossed the chamber membrane were fixed in methanol and stained with 0.05% crystal violet. Transversed cells were counted in four fields of view per chamber at 20X using a Motic AE31E light microscope. Motic Motican72 technology. The percent invasion was determined via the following equation:

$$\%\ Invasion = \frac{\text{mean number of cells invaded through Matrigel} - \text{coated transwell}}{\text{mean number of cells migrated through uncoated transwell}} x100$$

5.2.8 *METABOLISM-FOCUSED GENE SET ENRICHMENT ANALYSIS (GSEA)*

Microarray gene expression data for MDA-MB-231 cells overexpressing ALDH1A3 (n=3; GSE103426), and microarray gene expression data Aldefluor-sorted (ALDH+ vs ALDH-) breast cancer patient samples (n=8; GSE52327) was assessed for differential transcription of metabolic enzymes[237,289]. A list of 1647 genes known to code for metabolic enzymes was accessed through the Comprehensive Mammalian Metabolic Enzyme Database[405]. The top 50 most up-regulated metabolism genes in the ALDH1A3-OE cells, and top 50 most up-regulated metabolism genes in ALDH+ breast cancer patient samples were submitted to GSEA.

Gene Set Enrichment Analysis (GSEA) was performed using available online software (http://software.broadinstitute.org/gsea/index.jsp) to compute overlaps in curated gene sets (C2). The top 50 overlapping gene sets identified by GSEA for each dataset were identified. Gene sets with similar function were identified between the datasets (12/50 gene sets were shared between ALDH+ and ALDH1A3-OE).

5.2.9 *MASS SPECTROMETRY-BASED METABOLOMICS*

Metabolites from cultured cells were collected by scraping subconfluent monolayers of cells directly into ice-cold 80% methanol. Metabolites were extracted from tumour samples by crushing 50 mg of a minced tumour into ice-cold 80% methanol. To eliminate large cellular debris, samples were centrifuged at 500 x g for 5 minutes and the supernatant was decanted to a new tube. Supernatant was diluted 1/10 with hydrophilic interaction liquid chromatography (HILIC) loading buffer (95% acetonitrile, 2 mM ammonium hydroxide, and 2 mM ammonium acetate). Samples were centrifuged at 13,000

x g for 5 minutes to remove any precipitate, and tumour sample supernatants (but not cultured cell sample supernatant) was further diluted 1/10 in HILIC buffer. Next, 50 µL injections were loaded on an Acquity UPLC BEH Amide, 1.7 µm particle size, 2.1 x 100 mm column (Waters #186004801). Multiple reaction monitoring (MRM) was performed using a Sciex 5500 QTRAP mass spectrometer using a previously described acquisition method[406]. This hybrid dual quadrupole linear ion trap mass spectrometer (MS) has been used previously for quantitative profiling of endogenous polar metabolites in both positive and negative modes from an *in vivo* source[406]. Peak heights for individual metabolites were extracted using Multiquant Software (Sciex). From a single MS analysis, Q1/Q3 MRM transition mass spectra in both ionization modes were normalized independently.

MS total useful signals (MSTUS)[407] is a simple and cited MS normalization method that uses total useful metabolite concentrations to normalize metabolite concentrations between samples. Samples were MSTUS normalized on the NOREVA platform[342]. Database sources including the Human Metabolome Database, KEGG and MetaboAnalyst were used for the identification of altered metabolic pathways.

5.2.10 *GABA TREATMENT OF MDA-MB-231 ALDH1A3-OE TUMOURS*

Eight to ten-week old female NOD/SCID mice, were orthotopically injected with 2×10^6 MDA-MB-231 vector control or ALDH1A3-OE cells admixed in 1:1 ratio with phenol red-free high concentration. Mice were intraperitoneally injected daily with 250 µg/kg γ-aminobutyric acid (GABA; Sigma) or the same volume of vehicle (phosphate buffered saline; PBS; Invitrogen). Primary tumours were palpable in 10 to 16 days, mice with poorly placed tumours (i.e. growing subcutaneously instead of on the mammary fat

pad) were excluded from the study. Primary tumour growth was quantified (length × width × height / 2).

5.2.11 *Lung and Brain Metastasis Quantification*

One lung from each more was subjected to RT-qPCR assessment of metastasis. Lung tissue was minced and then digested in Trizol. RNA extraction, cDNA synthesis was performed as previously described. Infiltration of human cells into the lung (metastasis) was determined using human-specific GAPDH primers, with Cq values interpolated to represent the # of metastatic cells by comparing to a standard curve generated by spiking known numbers of MDA-MB-231 cells (0, 10, 100, 1000, 100000, 1000000) into samples of naïve lung tissue.

The remaining lungs and brains were harvested, fixed, paraffin embedded and sectioned (5 μM) for metastasis visualization by haematoxylin and eosin (H&E) staining. Images were captured on a Zeiss Axio Imager Z1 W/ Color & Monochrome camera at 2.5x Magnification. Three H&E stained sections per lung were visualized. Quantified sections were taken from equal thirds to represent the entire tissue. In a blinded design, captured images were quantified for % metastatic surface area by Image J.

5.2.12 *Patient Dataset Analysis*

Breast Cancer (METABRIC, Nature 2012 & Nat Commun 2016; n=1904) and Breast Invasive Carcinoma (TCGA, Cell 2015; n=816) clinical data and RNA-Seq log2 V2 RSEM gene expression data were accessed via cBioportal[285,286].

Microarray-based gene expression (Affymetrix HG-U133 Plus 2.0 array) of pre-chemotherapy biopsies from breast cancer patients was acquired from GSE28844[287]; with histopathological response based on Miller & Payne grading system (Non-Responders n=14; Intermediate responder n=10; Responders n=8). Microarray-based gene expression of primary breast tumours which had associated clinical data for metastasis was accessed from GSE2034 (n=286), GSE12276 (n=204), GSE2603 (n=81), and GSE5327 (n=48).

5.2.13 *STATISTICAL ANALYSES*

All statistical analyses were performed in GraphPad Prism 8. Statistical tests and significance are indicated in all figure captions.

5.3 RESULTS

5.3.1 *ALDH1A3 INCREASES TUMOUR GROWTH AND METASTASIS OF TNBC MDA-MB-231 AND MDA-MB-436*

As previously established (in Chapter 4 and in other publications[138]), MDA-MB-231 cells overexpressing ALDH1A3 grow faster as tumours and are more metastatic to the lungs than control MDA-MB-231 cells (Figure 5.1A). Treating mice with all-trans retinoic acid (which is the product of ALDH1A3) causes a similar increase in MDA-MB-231 tumour growth and metastasis[138,289]. Identifying an additional breast cancer cell line which recapitulates the pro-tumourigenic and pro-metastatic effects of elevated ALDH1A3 in MDA-MB-231 is desirable for validating potential mechanisms driving ALDH1A3-mediated tumour growth and spread.

To this end, ALDH1A3 was successfully knocked down in the MDA-MB-436 breast cancer cell line and validated at the mRNA level (shRNA1 88% and shRNA2 85% efficient) and by Aldefluor fluorescence (shRNA1 71% and shRNA2 75% efficient; Figure 5.1B). As expected, expression of all-trans retinoic acid (ATRA)-inducible genes (DHRS3, RARβ, and RARRES1) was reduced in the MDA-MB-436 ALDH1A3-KD cells (Figure 5.1C).

MDA-MB-436 ALDH1A3-KD tumours were generally smaller than control tumours; however only ALDH1A3-KD shRNA 2 tumours were of significantly smaller volume than control tumours (Figure 5.1D). As previously published[289], MDA-MB-436 tumours grew faster in mice harbouring subcutaneous ATRA pellets, though this effect was not significant here (Figure 5.1F).

For ATRA-treated and ALDH1A3-KD experimental mice, both lungs were harvested at endpoint, with one lobe formalin fixed and paraffin embedded for H&E staining, and the other lobe undergoing RNA extraction for downstream RT-qPCR analysis. Expression of human GAPDH in mouse lungs is a rapid and accurate measure of human cell infiltration (aka metastasis) in the lungs. There was no detectable human GAPDH in any of the mouse lungs suggesting there was a lack of lung metastasis, thus H&E staining was not performed. Though there was no *in vivo* metastasis observed, MDA-MB-436 ALDH1A3-KD cells had less invasive potential in an *in vitro* trans-well invasion assay (Figure 5.1E), consistent with previous findings in the MDA-MB-231 model[138].

While the MDA-MB-436 ALDH1A3-KD model is appropriate for some *in vitro* applications (i.e. invasion); because it does not metastasize *in vivo*, the MDA-MB-231 ALDH1A3-OE model is retained for most future experiments characterizing the function

of ALDH1A3. The focus now shifts to determining what characteristics of ALDH1A3-hi cells are causing this aggressive pro-metastatic phenotype.

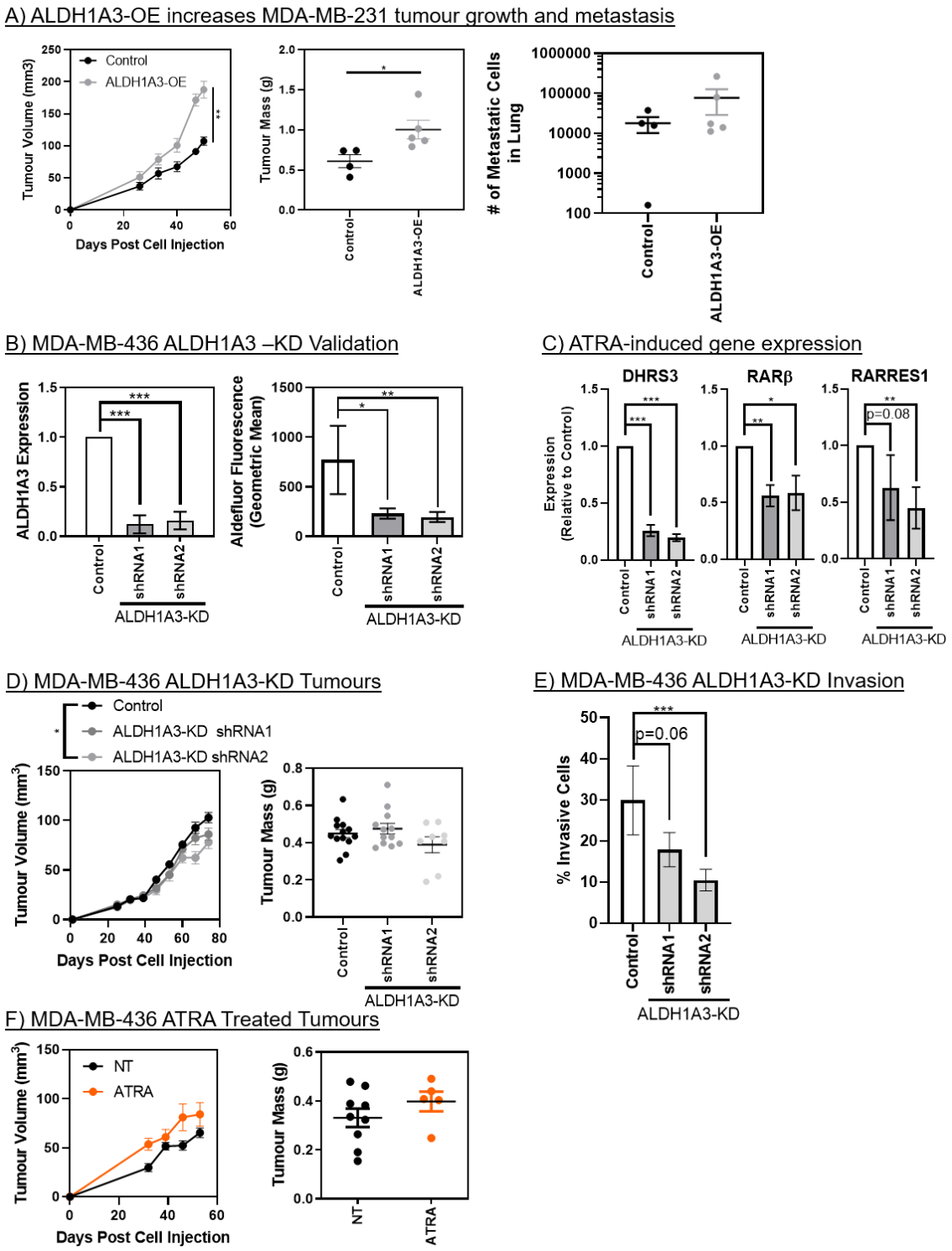

Figure 5.1: Elevated ALDH1A3 increases tumour growth and invasion/metastasis of TNBC MDA-MB-231 and MDA-MB-436 cells. A) MDA-MB-231 ALDH1A3-OE tumours grow faster than control tumours, one-tailed t-test (Control n=4, ALDH1A3-OE n=5; mean and SEM error bars), and have increased lung metastasis (median and SEM error bars). **B)** RT-qPCR and Aldefluor validation of MDA-MB-436 ALDH1A3 knockdown efficiency. ALDH1A3 mRNA abundance relative to vector control and geometric mean fluorescence of Aldefluor assay; one-way ANOVA with Dunnett's post-hoc test (n=4; SD error bars). **C)** Reduced expression of ATRA-induced genes (DHRS3, RARβ, and RARRES1) in MDA-MB-436 ALDH1A3-KD cells. ATRA-induced gene mRNA abundance relative to vector control cells. One-way ANOVA with Dunnett's post-hoc test (n=4; SD error bars). **D)** MDA-MB-436 control or ALDH1A3-KD tumours, one-way ANOVA with Dunnett's post-hoc test (control n=13, ALDH1A3 shRNA1 n=13, ALDH1A3 shRNA2 n=8; SEM error bars). **E)** Invasive potential of MDA-MB-436 ALDH1A3-KD cells in replete FBS conditions (one-way ANOVA with Dunnett's post-hoc test; n=5, SD error bars). **F)** NOD/SCID mice harbouring an MDA-MB-436 tumour +/- ATRA pellet, one-tailed unpaired t-test (NT n=9, ATRA n=5; SEM error bars). Tumour volume mm^3, length x width x height / 2. $p<0.05$*; $p<0.01$**; $p<0.001$***. CD performed RT-qPCR analysis of lung metastasis, PM surgically implanted ATRA pellets.

5.3.2 *DIFFERENTIAL TRANSCRIPTION OF ENZYMES IMPLICATES DYSREGULATED PLASMIN, RETINOID, AND PROSTAGLANDIN SYNTHESIS IN ALDH1A3/ALDH+ BREAST CANCER CELLS*

To investigate the pro-metastatic capacities of ALDH1A3-hi breast cancer cells; I begin with assessing differential gene expression of MDA-MB-231 ALDH1A3-OE cells and then compare this differential gene expression to ALDH+ breast cancer stem cells. Through these analyses I identify a potential mechanisms for the increased invasive capacity of ALDH1A3-expressing cells through altered plasminogen activation.

In the previously published Affymetrix Human Gene 2.0ST microarray gene expression dataset (GSE103426), extensive differences in gene transcription between MDA-MB-231 ALDH1A3-OE and MDA-MB-231 control cells were observed[138]. It was determined that a large portion of ALDH1A3-OE-driven transcription was due to the

increased production of retinoic acid which is a well-characterized nuclear hormone ligand and mediates expression of hundreds of genes[289].

The mechanism by which ALDH1A3 confers increased invasive potential to MDA-MB-231 cells *in vitro* has not previously been determined. Therefore, I focused on differential expression of genes that have known contributions to invasion and/or metastasis. Among the 139 transcripts significantly up-regulated by ≥1.5-fold in MDA-MB-231 cells overexpressing ALDH1A3, it was noted that two pro-plasminogen activation (tissue plasminogen activator [PLAT] and plasminogen activator, urokinase [PLAU]) and a plasminogen activator urokinase receptor gene (PLAUR) were up-regulated. Concurrently, there was significant downregulation of plasminogen activator inhibitor-2 (SERPINB2) (Figure 5.2).

Plasmin can play a critical role in cancer invasion and metastasis via its ability to degrade extracellular matrix (ECM) proteins, liberate growth factors that had been sequestered in the ECM, and by activating several matrix metalloproteases[402]. The activation of plasminogen to plasmin is a tightly regulated process which is governed by the two main plasminogen activators (encoded by PLAT and PLAU) and two main plasminogen activator inhibitors (encoded by SERPINE1 and SERPINB2). The gene expression profile of MDA-MB-231 ALDH1A3-OE cells suggests an increased plasminogen activation capacity and a potential mechanism for the increased invasion seen in cells with high ALDH1A3 activity (MDA-MB-436 cells Figure 5.1E) and is previously published in MDA-MB-231 cells[138].

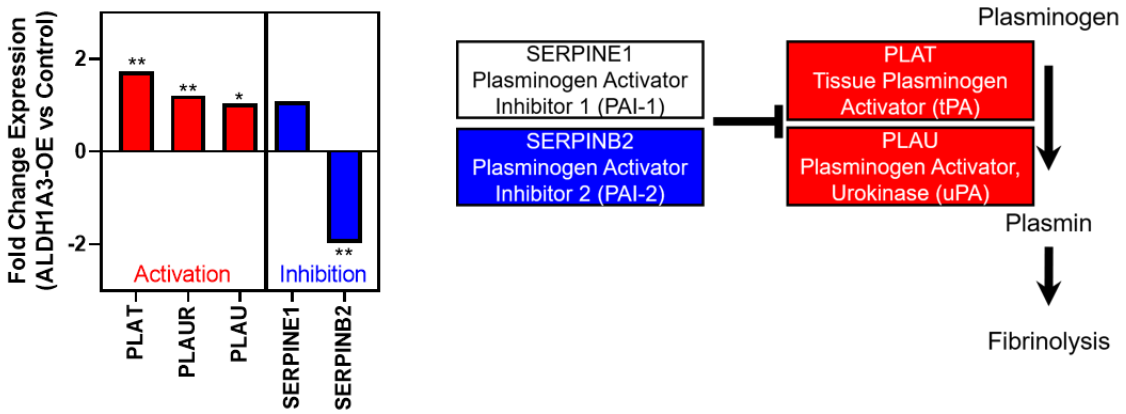

Figure 5.2: Microarray-based plasminogen activation/inhibition gene expression of MDA-MB-231 ALDH1A3-OE cells relative to control cells (Affymetrix Human Gene 2.0ST ; n=3; ANOVA). $p<0.05$*; $p<0.01$**; $p<0.001$***. KMC submitted MDA-MB-231 ALDH1A3 and Control RNA for microarray analysis.

The majority of ALDH1A3-mediated gene expression is attributed to elevated retinoic acid. As a potent transcriptional mediator, RA controls the expression of hundreds of genes- most of which likely do not contriube to ALDH1A3-mediated metatasis. In an attempt to provide insight to the ALDH1A3-hi phenotype downstream of this extensive RA-mediated transcription, differential regulation of genes which code for metabolic enzymes was assessed in the MDA-MB-231 ALDH1A3-OE cells (Figure 5.3). To provide greater relevance to patients—where the greatest activity of ALDH1A3 is not observed in bulk tumour cells, but in ALDH+ cancer stem cells— I compared the metabolism-associated transcriptional overlap of ALDH+ CSCs (Figure 5.3) and MDA-MB-231 ALDH1A3-OE cells. Overall, there was a striking overlap of metabolic pathways that contained up-regulated genes in both ALDH+ breast CSCs and MDA-MB-231 ALDH1A3-OE cells (Figure 5.4 & Table 5.3).

Gene Set Enrichment Analysis (GSEA) was performed for the top 50 most up-regulated genes in MDA-MB-231 ALDH1A3-OE cells and also for the top 50 most up-regulated genes in ALDH+ breast cancer patients cells. Though the genes up-regulated in ALDH1A3-OE and ALDH+ were not identical, the genes were enriched in 12/50 of the same gene sets, including: retinol biosynthesis (REACTOME_SIGNALING_BY_ RETINOIC_ACID, REACTOME_RA_BIOSYNTHESIS_ PATHWAY, and REACTOME_METABOLISM_OF_VITAMINS_AND_ COFACTORS), prostaglandin metabolism (REACTOME_METABOLISM_OF_LIPIDS and REACTOME_ SYNTHESIS_OF_PROSTAGLANDINS_PG_AND_THROMBOXANES_TX), and cytochrome p450 drug metabolism (KEGG_METABOLISM_OF_XENOBIOTICS_BY_ CYTOCHROME _P450, HSIAO_LIVER_SPECIFIC_GENES, and KEGG_DRUG_ METABOLISM_ CYTOCHROME_P450) (Figure 5.4).

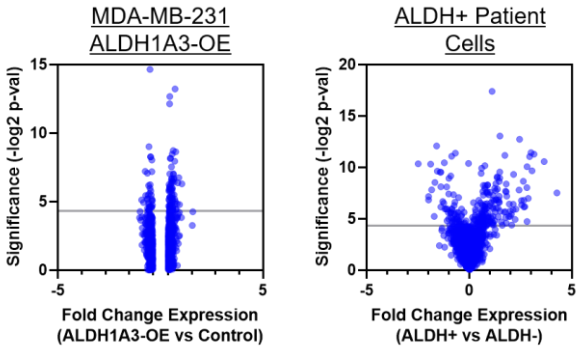

Figure 5.3: Differential expression of metabolism-associated genes in MDA-MB-231 ALDH1A3-OE and ALDH+ Aldefluor-sorted breast cancer patient samples. Microarray-based differential gene expression in MDA-MB-231 ALDH1A3-OE vs control cells (Affymetrix Human Gene 2.0ST ; n=3) and from Aldefluor-sorted primary breast tumour samples (Affymetrix Human Genome U133 Plus 2.0 Array; GSE52327[237]; n=8). Shown here is differential transcription of 1647 genes coding for metabolic enzymes (from the Comprehensive Mammalian Metabolic Enzyme Database gene list); one-way ANOVA; gray line represents p=0.05. KMC submitted MDA-MB-231 ALDH1A3 and Control RNA for microarray analysis.

Table 5.3: Up-regulated transcription of metabolic enzymes in ALDH+ breast cancer patient cells and MDA-MB-231 ALDH1A3-OE cells. The top 20 most up-regulated genes in both datasets are shown here.

		ALDH+ Breast Cancer Patient Cells		MDA-MB-231 ALDH1A3-OE Cells	
Gene Symbol	**Gene Name**	**Fold-Change Expression**	**ANOVA p-value**	**Fold-Change Expression**	**ANOVA p-value**
DHRS3	short-chain dehydrogenase/reductase 3	1.31	0.0151	10.36	0.0023
ADH1B	alcohol dehydrogenase 1B isoform 2	4.28	0.0055	1.22	0.8111
STEAP1	metalloreductase STEAP1	3.07	0.0012	1.48	0.1746
STEAP2	metalloreductase STEAP2	3.01	0.0004	1.36	0.2315
ALDH1A3	aldehyde dehydrogenase family 1 member A3	2.95	0.0005	1.24	0.1176
PTGES	prostaglandin E synthase	2.16	0.0016	2.02	0.1047
PLA2G2A	phospholipase A2, membrane associated precursor	2.88	0.0079	1.03	0.1442
PLOD2	procollagen-lysine,2-oxoglutarate 5-dioxygenase 2 isoform 2 precursor	2.82	0.0038	1.08	0.0756
PTGIS	prostacyclin synthase precursor	2.82	0.0380	1.03	0.8637
PRTFDC1	phosphoribosyltransferase domain-containing protein 1	2.63	0.0025	1.16	0.0177
PRG4	lipid phosphate phosphatase-related protein type 2	2.55	0.0124	1.14	0.3038
AKR1C1	aldo-keto reductase family 1, member C1	2.54	0.0092	1.05	0.0841
PDK4	pyruvate dehydrogenase kinase, isozyme 4	2.28	0.0164	1.08	0.9146
ALDH1L2	10-formyltetrahydrofolate dehydrogenase ALDH1L2	2.14	0.0118	1.06	0.2474
PDE1A	calcium/calmodulin-dependent 3',5'-cyclic nucleotide phosphodiesterase 1A	1.81	0.0419	1.28	0.0276
BHMT2	S-methylmethionine--homocysteine S-methyltransferase BHMT2	1.83	0.0068	1.25	0.7656
AADAC	arylacetamide deacetylase	1.47	0.0104	1.58	0.0127
HNMT	histamine N-methyltransferase	1.93	0.0269	1.03	0.0279
ACSS3	acyl-CoA synthetase short-chain family member 3, mitochondrial isoform X3	1.77	0.0049	1.18	0.0558
COX7A1	cytochrome c oxidase subunit 7A1, mitochondrial	1.78	0.0288	1.10	0.5651

A) Gene Set Enrichment Analysis of Upregulated Metabolism-Associated Genes

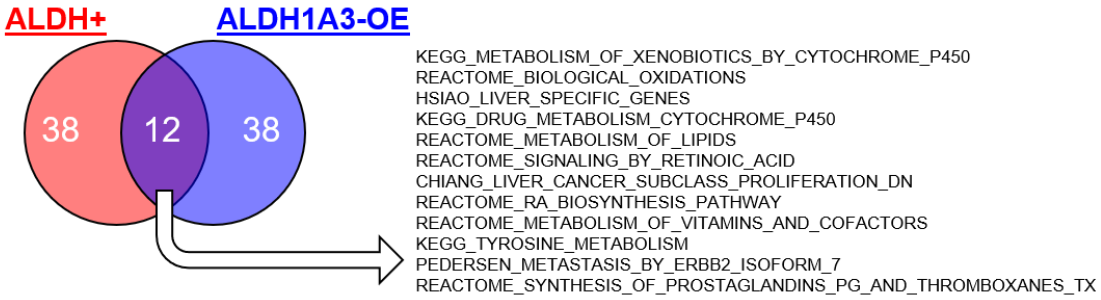

B) RA and Prostaglandin Metabolism Genes Up-regulated in ALDH+ Cells

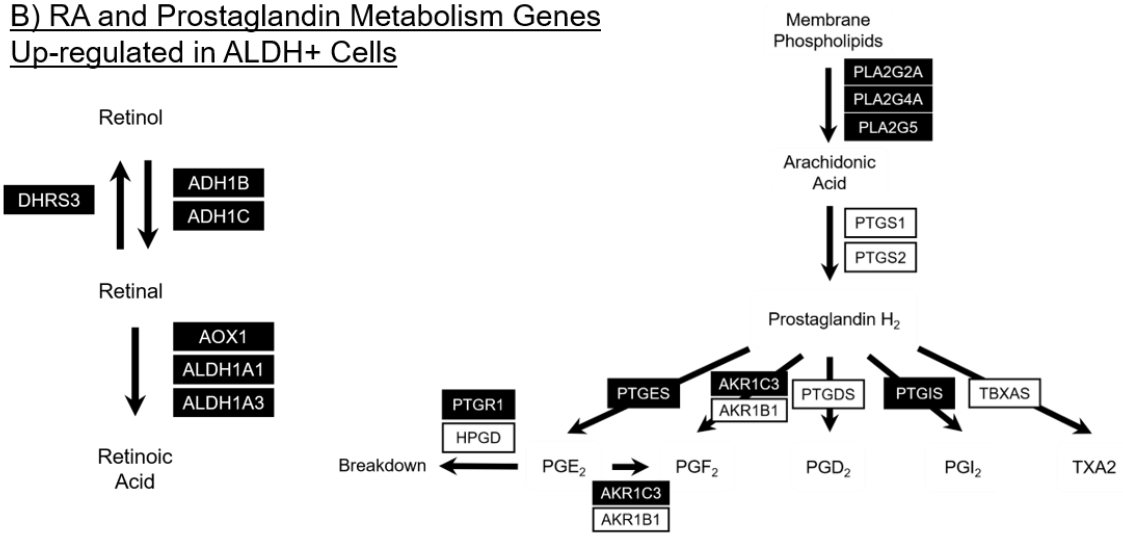

C) RA and Prostaglandin Metabolism Genes Up-regulated in ALDH1A3-OE Cells

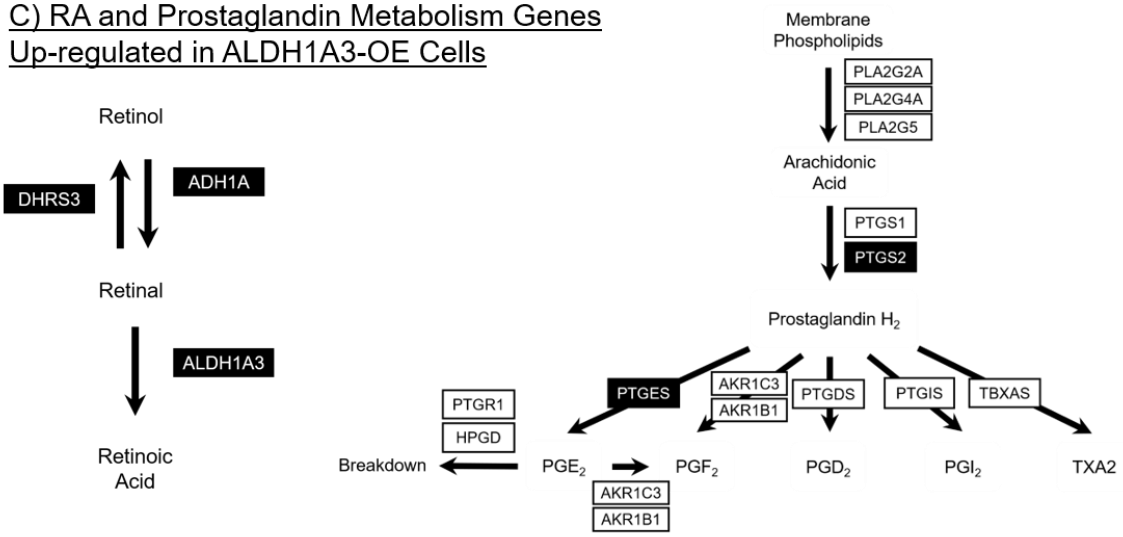

Figure 5.4: Retinoic Acid and prostaglandin metabolism is up-regulated in ALDH1A3-OE and ALDH+ breast cancer. A) Top 50 gene sets identified in Gene Set Enrichment Analysis of genes enriched in MDA-MB-231 ALDH1A3-OE or ALDH+ breast cancer cells. Specifically, which genes are up-regulated in **B)** ALDH+ breast cancer patient cells, and **C)** ALDH1A3-OE MDA-MB-231 for retinoic acid (RA) synthesis and prostaglandin metabolism are depicted with black boxes. KMC submitted MDA-MB-231 ALDH1A3 and Control RNA for microarray analysis.

Retinol biosynthesis was the metabolic pathway most likely to emerge in the ALDH-hi breast cancer cells (Figure 5.4). Increased retinoic acid synthesis is inescapable in cells with enhanced ALDH1A3 activity, as ALDH1A3 functions as a retinaldehyde dehydrogenase converting retinal to retinoic acid. Also expected is the strong induction of the retinoic acid synthesis negative feedback enzyme short-chain dehydrogenase/reductase 3 (DHRS3) which converts retinal back to retinol. Increased expression of prostaglandin biosynthesis genes was also anticipated. Expression of prostaglandin synthesis genes (e.g. PTGES and PTGS2) is known to be induced by retinoic acid and prostaglandin E2 signaling has been implicated in breast cancer stem cells previously[289,401].

Overall, the relationship between ALDH1A3 and retinoic acid/prostaglandin synthesis was also reflected in breast cancer patient data. In biopsies of n=806 primary breast tumours, there is a strong positive correlation for expression of ALDH1A3 and expression of retinoic acid biosynthesis and prostaglandin synthesis genes (Figure 5.5). However, expression of prostaglanden E2 synthase (PTGES) was not significantly correlated with ALDH1A3 in these bulk tumour biopsies (Pearson r = -0.005, p=0.4448).

Of clinical relevance is the up-regulation of cytochrome p450 drug metabolism pathways (Figure 5.4) seen in ALDH1A3-hi breast cancer cells. As ALDH+ cancer stem cells are inherently resistant to chemotherapy, an ALDH1A3/cytochrome p450 axis might

present a new target for improving chemotherapy sensitivity. Importantly, chemoresistance and metastasis use interconnected pathways. For example, Twist increases both invasive potential and chemotherapy resistance of breast cancer cells by dowregulating estrogen receptor-α and upregulating AKT[408,409]. However, none of the genes that code for the cytochrome p450 drug metabolism proteins themselves (CYP1A2/2A13/2A6/2A7 /2B6/2C18/2C19/2C8/2C9/2D6/2E1/3A4/3A43/3A5/3A7) were up-regulated in ALDH-hi cells. Instead, accessory enzymes which feed into cytochrome p450 were up-regulated (e.g. ALDH3B2, ADH1A, and ADH1B). Without a clear chemoresistance expression profile, I cannot glean any insights into combined chemoresistance/metastasis pathways mediated by ALDH1A3. Based on transcriptional data alone, the best novel candidate for explaining ALDH1A3-mediated metastasis may involve plasminogen activation (Figure 5.2)

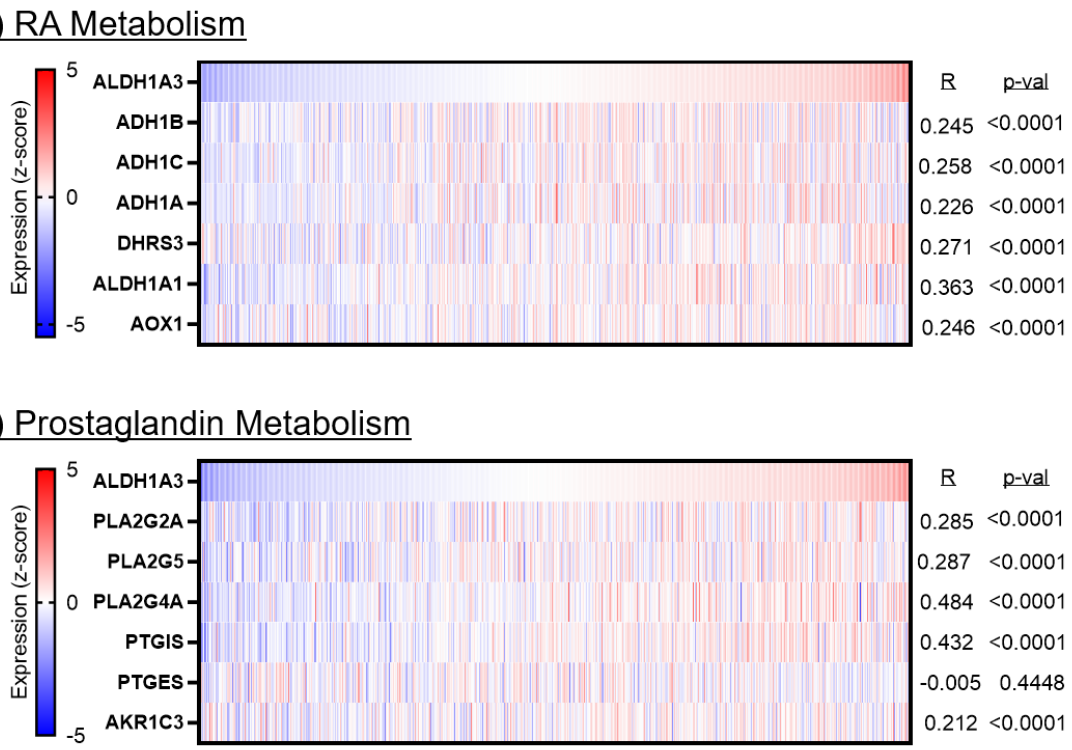

Figure 5.5: Correlation of RA and prostaglandin metabolism gene expression with ALDH1A3 expression in breast cancer patient samples. RNA-seq (V2 RSEM; z-score)-based expression data for n=816 primary breast tumour samples (TCGA, Cell 2015) for ALDH1A3, retinoic acid, and prostaglandin metabolism genes upregulated in MDA-MB-231 ALDH1A3-OE and/or ALDH+ breast cancer cells. Pearson correlation R- and p-values for each metabolism gene vs ALDH1A3.

5.3.3 *INCREASED PLASMIN GENERATION MAY CONTRIBUTE TO ALDH1A3-MEDIATED INVASION*

The increased expression of plasminogen activators PLAT and PLAU with concurrent downregulation of plasminogen activator inhibitor SERPINB2 in the MDA-MB-231 ALDH1A3-OE cells (Figure 5.2) suggested that ALDH1A3's pro-metastatic phenotype may be due to elevated plasminogen activation. To directly quantify plasminogen activation activity, a chromogenic plasminogen assay was performed. Briefly, a chromogenic substrate for plasmin is added to the cells in culture and this substrate will change color in the presence of plasmin (the activated form of plasminogen) in a time-dependent manner. In both MDA-MB-231 and MDA-MB-436 cells, when there is elevated ALDH1A3 there is subsequently increased plasminogen activation (Figure 5.6A).

Enhanced plasminogen activation is associated with increased invasive and metastatic potential in many cancer models[402]. The enhanced invasive capacity of MDA-MB-231 ALDH1A3-OE cells has been characterized previously, but not in the context of plasminogen activation. All previous invasion experiments assessing the invasive potential of MDA-MB-231 ALDH1A3-OE cells were performed with replete FBS (which would contain variable levels of endogenous bovine plasminogen). To test the role of plasminogen activation more exclusively in ALDH1A3-mediated MDA-MB-231 cell invasion, the conventional transwell invasion assay was performed, but with plasminogen-stripped FBS +/- 0.25μM human plasminogen. With plasminogen-stripped FBS, MDA-MB-231 ALDH1A3-OE only has an invasive advantage over control cells in the presence of plasminogen (Figure 5.6B). Similarly, in replete FBS (which contains trace levels of bovine plasminogen that can be activated by human PLAT and PLAU to plasmin) MDA-MB-436 ALDH1A3-KD cells were less invasive than control cells (Figure 5.1E).

Mirroring the effect seen in MDA-MB-231 ALDH1A3-OE cells, reduced plasminogen activation was observed in MDA-MB-436 ALDH1A3-KD cells (Figure 5.6A); but, unlike MDA-MB-231 there was no significant differential expression of plasminogen activation genes (Figure 5.6C). Indeed ALDH1A3-KD cells expressed lower levels of plasminogen activator-2 (SERPINB2) than control cells which would incorrectly imply that MDA-MB-436 ALDH1A3-KD cells have improved plasminogen activation over control cells.

The plasminogen activation transcription profile was also assessed in ALDH+ breast cancer stem cells. In ALDH+ CSCs there is increased expression of plasminogen activators PLAT and PLAU, while plasminogen inhibitor SERPINE1 is significantly elevated in ALDH+ cells (Figure 5.6D). Due to the discrepancy of actual plasminogen activation (chromogenic assay) versus the predicted activity (transcription profile) observed in the MDA-MB-436 ALDH1A3-KD cells, the extent of plasminogen activation capacity in ALDH+ breast cancer stem cells should be assessed with the direct chromogenic plasminogen assay. Plasminogen activation may be a paradigm for how transcriptional data alone cannot capture the true phenotype of ALDH1A3-OE cells and underscores a need to complement gene expression data with additional methods like metabolomics.

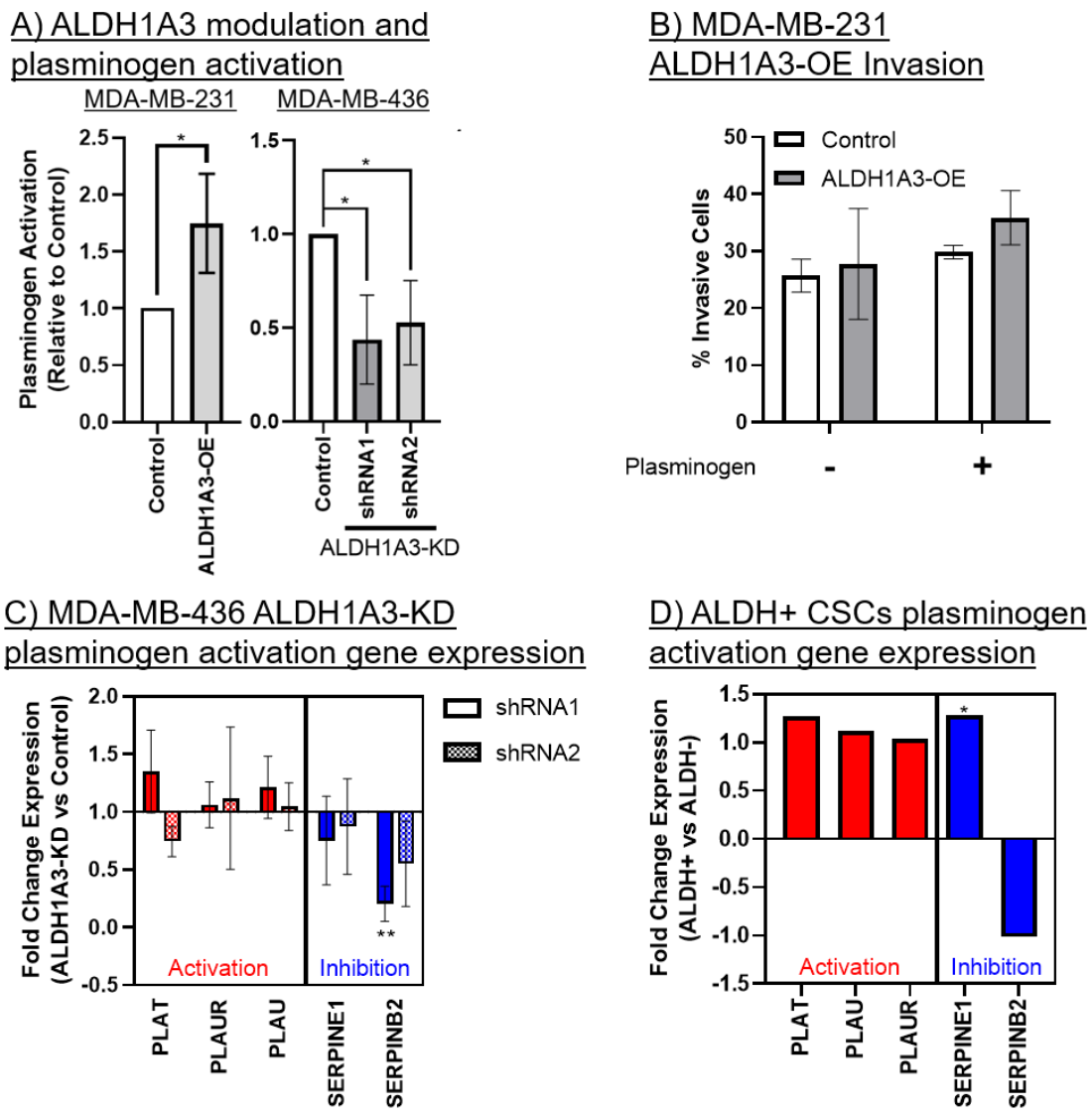

Figure 5.6: Plasminogen activation is enhanced by ALDH1A3 and may contribute to the invasive potential of MDA-MB-231 and MDA-MB-436 cells. A) Colorimetric plasminogen activation assay applied to MDA-MB-231 ALDH1A3-OE (one sample t-test) and MDA-MB-436 ALDH1A3-KD (one-way ANOVA with Dunnett's post-hoc test) cells (n=4, SD error bars). **C)** Invasive potential of MDA-MB-231 ALDH1A3-OE cells +/- 0.25µM plasminogen (n=2, bars represent range). **D)** RT-qPCR based gene expression of plasminogen activation/inhibition gene expression in MDA-MB-436 ALDH1A3-KD cells relative to control cells (one-way ANOVA with Dunnett's post-hoc test; n=4, SD error bars). $p<0.05$*; $p<0.01$**. DB performed plasminogen activation assays.

5.3.4 *METABOLOMICS ANALYSIS REVEALED THAT GABA DEGRADATION IS DYSREGULATED IN MDA-MB-231 ALDH1A3-OE TUMOURS*

Due to the discrepancy between transcription and phenotype observed in the plasminogen activation pathway, it occurred to us that complementing transcriptomics with metabolomics is a potential strategy to identify pro-metastatic pathways that are not obvious by gene expression data alone. HPLC-MS metabolomic analysis of MDA-MB-231 ALDH1A3-OE tumours and MDA-MB-231 ALDH1A3-OE cells grown in monolayer adherent culture revealed remarkably similar metabolite profiles between *in vivo* and *in vitro* ALD1A3-OE samples (Figure 5.7A & 5.7B). Control tumours had a significantly different metabolite profile than ALDH1A3-OE tumours, exemplified by the number of differentially abundant metabolites (23/72), and distinguishable subgroups in principal component analysis (Figure 5.7C). The ALDH1A3-OE cells grown in culture did not have as distinct a metabolite profile as their control cell counterparts, with 4/72 differentially abundant metabolites and poorly separated subgroups via principal component analysis (Figure 5.7D).

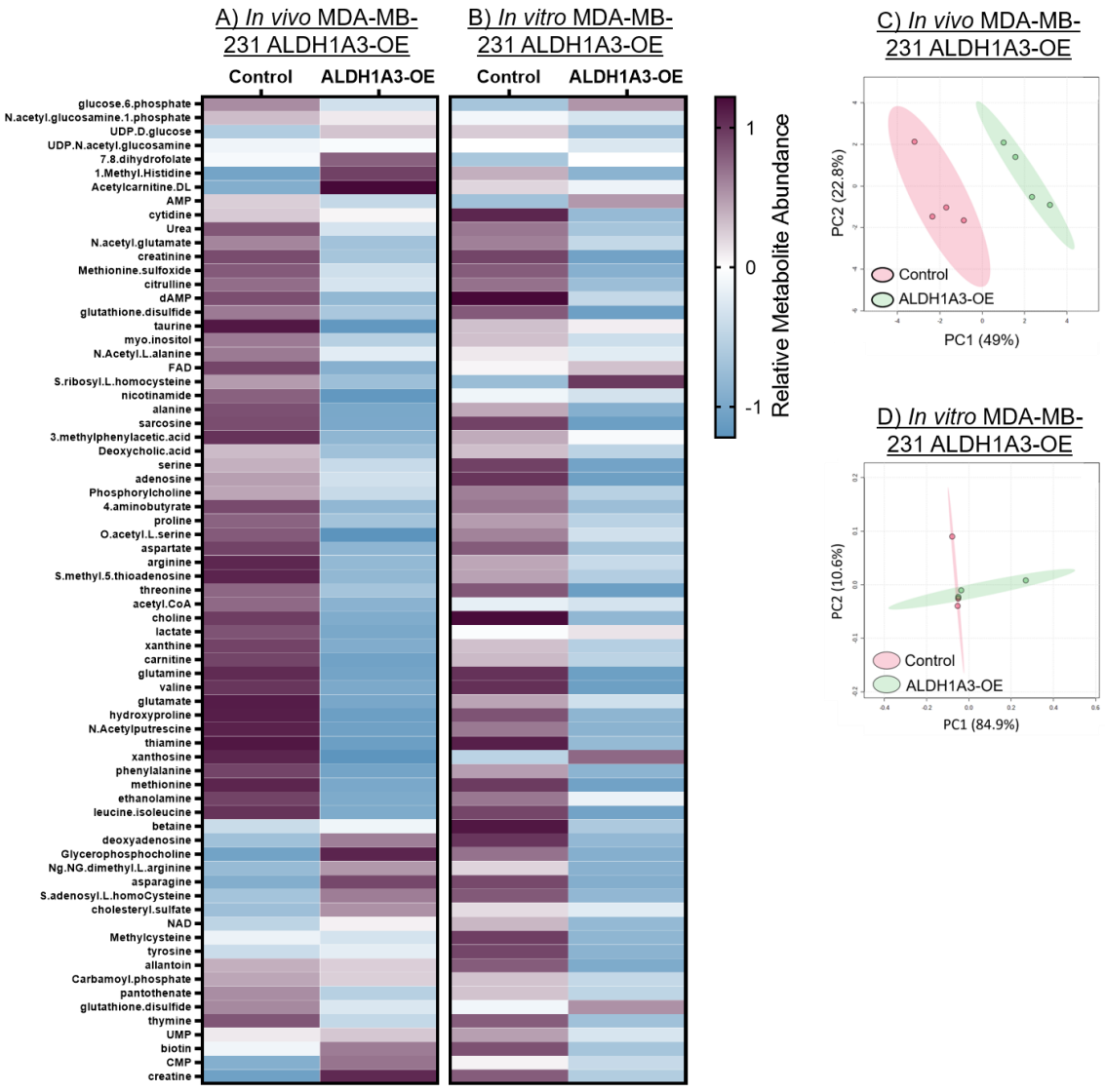

Figure 5.7: HPLC- MS Metabolomics identifies GABA metabolism as a dysregulated pathway in MDA-MB-231 breast cancer cells overexpressing ALDH1A3. Heatmap of mean normalized metabolite levels detected by Sciex 5500 QTRAP mass spectrometer[406]; 72 metabolites clustered using Euclidean Distances based on the *in vivo* ALDH1A3-OE samples. **A)** *In vivo* samples taken from MDA-MB-231 tumours +/- ALDH1A3-overexpresion (ALDH1A3-OE) after 53 days of tumour growth (Control n=4, ALDH1A3-OE n=4). **B)** *In vitro* samples from MDA-MB-231 cells grown in subconfluent adherent monolayers; n=3 per group. JPM, MAG, AC, and HW developed targeted metabolomics method, ran the mass spectrometer, and assisted in data analysis

The changes in metabolite abundance in the MDA-MB-231 ALDH1A3 cells/tumours were combined with the metabolism-associated gene expression data to form a transcriptomic-metabolomic map and identify dysregulated pathways (Figure 5.8). The central subnetwork contains the metabolites glutamate (L-glutamic acid) and 4-aminobutyrate (GABA), as well as gene expression for 4-aminobutyrate aminotransferase (ABAT) (Figure 5.8A). These components form a "GABA degradation" node and have a high degree centrality (the number of connections made to other nodes) and betweenness centrality (the number of shortest paths going through the node) (Table 5.4). This places GABA metabolism as a central component of the ALDH1A3-OE phenotype. GABA metabolites were among the metabolites that were similarly altered in both *in vivo* and *in vitro* ALDH1A3-OE samples (γ-aminobutyric acid and its intermediate metabolites N-acetylputrescine and glutamate) (Figure 5.9). As a pathway that has been implicated in tumour growth and metastasis, GABA metabolism was prioritized for further study.

A) Integrated Gene-Metabolite Interaction Network of MDA-MB-231 ALDH1A3-OE

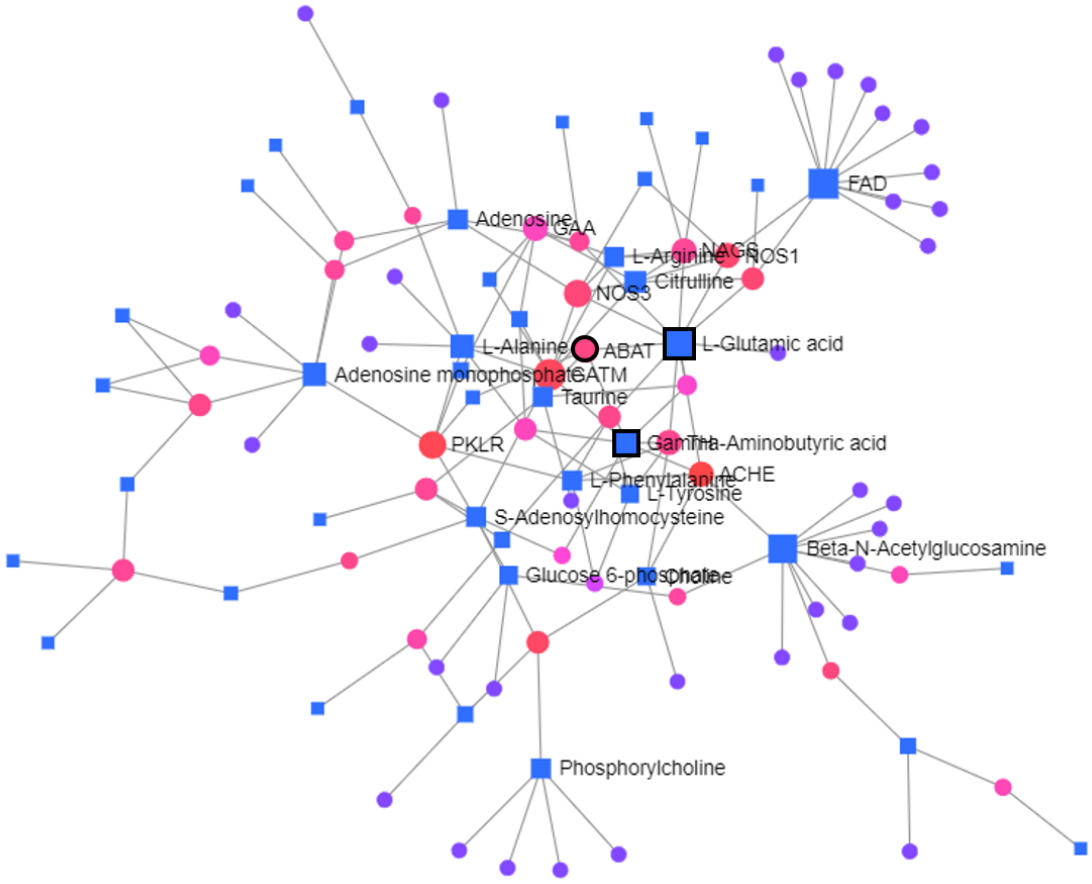

B) Downregulated in ALDH1A3-OE

Pathway	p-value
Catecholamine biosynthesis	2.09E-07
Glycosphingolipid metabolism	1.22E-05
Amine-derived hormones	1.85E-05
Glyoxylate metabolism	0.000145
The activation of arylsulfatases	0.00111
Nitric oxide stimulates guanylate cyclase	0.00482
Phagosomal maturation (early endosomal stage)	0.00758
Proline catabolism	0.00777
NOSIP mediated eNOS trafficking	0.00777
Degradation of GABA	0.00777

C) Up-regulated in ALDH1A3-OE

Pathway	p-value
Resolution of AP sites via the multiple-nucleotide patch replacement pathway	3.05E-05
Base Excision Repair	4.32E-05
N-glycan antennae elongation in the medial/trans-Golgi	4.32E-05
Asparagine N-linked glycosylation	0.000264
Transport to the Golgi and subsequent modification	0.00028
Removal of the Flap Intermediate from the C-strand	0.000595
Keratan sulfate biosynthesis	0.00446
Cysteine formation from homocysteine	0.00747
Ceramide signalling	0.0112
Reactions specific to the complex N-glycan synthesis pathway	0.0112

Figure 5.8: Gene Expression/Metabolite interaction network places GABA metabolism at center of ALDH1A3-OE phenotype. **A)** Gene-Metabolite interaction network for ALDH1A3-OE tumours/cells showing the central network and distal nodes. The GABA degradation gene (ABAT) and metabolites (Gamma-aminobutyric acid and L-glutamic acid) are outlined in black. The top 10 **B)** Downregulated and **C)** upregulated Reactome pathways in ALDH1A3-OE tumours/cells identified by Gene-Metabolite interaction network. JPM, MAG, AC, and HW developed targeted metabolomics method, ran the mass spectrometer, and assisted in data analysis. KMC submitted MDA-MB-231 ALDH1A3 and Control RNA for microarray analysis.

Table 5.4: Node centrality within gene-metabolite interaction map of ALDH1A3-OE tumours/cells[343]

Id	Label	Degree Centrality	Betweenness Centrality
C00016	FAD	12	986.29
C00025	**L-Glutamic acid**	11	1570.85
C03878	Beta-N-Acetylglucosamine	11	1406.99
2628	GATM	8	891.34
C00020	Adenosine monophosphate	7	890.48
C00041	L-Alanine	7	689.59
C00334	**Gamma-Aminobutyric acid**	7	427.67
5313	PKLR	6	1047.12
4846	NOS3	6	469.81
C00327	Citrulline	6	407.97
43	ACHE	5	1445.53
C00021	S-Adenosylhomocysteine	5	761.02
4842	NOS1	5	632.9
C00079	L-Phenylalanine	5	491.17
C00212	Adenosine	5	459.16
C00588	Phosphorylcholine	5	406
18	**ABAT**	5	347.13
7054	TH	5	281.74
C00245	Taurine	5	252.05
C00062	L-Arginine	5	236.8

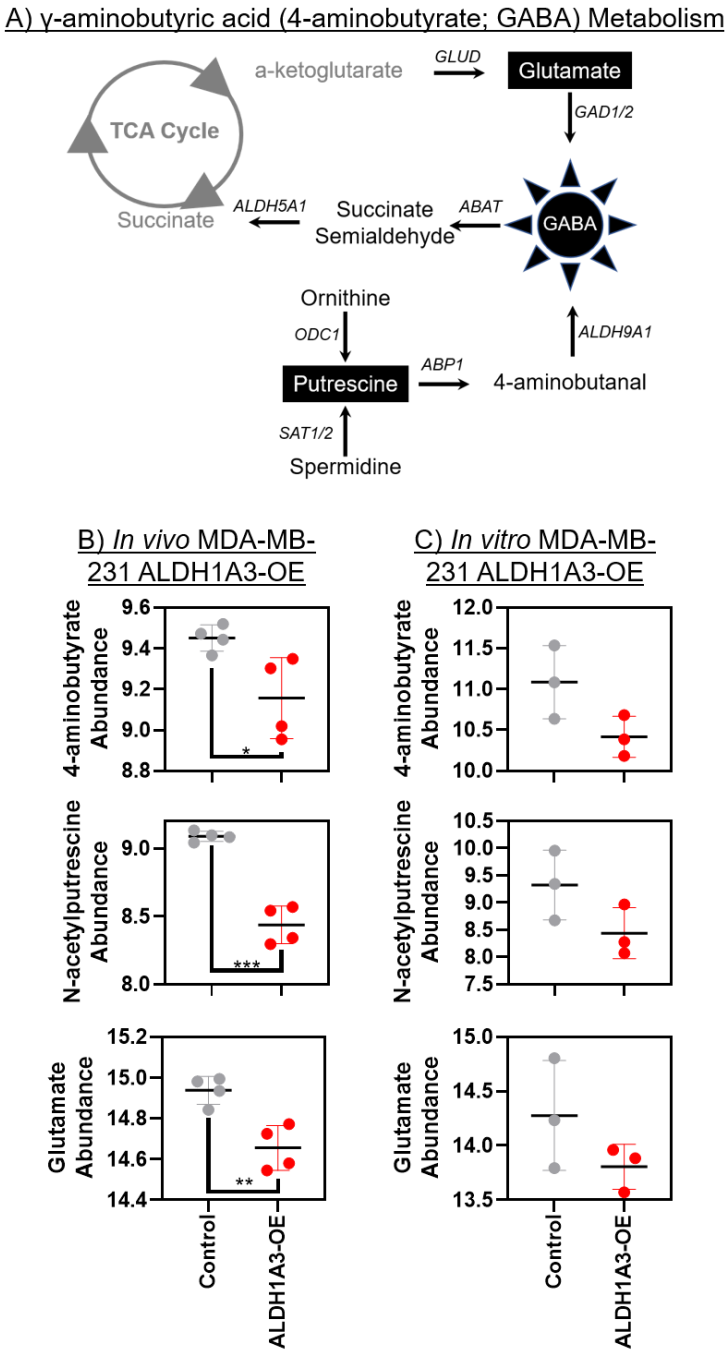

Figure 5.9: GABA and GABA metabolism intermediates are less abundant in MDA-MB-231 ALDH1A3-OE tumours and cell cultures but not in ATRA-treated cells. A) GABA metabolism with detected metabolites in black boxes. **B-D)** GABA and GABA intermediate metabolite abundance (N-acetylputrescine and glutamate/L-glutamic acid); mean, SD error bars, unpaired two-tailed t-test (n=4 ALDH1A3-OE *in vivo*, n=4 *in vivo* NT and *in vitro* ALDH1A3-OE and ATRA-treatment). $p<0.05$*; $p<0.01$**, $p<0.001$***. JPM, MAG, AC, and HW developed targeted metabolomics method, ran the mass spectrometer, and assisted in data analysis.

5.3.5 *GABA TREATMENT ENHANCES METASTASIS OF MDA-MB-231 TUMOURS*

The gene-metabolite interaction network suggests that there is dysregulated GABA signaling/metabolism in ALDH1A3-OE cells; but metabolomics provides a snapshot of metabolite abundance with little insight into the direction of metabolism. The reduced GABA observed in ALDH1A3-OE tumours/cells could be due to rapid flux of GABA metabolism based on high usage, or due to GABA metabolism being avoided altogether. To determine whether GABA is utilized by MDA-MB-231 cells as an oncometabolite/signaling molecule to drive tumour growth or metastasis, mice harbouring MDA-MB-231 control or ALDH1A3-OE tumours were treated with systemic GABA.

As expected, MDA-MB-231 ALDH1A3-OE tumours were larger in both volume and mass when compared to control tumours (Figure 5.10A 5.10B). Systemic treatment with 250 µg/kg GABA did not significantly impact tumour growth. Assessment of lung metastasis via human GAPDH RT-qPCR assay revealed that mice treated with GABA or with ALDH1A3-OE primary tumours had more MDA-MB-231 cells in their lungs, and ALDH1A3-OE did not enhance GABA's pro-lung metastasis effect (Figure 5.10C). The RT-qPCR lung metastasis assay is confirmed by H&E stained lung sections (Figure 5.10D) where ALDH1A3-OE tumours colonized a greater portion of lung tissue (Figure 5.10E). Though the % of metastatic lung tissue is not significantly different between untreated and GABA-treated mice harbouring control tumours, a larger portion of GABA-treated mice had detectable lung metastasis (8/13; 61.5%) compared to untreated control MDA-MB-231 (5/15; 33%). The incidence of metastasis was similar in GABA-treated mice (8/10; 80%) versus untreated mice (11/11; 100%) harbouring ALDH1A3-OE tumours

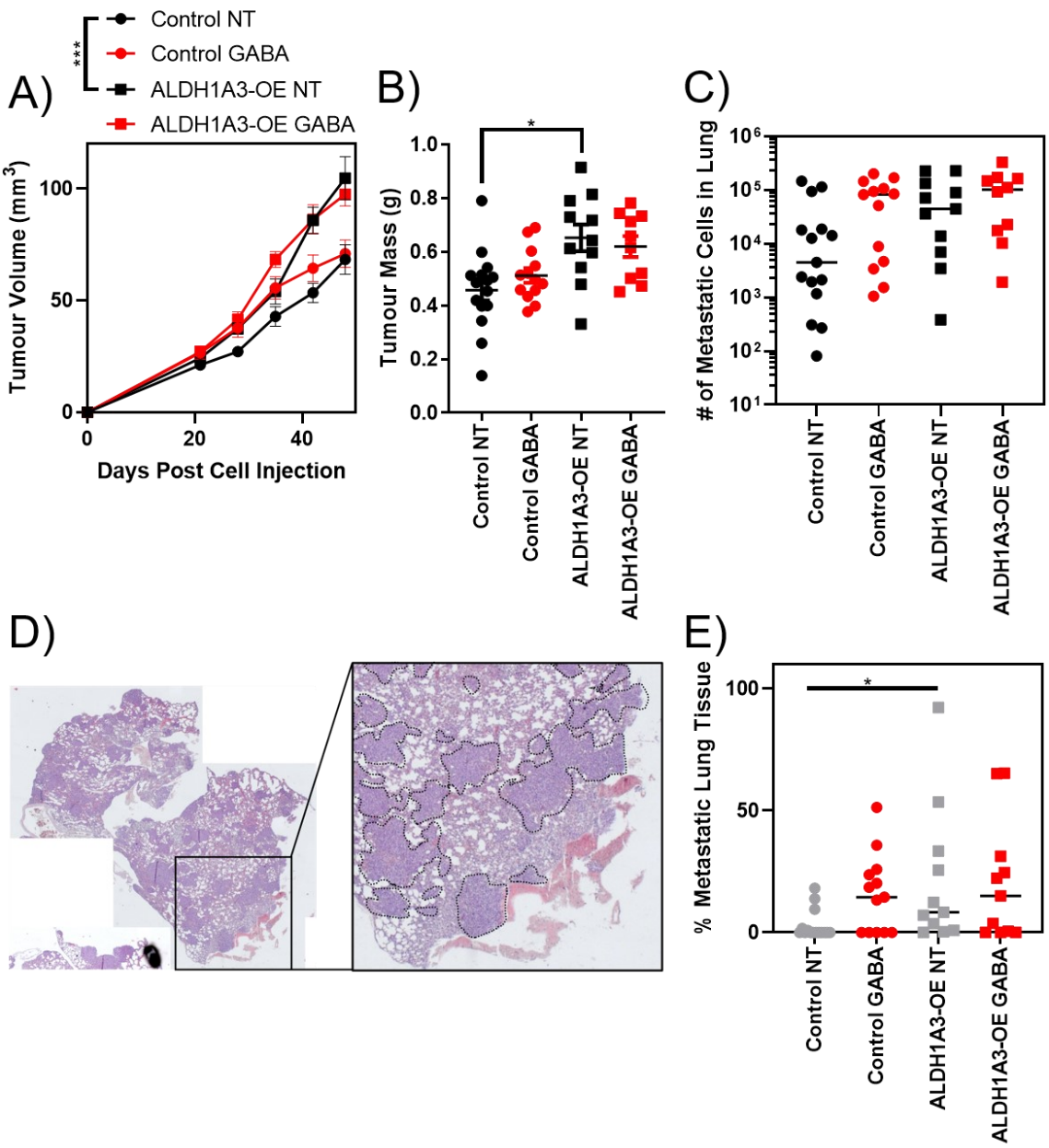

Figure 5.10: Systemic GABA treatment may increase metastatic potential of MDA-MB-231 tumours. A) ALDH1A3 overexpression increases MDA-MB-231 tumour volume and **B)** tumour mass. Treatment with systemic GABA (daily 250 µg/kg IP injections) does not alter tumour volume/mass (Control NT n=15; Control GABA n=13; ALDH1A3-OE NT n=11, ALDH1A3-OE GABA n=10; SEM error bars). **C)** RT-qPCR quantified lung metastasis (median, SEM error bars). **D)** Light microscopy image of H&E stained lung section; example from GABA-treated control tumour bearing mouse with metastatic nodes outlined. **E)** Histology quantified lung metastasis (median, SEM error bars); $p<0.05$*. HW assisted with intraperitoneal injections, CD performed RT-qPCR and H&E lung metastasis quantification.

Since enhanced GABA metabolism has been implicated in breast cancer cells that preferentially metastasize to the brain[403], the incidence of brain metastasis in GABA-treated mice is being assessed. Mouse brains were formalin fixed and paraffin embedded and are being H&E stained. In our hands, the MDA-MB-231 tumours do not typically metastasize to the brain of NOD/SCID mice at 48 days post cell injection. However, the first brain assessed for metastasis—from a mouse harbouring an MDA-MB-231 ALDH1A3-OE tumour treated with GABA—showed detectable micrometastases in 2/3 brain sections (one section shown in Figure 5.11). The remainder of mouse brains will be sectioned and stained.

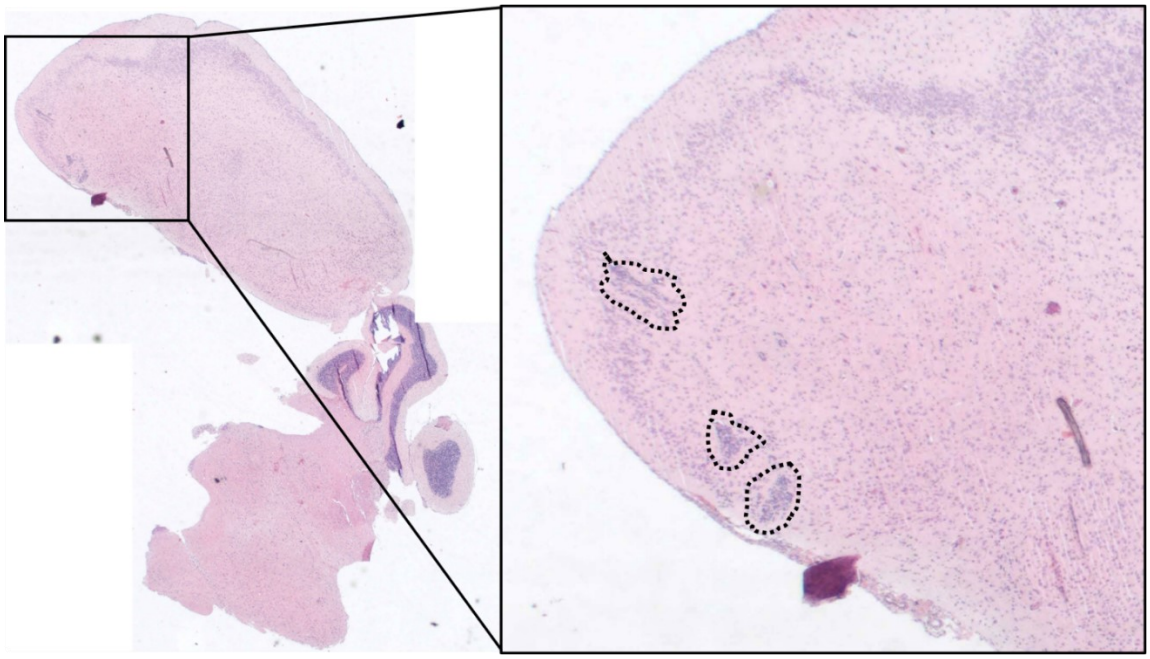

Figure 5.11: Brain micrometastases observed in a mouse harbouring MDA-MB-231 ALDH1A3-OE tumour treated with systemic GABA (n=1). Light microscopy image, H&E stained, metastatic nodes outlined in dotted black line. CD performed H&E staining.

5.3.6 *ABAT EXPRESSION IS LOWER IN BREAST TUMOURS WITH HIGH ALDH1A3 EXPRESSION AND IN BREAST TUMOURS THAT METASTASIZE*

Exogenous GABA treatment increased metastasis of MDA-MB-231 control tumours but not ALDH1A3-OE tumours. The interaction between GABA signaling/metabolism and ALDH1A3 is unclear, so the MDA-MB-231 ALDH1A3-OE microarray gene expression data was revisited to determine if there is differential expression of GABA signaling/metabolism genes that could suggest the directionality of GABA signaling/metabolism in the ALDH1A3-OE cells (Figure 5.12A). In MDA-MB-231 ALDH1A3-OE cells there was significantly reduced expression of γ-aminobutyrate aminotransferase (ABAT); with significant up-regulation of γ-aminobutyric acid receptor subunit ε (GABRE), γ-aminobutyric acid receptor subunit α-6 (GABRA6), glutamate decarboxylase 1 (GAD1), and succinic semialdehyde dehydrogenase (ALDH5A1) (Figure 5.12B).

In two independent breast cancer patient datasets (TCGA, Cell 2015 and METABRIC), expression of ABAT was negatively correlated (Pearson correlation r= -0.175 and -0.2734 respectively) while expression of GABRE was positively correlated (Pearson correlation r= 0.3585 and 0.3075) with ALDH1A3 expression (Figures 5.12C & 5.12D). Neither GABRA6, GAD1, or ALDH5A1 were significantly and consistently correlated with ALDH1A3 expression in the TCGA or METABRIC datasets (Pearson r: GABRA6 -0.0528 & 0.0117; GAD1 -0.0343 & -0.1308; ALDH5A1 0.0794 & -0.2195 respectively).

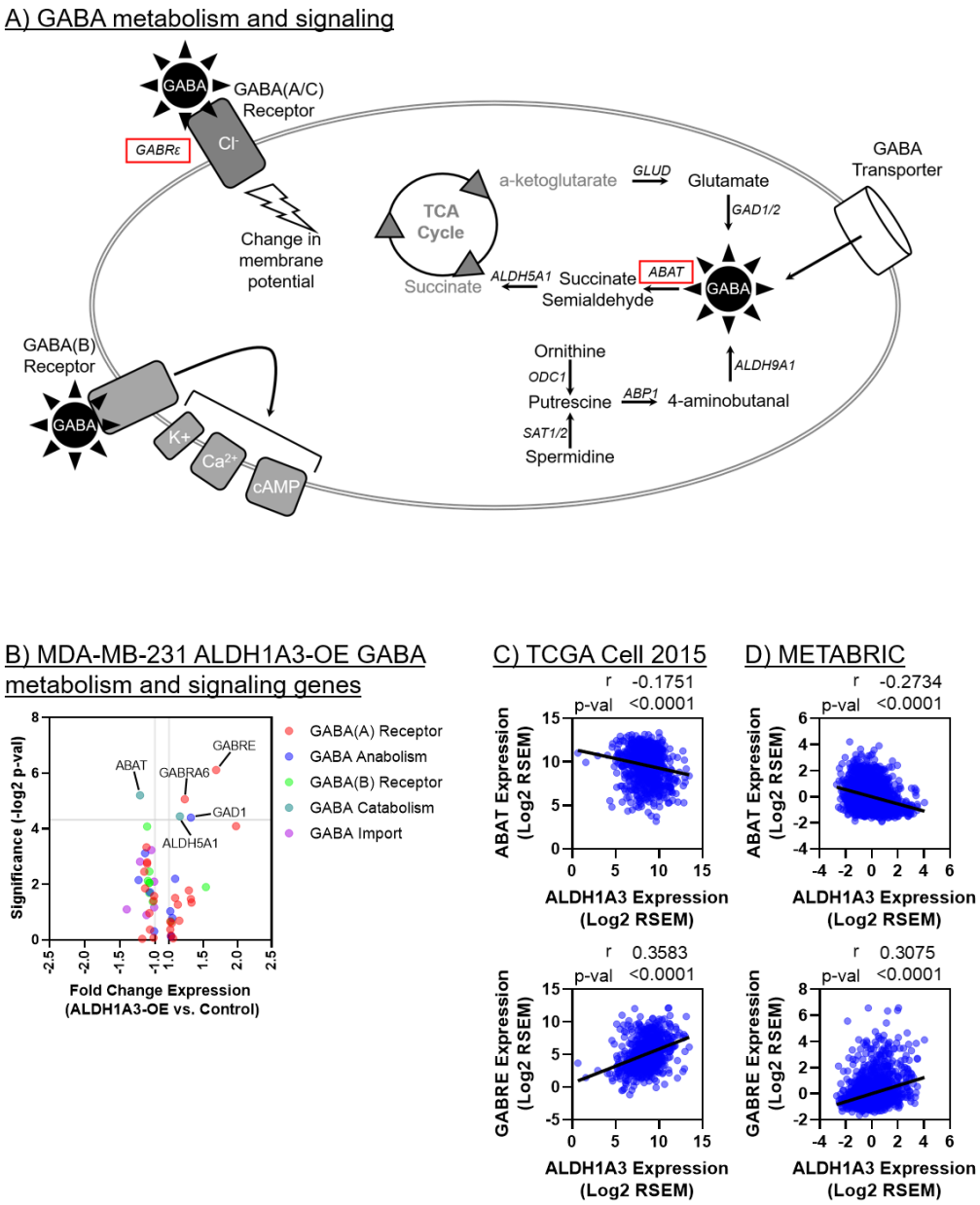

Figure 5.12: GABA signaling/metabolism genes are differentially expressed in MDA-MB-231 cells and breast tumours with high ALDH1A3 levels. A) The GABA signaling/metabolism pathway with receptors, channels, and metabolism. **B)** Transcriptome analysis of MDA-MB-231 cells (ALDH1A3 overexpression versus control cells) was completed by Affymetrix Human Gene 2.0ST Array (n=3) identifies differential expression of some GABA signaling/metabolism (e.g. downregulation of ABAT and upregulation of GABRE upon ALDH1A3 overexpression); grey line p=0.05. **C** and **D)** The changes in expression in GABA signaling pathway players ABAT and GABRE induced by ALDH1A3 overexpression in MDA-MB-231 cells is mirrored in expression correlations in breast cancer patient tumour data sets (METABRIC n=1904, and TCGA, Cell 2015 n=816; RNA-Seq RSEM log2; Pearson correlations). KMC submitted MDA-MB-231 ALHD1A3-OE and Control RNA for microarray analysis.

As a major inhibitory neurotransmitter in the central nervous system, GABA is most abundant in the brain[410]. If ALDH1A3-hi breast cancer cells can "hijack" GABA signaling/metabolism, these cells may be more likely to metastasize to the GABA-enriched brain microenvironment. To determine if ABAT or GABRE coordinate with ALDH1A3 to promote brain metastasis, two independent datasets for gene expression of primary breast tumours were assessed (GSE2034 and GSE12276). As in the TCGA and METABRIC datasets (Figure 5.12C), expression of ABAT was negatively correlated (r=-0.2823 and -0.3264) while GABRE was positively correlated (r=0.3336 and 0.3574) with ALDH1A3 expression (Figure 5.13A & 5.13B). In both patient groups, low ABAT expression in the primary breast tumour was significantly and strongly associated with increased risk of brain metastasis (HR=4.486 & p=0.0372; HR=4.043 & p=0.0044), while GABRE was not.

The lung is a common site of breast cancer metastasis, especially for TNBC[411]. ALDH1A3-driven lung metastasis is well established in the MDA-MB-231 model (Figures 5.1 and 5.10)[138], and now I have observed GABA-driven lung metastasis of MDA-MB-231 tumours (Figure 5.10) as well. When primary breast tumours have low ABAT expression, there is a higher risk for metastasis to all distal sites excluding brain (GSE12276; HR=1.898; p<0.0001), and a higher risk for lung-specific metastasis (GSE2603; HR=7.334; p=0.0022 & GSE5327; HR=2.532; p=0.0156). GABRE expression did not impact the risk of distant metastasis (Figure 5.13).

ABAT-lo/ALDH1A3-hi primary tumours are more likely to metastasize to several distal sites, implying that these cells (the "seeds") have an inherent metastatic capacity not wholly dependent on the microenvironment of the metastatic site (the "soil). Since ABAT

is the key enzyme which degrades GABA, reduced ABAT levels in these highly metastatic primary tumours suggests that there is more available endogenous GABA for signaling/metabolism. Together, this brain and lung metastasis data suggests that ABAT-low primary breast tumours (often with concurrent high ALDH1A3 expression) are highly metastatic and are agnostic to whether the metastatic site is enriched for GABA (i.e., the brain) or is depleted for GABA (i.e. the lung). Completed analysis of ALDH1A3-mediated brain metastasis in my experimental GABA-treated model can clarify this concept.

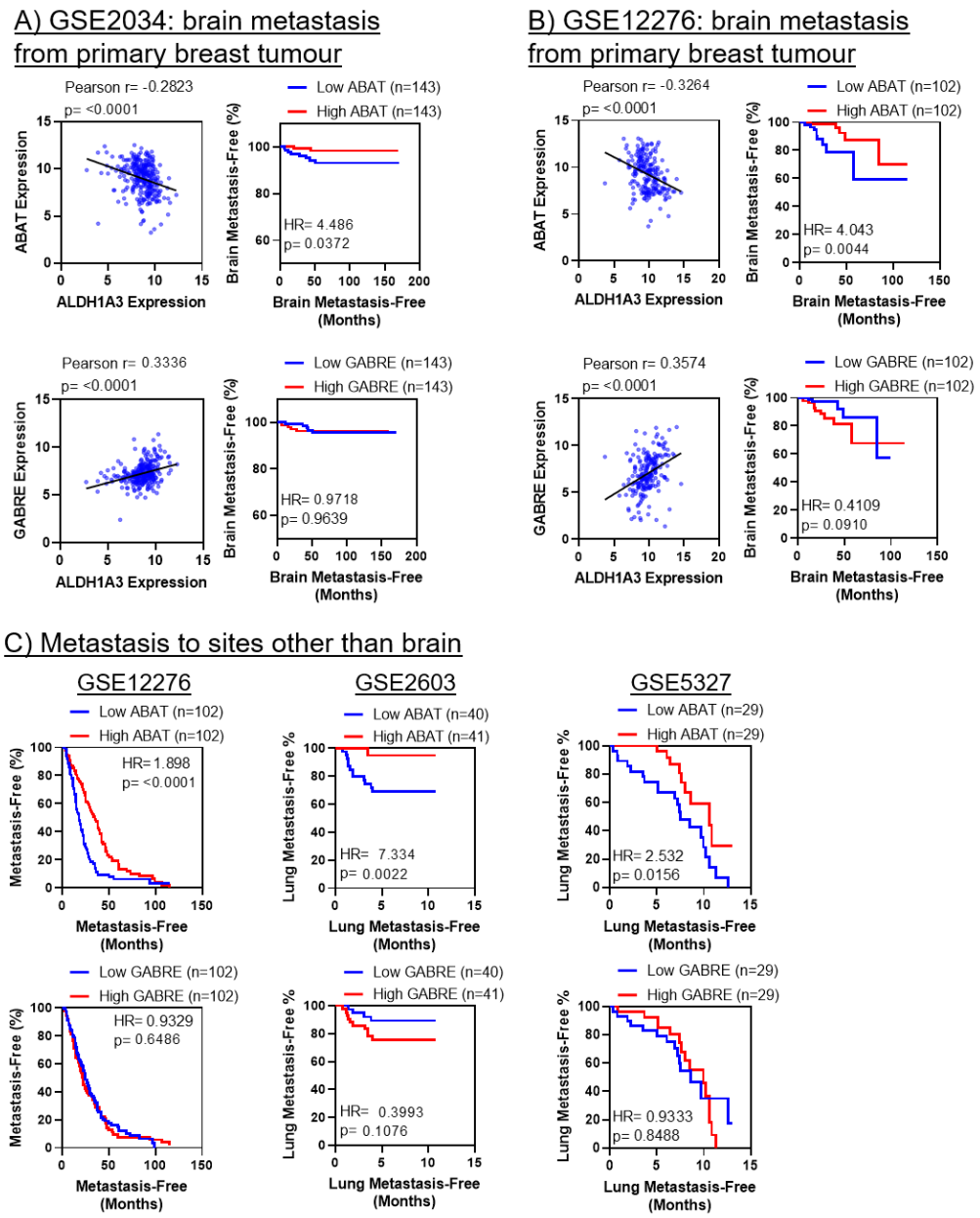

Figure 5.13: Metastasis is associated with reduced ABAT expression in primary breast tumours. Microarray-based gene expression of ABAT or GABRE correlated with ALDH1A3 expression. High and low expression of ABAT and GABRE was categorized based on median expression for Kaplan-Meier metastasis-free survival analysis. **A)** GSE2034: Affymetrix Human Genome U133A Array log2 expression from primary tumours of 286 lymph node negative breast cancer patients[412]. **B)** GSE12276: Affymetrix Human Genome U133 Plus 2.0 Array log2 expression of 204 primary breast tumours from patients all of whom experienced local or distant relapse[413]. **C)** GSE2603: Affymetrix Human Genome U133A Array log2 expression from primary tumours of 81 breast cancer patients; GSE5327: Affymetrix Human Genome U133A Array log2 expression from 48 primary ER- breast tumours.

5.4 DISCUSSION

In this study, the transcriptome and metabolome of TNBC cells with elevated ALDH1A3 activity were studied. This was done to identify novel ways in which ALDH1A3 contributes to the aggressive nature of TNBC cells. I find that high aldehyde dehydrogenase activity from ALDH1A3 is not just a marker, but a functional mediator of growth and metastasis in breast cancer. The direct contribution of ALDH1A3 to metastasis may be mediated through enhanced plasminogen activation and aberrant GABA signaling/metabolism.

Though MDA-MB-231 ALDH1A3-OE cells are not true breast cancer stem cells, this cell line does recapitulate many features of breast CSCs such as enhanced colony-formation, tumour growth, and metastatic capacity[138]. When compared to ALDH+ breast cancer stem cells, the metabolism-associated gene expression profile of MDA-MB-231 ALDH1A3-OE cells contains up-regulation of the same retinoid and prostaglandin synthesis programs.

In retinoid biosynthesis, retinol is reversibly oxidized by ADHs to retinaldehyde, which is then irreversibly oxidized to RA by cytosolic ALDH1 (human ALDH1A1, ALDH1A2, ALDH1A3) or aldehyde oxidase (AOX1)[135]. As an important mediator of stem cell differentiation versus expansion, retinoid signaling is an establish feature of ALDH+ breast cancer stem cells[414]. Unfortunately, retinoid-based treatments for solid tumours have contradictory results in clinical trials- at times reducing tumour burden but in other cases accelerating disease progression[226]. It is unlikely that retinoid-based therapies for solid tumours will be generally applied in the clinic due to these unpredictable clinical responses.

Analysis of the metabolome is a useful complement to the transcriptome analyses that has been performed for ALDH-hi breast cancer cells in this study (and in many others). As the downstream end product of interactions between the genome, transcriptome, and proteome the metabolome of breast cancer stem cells may give us new insights into the true character of aggressive ALDH-hi cells. Unfortunately, all methods to isolate or enrich for cancer stem cells contain a FACS cell sorting step which directly alters the metabolome of cells[415,416]. Since the MDA-MB-231 ALDH1A3-OE cells re-capitulate many of the features of ALDH+ breast cancer stem cells and since the transcriptional overlap of metabolic enzymes is similar; it is possible to glean new insights into how ALDH1A3 contributes to metastasis of ALDH-hi cells and potentially CSCs.

I performed mass spectroscopy-based metabolomics on TNBC MDA-MB-231 tumours and cells, with or without ALDH1A3 overexpression, and noted ALDH1A3-dependent changes in the metabolism of the inhibitory neurotransmitter γ-aminobutyric acid (GABA). GABA is the ligand of the GABAergic signaling pathway[417] and the pathway plays a role in the metastasis of breast cancer, especially to the brain[403,418–421]. Importantly, systemic GABA treatment did not affect MDA-MB-231 tumour growth, but both ALDH1A3 and systemic GABA increased lung metastasis. Quantification of brain metastasis is ongoing. Transcriptome analysis of MDA-MB-231 cells revealed ALDH1A3-dependent changes in expression of some GABA signaling components including upregulation of receptor subunits (GABRE) and downregulation of GABA catabolic enzyme ABAT. These gene expression changes were reflected in breast cancer patient tumours. The importance of GABA signaling/metabolism in breast cancer metastasis is illustrated by the four independent patient datasets wherein decreased ABAT

expression (and inferred increased GABA signaling/metabolism) was strongly and significantly associated with an increased risk of brain and lung metastasis (Figure 5.13).

While only one brain from the GABA-treated MDA-MB-231 ALDH1A3-OE mouse cohort has been analyzed, it is striking to see the presence of any brain metastasis. Though it is considered an aggressive and metastatic TNBC model, MDA-MB-231 cells typically do not metastasize to the brains of NOD/SCID mice. Indeed, MDA-MB-231 brain metastasis models follow two paradigms: 1) MDA-MB-231 cells are injected intracardially or 2) intracranially[422–425]. Even the "brain-seeking" MDA-MB-231BR cell line— derived from intracardiac-injected MDA-MB-231 cells which formed a brain lesion— must be injected intracranially to reliably form brain metastases[426–428]. It is possible that the humane endpoint (based on extensive lung metastasis; Figures 5.10C-E) is often reached prior to development of brain metastases in the MDA-MB-231 model. With completed analysis of brain metastasis, I can determine whether ABAT-low/ALDH1A3-OE MDA-MB-231 tumours are able to hone to both metastatic sites that are enriched for GABA (i.e. the brain) or depleted for GABA (i.e. the lung).

If an interaction between ALDH1A3 and GABA signaling/metabolism primes TNBC cells to establish brain or lung metastases, some common clinical practices should be re-assessed. Peripheral nerve pain is a dose-limiting and long-lasting side effect observed in 31-42% of patients receiving taxane chemotherapy[429,430]. These individuals are eligible to receive treatment with gabapentin which is a structural analog of GABA and is able to dampen neuropathic pain[404,431–434]. Though the complete mechanism of action is still under investigation, gabapentin does not act through GABA(A) or GABA(B) receptor binding, but by indirectly increasing intracellular GABA synthesis[435]. ALDH1A3-hi breast

cancer cells are intrinsically resistant to taxane-based therapy— if these cells are also adept at using intracellular GABA to metastasize, gabapentin administration could create a permissive environment for metastasis and relapse. Further investigation of the ALDH1A3/GABA axis is needed to determine whether patients may be at increased risk of metastasis if given gabapentin or other GABA agonists.

CHAPTER 6: DISCUSSION

6.1 SUMMARY OF WORK:

This work has assessed the potential of two distinct targets in the treatment of breast cancer: DNA methylation and ALDH1A3. Targetable DNA methylation was studied through the lens of DNA hypomethylating agent decitabine, and ALDH1A3 was investigated as an inhibitable pro-growth and metastasis molecule. In summary, the goals were to:

1. Identify determinants of decitabine response in breast cancer cells:
    - Characterize the sensitivity of a panel of breast cancer cells to decitabine treatment (Chapter 2)
    - Examine known or suspected mediators of decitabine response to identify key features of decitabine response (Chapter 2)
    - Functionally screen for hypermethylated tumour suppressor genes that when resurrected by hypomethylating therapy slow breast tumour growth. (Chapter 3)
    - Functionally screen for other novel mediators which dictate decitabine response (Chapter 3)

2. Determine if ALDH1A3 is a potential target for breast cancer treatment:
    - Develop an *in vivo* ALDH1A3 inhibition breast cancer model (Chapter 4)
    - Study the role of ALDH1A3 in breast cancer metastasis (Chapter 5)

Broadly, the results of this work suggest that:

- Nucleoside-based DNA de-methylating therapy alone is an ineffective approach for treating breast cancer in general.
- The one-carbon metabolism system governed by MTHFD2 is an emerging target for breast cancer therapy and may render cells susceptible to cytotoxic drugs like decitabine.
- ALDH1A3 inhibition has the potential to suppress tumour growth.
- ALDH1A3/TNBC may utilize plasminogen activation and the GABAergic system during metastasis.

6.2 DECITABINE ALONE IS INEFFECTIVE FOR BREAST CANCER TREATMENT APPLIED WITHOUT PRECISION

For decades the aberrant promoter hypermethylation observed across cancer types has been speculated upon as a drug target[23,51,440–442,76,88,319,363,436–439]. The first generation of hypomethylating agents was nucleoside-based (azacytidine and decitabine), and was successfully applied to haematological malignancies (MDS, and AML)[95]. However, this success has not yet translated over to the treatment of any solid tumour type. In my first aim I used a panel of breast cancer cell lines to characterize how decitabine treatment affects breast cancer cells in particular—perhaps decitabine would be more clinically efficacious if applied to patients who are already primed to respond. In the breast cancer cell lines, I searched for features that could be used to pre-determine which breast cancers are more susceptible to hypomethylating therapy.

I was unable to identify any molecular markers that could be used to stratify breast cancers based on decitabine response. What I found is that there is a significant cytotoxic outcome to decitabine therapy that is not reflected in changes to DNA methylation. Instead, the only molecule which seemed essential to decitabine response was deoxycytidine kinase (DCK). DCK controls the entry of decitabine (but not azacytidine) into DNA[443,444]. Loss of DCK confers resistance to decitabine in breast cancer cells. This is consistent with what is seen in AML patients who gain resistance to decitabine via down-regulation of DCK. Fortunately, down-regulation of DCK does not seem to be caused by the first-line therapies that breast cancer patients receive, and taxane-resistance does not translate to decitabine-resistance. All this implies that even after heavy pre-treatment, breast cancer patients enrolled in a decitabine clinical trial would not have resistance to decitabine. Unfortunately, decitabine is a weakly cytotoxic agent (Chapter 2 Figure 2.25; paclitaxel treatment inhibited growth of taxol-resistant cells to the same extent as decitabine treatment) and does not seem to consistently hypomethylate DNA of breast cancer cells.

The lack of correlation between the pattern of DNA hypomethylation and response to hypomethylating agents has been observed in pre-clinical and clinical studies in many cancer models[277,445–447]. This underlines our lack of understanding of A) how much DNA methylation truly contributes to breast tumour growth and B) the mechanism of action of hypomethylating agents. This led me to investigate if there were key hypermethylated tumour suppressor genes or novel genes that are integral to decitabine's mechanism of action which would govern hypomethylating agent response in breast cancer.

6.3 REACTIVATION OF A SINGLE HYPERMETHYLATED TUMOUR SUPPRESSOR GENE IS INSUFFICIENT TO SUPPRESS XENOGRAFT GROWTH

Hypermethylation of promoter regions is an early and ubiquitous event in breast tumour carcinogenesis. This observation led to many years of research which have catalogued the differential methylation patterns of ductal carcinoma *in situ*, breast cancer subtypes, and metastatic lesions. Ultimately, these studies have portrayed DNA methylation as correlative with breast cancer progression but not necessarily causative. This is due in part to the plethora of differentially methylated CpGs which make it difficult to parse the functionally relevant "driver" methylation events from hundreds of "passengers." This is assuming of course that "driver" methylation events exist.

I used a genome-wide shRNA screen in the MDA-MB-231 TNBC cells to search for individual hypermethylated tumour suppressor genes which impact *in vivo* cell growth. To add a layer of translational applicability, hypermethylated tumour suppressor genes were sought in the context of a hypomethylating therapy (decitabine). Only those hypermethylated TSGs which could be induced by hypomethylating therapy and had a significant impact on cell growth would be identified in this screen. Disappointingly, no single hypermethylated TSG (e.g. APOD) could be validated as an essential mediator of decitabine response. The two best explanations for this may be: A) MDA-MB-231 growth is not driven by any individual hypermethylated TSG or B) decitabine treatment did not effectively resurrect the expression of tumour suppressor genes *in vivo*.

6.3.1 *THE FUTURE OF DNA METHYLATION THERAPY FOR BREAST CANCER*

Non-nucleoside DNMTi agents

After many clinical failures of nucleoside-based hypomethylating drugs in solid tumours, non-nucleoside DNMT inhibitors (DNMTi) are being sought. Since the nucleoside analogs induce extensive DNA damage and cytotoxicity, it is not possible to study their DNMT inhibitory effects in isolation. Therefore, it is challenging to extrapolate the methylome-specific effects of nucleoside-based DNMTi's in breast cancer cells— this is the problem I encountered in Chapter 2. Novel DNMTi which directly bind to the catalytic domain of DNMTs without incorporation into DNA could be better tools by which to study the consequences of DNMT depletion in cancer cells.

These new non-nucleoside DNMTi's include curcumin, procaine, hydralazine, epigallocatechin gallate, RG-108, 3-nitro-2-(3-nitrophenyl) flavone and isooxazoline. A downside of these current non-nucleoside DNMTi is their poor selectivity for DNMTs and low potency[448]. The 4-aminoquinoline-based inhibitor "analog 5" of SGI-1027 shows potent inhibition of DNMT1 (at ≈5μM) *in silico* and effectively inhibited proliferation of several cancer cell lines *in vitro* including MDA-MB-231[361,449]. Unfortunately, the authors did not verify if DNA methylation was reduced in the analog 5-treated MDA-MB-231 cells. To date, none of these compounds have been assessed *in vivo* and are far from the clinical trial stage.

There is an untapped market for non-nucleoside DNMTi compounds. A potent, selective, and stable inhibitor for DNMT1 could be useful in pre-clinical studies to segregate the hypomethylation-specific and DNA damage effects that are pooled together

in the current studies which use decitabine or azacytidine. Until these experiments are performed, I think it will be challenging to determine whether DNA methylation truly is a relevant target for breast cancer therapy.

Strategic combination therapies

If hypomethylating agents are eventually used as a breast cancer therapy, it is highly likely that they will be used in tandem with other therapies. Chemotherapeutic pairings should include DNA-damaging agents. Synergy has been achieved between DNMTi and DNA damaging agents, as DNMTi promotes chromatin relaxation which both interferes with DNA damage repair and also is more permissive for DNA damage by genotoxic agents[450].

As with many cancer treatments, the immunomodulatory angle is being pursued in the application of decitabine to solid tumours. This is based off of evidence that hypomethylation induces the expression of cancer testis antigens and a human endogenous retrovirus "viral mimicry" response (Chapter 2)[271,451,452]. The first published trial with a low "hypomethylating" dose of decitabine posited to enhance immunotherapy was unsuccessful. In a Phase I/II study of heavily pre-treated advanced hepatocellular carcinoma patients, treatment with cytokine-induced killer T cells extended progression-free survival but this was not improved by concurrent administration of a low-dose decitabine regimen (NCT01799083)[365]. An increasingly popular angle is to use decitabine to enhance PD1/PDL1 therapies. Encouraging results from a trial of relapsed/refractory classic Hodgkin lymphoma show that combined decitabine + camrelizumab (Anti-PD1) treatment garnered a 100% complete response rate at 6 months compared to 76% complete

response rate with camrelizumab monotherapy[453]. There are several ongoing trials pairing decitabine with various immunotherapies (e.g. pembrolizumab anti-PD1), but at this time it is unclear how effective these combinations will be against different solid tumour types (NCT03233724, NCT03250962, NCT02961101, and NCT03346642).

6.4 MITOCHONDRIAL ONE-CARBON METABOLISM AND MTHFD2 AS A KEY FEATURE OF BREAST CANCER GROWTH

One-carbon metabolism is a vital metabolic pathway which includes key metabolites that sustain the synthesis of nucleotides, proteins, and lipids; while also generating S-adenosyl methionine (SAM) to maintain the epigenetic landscape; and supporting redox metabolism. For reasons we are just beginning to understand, mitochondrial one-carbon metabolism (instead of cytoplasmic) is favored in almost all cancer types and is ruled by methylene tetrahydrofolate dehydrogenase 2 (MTHFD2)[334].

The genome-wide shRNA screen performed in Chapter 3 was intended to reveal either hypermethylated tumour suppressor genes or genes which mediate decitabine's mechanism of action. Instead, likely due to the dependence of decitabine on cell proliferation, I have uncovered MTHFD2 as a potent oncogene in the MDA-MB-231 TNBC cells, which imparts increased sensitivity to decitabine. As MTHFD2's far-reaching role in cancer cell metabolism and proliferation becomes obvious, novel inhibitors are being developed to target this enzyme.

6.4.1 *ONE-CARBON METABOLISM TO GENERATE NUCLEOTIDES*

One-carbon metabolism is organized around two parallel cycles of methylation which use folate derivatives as methyl group carriers— one cycle is located in the cytosol and the other in the mitochondria. In the cancer-favored mitochondrial one-carbon pathway, serine donates a carbon through serine hydroxymethyltransferase (SHMT) which is then attached to tetrahydrofolate (THF) to create 5,10-methylenetetrahydrofolate (5,10-mTHF). MTHFD2 is a dual-action enzyme (dehydrogenase and cyclohydrolase) which then catalyzes the reversible conversion of methylene-THF into 10-formyl-THF which is subsequently oxidized to formate by MTHFD2L[357,454]. Formate then diffuses into the cytoplasm, joins a THF molecule and is further reduced to either 1) contribute to *de novo* purine synthesis, 2) pyrimidine synthesis, or 3) methionine synthesis[354,455–458]. All these functions are critical to maintenance of cancer cell growth, but perhaps none more so than nucleotide synthesis.

In the metabolomic analysis of MDA-MB-231 MTHFD2-KD tumours, I found depleted levels of almost all metabolites in purine or pyrimidine biosynthesis, but no effect on LINE1 DNA methylation (Chapter 3). This parallels results from lung and breast cancer metabolomes which exhibited reduced purine biosynthesis in cells harbouring MTHFD2 shRNAs[350,352]. Inhibition of MTHFD2 has also been shown to induced fatal levels of DNA replication stress by slowing the production of the pyrimidine thymidine[459]. Importantly, knockdown of MTHFD2 seems to have the most dramatic impact on breast cancer cell growth and nucleotide metabolism in glycine-depleted conditions (Chapter 3)[331]. This confirms MTHFD2's status as a key one-carbon metabolism mediator which fuels

nucleotide biosynthesis in addition to the other purposes it may serve such as redox metabolism.

This one-carbon metabolism detour through the mitochondria is a curious feature of cancer cells. The mitochondrial and cytosolic pathways are identical except that cytosolic MTHFD1 accomplishes the tasks of both MTHFD2 and MTHFD2L by reversibly converting 5,10-mTHF completely to formate. Nevertheless, the majority of one-carbon units used in the cytoplasm are derived from the mitochondria, and MTHFD2 is consistently upregulated across cancer types[334,460,461]. This implies some inherent benefit to preferring mitochondrial over cytoplasmic one-carbon metabolism.

MTHFD2 is undeniably facilitating mitochondrial one-carbon metabolism, but other folate metabolism-independent mechanisms may contribute to the MTHFD2 phenotype. This is best exemplified in a study where inhibition of MTHFD2 in cancer cells was partially compensated by shifting folate metabolism to the cytosol; but strikingly folate supplementation did not fully rescue MTHFD2-KD cells[357]. Formate is the end product of MTHFD2's one-carbon metabolism function, so the observation that adding formate was insufficient to save MTHFD2-KD cells implies that MTHFD2 may have a purpose independent of folate-metabolism[334,462].

6.4.2 *Mitochondrial Redox*

Reactive oxygen species (ROS) are chemically reactive molecules which are produced under oxidative stressors, can cause damage to cell structures, and are potent signaling species. ROS production and scavenging is a tightly regulated process, and cells

are protected from ROS-mediated stress by the major ROS scavenger: reduced glutathione (GSH). Oxidized glutathione (GSSG) is recycled back to GSH in an NADPH-dependent manner; therefore, NADPH generating enzymes play a key role in stabilizing redox homeostasis.

Redox metabolism is siloed into cytosolic and mitochondria pools. In cancer cells, the major cytosolic source of NADPH is the pentose phosphate pathway and G6PD; while the major mitochondrial source is one-carbon metabolism and MTHFD2[357,463,464]. MTHFD2 is an important contributor to mitochondrial redox metabolism and protection from oxidative stress. Depleting MTHFD2 decreased the ratios of NADPH/NADP+ and GSH/GSSH and resulted in HEK293T cells that were vulnerable to hydrogen peroxide oxidative stress[463]. Similarly, in colorectal cancer cells, knockdown of MTHFD2 sensitized cells to hypoxia-induced oxidative stress and impaired tumour growth and metastasis[465]. This illustrates the possibility of targeting MTHFD2 not just for impairing nucleotide biosynthesis but also for potentiating oxidative stress in tumours.

6.4.3 *Alternative MTHFD2 mechanisms*

MTHFD2 has dual redox cofactor specificity, so in addition to generating NADPH, it also generates a substantial volume of NADH in cancer cells[466]. Meiser *et al*. 2016 observed that some cancer cell lines run mitochondrial one-carbon metabolism in excess of the biosynthetic demands of one-carbon units, and excess one-carbon units get released from the cell as formate. Reducing 5,10-m-THF to formate can produce 3.5 molecules of ATP if the NADH produced by MTHFD2 is coupled to oxidative phosphorylation[467]. So,

enhanced MTHFD2 may produce excess formate to quickly spike energy production, similar to the Warburg effect.

Other phenotypes observed with either genetically engineered or small molecule mediated MTHFD2 inhibition are not directly explained by nucleotide synthesis, redox metabolism, or ATP generation. These observations imply a nuclear role for MTHFD2 that warrants further investigation. In one study, MTHFD2 was observed to bind to newly synthesized DNA and have an uncharacterized DNA repair function[351]. Ribosomal and RNA processing proteins also associate with MTHFD2 in cancer cells with an unidentified end result[468]. How MTHFD2 contributes to cancer growth could be affected by the mode of MTHFD2 inhibition. For example, a study comparing global shRNA versus CRISPR-based screens (in 501 and 342 cancer cell lines respectively), found that metabolic disruption dominates the effects on cell proliferation in CRISPR MTHFD2-knockouts while in shRNA knockdowns other MTHFD2 functions were playing a role[468].

6.4.4 *MTHFD2 INHIBITION*

The seminal work which instigated much of the interest in MTHFD2 was done in 2014. This began with an analysis RNA-Seq data for metabolic gene expression across 19 cancer types in the TCGA database. MTHFD2 was significantly and consistently overexpressed in almost every cancer type[334]. Subsequent analysis of survival data found that upregulation of MTHFD2 was associated with poor survival and aggressive pathological characteristics (such as TNM staging, grade, and metastasis) in invasive breast carcinoma, pancreatic cancer, renal cell carcinoma, and hepatocellular carcinoma[330,332,333,335]. Yet, MTHFD2 is not just a prognostic biomarker for multiple cancer

types. In an analysis of global RNAi and CRISPR screening data, inhibition of MTHFD2 consistently and potently reduced cell viability or proliferation[468]. The results of these studies communicated a need for MTHFD2 inhibitors to test clinically in multiple cancer types[469].

New targets for cancer therapy would ideally be specific to cancer cells. It is therefore encouraging that MTHFD2 is detected in transformed cell lines, primary tumours, and metastatic lesions; yet is undetectable or low in normal cell lines and adjacent normal stroma[334,465]. In fact, the only normal tissue type with high levels of MTHFD2 expression is pluripotent embryonal stem cells[470,471]. This further supports MTHFD2 as a viable drug target for cancer therapy which may spare healthy cells. The focus has now shifted into how these inhibitors will be designed.

Based on its clear role in one-carbon metabolism, several MTHFD2 inhibitors have been designed with inhibition of MTHFD2's dehydrogenase activity in mind. But, based on MTHFD2's participation in other pathways (e.g. DNA replication and RNA processing) perhaps inhibitors which can disrupt protein-protein interactions are also required. The first characterized MTHFD2 inhibitor was LY345899 which when bound to MTHFD2 prevents correct alignment of 5,10-mTHF for cyclohydrase activity, with an IC_{50} of 663 nM[353]. However, LY345899 has a higher affinity for MTHFD1 (IC_{50} 90 nM). Novel inhibitors DS18561882 and DS44960156 are more selective for MTHFD2[367,368]. DS18561882 is an orally available compound and was able to abolish *in vivo* MDA-MB-231 tumour growth when administered a 300 mg/kg dose bidaily. However, both DS18561882 and DS44960156 seem to exclusively inhibit the dehydrogenase activity of MTHFD2, leaving the interactions between MTHFD2 and DNA/proteins unaccounted for.

As additional MTHFD2 inhibitors are developed[472], and the role of MTHFD2 in cancer cells is further elucidated, I believe that there is enormous promise for MTHFD2 inhibitors in treating multiple cancer modalities including breast cancer. However, there may be one important caveat to the use of MTHFD2 inhibitors. When MTHFD2 was inhibited with shRNA in Chapter 3, decitabine was relatively less effective at suppressing tumour growth, and expression of chemotherapy resistance gene CCL20 was strongly induced. This may suggest some unknown mechanism by which MTHFD2 inhibition imparts resistance to cytotoxic chemotherapies. Further evaluation of MTHFD2 inhibition and drug resistance is required before MTHFD inhibitors are used in tandem with other agents in clinical trials.

6.5 TARGETING ALDH1A3 *IN VIVO*

Breast cancer cells with high ALDH activity caused by elevated levels of ALDH1A3 are a highly aggressive subpopulation[227]. These ALDH+ cells are often found in triple-negative or basal-like tumours which are intrinsically more prone to relapse and metastasis[473]. The contributions of ALDH1A3 to tumour growth and metastasis in TNBC was investigated here in Chapters 4 and 5. Cancer stem cells (CSCs) with high ALDH activity (ALDH+) have enhanced metastatic potential that is mirrored by the MDA-MB-231 ALDH1A3-OE cells[138,288]. While my model does not use the true ALDH+ cancer stem cells that would be present in heterogeneous primary tumours, observations in this model may be translatable not only to bulk tumour cells with high ALDH1A3 but also to CSCs.

A primary goal of this project was to establish an effective model of *in vivo* ALDH1A3 inhibition which had not been achieved by other groups. To this end, the MDA-

MB-231 TNBC cell line with engineered overexpression of ALDH1A3 was orthotopically injected in mice—these ALDH1A3-OE tumours grow significantly faster than control MDA-MB-231 tumours. If ALDH1A3 is effectively inhibited in these rapidly growing ALDH1A3-OE tumours, then growth will slow to the level of control MDA-MB-231 tumours. The non-specific but potent ALDH1A3i that was chosen for *in vivo* administration was nanoparticle encapsulated citral. This compound was able to significantly reduce ALDH1A3-mediated tumour growth. This *in vivo* proof-of-concept is significant because it provides a breast cancer model in which to test ALDH1A3i compounds that may be more clinically viable than citral.

6.5.1 *THE DEVELOPMENT OF ALDH1A3-SPECIFIC INHIBITORS*

Due to the role of ALDH1 isoforms in tumourigenesis, metastasis, drug resistance, and recurrence, many inhibitors are under development. Though ALDH isoforms are similar in structure and can bind the same substrates, each isoform has a distinct aldehyde binding site[256]. Therefore, there are two classes of ALDHi (ALDH inhibitor): those designed to inhibit multiple isoforms, and those specific to single isoforms. Multi-ALDH isoform inhibitors include N,N-diethylaminobenzaldehyde (DEAB), 4-dimethylamino-4-methylepent-2-ynthioic acid-S-methylester (DIMATE), ALDH inhibitors (aldis)-1, 2, 3, 4 and 6, dyclonine, and citral[474–478]. Isoform-specific ALDH inhibitors include the ALDH1A1 specific inhibitors Cpd 3, CM037, CM026, NCT-501, NCT-505, NCT-506, 13g and 13h; the ALDH2 specific inhibitor CVT10216; and the ALDH3A1 specific inhibitors CB7 and CB29[131,220,479–486]. Only two compounds (13h and compound 64) have been reported with modestly selective activity for ALDH1A3 and could inhibit ALDH1A3

activity when administered intraperitoneally[487–492]. Isoform-specific inhibitors have utility for isolating the function of individual ALDH isoforms. But, inhibitors that target a strategic combination of ALDH isoforms may be most clinically effective at targeting CSCs and drug resistance.

Though cancer types have distinct ALDH isoform activity that characterizes their ALDH+ (Aldefluor-positive) CSC population, 9/19 ALDH isoforms can contribute to Aldefluor fluorescence[482]. So, the ALDH activity in CSCs is a composite of multiple isoforms, and while targeting the major ALDH isoform (for breast cancer, ALDH1A3) is essential, inhibition of other ALDH isoforms may also be desirable. The application of multi-isoform ALDHi needs to consider the function of ALDH isoforms in normal tissues—importantly, the Aldefluor assay was originally developed to identify normal hematopoietic stem cells. In culture, inhibition of ALDH1 isoforms seems to actually expand the hematopoietic stem cell population[493,494]. If ALDH-targeted therapies cause aberrant expansion of hematopoietic stem cells *in vivo* and simultaneously remove the ALDH1-mediated cytoprotective capacity of hematopoietic stem cells, this could be a recipe for myelodysplastic disease. Fortunately, it seems that inhibition of a single ALDH1 isoform can be compensated by upregulation of the other two isoforms to rescue normal hematopoietic stem cell function[220]. Studies where ALDH1 isoform-specific inhibitors are administered *in vivo* are lacking, but the few studies do not report any adverse hematological events[474,495–498]. The optimal combination of ALDH isoform inhibition for effective CSC-targeting has yet to be determined.

6.5.2 *EXPLOITING THE ALDH-HI STATUS OF BREAST CANCER CELLS*

One promising approach to CSC-targeted therapy is to "lean in" to the elevated ALDH1 activity of CSCs. An interesting nifuroxazide compound was developed by Sarvi *et al.*, which is non-toxic until converted by intracellular ALDH1, this generates a reactive nitrogen species and cell death while concomitantly oxidizing and inactivating ALDH1[499]. This strategy was very effective at eliminating ALDH+ melanoma cells (with high ALDH1A1 and 1A3 activity), in an *in vivo* model and impaired the ability of nifuroxazide-treated tumours to initiate new tumours in a serial transplantation. This strategy could prevent other ALDH1 isoforms from compensating for inhibition of a single ALDH1 isoform by killing the ALDH+ cell before it can adapt. Further optimization of these types of compounds for specific ALDH isoforms could be very useful at limiting off-target toxicity and eliminating CSCs.

6.6 CHARACTERIZING THE ROLE OF ALDH1A3 IN BREAST CANCER METASTASIS

Metastasis of primary breast tumours to distal sites is ultimately what claims the lives of most breast cancer patients. Thus, identifying novel targets and strategies to prevent metastasis is essential. One such target may be ALDH1A3 which has recently been endorsed as a driver of breast-to-brain metastasis[500]. Indeed, the true goal of ALDH1A3-based therapies may be preventing metastasis as clinical models may suggests that ALDH1A3 is a negligible contributor to bulk tumour proliferation and instead is vital for metastasis.

The most obvious pathway that ALDH1A3 may use to facilitate metastasis is retinoic acid signaling. As an efficient retinaldehyde dehydrogenase, ALDH1A3 generates

large quantities of retinoic acid which exerts a wide array of effects on different cellular pathways and functions[135]. The key role of retinoic acid signaling in ALDH1A3-mediated breast tumour growth and metastasis has been well described by Marcato *et al.* 2015. However, retinoid-based therapies have not experienced the anticipated clinical success (which will be detailed later).

Defining which pathways—aside from RA signaling—are implicated in ALDH1A3-mediated metastasis can help shape our strategies to prevent metastasis. Through transcriptomic and metabolomic assays I have found that MDA-MB-231 ALDH1A3-OE cells resemble the ALDH+ CSCs and that plasminogen activation and the GABAergic system are involved in invasion/metastasis. One pathway that was identified in common between MDA-MB-231 ALDH1A3-OE cells and ALDH+ CSCs but was not functionally characterized here is prostaglandin synthesis. This pathway could play a major role in CSC-based metastasis and warrants further investigation. In addition to ALDH1A3 inhibitors, complementary therapies to ameliorate metastasis could target plasminogen activation, prostaglandin E2, and the GABAergic system

6.6.1 *RETINOID-BASED THERAPIES*

ALDH1A3 is an oncogene and its major product (retinoic acid) accelerates tumour growth and metastasis in some pre-clinical breast cancer models. So, it seems counterintuitive to use retinoids as a cancer therapy[138,289,501]. The main conceit of retinoid-therapy is based off observations made in haematological malignancies: namely that retinoic acid induces differentiation of acute promyelocytic leukemia (PML) cells. Eliminating the leukemic stem cell population via retinoid treatment can be curative for

some PML patients[502]. Therefore, the theory was that exogenous retinoic acid would shift the ALDH+ cancer stem cell program from a pro-self renewal state to a pro-differentiation state.

Overall, the results of retinoid treatment for solid tumours have been lackluster[503]. In two Phase II clinical trials for recurrent or metastatic breast cancer, *all-trans* retinoic acid did not have any clinical benefit[504,505]. The 13-cis-retinoic acid isomer similarly has little/no clinical benefit in glioma, pancreatic carcinoma, renal cell carcinoma, esophageal carcinoma, carcinoma of the cervix, or breast carcinoma[506–510]. There are 36 open clinical trials applying *all-trans* retinoic acid in cancer, most are in haematological malignancies (APL n=11, acute myelocytic leukemia n=11), with the remaining studies in solid tumours focused on neuroblastoma, non-small cell lung cancer, multiple myeloma, and melanoma. At this point in time, retinoid therapies are at a standstill for breast cancer therapy.

6.6.2 *PLASMINOGEN ACTIVATION SYSTEM*

One of the early events which may be required for distant metastasis is the escape of primary tumour cells through the extracellular matrix (ECM) and basement membrane. Several proteolytic systems contribute to the degradation of the ECM, digesting the basal lamina components and permitting tumour cell movement[511]. Matrix metalloproteinases (MMPs) are an important family of endopeptidases with the primary function of ECM degradation[512511]. Of the 28 MMP proteins, 14 have been implicated in breast cancer progression[513]. These MMPs are often not produced by the tumour cells themselves, but are released from the surrounding stromal cells after stimulation by tumours cells[514]. In addition to MMPs, cytokines and growth factors work in concert with tumour cells to

promote cellular invasion. The plasminogen activation system is hypothesized to contribute not only its own proteolytic function to degrading the ECM, but also activation of MMPs and liberation of growth factors in the ECM[402].

The plasminogen activation system is dysregulated in the microenvironment of many cancer types including breast cancer. There are two plasminogen activators which promote the conversion of plasminogen to plasmin: tissue plasminogen activator (tPA) and urokinase plasminogen activator (uPA). Generally, tPA is present in both normal and malignant tissue, while uPA seems to be more specific to cancer cells[515]. In node-negative breast cancer patients, an ELISA based test for uPA activity has been used to anticipate patients with a high risk of metastasis who require more aggressive treatment[516,517]. In terms of potential treatments for inhibiting breast cancer metastasis, this makes uPA a desirable target.

uPA works in tandem with its receptor urokinase plasminogen activator receptor (uPAR; PLAUR) which helps to localize and to enhance the activity of uPA by up to 50-fold[518,519]. uPA and uPAR are associated with advanced disease and metastasis clinically, and both have been shown to increase breast tumour growth and metastasis in pre-clinical models[520–522]. Small molecule inhibitors designed to block the binding of uPA to uPAR have not been successful at suppressing uPA activity, probably due to technical challenges in blocking the binding site on uPAR[523]. Inhibitors which were designed to block the plasminogen binding site on uPA were able to inhibit metastasis of prostate, colorectal, and MDA-MB-231 breast tumours[524–527].

Altogether, this presents the increased plasminogen activation I observed in MDA-MB-231 and MDA-MB-436 TNBC cells with high ALDH1A3 (Chapter 5) as a facilitator

of ALDHA3-mediated metastasis and a target for therapy. Limiting the clinical translation of all uPA/uPAR targeted therapies however, is the extreme species specificity of uPA-uPAR interactions[524]. Human uPA/uPAR inhibitors only impact the tumour cells and do not effect the normal mouse tissue. So, even if we were to show that uPA/uPAR inhibition slows ALDH1A3-mediated metastasis *in vivo*, we will not be able to assess the relevance of uPA/uPAR inhibition across the entire metastatic cascade. This species specificity might cause us to underestimate the toxicity profile of these drugs as well. In a clinical trial, systemic inhibition of normal uPA-mediated fibrinolysis could have dire consequences for clotting. Perhaps ALDH1A3 inhibition could prevent downstream plasminogen activation and bypass the need for uPA/uPAR clinical inhibitors.

6.6.3 *THE ROLE OF PROSTAGLANDIN E2 SYNTHESIS IN BREAST CANCER*

For decades it has been observed that many solid tumours exist in a prostaglandin E2 (PGE2)-enriched microenvironment[528–530]. This has been attributed to overexpression of cyclooxygenase-2 (COX-2 encoded by the PTGS2 gene) and prostaglandin E2 synthase (PTGES) in both tumour cells and surrounding normal fibroblasts/normal stem cells[531–535]. Abundant PGE2 is associated with poor clinical outcomes in solid tumours, and how PGE2 mechanistically contributes to tumour growth and spread is under active investigation[535–537]. Based on my transcriptome evaluation of MDA-MB-231 ALDH1A3-OE and ALDH+ breast CSCs, a major source of PGE2 in breast cancer may these aggressive ALDH-hi cells.

A key component of prostaglandin synthesis which was up-regulated in the MDA-MB-231 ALDH1A3-OE cells is COX-2. Arachidonic acid is converted to prostaglandin

H2 by either COX-1 (PTGS1) or COX-2 (PTGS2). COX-1 seems to be constitutively active in normal tissue, while COX-2 can be induced by inflammatory signals or during oncogenic transformation[538–540]. In transgenic mice with mammary gland-specific overexpression of COX-2, this increase in COX-2 was sufficient to induce mammary gland tumourigenesis[541]. This tumour formation could be abrogated by treatment with COX2 inhibitor celecoxib[542]. In addition to tumourigenesis, COX-2 also seems to prime MDA-MB-231BR "brain seeking" cells for extravasation and establishment of brain metastases[413].

There are connections being drawn between CSCs and PGE2 signaling. Breast cancer cell lines with endogenously high COX-2 (PTGS2) or with engineered COX-2 overexpression display increased migratory and invasive capabilities linked to an enhanced production/release of prostaglandin E2 and signaling through prostaglandin E2 cell surface receptors[401,543]. PGE2 signaling through the prostaglandin E2 cell surface receptor type 4 (EP4) specifically was able to create an ALDH+ cancer stem cell-like population in MCF7 and SKBR3 breast cancer cells through the PI3K/AKT/Notch/Wnt axis[401]. Similarly, in an *in vivo* model, PGE2 expanded colorectal CSCs and increased liver metastasis by EP4-NFKB and EP4-MAPK signaling[544,545]. In a PGE2 receptor-independent fashion, Wnt signaling in glioma stem cells is responsible for overexpression of COX-2 and subsequent self-renewal[546]. The source of PGE2 does not have to be tumour cells; both myeloid derived suppressor cells and dying bulk tumour cells may supply PGE2 to support CSCs. PGE2 provided by myeloid derived suppressor cells induced an ALDH+ CSC phenotype on uterine cervical carcinoma cells[547]. The most convincing evidence is from a study of bladder cancer patient derived xenografts (PDXs) where PGE2 release due

to chemotherapy-induced cell damage expanded the CSC population and drove post-chemotherapy tumour repopulation. Importantly, administration of COX-2 inhibitor (celecoxib) quashed PGE2-driven chemotherapy resistance mediated by cancer stem cells[548]. Unfortunately, the clinical evidence for COX-2 inhibition is not as convincing.

The best studied COX-2 inhibitor is the nonsteroidal anti-inflammatory drug (NSAID) aspirin. While there is evidence to support a role of aspirin in breast cancer prevention, there are conflicting or null reports for aspirin's role in improving relapse-free survival[549–557]. The COX-2 specific inhibitor celecoxib has also been through clinical trials for breast cancer therapy. Celecoxib treatment (400 mg daily) did not improve disease-free survival in a randomised placebo controlled study of 2639 patients with resected HER2- breast cancer that had previously received local and systemic adjuvant therapy[558]. These negative results suggest that perhaps targeting the enzyme which generates PGE2 is ineffective, and instead targeting the PGE2 receptors could be superior.

Inhibition of the prostaglandin E2 receptor EP4, does not have the long-term adverse gastrointestinal side effects of traditional or selective COX-2 inhibitors (like aspirin and celecoxib). Small molecule inhibitors for EP4 are in development and well tolerated (no gastrointestinal side effects or other adverse events observed in initial studies)[559]. Preclinical evidence shows that an EP4 inhibitor (L-161,982) can reduce resistance to oxaliplatin, slow proliferation, and prevent tumoursphere formation[546,560,561]. EP4 is also a key mediator of prostaglandin-based inflammation and pain. The market for new non-opioid analgesics is substantial, so development of clinically viable EP4 inhibitors is occurring rapidly. If EP4 inhibitors are not directly tested as cancer therapies,

there may be at least correlative studies performed (like aspirin and celecoxib) in the future.

6.6.4 *GABA SIGNALING/METABOLISM IN METASTASIS*

Cancer cells can co-opt normal signaling processes to accomplish rapid growth and to metastasize. Apparently, neurotransmitters like GABA are not exempt from a breast cancer cell's ability to hijack cellular signaling pathways. My observation that systemic GABA treatment increases lung metastasis of MDA-MB-231 tumours implicates the GABAergic system in metastasis (Chapter 5). This is supported by my analysis of breast cancer patient datasets where high ALDH1A3 expression is associated with loss of aminobutyric acid transaminase (ABAT) in primary tumours. This implies ALDH1A3-hi breast cancer has an increased GABAergic capacity. Importantly, I found that this loss of ABAT was a significant risk factor for lung and brain metastasis (Chapter 5)[420]. The role of GABA in cancer metastasis is poorly defined at present.

Clinically, GABA seems to have an oncogenic role in primary breast tumours, as homogenates of stage I and II breast tumours with high extracellular GABA (>90 μM) were associated with shorter disease-free survival[418]. My observation that primary breast tumours which have lost ABAT expression are more metastatic implies that this loss of ABAT might result in an impaired ability to degrade GABA and cause subsequent elevated extracellular GABA levels. The pro-metastatic function that this extra GABA serves may come down to its activation of GABA(A/B/C) receptors or its use as an oncometabolite to fuel the TCA cycle.

GABA is the main inhibitory neurotransmitter in the brain; however, functional GABA receptors have also been identified in non-neuronal tissues (e.g. lung, liver, gastrointestinal tract, sperm, testes, mammary gland, colon, liver)[254,562–564]. The ionotropic GABA(A) and GABA(C) receptors are pentameric chloride channels comprised of several subunits (α1-6, β1–4, γ1–3, δ, ε, π, and ρ) or exclusively ρ subunits respectively[565,566]. GABA(A) receptors composed of different subunits can have different affinities to GABA or GABA agonists and seem to have diverse functions in GABA-related metastasis and growth models.

Activation of GABA(A) receptors is typically pro-metastatic in breast cancer models. GABA treatment of MDA-MB-231 cells increased invasive potential by activating GABA(A) receptors, increasing intracellular $Ca2^{+}$, and activating the transcription factor NFAT1[420]. However, in HER2+ breast cancer cells derived from a patient's brain metastasis, treatment with a GABA(A) receptor agonist isoguvacine resulted in apoptosis[567]. It is possible that the function of GABA(A) receptors is dependent on primary tumour subtype (HER2+ versus TNBC) and/or the composition of subunits in the predominant GABA(A) receptor. Expression of the GABA(A) receptor subunit α3 (GABRA3) is associated with poor prognosis and enhances lung metastasis of MDA-MB-436 TNBC tumours[421]. The presence of GABA(A) receptor subunit π (GABRP) is subtype specific. GABRP is often lost in primary breast tumours[568], yet another group found GABRP specifically in basal-like breast tumours where it promotes tumourigenesis and metastasis[419]. GABA is a chemoattractant for MDA-MB-231BR "brain seeking" cells; and this seems to be mediated by GABRP localized to the invadopodia of MDA-MB-231BR

cells[569]. Together, this suggest that activation of GABA(A) receptors promotes metastasis of experimental TNBC.

The other category of GABA receptors, are the metabotropic GABA(B) receptors which belong to the G protein-coupled receptor superfamily and exist as R1a, R1b, and R2 isoforms[570]. The only study to my knowledge which focused on the metastatic role of GABA(B) receptor in breast cancer used the 4T1 triple-negative murine mammary carcinoma model[571,572]. Intraperitoneal administration of 30 mg/kg baclofen (GABA(B) agonist) increased lung metastasis mediated through ERK1/2. While this requires further characterization, activation of GABA(B) receptors also appears to increase TNBC metastasis.

These studies of GABA receptors and the observation ABAT-lo primary tumours are highly metastatic suggest that TNBC can enhance GABA signaling by downregulating ABAT and preventing intracellular degradation of GABA. This autocrine GABA production and self-signaling may explain why primary breast tumours with elevated GABA are at greater risk for metastasis[418]. Interestingly, the role of GABA shifts dramatically once primary breast tumours have established a brain metastasis. In a rare opportunity to study surgically resected breast-to-brain metastases, it was observed that GABA import proteins and ABAT activity were actually up-regulated[403]. In this context, GABA was used as an oncometabolite, with breast-to-brain metastatic cells importing GABA from the GABA-rich brain environment and shuttling GABA into the TCA cycle. These metastatic cells were highly proliferative in the presence of GABA, with elevated NADH production that was abolished by the addition of ABAT inhibitor vigabatrin. The

dichotomy of GABA as an oncometabolite and signaling molecule may be dependent on exogenous levels of GABA and intracellular ABAT activity.

Unraveling the interactions between TNBC cells and GABA is important because GABA memetics are commonly prescribed to alleviate peripheral nerve pain[404]. Gabapentin is the best studied GABA analog in the context of cancer. Gabapentin indirectly increases the intracellular production of GABA through binding the alpha-2/delta subunit at voltage-gated sensitive calcium channels[573,574]. Gabapentin (and other gabapentinoids) are liberally prescribed in the United States, with an estimated 4% of Americans using gabapentinoids at least once in 2015[575]. Fortunately, there does not seem to be an association of gabapentin use and development of cancer. A large Californian study of 6,608,681 individuals, 109,879 of whom were prescribed gabapentin at some point, determined that there was no significant association between gabapentin exposure and risk of cancer development[576]. We are lacking follow-up studies to determine if gabapentin use affects the rates of relapse or metastasis in cancer patients. These studies are necessary because an estimated 5.6% of Americans with cancer use gabapentin, and this rate is increasing[577].

My data supporting a relationship between the GABAergic system, ALDH1A3, and metastasis provides the impetus for future experiments which will fully dissect this pro-metastatic axis. The completion of these experiments will clarify the contradictory and context-dependent role of GABA in metastasis.

6.7 SUMMARY OF LIMITATIONS AND FUTURE WORK

6.7.1 *GENOME-WIDE SCREENS*

The shRNA-based genome-wide screen for knockdowns which bestow decitabine resistance could be improved in several ways. The ThermoFisher Decode shRNA library, which was innovative at the outset of this project, is outclassed by more recent shRNA screens which can contain ≈25 shRNAs per gene to identify hits with a high level of confidence[578]. These next generation shRNA screens could be applied to the MDA-MB-231 TNBC cells to re-create this *in vivo* decitabine experiment. This could salvage potential gene hits that were lost by the ATARiS algorithm's exclusion of genes targeted by single shRNAs. It is also possible that hypermethylation of TSGs is not a major driver of MDA-MB-231 tumour growth, so additional TNBC cell lines should be used for a more thorough search of potent hypermethylated TSGs. In the execution of these future experiments, technical challenges should be addressed such as characterizing the relative abundance of shRNAs in the pools prior to implantation in the mice to remove stochastic gene hits that are a result of shRNA drop-out during the establishment of tumours.

Overall, the design of the screen was sufficient and has one major advantage over similar studies: the screen was performed *in vivo.* Knockdown of MTHFD2 does not impart a significant growth disadvantage to MDA-MB-231 cells in replete culture conditions (Chapter 5), yet it dramatically impairs tumour growth. The large databases of shRNA- and CRISPR-based screen (i.e. Achilles) are generally obtained through culturing cells in replete conditions and may underestimate the role of genes like MTHFD2 under more realistic *in vivo* conditions. Strategies to increase the scale of *in vivo* genome-wide screening data could identify other such key components of tumour growth.

6.7.2 *CITRAL AS AN ALDH1A3 INHIBITOR*

Nanoparticle encapsulated citral was able to significantly inhibit ALDH1A3-mediated growth of MDA-MB-231 tumours (Chapter 4). This was the first published breast cancer model to use a small molecule inhibitor against ALDH1A3 to suppress tumour growth and was performed as a proof-of-concept. Realistically, citral has several major issues that preclude it from consideration as a clinical ALDH1A3i. First, citral does not specifically inhibit ALDH1A3; instead also inhibiting at least ALDH2 and ALDH1A1. Secondly, citral has poor bioavailability unless encapsulated. Finally, citral has non-ALDH1A3 associated cytotoxic activity in other breast cancer models, making it difficult to distinguish its ALDH1A3-specific activity unless citral is used in an ALDH1A3-modified system like I have done[385].

To improve the translational application of ALDH1A3i studies, metastasis should be assessed after *in vivo* ALDH1A3i treatment. Unfortunately, the MDA-MB-231 ALDH1A3-OE xenograft +/- Citral-NP experiment was terminated at day 38, which is too early to observe lung metastases. Future experiments should be designed to have an extended timeline to capture any anti-metastatic effects of ALDH1A3i.

Monoclonal cell lines are acceptable as the initial pre-clinical model to show mechanism, but patient-derived xenografts (PDXs) are superior *in vivo* models to re-capitulate clinical features and to model CSCs[105,579]. *In vivo* ALDH1A3i experiments in the future should use these PDX models as they contain true ALDH+ CSCs. Serial transplantation experiments are also essential to show that a CSC-like population has been depleted by ALDH1A3i. The next generation of ALDH1A3i *in vivo* experiments would ideally have these elements: a PDX from a recent passage, use of an ALDH1-specific and

bioavailable compound, an assessment of metastasis, and performance of serial transplantation at endpoint.

6.7.3 *CHARACTERIZING CANCER STEM CELL METABOLOMES*

Evaluating the metabolic pathways that CSCs use for self-renewal and metastasis could reveal novel CSC-specific targets. While not the express aim of my study of MDA-MB-231 ALDH1A3-OE cells, this cell line has many of the features of CSCs and might be extrapolated to imply that breast CSCs harbour enhanced GABAergic signaling/metabolism (Chapter 5). This indirect profiling of breast CSCs is relevant because there are few metabolomics methods that can accurately evaluate CSCs.

Methods to isolate CSCs are often dependent on FACS (i.e. Aldefluor assay). However, several controversial reports claim that FACS drastically alters the cellular metabolome. In one study, FACS altered the composition of eicosanoids (like prostaglandin), fatty acids, and carboxylic acid derivatives (the output of ALDHs). This was attributed to mechanosensory signaling pathways being activated by the physical impact cells experience as they pass through the instrument[416]. Another study observed that nearly half of the profiled metabolites changed by at least 1.5-fold after sorting, including glycogen, nucleosides, amino acids, central carbon metabolites, and acylcarnitines[415]. Therefore, accurate metabolomic analysis of live CSCs is lacking, as studies including flow cytometry present a distorted view of the CSC metabolome[580,581].

Lately, several creative workarounds have been applied to the metabolomic profiling of CSCs. An innovative single cell mass spectrometry platform was used to

examine “stem-like” colorectal HCT116 cell cultures, and identified that TCA cycle metabolites are more abundant in CSCs versus non-CSCs[580]. Glioma stem cells enriched in non-adherent conditions exhibited dysregulated glycerophospholipid metabolism compared to normal neural stem cells[582]. These studies are two good examples of how the metabolome of breast CSCs could be profiled in a FACS-free manner. For future studies, I would propose the use of PDXs cultured *ex vivo* in low-adherent conditions to enrich for ALDH+ CSCs[583].

6.7.4 *CONTRIBUTION OF GABA TO METASTASIS*

My observation that systemic GABA administration enhanced the lung metastasis of MDA-MB-231 tumours should be followed-up with experiments to determine the pro-metastatic mechanism of GABA. Based on the literature, it appears that GABA has opposing roles: 1) imported extracellular GABA is fed into the TCA cycle to fuel proliferation or 2) ABAT is lost and GABA is released for autocrine/paracrine GABAergic signaling to promote invasion/metastasis (Figure 6.1). ABAT-lo primary tumours are at greater risk for brain metastasis, yet breast cancer cells that have established metastatic brain lesion are ABAT-hi. This suggests that somewhere in the metastatic cascade the function of GABA shifts from pro-invasive to pro-growth. Future experiments should be carefully designed to discriminate between these two functions.

To determine whether GABA-fueled TCA cycling is important to tumourigenesis and growth, the mammosphere forming assay and typical growth rate assays should be used. PDXs should be grown *ex vivo* as mammospheres (a readout of tumourigenesis that enriches for ALDH+ cells); and TNBC cell lines with modified ALDH1A3 activity (i.e.

MDA-MB-231 ALDH1A3-OE) should be used. Exogenous GABA's entry into the TCA cycle would be prevented by addition of tiagabine (GABA importer inhibitor) or vigabatrin (ABAT inhibitor). If exogenous GABA contributes to proliferation, then both vigabatrin and tiagabine should suppress growth in GABA supplemented conditions. It is possible that GABA's position as an oncometabolite is restricted to breast cancer cells that are adapting to the brain microenvironment[403].

To determine whether GABAergic signaling mediates the initial invasion step of metastasis, those same PDX or TNBC cells should be applied to the Matrigel transwell invasion assay. Addition of muscimol (GABA(A) receptor agonist) or baclofen (GABA(B) receptor agonist)—which cannot be fed into the TCA cycle like GABA—will stimulate GABA receptors and reveal whether this signaling enhances invasion. Completion of these studies will provide evidence for a potential ALDH1A3/GABA axis of metastasis.

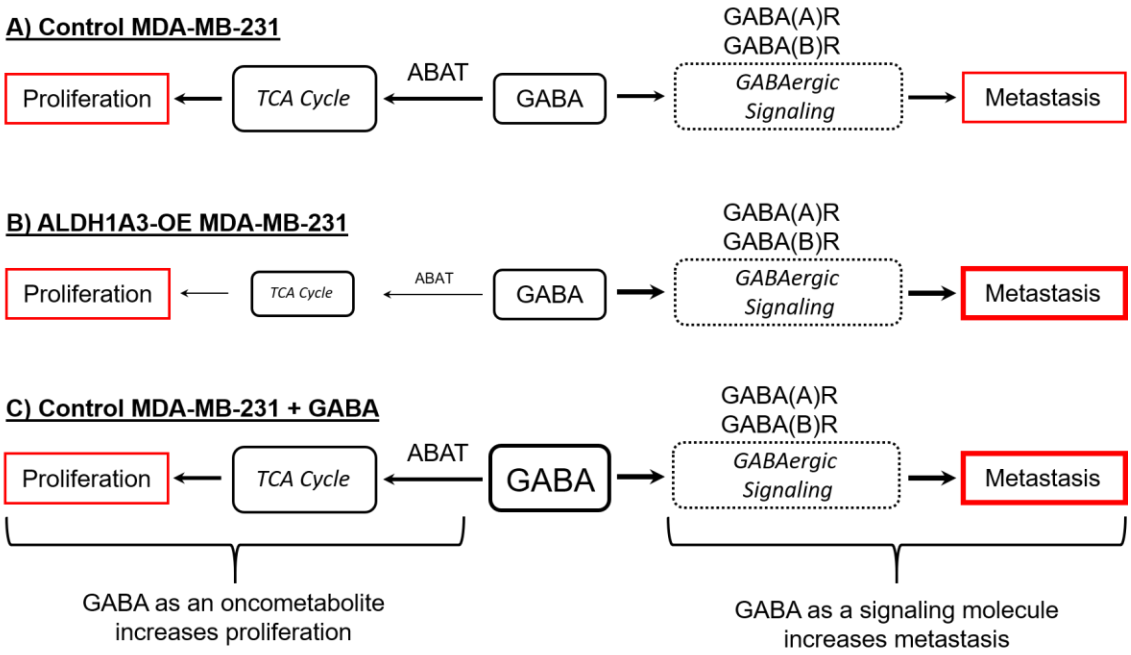

Figure 6.1 Working model for the relationship between ALDH1A3-OE and GABA treatment. A) Control MDA-MB-231 cells with ABAT activity modestly use GABA both as a proliferative oncometabolite and as a pro-metastatic/invasion signaling molecule. **B)** MDA-MB-231 ALDH1A3-OE cells have lost ABAT activity and direct intracellular GABA towards invasive GABAergic signaling. **C)** MDA-MB-231 control cells treated with exogenous GABA can now direct more GABA towards invasive GABAergic signaling resembling the elevated metastasis seen in the MDA-MB-231 ALDH1A3-OE cells.

6.8 Conclusions

The preceding work has evaluated two potential targets for breast cancer therapy: DNA methylation and ALDH1A3. I was not able to identify predictive biomarkers or resurrected hypermethylated TSGs which govern the response of breast cancer to decitabine. Instead, the emerging drug target MTHFD2 was revealed as a driver of MDA-MB-231 tumour growth and nucleotide synthesis. MTHFD2 appears to be an excellent target for inhibition— perhaps a better target than DNMT in breast cancer. *At this time,*

DNA methylation inhibitors are unlikely to provide clinical benefit to most breast cancer patients when applied as single agents, without a patient stratification strategy.

The CSC-marker ALDH1A3 has been speculated to be a potentially druggable target for breast cancer. Here, I show that inhibition of ALDH1A3 was indeed able to reduce *in vivo* MDA-MB-231 tumour growth in an ALDH1A3-dependent fashion. ALDH1A3 has a cryptic role in breast cancer metastasis, which based off my analyses may be due to plasminogen activation or the GABAergic system. Further dissection of the GABAergic system in ALDH-hi breast cancer cells could shed light on how breast cancer invades surrounding tissue and hones to metastatic sites (especially the brain). *Inhibition of ALDH1A3 warrants further investigation especially surrounding its potential anti-metastatic benefits.*

REFERENCES

1. Brenner DR, Weir HK, Demers AA, et al. Projected estimates of cancer in Canada in 2020. *CMAJ*. 2020;192(9):E199-E205. doi:10.1503/cmaj.191292

2. *Age Standardized (World) Incidence Rates, Breast, All Ages*.; 2018. http://gco.iarc.fr/today. Accessed May 3, 2020.

3. Lo P-K, Wolfson B, Zhou Q. Cancer stem cells and early stage basal-like breast cancer. *World J Obstet Gynecol*. 2016;5(2):150. doi:10.5317/wjog.v5.i2.150

4. Cornejo KM, Kandil D, Khan A, Cosar EF. Theranostic and molecular classification of breast cancer. *Arch Pathol Lab Med*. 2014;138(1):44-56. doi:10.5858/arpa.2012-0442-RA

5. Goldhirsch A, Wood WC, Coates AS, Gelber RD, Thürlimann B, Senn HJ. Strategies for subtypes-dealing with the diversity of breast cancer: Highlights of the St Gallen international expert consensus on the primary therapy of early breast cancer 2011. *Ann Oncol*. 2011;22(8):1736-1747. doi:10.1093/annonc/mdr304

6. Eliyatkin N, Yalcin E, Zengel B, Aktaş S, Vardar E. Molecular Classification of Breast Carcinoma: From Traditional, Old-Fashioned Way to A New Age, and A New Way. *J Breast Heal*. 2015;11(2):59-66. doi:10.5152/tjbh.2015.1669

7. Trivers KF, Lund MJ, Porter PL, et al. The epidemiology of triple-negative breast cancer, including race. *Cancer Causes Control*. 2009;20(7):1071-1082. doi:10.1007/s10552-009-9331-1

8. Anders CK, Carey LA. Biology, metastatic patterns, and treatment of patients with triple-negative breast cancer. *Clin Breast Cancer*. 2009;9(SUPPL.2):S73. doi:10.3816/CBC.2009.s.008

9. Li H, Ma F, Wang H, et al. Stem cell marker aldehyde dehydrogenase 1 (ALDH1)-expressing cells are enriched in triple-negative breast cancer. *Int J Biol Markers*. 2013;28(4):357-364. doi:10.5301/jbm.5000048

10. Giatromanolaki A, Sivridis E, Fiska A, Koukourakis MI. The CD44+/CD24- phenotype relates to "triple-negative" state and unfavorable prognosis in breast cancer patients. *Med Oncol*. 2011;28(3):745-752. doi:10.1007/s12032-010-9530-3

11. Wu Y, Sarkissyan M, Elshimali Y, Vadgama J V. Triple Negative Breast Tumors in African-American and Hispanic/Latina Women Are High in CD44+, Low in CD24+, and Have Loss of PTEN. *PLoS One*. 2013;8(10):1-12. doi:10.1371/journal.pone.0078259

12. Tsang JYS, Huang Y-H, Luo M-H, et al. Cancer stem cell markers are associated with adverse biomarker profiles and molecular subtypes of breast cancer. *Breast Cancer Res Treat*. 2012;136(2):407-417. doi:10.1007/s10549-012-2271-6

13. Perrone G, Gaeta LM, Zagami M, et al. In Situ Identification of CD44+/CD24- Cancer Cells in Primary Human Breast Carcinomas. *PLoS One*. 2012;7(9):1-9. doi:10.1371/journal.pone.0043110

14. Ricardo S, Vieira AF, Gerhard R, et al. Breast cancer stem cell markers CD44, CD24 and ALDH1: expression distribution within intrinsic molecular subtype. *J ClinPathol*. 2011;64(1472-4146):937-946. doi:10.1136/jcp.2011.090456

15. Idowu MO, Kmieciak M, Dumur C, et al. CD44+/CD24-/lowcancer stem/progenitor cells are more abundant in triple-negative invasive breast carcinoma phenotype and are associated with poor outcome. *Hum Pathol*. 2012;43(3):364-373. doi:10.1016/j.humpath.2011.05.005

16. Honeth G, Bendahl PO, Ringnér M, et al. The CD44+/CD24-phenotype is enriched in basal-like breast tumors. *Breast Cancer Res*. 2008;10(3):R53. doi:10.1186/bcr2108

17. Ma F, Li H, Wang H, et al. Enriched CD44+/CD24- population drives the aggressive phenotypes presented in triple-negative breast cancer (TNBC). *Cancer Lett*. 2014;353(2):153-159. doi:10.1016/j.canlet.2014.06.022

18. Louhichi T, Ziadi S, Saad H, Dhiab M Ben, Mestiri S, Trimeche M. Clinicopathological significance of cancer stem cell markers CD44 and ALDH1 expression in breast cancer. *Breast Cancer*. 2018;25(6):698-705. doi:10.1007/s12282-018-0875-3

19. Riaz N, Idress R, Habib S, Azam I, Lalani ENM. Expression of Androgen Receptor and Cancer Stem Cell Markers (CD44+/CD24− and ALDH1+): Prognostic Implications in Invasive Breast Cancer. *Transl Oncol*. 2018;11(4):920-929. doi:10.1016/j.tranon.2018.05.002

20. Dalerba P, Cho RW, Clarke MF. Cancer Stem Cells: Models and Concepts. *AnnuRevMed*. 2006;(0066-4219).

21. Chemoresistance in Cancer Stem Cells and Strategies to Overcome Resistance. *Chemother Open Access*. 2014;03(01). doi:10.4172/2167-7700.1000125

22. Hanahan D, Weinberg RA. Hallmarks of cancer: the next generation. *Cell*. 2011;144(5):646-674. doi:10.1016/j.cell.2011.02.013

23. Jones PA, Baylin SB. The fundamental role of epigenetic events in cancer. *Nat Rev Genet 2002 36*. 2002;3(6):415. doi:10.1038/nrg816

24. Holliday R. Epigenetics: A Historical Overview. *Epigenetics*. 2006;1(2):76-80. doi:10.4161/epi.1.2.2762

25. The Human Genome Project FAQ | NHGRI. https://www.genome.gov/human-genome-project/Completion-FAQ. Accessed May 4, 2020.

26. Bednar J, Horowitz RA, Grigoryev SA, et al. Nucleosomes, linker DNA, and linker histone form a unique structural motif that directs the higher-order folding and compaction of chromatin. *Proc Natl Acad Sci U S A*. 1998;95(24):14173-14178. doi:10.1073/PNAS.95.24.14173

27. Davie JR, Chadee DN. Regulation and regulatory parameters of histone modifications. *J Cell Biochem Suppl*. 1998;30-31:203-213.

28. Taverna SD, Li H, Ruthenburg AJ, Allis CD, Patel DJ. How chromatin-binding modules interpret histone modifications: lessons from professional pocket pickers. *Nat Struct Mol Biol*. 2007;14(11):1025-1040. doi:10.1038/nsmb1338

29. Kouzarides T. Chromatin Modifications and Their Function. *Cell*. 2007;128(4):693-705. doi:10.1016/j.cell.2007.02.005

30. Zhang T, Cooper S, Brockdorff N. The interplay of histone modifications - writers that read. *EMBO Rep*. 2015;16(11):1467-1481. doi:10.15252/embr.201540945

31. Horikoshi N, Kumar P, Sharma GG, et al. Genome-wide distribution of histone H4 Lysine 16 acetylation sites and their relationship to gene expression. *Genome Integr*. 2013;4(1):3. doi:10.1186/2041-9414-4-3

32. Taylor GCA, Eskeland R, Hekimoglu-Balkan B, Pradeepa MM, Bickmore WA. H4K16 acetylation marks active genes and enhancers of embryonic stem cells, but does not alter chromatin compaction. *Genome Res*. 2013;23(12):2053-2065. doi:10.1101/gr.155028.113

33. Kurdistani SK. Histone modifications in cancer biology and prognosis. *Prog Drug Res*. 2011;67:91-106.

34. Fraga MF, Ballestar E, Villar-Garea A, et al. Loss of acetylation at Lys16 and trimethylation at Lys20 of histone H4 is a common hallmark of human cancer. *Nat Genet*. 2005;37(4):391-400. doi:10.1038/ng1531

35. Doyen C-M, Montel F, Gautier T, et al. Dissection of the unusual structural and functional properties of the variant H2A.Bbd nucleosome. *EMBO J*. 2006;25(18):4234-4244. doi:10.1038/sj.emboj.7601310

36. Buschbeck M, Hake SB. Variants of core histones and their roles in cell fate decisions, development and cancer. *Nat Rev Mol Cell Biol*. 2017;18(5):299-314. doi:10.1038/nrm.2016.166

37. Hua S, Kallen CB, Dhar R, et al. Genomic analysis of estrogen cascade reveals histone variant H2A.Z associated with breast cancer progression. *Mol Syst Biol*. 2008;4:188. doi:10.1038/msb.2008.25

38. Vardabasso C, Gaspar-Maia A, Hasson D, et al. Histone Variant H2A.Z.2 Mediates Proliferation and Drug Sensitivity of Malignant Melanoma. *Mol Cell*.

2015;59(1):75-88. doi:10.1016/j.molcel.2015.05.009

39. Amaral PP, Dinger ME, Mercer TR, Mattick JS. The Eukaryotic Genome as an RNA Machine. *Science (80-)*. 2008;319(5871):1787-1789. doi:10.1126/science.1155472

40. Gibb EA, Brown CJ, Lam WL. The functional role of long non-coding RNA in human carcinomas. *Mol Cancer*. 2011;10(1):38. doi:10.1186/1476-4598-10-38

41. Lu J, Getz G, Miska EA, et al. MicroRNA expression profiles classify human cancers. *Nature*. 2005;435(7043):834-838. doi:10.1038/nature03702

42. Wang KC, Chang HY. Molecular mechanisms of long noncoding RNAs. *Mol Cell*. 2011;43(6):904-914. doi:10.1016/j.molcel.2011.08.018

43. Carthew RW, Sontheimer EJ. Origins and Mechanisms of miRNAs and siRNAs. *Cell*. 2009;136(4):642-655. doi:10.1016/j.cell.2009.01.035

44. Fabris L, Calin GA. Circulating free xeno-microRNAs - The new kids on the block. *Mol Oncol*. 2016;10(3):503-508. doi:10.1016/j.molonc.2016.01.005

45. Haemmerle M, Gutschner T. Long Non-Coding RNAs in Cancer and Development: Where Do We Go from Here? *Int J Mol Sci*. 2015;16(1):1395-1405. doi:10.3390/ijms16011395

46. Johnson TB, Coghill RD. Researches on pyrimidines. C111. The discovery of 5-methyl-cytosine in tuberculinic acid, the nucleic acid of the Tubercle Bacillus. *J Am Chem Soc*. 1925;47(11):2838-2844. doi:10.1021/ja01688a030

47. Saxonov S, Berg P, Brutlag DL. A genome-wide analysis of CpG dinucleotides in the human genome distinguishes two distinct classes of promoters. *Proc Natl Acad Sci U S A*. 2006;103(5):1412-1417. doi:10.1073/pnas.0510310103

48. Han H, Cortez CC, Yang X, Nichols PW, Jones PA, Liang G. DNA methylation directly silences genes with non-CpG island promoters and establishes a nucleosome occupied promoter. *Hum Mol Genet*. 2011;20(22):4299-4310. doi:10.1093/hmg/ddr356

49. Larsen F, Gundersen G, Lopez R, Prydz H. CpG islands as gene markers in the human genome. *Genomics*. 1992;13(4):1095-1107.

50. Illingworth RS, Bird AP. CpG islands – 'A rough guide.' *FEBS Lett*. 2009;583(11):1713-1720. doi:10.1016/J.FEBSLET.2009.04.012

51. Ehrlich M. DNA hypomethylation in cancer cells. *Epigenomics*. 2009;1(2):239-259. doi:10.2217/epi.09.33

52. Sheaffer KL, Elliott EN, Kaestner KH. DNA Hypomethylation Contributes to

Genomic Instability and Intestinal Cancer Initiation. *Cancer Prev Res*. 2016;9(7):534-546. doi:10.1158/1940-6207.CAPR-15-0349

53. Song L, James SR, Kazim L, Karpf AR. Specific Method for the Determination of Genomic DNA Methylation by Liquid Chromatography-Electrospray Ionization Tandem Mass Spectrometry. *Anal Chem*. 2005;77(2):504-510. doi:10.1021/ac0489420

54. Yang AS, Estécio MRH, Doshi K, Kondo Y, Tajara EH, Issa J-PJ. A simple method for estimating global DNA methylation using bisulfite PCR of repetitive DNA elements. *Nucleic Acids Res*. 2004;32(3):e38. doi:10.1093/nar/gnh032

55. Karimi M, Johansson S, Ekström TJ. Using LUMA: a Luminometric-based assay for global DNA-methylation. *Epigenetics*. 1(1):45-48.

56. Tost J, Gut IG. DNA methylation analysis by pyrosequencing. *Nat Protoc*. 2007;2(9):2265-2275. doi:10.1038/nprot.2007.314

57. Soto J, Rodriguez-Antolin C, Vallespín E, de Castro Carpeño J, Ibanez de Caceres I. The impact of next-generation sequencing on the DNA methylation–based translational cancer research. *Transl Res*. 2016;169:1-18.e1. doi:10.1016/J.TRSL.2015.11.003

58. Pidsley R, Zotenko E, Peters TJ, et al. Critical evaluation of the Illumina MethylationEPIC BeadChip microarray for whole-genome DNA methylation profiling. *Genome Biol*. 2016;17(1):208. doi:10.1186/s13059-016-1066-1

59. Herman JG, Graff JR, Myöhänen S, Nelkin BD, Baylin SB. Methylation-specific PCR: a novel PCR assay for methylation status of CpG islands. *Proc Natl Acad Sci U S A*. 1996;93(18):9821-9826.

60. Tammen SA, Friso S, Choi SW. Epigenetics: The link between nature and nurture. *Mol Aspects Med*. 2013;34(4):753-764. doi:10.1016/j.mam.2012.07.018

61. Herman JG, Baylin SB. Gene Silencing in Cancer in Association with Promoter Hypermethylation. *N Engl J Med*. 2003;349(21):2042-2054. doi:10.1056/NEJMra023075

62. Valinluck V, Tsai H-H, Rogstad DK, Burdzy A, Bird A, Sowers LC. Oxidative damage to methyl-CpG sequences inhibits the binding of the methyl-CpG binding domain (MBD) of methyl-CpG binding protein 2 (MeCP2). *Nucleic Acids Res*. 2004;32(14):4100-4108. doi:10.1093/nar/gkh739

63. Auclair G, Weber M. Mechanisms of DNA methylation and demethylation in mammals. *Biochimie*. 2012;94(11):2202-2211. doi:10.1016/j.biochi.2012.05.016

64. Hajkova P, Jeffries SJ, Lee C, Miller N, Jackson SP, Surani MA. Genome-wide reprogramming in the mouse germ line entails the base excision repair pathway.

Science (80-). 2010;329(5987):78-82. doi:10.1126/science.1187945

65. Rasmussen KD, Helin K. Role of TET enzymes in DNA methylation, development, and cancer. *Genes Dev*. 2016;30(7):733-750. doi:10.1101/gad.276568.115

66. Leitch HG, Surani MA, Hajkova P. DNA (De)Methylation: The Passive Route to Naïvety? *Trends Genet*. 2016;32(10):592-595. doi:10.1016/j.tig.2016.08.005

67. Lister R, Ecker JR. Finding the fifth base: Genome-wide sequencing of cytosine methylation. *Genome Res*. 2009;19(6):959-966. doi:10.1101/gr.083451.108

68. Lienert F, Wirbelauer C, Som I, Dean A, Mohn F, Schübeler D. Identification of genetic elements that autonomously determine DNA methylation states. *Nat Genet*. 2011;43(11):1091-1097. doi:10.1038/ng.946

69. Straussman R, Nejman D, Roberts D, et al. Developmental programming of CpG island methylation profiles in the human genome. *Nat Struct Mol Biol*. 2009;16(5):564-571. doi:10.1038/nsmb.1594

70. Liu L, Wylie RC, Andrews LG, Tollefsbol TO. Aging, cancer and nutrition: The DNA methylation connection. *Mech Ageing Dev*. 2003;124(10-12):989-998. doi:10.1016/j.mad.2003.08.001

71. Cedar H, Bergman Y. Programming of DNA Methylation Patterns. *Annu Rev Biochem*. 2012;81(1):97-117. doi:10.1146/annurev-biochem-052610-091920

72. Soares J, Pinto AE, Cunha C V, et al. Global DNA hypomethylation in breast carcinoma: correlation with prognostic factors and tumor progression. *Cancer*. 1999;85(1):112-118.

73. Li J, Gao F, Li N, et al. An improved method for genome wide DNA methylation profiling correlated to transcription and genomic instability in two breast cancer cell lines. *BMC Genomics*. 2009;10:223. doi:10.1186/1471-2164-10-223

74. Ruike Y, Imanaka Y, Sato F, Shimizu K, Tsujimoto G. Genome-wide analysis of aberrant methylation in human breast cancer cells using methyl-DNA immunoprecipitation combined with high-throughput sequencing. *BMC Genomics*. 2010;11(1):137. doi:10.1186/1471-2164-11-137

75. Jovanovic J, Rønneberg JA, Tost J, Kristensen V. The epigenetics of breast cancer. *Mol Oncol*. 2010;4(3):242-254. doi:10.1016/j.molonc.2010.04.002

76. Widschwendter M, Jones PA. DNA methylation and breast carcinogenesis. *Oncogene*. 2002;21-35(3):5462-5482. doi:10.1038/sj.onc.1205606

77. Roll JD, Rivenbark AG, Jones WD, Coleman WB. DNMT3b overexpression contributes to a hypermethylator phenotype in human breast cancer cell lines. *Mol*

Cancer. 2008;7(1):15. doi:10.1186/1476-4598-7-15

78. Girault I, Tozlu S, Lidereau R, Bièche I. Expression analysis of DNA methyltransferases 1, 3A, and 3B in sporadic breast carcinomas. *Clin Cancer Res*. 2003;9(12):4415-4422.

79. Donninger H, Vos MD, Clark GJ. The RASSF1A tumor suppressor. *J Cell Sci*. 2007;120(18):3163-3172. doi:10.1242/jcs.010389

80. Fackler MJ, McVeigh M, Evron E, et al. DNA methylation of RASSF1A, HIN-1, RAR-β, cyclin D2 and twist in in situ and invasive lobular breast carcinoma. *Int J Cancer*. 2003;107(6):970-975. doi:10.1002/ijc.11508

81. Harvey JM, Clark GM, Osborne CK, Allred DC. Estrogen receptor status by immunohistochemistry is superior to the ligand-binding assay for predicting response to adjuvant endocrine therapy in breast cancer. *J Clin Oncol*. 1999;17(5):1474-1481. doi:10.1200/JCO.1999.17.5.1474

82. Van Grembergen O, Bizet M, de Bony EJ, et al. Portraying breast cancers with long noncoding RNAs. *Sci Adv*. 2016;2(9):e1600220. doi:10.1126/sciadv.1600220

83. Chen C, Li Z, Yang Y, Xiang T, Song W, Liu S. Microarray expression profiling of dysregulated long non-coding RNAs in triple-negative breast cancer. *Cancer Biol Ther*. 2015;16(6):856-865. doi:10.1080/15384047.2015.1040957

84. Chen XQ, Zhang F, Su QC, Zeng C, Xiao FH, Peng Y. Methylome and transcriptome analyses reveal insights into the epigenetic basis for the good survival of hypomethylated ER-positive breast cancer subtype. *Clin Epigenetics*. 2020;12(1):16. doi:10.1186/s13148-020-0811-1

85. Gaudet MM, Campan M, Figueroa JD, et al. DNA Hypermethylation of ESR1 and PGR in Breast Cancer: Pathologic and Epidemiologic Associations. *Cancer Epidemiol Biomarkers Prev*. 2009;18(11):3036-3043. doi:10.1158/1055-9965.EPI-09-0678

86. Martínez-Galán J, Torres-Torres B, Núñez MI, et al. ESR1gene promoter region methylation in free circulating DNA and its correlation with estrogen receptor protein expression in tumor tissue in breast cancer patients. *BMC Cancer*. 2014;14(1):59. doi:10.1186/1471-2407-14-59

87. Widschwendter M, Siegmund KD, Müller HM, et al. Association of Breast Cancer DNA Methylation Profiles with Hormone Receptor Status and Response to Tamoxifen. *Cancer Res*. 2004;64(11):3807-3813. doi:10.1158/0008-5472.CAN-03-3852

88. Connolly R, Stearns V. Epigenetics as a Therapeutic Target in Breast Cancer. 2012;(July):191-204. doi:10.1007/s10911-012-9263-3

89. Stearns V, Zhou Q, Davidson NE. Epigenetic regulation as a new target for breast cancer therapy. *Cancer Invest*. 2007;25(8):659-665. doi:10.1080/07357900701719234

90. Kristensen LS, Nielsen HM, Hansen LL. Epigenetics and cancer treatment. *Eur J Pharmacol*. 2009;625(1-3):131-142. doi:10.1016/j.ejphar.2009.10.011

91. Momparler RL. Pharmacology of 5-Aza-2′-deoxycytidine (decitabine). *Semin Hematol*. 2005;42(3 Suppl 2):S9-S16. doi:10.1053/j.seminhematol.2005.05.002

92. Gros C, Fahy J, Halby L, et al. DNA methylation inhibitors in cancer: Recent and future approaches. *Biochimie*. 2012;94(11):2280-2296. doi:10.1016/j.biochi.2012.07.025

93. Appleton K, Mackay HJ, Judson I, et al. Phase I and pharmacodynamic trial of the DNA methyltransferase inhibitor decitabine and carboplatin in solid tumors. *J Clin Oncol*. 2007;25(29):4603-4609. doi:10.1200/JCO.2007.10.8688

94. Nie J, Liu L, Li X, Han W. Decitabine , a new star in epigenetic therapy : the clinical application and biological mechanism in solid tumors. *Cancer Lett*. 2014;354(1):12-20. doi:10.1016/j.canlet.2014.08.010

95. Kaminskas E, Farrell A, Abraham S, et al. Approval summary: Azacitidine for treatment of myelodysplastic syndrome subtypes. *Clin Cancer Res*. 2005;11(10):3604-3608. doi:10.1158/1078-0432.CCR-04-2135

96. Braiteh F, Soriano AO, Garcia-Manero G, et al. Phase I study of epigenetic modulation with 5-azacytidine and valproic acid in patients with advanced cancers. *Clin Cancer Res*. 2008;14(19):6296-6301. doi:10.1158/1078-0432.CCR-08-1247

97. Al-Hajj M, Wicha MS, Benito-Hernandez A, Morrison SJ, Clarke MF. Prospective identification of tumorigenic breast cancer cells. *Proc Natl Acad Sci U S A*. 2003;100(7):3983-3988. doi:10.1073/pnas.0530291100

98. Bonnet D, Dick JE. Human acute myeloid leukemia is organized as a hierarchy that originates from a primitive hematopoietic cell. *Nat Med*. 1997;3(7):730-737. doi:10.1038/nm0797-730

99. Carpentino JE, Hynes MJ, Appelman HD, et al. Aldehyde dehydrogenase-expressing colon stem cells contribute to tumorigenesis in the transition from colitis to cancer. *Cancer Res*. 2009;69(20):8208-8215. doi:10.1158/0008-5472.CAN-09-1132

100. Charafe-Jauffret E, Ginestier C, Iovino F, et al. Breast cancer cell lines contain functional cancer stem sells with metastatic capacity and a distinct molecular signature. *Cancer Res*. 2009;69(4):1302-1313. doi:10.1158/0008-5472.CAN-08-2741

101. Charafe-Jauffret E, Ginestier C, Iovino F, et al. Aldehyde dehydrogenase 1-positive cancer stem cells mediate metastasis and poor clinical outcome in inflammatory breast cancer. *Clin Cancer Res*. 2010;16(1):45-55. doi:10.1158/1078-0432.CCR-09-1630

102. Choi D, Lee HW, Hur KY, et al. Cancer stem cell markers CD133 and CD24 correlate with invasiveness and differentiation in colorectal adenocarinoma. *World J Gastroenterol*. 2009;15(18):2258-2264. doi:10.3748/wjg.15.2258

103. Dalerba P, Cho RW, Clarke MF. Cancer Stem Cells: Models and Concepts. *Annu Rev Med*. 2007;58(1):267-284. doi:10.1146/annurev.med.58.062105.204854

104. Ginestier C, Hur MH, Charafe-Jauffret E, et al. ALDH1 Is a Marker of Normal and Malignant Human Mammary Stem Cells and a Predictor of Poor Clinical Outcome. *Cell Stem Cell*. 2007;1(5):555-567. doi:10.1016/j.stem.2007.08.014

105. Frame FM, Maitland NJ. Cancer Stem Cells, Models of Study and Implications of Therapy Resistance Mechanisms. In: *Advances in Experimental Medicine and Biology*. Vol 720. ; 2011:105-118. doi:10.1007/978-1-4614-0254-1_9

106. Dylla SJ, Beviglia L, Park I-K, et al. Colorectal Cancer Stem Cells Are Enriched in Xenogeneic Tumors Following Chemotherapy. Gilliland DG, ed. *PLoS One*. 2008;3(6):e2428. doi:10.1371/journal.pone.0002428

107. Eramo A, Ricci-Vitiani L, Zeuner A, et al. Chemotherapy resistance of glioblastoma stem cells. *Cell Death Differ*. 2006;13(7):1238-1241. doi:10.1038/sj.cdd.4401872

108. Gong X, Schwartz PH, Linskey ME, Bota DA. Neural stem/progenitors and glioma stem-like cells have differential sensitivity to chemotherapy. *Neurology*. 2011;76(13):1126-1134. doi:10.1212/WNL.0b013e318212a89f

109. Hirschmann-Jax C, Foster AE, Wulf GG, et al. A distinct “side population” of cells with high drug efflux capacity in human tumor cells. *Proc Natl Acad Sci U S A*. 2004;101(39):14228-14233. doi:10.1073/pnas.0400067101

110. Hu G, Li F, Ouyang K, et al. Intrinsic gemcitabine resistance in a novel pancreatic cancer cell line is associated with cancer stem cell-like phenotype. *Int J Oncol*. 2012;40(3):798-806. doi:10.3892/ijo.2011.1254

111. Kucerova L, Feketeova L, Kozovska Z, et al. In vivo 5FU-exposed human medullary thyroid carcinoma cells contain a chemoresistant CD133+ tumor-initiating cell subset. *Thyroid*. 2014;24(3):520-532. doi:10.1089/thy.2013.0277

112. Marcato P, Dean CA, Giacomantonio CA, Lee PWK. If cancer stem cells are resistant to current therapies what’s next? *Futur Oncol*. 2009;5(6):747-750. doi:10.2217/fon.09.58

113. Tanei T, Morimoto K, Shimazu K, et al. Association of breast cancer stem cells identified by aldehyde dehydrogenase 1 expression with resistance to sequential paclitaxel and epirubicin-based chemotherapy for breast cancers. *Clin Cancer Res*. 2009;15(12):4234-4241. doi:10.1158/1078-0432.CCR-08-1479

114. Tomuleasa C, Soritau O, Rus-Ciuca D, et al. Isolation and characterization of hepatic cancer cells with stem-like properties from hepatocellular carcinoma. *J Gastrointest Liver Dis*. 2010;19(1):61-67.

115. Touil Y, Igoudjil W, Corvaisier M, et al. Colon cancer cells escape 5FU chemotherapy-induced cell death by entering stemness and quiescence associated with the c-Yes/YAP axis. *Clin Cancer Res*. 2014;20(4):837-846. doi:10.1158/1078-0432.CCR-13-1854

116. Storms RW, Trujillo AP, Springer JB, et al. Isolation of primitive human hematopoietic progenitors on the basis of aldehyde dehydrogenase activity. *Proc Natl Acad Sci U S A*. 1999;96(16):9118-9123. doi:10.1073/pnas.96.16.9118

117. Cheung AMS, Wan TSK, Leung JCK, et al. Aldehyde dehydrogenase activity in leukemic blasts defines a subgroup of acute myeloid leukemia with adverse prognosis and superior NOD/SCID engrafting potential. *Leukemia*. 2007;21(7):1423-1430. doi:10.1038/sj.leu.2404721

118. Basak SK, Veena MS, Oh S, et al. The Malignant Pleural Effusion as a model to investigate intratumoral heterogeneity in lung cancer. *PLoS One*. 2009;4(6):e5884. doi:10.1371/journal.pone.0005884

119. Boonyaratanakornkit JB, Yue L, Strachan LR, et al. Selection of tumorigenic melanoma cells using ALDH. *J Invest Dermatol*. 2010;130(12):2799-2808. doi:10.1038/jid.2010.237

120. Bortolomai I, Canevari S, Facetti I, et al. Tumor initiating cells: Development and critical characterization of a model derived from the A431 carcinoma cell line forming spheres in suspension. *Cell Cycle*. 2010;9(6):1194-1206. doi:10.4161/cc.9.6.11108

121. Chu P, Clanton DJ, Snipas TS, et al. Characterization of a subpopulation of colon cancer cells with stem cell-like properties. *Int J Cancer*. 2009;124(6):1312-1321. doi:10.1002/ijc.24061

122. Clay MR, Tabor M, Owen JH, et al. Single-marker identification of head and neck squamous cell carcinoma cancer stem cells with aldehyde dehydrogenase. *Head Neck*. 2010;32(9):1195-1201. doi:10.1002/hed.21315

123. Deng S, Yang X, Lassus H, et al. Distinct expression levels and patterns of stem cell marker, aldehyde dehydrogenase isoform 1 (ALDH1), in human epithelial cancers. *PLoS One*. 2010;5(4):e10277. doi:10.1371/journal.pone.0010277

124. Huang EH, Hynes MJ, Zhang T, et al. Aldehyde dehydrogenase 1 is a marker for normal and malignant human colonic stem cells (SC) and tracks SC overpopulation during colon tumorigenesis. *Cancer Res*. 2009;69(8):3382-3389. doi:10.1158/0008-5472.CAN-08-4418

125. Feng J, Qi Q, Khanna A, et al. Aldehyde dehydrogenase 1 is a tumor stem cell-Associated marker in lung cancer. *Mol Cancer Res*. 2009;7(3):330-338. doi:10.1158/1541-7786.MCR-08-0393

126. Li T, Su Y, Mei Y, et al. ALDH1A1 is a marker for malignant prostate stem cells and predictor of prostate cancer patients outcome. *Lab Investig*. 2010;90(2):234-244. doi:10.1038/labinvest.2009.127

127. Ma S, Kwok WC, Lee TKW, et al. Aldehyde dehydrogenase discriminates the CD133 liver cancer stem cell populations. *Mol Cancer Res*. 2008;6(7):1146-1153. doi:10.1158/1541-7786.MCR-08-0035

128. Rasheed ZA, Yang J, Wang Q, et al. Prognostic significance of tumorigenic cells with mesenchymal features in pancreatic adenocarcinoma. *J Natl Cancer Inst*. 2010;102(5):340-351. doi:10.1093/jnci/djp535

129. Todaro M, Iovino F, Eterno V, et al. Tumorigenic and metastatic activity of human thyroid cancer stem cells. *Cancer Res*. 2010;70(21):8874-8885. doi:10.1158/0008-5472.CAN-10-1994

130. Ucar D, Cogle CR, Zucali JR, et al. Aldehyde dehydrogenase activity as a functional marker for lung cancer. *Chem Biol Interact*. 2009;178(1-3):48-55. doi:10.1016/j.cbi.2008.09.029

131. Van Den Hoogen C, Van Der Horst G, Cheung H, et al. High aldehyde dehydrogenase activity identifies tumor-initiating and metastasis-initiating cells in human prostate cancer. *Cancer Res*. 2010;70(12):5163-5173. doi:10.1158/0008-5472.CAN-09-3806

132. Wang L, Park P, Zhang H, La Marca F, Lin CY. Prospective identification of tumorigenic osteosarcoma cancer stem cells in OS99-1 cells based on high aldehyde dehydrogenase activity. *Int J Cancer*. 2011;128(2):294-303. doi:10.1002/ijc.25331

133. Jackson B, Brocker C, Thompson DC, et al. Update on the aldehyde dehydrogenase gene (ALDH) superfamily. *Hum Genomics*. 2011;5(4):283-303. doi:10.1186/1479-7364-5-4-283

134. Vasiliou V, Nebert DW. Analysis and update of the human aldehyde dehydrogenase (ALDH) gene family. *Hum Genomics*. 2005;2(2):138-143. doi:10.1186/1479-7364-2-2-138

135. Kedishvili NY. Enzymology of retinoic acid biosynthesis and degradation. *J Lipid*

Res. 2013;54(7):1744-1760. doi:10.1194/jlr.R037028

136. Marcato P, Dean CA, Da P, et al. Aldehyde dehydrogenase activity of breast cancer stem cells is primarily due to isoform ALDH1A3 and its expression is predictive of metastasis. *Stem Cells*. 2011;29(1):32-45. doi:10.1002/stem.563

137. Marchitti SA, Brocker C, Stagos D, Vasiliou V. Non-P450 aldehyde oxidizing enzymes: The aldehyde dehydrogenase superfamily. *Expert Opin Drug Metab Toxicol*. 2008;4(6):697-720. doi:10.1517/17425255.4.6.697

138. Marcato P, Dean CA, Liu RZ, et al. Aldehyde dehydrogenase 1A3 influences breast cancer progression via differential retinoic acid signaling. *Mol Oncol*. 2015;9(1):17-31. doi:10.1016/j.molonc.2014.07.010

139. Chen Y, Orlicky DJ, Matsumoto A, Singh S, Thompson DC, Vasiliou V. Aldehyde dehydrogenase 1B1 (ALDH1B1) is a potential biomarker for human colon cancer. *Biochem Biophys Res Commun*. 2011;405(2):173-179. doi:10.1016/j.bbrc.2011.01.002

140. Landen CN, Goodman B, Katre AA, et al. Targeting aldehyde dehydrogenase cancer stem cells in ovarian cancer. *Mol Cancer Ther*. 2010;9(12):3186-3199. doi:10.1158/1535-7163.MCT-10-0563

141. Liebscher CA, Prinzler J, Sinn BV, et al. Aldehyde dehydrogenase 1/epidermal growth factor receptor coexpression is characteristic of a highly aggressive, poor-prognosis subgroup of high-grade serous ovarian carcinoma. *Hum Pathol*. 2013;44(8):1465-1471. doi:10.1016/j.humpath.2012.12.016

142. Luo Y, Dallaglio K, Chen Y, et al. ALDH1A isozymes are markers of human melanoma stem cells and potential therapeutic targets. *Stem Cells*. 2012;30(10):2100-2113. doi:10.1002/stem.1193

143. Mao P, Joshi K, Li J, et al. Mesenchymal glioma stem cells are maintained by activated glycolytic metabolism involving aldehyde dehydrogenase 1A3. *Proc Natl Acad Sci U S A*. 2013;110(21):8644-8649. doi:10.1073/pnas.1221478110

144. Shao C, Sullivan JP, Girard L, et al. Essential role of aldehyde dehydrogenase 1A3 for the maintenance of non-small cell lung cancer stem cells is associated with the STAT3 pathway. *Clin Cancer Res*. 2014;20(15):4154-4166. doi:10.1158/1078-0432.CCR-13-3292

145. Cheng P, Wang J, Waghmare I, et al. Tumor and Stem Cell Biology FOXD1-ALDH1A3 Signaling Is a Determinant for the Self-Renewal and Tumorigenicity of Mesenchymal Glioma Stem Cells. 2016. doi:10.1158/0008-5472.CAN-15-2860

146. Burrell RA, Swanton C. Tumour heterogeneity and the evolution of polyclonal drug resistance. *Mol Oncol*. 2014;8(6):1095-1111. doi:10.1016/j.molonc.2014.06.005

147. Ponti D, Costa A, Zaffaroni N, et al. Isolation and in vitro propagation of tumorigenic breast cancer cells with stem/progenitor cell properties. *Cancer Res*. 2005;65(13):5506-5511. doi:10.1158/0008-5472.CAN-05-0626

148. Bunting KD. ABC Transporters as Phenotypic Markers and Functional Regulators of Stem Cells. *Stem Cells*. 2002;20(3):274-274. doi:10.1634/stemcells.20-3-274

149. Chiba P, Mihalek I, Ecker G, Kopp S, Lichtarge O. Role of Transmembrane Domain/Transmembrane Domain Interfaces of PGlycoprotein (ABCB1) in Solute Transport. Convergent Information from Photoaffinity Labeling, Site Directed Mutagenesis and in Silico Importance Prediction. *Curr Med Chem*. 2006;13(7):793-805. doi:10.2174/092986706776055607

150. Haraguchi N, Utsunomiya T, Inoue H, et al. Characterization of a Side Population of Cancer Cells from Human Gastrointestinal System. *Stem Cells*. 2006;24(3):506-513. doi:10.1634/stemcells.2005-0282

151. Kim M, Turnquist H, Sgagias M, et al. The multidrug resistance transporter ABCG2 (breast cancer resistance protein 1) effluxes Hoechst 33342 and is overexpressed in hematopoietic stem cells. *Clin Cancer Res*. 2002;8(1):22-28.

152. Loebinger MR, Giangreco A, Groot KR, et al. Squamous cell cancers contain a side population of stem-like cells that are made chemosensitive by ABC transporter blockade. *Br J Cancer*. 2008;98(2):380-387. doi:10.1038/sj.bjc.6604185

153. Zhu Z, Hao X, Yan M, et al. Cancer stem/progenitor cells are highly enriched in CD133 +CD44+ population in hepatocellular carcinoma. *Int J Cancer*. 2010;126(9):2067-2078. doi:10.1002/ijc.24868

154. Gottesman MM, Fojo T, Bates SE. Multidrug resistance in cancer: Role of ATP-dependent transporters. *Nat Rev Cancer*. 2002;2(1):48-58. doi:10.1038/nrc706

155. Keshet GI, Goldstein I, Itzhaki O, et al. MDR1 expression identifies human melanoma stem cells. *Biochem Biophys Res Commun*. 2008;368(4):930-936. doi:10.1016/j.bbrc.2008.02.022

156. Schatton T, Murphy GF, Frank NY, et al. Identification of cells initiating human melanomas. *Nature*. 2008;451(7176):345-349. doi:10.1038/nature06489

157. Hollenstein K, Dawson RJ, Locher KP. Structure and mechanism of ABC transporter proteins. *Curr Opin Struct Biol*. 2007;17(4):412-418. doi:10.1016/j.sbi.2007.07.003

158. Rice AJ, Park A, Pinkett HW. Diversity in ABC transporters: Type I, II and III importers. *Crit Rev Biochem Mol Biol*. 2014;49(5):426-437. doi:10.3109/10409238.2014.953626

159. Schinkel AH, Jonker JW. Mammalian drug efflux transporters of the ATP binding cassette (ABC) family: An overview. *Adv Drug Deliv Rev*. 2003;55(1):3-29. doi:10.1016/S0169-409X(02)00169-2

160. Shaffer BC, Gillet JP, Patel C, Baer MR, Bates SE, Gottesman MM. Drug resistance: Still a daunting challenge to the successful treatment of AML. *Drug Resist Updat*. 2012;15(1-2):62-69. doi:10.1016/j.drup.2012.02.001

161. Goldstein LJ, Galski H, Fojo A, et al. Expression of a multidrug resistance gene in human cancers. *J Natl Cancer Inst*. 1989;81(2):116-124. doi:10.1093/jnci/81.2.116

162. Trock BJ, Leonessa F, Clarke R. Multidrug Resistance in Breast Cancer: a Meta-analysis of MDR1/gp170 Expression and Its Possible Functional Significance. *JNCI J Natl Cancer Inst*. 1997;89(13):917-931. doi:10.1093/jnci/89.13.917

163. Larkin A, O'Driscoll L, Kennedy S, et al. Investigation of MRP-1 protein and MDR-1 P-glycoprotein expression in invasive breast cancer: A prognostic study. *Int J Cancer*. 2004;112(2):286-294. doi:10.1002/ijc.20369

164. Rudas M, Filipits M, Taucher S, et al. Expression of MRP1, LRP and Pgp in breast carcinoma patients treated with preoperative chemotherapy. *Breast Cancer Res Treat*. 2003;81(2):149-157. doi:10.1023/A:1025751631115

165. Jin W, Liu Y, Xu SG, et al. UHRF1 inhibits MDR1 gene transcription and sensitizes breast cancer cells to anticancer drugs. *Breast Cancer Res Treat*. 2010;124(1):39-48. doi:10.1007/s10549-009-0683-8

166. Sung PH, Wen J, Bang S, Park S, Si YS. CD44-positive cells are responsible for gemcitabine resistance in pancreatic cancer cells. *Int J Cancer*. 2009;125(10):2323-2331. doi:10.1002/ijc.24573

167. Wang D, Zhu H, Zhu Y, et al. CD133+/CD44+/Oct4+/Nestin+ stem-like cells isolated from Panc-1 cell line may contribute to multi-resistance and metastasis of pancreatic cancer. *Acta Histochem*. 2013;115(4):349-356. doi:10.1016/j.acthis.2012.09.007

168. Rentala S, Mangamoori LN. Isolation, characterization and mobilization of prostate cancer tissue derived CD133+ MDR1+ cells. *J Stem Cells*. 2010;5(2):75-81.

169. Fong MY, Kakar SS. The role of cancer stem cells and the side population in epithelial ovarian cancer. *Histol Histopathol*. 2010;25(1):113-120. doi:10.14670/HH-25.113

170. Nakai E, Park K, Yawata T, et al. Enhanced mdr1 expression and chemoresistance of cancer stem cells derived from glioblastoma. *Cancer Invest*. 2009;27(9):901-908. doi:10.3109/07357900801946679

171. Ho MM, Hogge DE, Ling V. MDR1 and BCRP1 expression in leukemic progenitors correlates with chemotherapy response in acute myeloid leukemia. *Exp Hematol*. 2008;36(4):433-442. doi:10.1016/j.exphem.2007.11.014

172. Wright MH, Calcagno AM, Salcido CD, Carlson MD, Ambudkar S V., Varticovski L. Brca1 breast tumors contain distinct CD44+/CD24-and CD133+cells with cancer stem cell characteristics. *Breast Cancer Res*. 2008;10(1). doi:10.1186/bcr1855

173. Lees-Miller SP, Godbout R, Chan DW, et al. Absence of p350 subunit of DNA-activated protein kinase from a radiosensitive human cell line. *Science (80-)*. 1995;267(5201):1183-1185. doi:10.1126/science.7855602

174. Ouyang H, Nussenzweig A, Kurimasa A, et al. Ku70 is required for DNA repair but not for T cell antigen receptor gene recombination in vivo. *J Exp Med*. 1997;186(6):921-929. doi:10.1084/jem.186.6.921

175. Zhang J, F.G. Stevens M, D. Bradshaw T. Temozolomide: Mechanisms of Action, Repair and Resistance. *Curr Mol Pharmacol*. 2011;5(1):102-114. doi:10.2174/1874467211205010102

176. Casorelli I, Russo M, Bignami M. Role of Mismatch Repair and MGMT in Response to Anticancer Therapies. *Anticancer Agents Med Chem*. 2012;8(4):368-380. doi:10.2174/187152008784220276

177. Liu G, Yuan X, Zeng Z, et al. Analysis of gene expression and chemoresistance of CD133+ cancer stem cells in glioblastoma. *Mol Cancer*. 2006;5:67. doi:10.1186/1476-4598-5-67

178. Pistollato F, Abbadi S, Rampazzo E, et al. Intratumoral hypoxic gradient drives stem cells distribution and MGMT expression in glioblastoma. *Stem Cells*. 2010;28(5):851-862. doi:10.1002/stem.415

179. Beier D, Röhrl S, Pillai DR, et al. Temozolomide preferentially depletes cancer stem cells in glioblastoma. *Cancer Res*. 2008;68(14):5706-5715. doi:10.1158/0008-5472.CAN-07-6878

180. Pallini R, Montano N, Larocca LM. Comment re: Temozolomide preferentially depletes cancer stem cells. *Cancer Res*. 2009;69(15):6364. doi:10.1158/0008-5472.CAN-09-0036

181. Persano L, Pistollato F, Rampazzo E, et al. BMP2 sensitizes glioblastoma stem-like cells to Temozolomide by affecting HIF-1α stability and MGMT expression. *Cell Death Dis*. 2012;3(10):e412. doi:10.1038/cddis.2012.153

182. Adams JM, Cory S. The Bcl-2 apoptotic switch in cancer development and therapy. *Oncogene*. 2007;26(9):1324-1337. doi:10.1038/sj.onc.1210220

183. Shervington A, Lu C. Expression of multidrug resistance genes in normal and cancer stem cells. *Cancer Invest*. 2008;26(5):535-542. doi:10.1080/07357900801904140

184. Ma S, Lee TK, Zheng BJ, Chan KW, Guan XY. CD133+ HCC cancer stem cells confer chemoresistance by preferential expression of the Akt/PKB survival pathway. *Oncogene*. 2008;27(12):1749-1758. doi:10.1038/sj.onc.1210811

185. Vangipuram SD, Buck SA, Lyman WD. Wnt pathway activity confers chemoresistance to cancer stem-like cells in a neuroblastoma cell line. *Tumour Biol*. 2012;33(6):2173-2183. doi:10.1007/s13277-012-0478-0

186. Yang W, Yan HX, Chen L, et al. Wnt/β-catenin signaling contributes to activation of normal and tumorigenic liver progenitor cells. *Cancer Res*. 2008;68(11):4287-4295. doi:10.1158/0008-5472.CAN-07-6691

187. Bisson I, Prowse DM. WNT signaling regulates self-renewal and differentiation of prostate cancer cells with stem cell characteristics. *Cell Res*. 2009;19(6):683-697. doi:10.1038/cr.2009.43

188. Anastas JN, Kulikauskas RM, Tamir T, et al. WNT5A enhances resistance of melanoma cells to targeted BRAF inhibitors. *J Clin Invest*. 2014;124(7):2877-2890. doi:10.1172/JCI70156

189. Chau WK, Ip CK, Mak ASC, Lai HC, Wong AST. C-Kit mediates chemoresistance and tumor-initiating capacity of ovarian cancer cells through activation of Wnt/β-catenin-ATP-binding cassette G2 signaling. *Oncogene*. 2013;32(22):2767-2781. doi:10.1038/onc.2012.290

190. Wang H, Fan L, Xia X, et al. Silencing Wnt2B by siRNA interference inhibits metastasis and enhances chemotherapy sensitivity in ovarian cancer. *Int J Gynecol Cancer*. 2012;22(5):755-761. doi:10.1097/IGC.0b013e3182540284

191. Zhao H, Wei W, Sun Y, Gao J, Wang Q, Zheng J. Interference with the expression of β-catenin reverses cisplatin resistance in A2780/DDP cells and inhibits the progression of ovarian cancer in mouse model. *DNA Cell Biol*. 2015;34(1):55-62. doi:10.1089/dna.2014.2626

192. Singh RR, Kunkalla K, Qu C, et al. ABCG2 is a direct transcriptional target of hedgehog signaling and involved in stroma-induced drug tolerance in diffuse large B-cell lymphoma. *Oncogene*. 2011;30(49):4874-4886. doi:10.1038/onc.2011.195

193. Sims-Mourtada J, Izzo JG, Ajani J, Chao KSC. Sonic Hedgehog promotes multiple drug resistance by regulation of drug transport. *Oncogene*. 2007;26(38):5674-5679. doi:10.1038/sj.onc.1210356

194. Santisteban M. ABC transporters as molecular effectors of pancreatic oncogenic pathways: The hedgehog-GLI model. *J Gastrointest Cancer*. 2010;41(3):153-158.

doi:10.1007/s12029-010-9144-1

195. Huang FT, Zhuan-Sun YX, Zhuang YY, et al. Inhibition of hedgehog signaling depresses self-renewal of pancreatic cancer stem cells and reverses chemoresistance. *Int J Oncol*. 2012;41(5):1707-1714. doi:10.3892/ijo.2012.1597

196. Yao J, An Y, Wei JS, et al. Cyclopamine reverts acquired chemoresistance and down-regulates cancer stem cell markers in pancreatic cancer cell lines. *Swiss Med Wkly*. 2011;141(MAY):w13208. doi:10.4414/smw.2011.13208

197. Chai F, Zhou J, Chen C, et al. The hedgehog inhibitor cyclopamine antagonizes chemoresistance of breast cancer cells. *Onco Targets Ther*. 2013;6:1643-1647. doi:10.2147/OTT.S51914

198. Singh S, Chitkara D, Mehrazin R, Behrman SW, Wake RW, Mahato RI. Chemoresistance in prostate cancer cells is regulated by miRNAs and Hedgehog pathway. *PLoS One*. 2012;7(6):e40021. doi:10.1371/journal.pone.0040021

199. Steg AD, Bevis KS, Katre AA, et al. Stem cell pathways contribute to clinical chemoresistance in ovarian cancer. *Clin Cancer Res*. 2012;18(3):869-881. doi:10.1158/1078-0432.CCR-11-2188

200. Ulasov I V., Nandi S, Dey M, Sonabend AM, Lesniak MS. Inhibition of sonic hedgehog and notch pathways enhances sensitivity of cd133+ glioma stem cells to temozolomide therapy. *Mol Med*. 2011;17(1-2):103-112. doi:10.2119/molmed.2010.00062

201. Aleksic T, Feller SM. Gamma-secretase inhibition combined with platinum compounds enhances cell death in a large subset of colorectal cancer cells. *Cell Commun Signal*. 2008;6:8. doi:10.1186/1478-811X-6-8

202. Zhang S, Balch C, Chan MW, et al. Identification and characterization of ovarian cancer-initiating cells from primary human tumors. *Cancer Res*. 2008;68(11):4311-4320. doi:10.1158/0008-5472.CAN-08-0364

203. Zhang Z-P, Sun Y-L, Fu L, Gu F, Zhang L, Hao X-S. Correlation of Notch1 expression and activation to cisplatin-sensitivity of head and neck squamous cell carcinoma. *Ai Zheng*. 2009;28(2):100-103.

204. Du X, Zhao Y pei, Zhang T ping, et al. Alteration of the Intrinsic Apoptosis Pathway Is Involved in Notch-induced Chemoresistance to Gemcitabine in Pancreatic Cancer. *Arch Med Res*. 2014;45(1):15-20. doi:10.1016/j.arcmed.2013.10.001

205. Kang M, Jiang B, Xu B, et al. Delta like ligand 4 induces impaired chemo-drug delivery and enhanced chemoresistance in pancreatic cancer. *Cancer Lett*. 2013;330(1):11-21. doi:10.1016/j.canlet.2012.11.015

206. Ma Y, Ren Y, Han EQ, et al. Inhibition of the Wnt-β-catenin and Notch signaling pathways sensitizes osteosarcoma cells to chemotherapy. *Biochem Biophys Res Commun*. 2013;431(2):274-279. doi:10.1016/j.bbrc.2012.12.118

207. Xu D, Hu J, De Bruyne E, et al. Dll1/Notch activation contributes to bortezomib resistance by upregulating CYP1A1 in multiple myeloma. *Biochem Biophys Res Commun*. 2012;428(4):518-524. doi:10.1016/j.bbrc.2012.10.071

208. Bonadonna G, Valagussa P, Moliterni A, Zambetti M, Brambilla C. Adjuvant Cyclophosphamide, Methotrexate, and Fluorouracil in Node-Positive Breast Cancer – The Results of 20 Years of Follow-up. *N Engl J Med*. 1995;332(14):901-906. doi:10.1056/NEJM199504063321401

209. Di Re F, Bohm S, Oriana S, Spatti GB, Zunino F. Efficacy and safety of high-dose cisplatin and cyclophosphamide with glutathione protection in the treatment of bulky advanced epithelial ovarian cancer. *Cancer Chemother Pharmacol*. 1990;25(5):355-360. doi:10.1007/bf00686237

210. Luce JK, Gamble JF, Wilson HE, et al. Combined cyclophosphamide vincristine, and prednisone therapy of malignant lymphoma. *Cancer*. 1971;28(2):306-317. doi:10.1002/1097-0142(197108)28:2<306::aid-cncr2820280208>3.0.co;2-n

211. Socié G, Clift RA, Blaise D, et al. Busulfan plus cyclophosphamide compared with total-body irradiation plus cyclophosphamide before marrow transplantation for myeloid leukemia: long-term follow-up of 4 randomized studies. *Blood*. 2001;98(13):3569-3574. doi:10.1182/blood.v98.13.3569

212. Thurman WG, Fernbach DJ, Sullivan MP. Cyclophosphamide therapy in childhood neuroblastoma. *N Engl J Med*. 1964;270:1336-1340. doi:10.1056/NEJM196406182702503

213. Emadi A, Jones RJ, Brodsky RA. Cyclophosphamide and cancer: Golden anniversary. *Nat Rev Clin Oncol*. 2009;6(11):638-647. doi:10.1038/nrclinonc.2009.146

214. Hilton J. Role of Aldehyde Dehydrogenase in Cyclophosphamide-resistant L 1210 Leukemia. *Cancer Res*. 1984;44(11):5156-5160.

215. Jones RJ, Barber JP, Vala MS, et al. Assessment of aldehyde dehydrogenase in viable cells. *Blood*. 1995;85(10):2742-2746.

216. Russo JE, Hilton J. Characterization of cytosolic aldehyde dehydrogenase from cyclophosphamide resistant L1210 cells. *Cancer Res*. 1988;48(11):2963-2968.

217. Magni M, Shammah S, Schiró R, Mellado W, Dalla-Favera R, Gianni AM. Induction of cyclophosphamide-resistance by aldehyde-dehydrogenase gene transfer. *Blood*. 1996;87(3):1097-1103. doi:10.1182/blood.v87.3.1097.bloodjournal8731097

218. Moreb JS, Muhoczy D, Ostmark B, Zucali JR. RNAi-mediated knockdown of aldehyde dehydrogenase class-1A1 and class-3A1 is specific and reveals that each contributes equally to the resistance against 4-hydroperoxycyclophosphamide. *Cancer Chemother Pharmacol*. 2007;59(1):127-136. doi:10.1007/s00280-006-0233-6

219. Sladek NE, Kollander R, Sreerama L, Kiang DT. Cellular levels of aldehyde dehydrogenases (ALDH1A1 and ALDH3A1) as predictors of therapeutic responses to cyclophosphamide-based chemotherapy of breast cancer: a retrospective study. Rational individualization of oxazaphosphorine-based cancer chemotherap. *Cancer ChemotherPharmacol*. 2002;49(0344-5704):309-321. doi:10.1007/s00280-001-0412-4

220. Levi BP, Yilmaz ÖH, Duester G, Morrison SJ. Aldehyde dehydrogenase 1a1 is dispensable for stem cell function in the mouse hematopoietic and nervous systems. *Blood*. 2009;113(8):1670-1680. doi:10.1182/blood-2008-05-156752

221. Awad O, Yustein JT, Shah P, et al. High ALDH activity identifies chemotherapy-resistant Ewing's sarcoma stem cells that retain sensitivity to EWS-Fli1 inhibition. *PLoS One*. 2010;5(11):e13943. doi:10.1371/journal.pone.0013943

222. Duong HQ, Hwang JS, Kim HJ, Kang HJ, Seong YS, Bae I. Aldehyde dehydrogenase 1A1 confers intrinsic and acquired resistance to gemcitabine in human pancreatic adenocarcinoma MIA PaCa-2 cells. *Int J Oncol*. 2012;41(3):855-861. doi:10.3892/ijo.2012.1516

223. Nishikawa S, Konno M, Hamabe A, et al. Aldehyde dehydrogenasehigh gastric cancer stem cells are resistant to chemotherapy. *Int J Oncol*. 2013;42(4):1437-1442. doi:10.3892/ijo.2013.1837

224. Raha D, Wilson TR, Peng J, et al. The cancer stem cell marker aldehyde dehydrogenase is required to maintain a drug-tolerant tumor cell subpopulation. *Cancer Res*. 2014;74(13):3579-3590. doi:10.1158/0008-5472.CAN-13-3456

225. Alamgeer M, Ganju V, Kumar B, et al. Changes in aldehyde dehydrogenase-1 expression during neoadjuvant chemotherapy predict outcome in locally advanced breast cancer. *Breast Cancer Res*. 2014;16(2):R44. doi:10.1186/bcr3648

226. Mohammad Sultan KMC. Retinoid Signaling in Cancer and Its Promise for Therapy. *J Carcinog Mutagen*. 2013;0(0):1-14. doi:10.4172/2157-2518.s7-006

227. Marcato P, Dean CA, Giacomantonio CA, Lee PWK. Aldehyde dehydrogenase its role as a cancer stem cell marker comes down to the specific isoform. *Cell Cycle*. 2011;10(9):1378-1384. doi:10.4161/cc.10.9.15486

228. Lord SJ, Marinovich ML, Patterson JA, et al. Incidence of metastatic breast cancer in an Australian population-based cohort of women with non-metastatic breast cancer at diagnosis. *Med J Aust*. 2012;196(11):688-692. doi:10.5694/mja12.10026

229. Weigelt B, Peterse JL, Van't Veer LJ. Breast cancer metastasis: Markers and models. *Nat Rev Cancer*. 2005;5(8):591-602. doi:10.1038/nrc1670

230. Hölzel D, Eckel R, Bauerfeind I, et al. Improved systemic treatment for early breast cancer improves cure rates, modifies metastatic pattern and shortens post-metastatic survival: 35-year results from the Munich Cancer Registry. *J Cancer Res Clin Oncol*. 2017;143(9):1701-1712. doi:10.1007/s00432-017-2428-0

231. Van Den Hurk CJG, Eckel R, Van De Poll-Franse L V., et al. Unfavourable pattern of metastases in M0 breast cancer patients during 1978-2008: A population-based analysis of the Munich Cancer Registry. *Breast Cancer Res Treat*. 2011;128(3):795-805. doi:10.1007/s10549-011-1372-y

232. Gerratana L, Fanotto V, Bonotto M, et al. Pattern of metastasis and outcome in patients with breast cancer. *Clin Exp Metastasis*. 2015;32(2):125-133. doi:10.1007/s10585-015-9697-2

233. Paget S. The distribution of secondary growths in cancer of the breast. *Lancet*. 1889;133(3421):571-573. doi:10.1016/S0140-6736(00)49915-0

234. Mehlen P, Puisieux A. Metastasis: A question of life or death. *Nat Rev Cancer*. 2006;6(6):449-458. doi:10.1038/nrc1886

235. Balic M, Lin H, Young L, et al. Most early disseminated cancer cells detected in bone marrow of breast cancer patients have a putative breast cancer stem cell phenotype. *Clin Cancer Res*. 2006;12(19):5615-5621. doi:10.1158/1078-0432.CCR-06-0169

236. Walsh HR, Cruickshank BM, Brown JM, Marcato P. The flick of a switch: Conferring survival advantage to breast cancer stem cells through metabolic plasticity. *Front Oncol*. 2019;9(AUG). doi:10.3389/fonc.2019.00753

237. Liu S, Cong Y, Wang D, et al. Breast cancer stem cells transition between epithelial and mesenchymal states reflective of their normal counterparts. *Stem Cell Reports*. 2014;2(1):78-91. doi:10.1016/j.stemcr.2013.11.009

238. Markiewicz A, Topa J, Nagel A, et al. Spectrum of epithelial-mesenchymal transition phenotypes in circulating tumour cells from early breast cancer patients. *Cancers (Basel)*. 2019;11(1). doi:10.3390/cancers11010059

239. Williams ED, Gao D, Redfern A, Thompson EW. Controversies around epithelial–mesenchymal plasticity in cancer metastasis. *Nat Rev Cancer*. 2019;19(12):716-732. doi:10.1038/s41568-019-0213-x

240. Luzzi KJ, MacDonald IC, Schmidt EE, et al. Multistep nature of metastatic inefficiency: Dormancy of solitary cells after successful extravasation and limited survival of early micrometastases. *Am J Pathol*. 1998;153(3):865-873. doi:10.1016/S0002-9440(10)65628-3

241. Liu X, Taftaf R, Kawaguchi M, et al. Homophilic CD44 interactions mediate tumor cell aggregation and polyclonal metastasis in patient-derived breast cancer models. *Cancer Discov*. 2019;9(1):96-113. doi:10.1158/2159-8290.CD-18-0065

242. Sharma U, Miller P, Medina Saenz K, et al. Abstract PD9-10: Circulating CAF/cancer stem cell co-clusters bolster breast cancer metastasis. In: *Cancer Research*. Vol 79. American Association for Cancer Research (AACR); 2019:PD9-10-PD9-10. doi:10.1158/1538-7445.sabcs18-pd9-10

243. Malanchi I, Santamaria-Martínez A, Susanto E, et al. Interactions between cancer stem cells and their niche govern metastatic colonization. *Nature*. 2012;481(7379):85-91. doi:10.1038/nature10694

244. Bartucci M, Dattilo R, Moriconi C, et al. TAZ is required for metastatic activity and chemoresistance of breast cancer stem cells. *Oncogene*. 2014;34:681-690. doi:10.1038/onc.2014.5

245. Bartosiewicz D, Krasowska A. Inhibitors of ABC transporters and biophysical methods to study their activity. *Zeitschrift fur Naturforsch - Sect C J Biosci*. 2009;64(5-6):454-458. doi:10.1515/znc-2009-5-625

246. Belpomme D, Gauthier S, Pujade-Lauraine E, et al. Verapamil increases the survival of patients with anthracycline-resistant metastatic breast carcinoma. *Ann Oncol Off J Eur Soc Med Oncol*. 2000;11(11):1471-1476. doi:10.1023/a:1026556119020

247. Millward MJ, Cantwell BMJ, Munro NC, Robinson A, Corris PA, Harris AL. Oral verapamil with chemotherapy for advanced non-small cell lung cancer: A randomised study. *Br J Cancer*. 1993;67(5):1031-1035. doi:10.1038/bjc.1993.189

248. Sonneveld P, Suciu S, Weijermans P, et al. Cyclosporin A combined with vincristine, doxorubicin and dexamethasone (VAD) compared with VAD alone in patients with advanced refractory multiple myeloma: An EORTC- HOVON randomized phase III study (06914). *Br J Haematol*. 2001;115(4):895-902. doi:10.1046/j.1365-2141.2001.03171.x

249. Lhommé C, Joly F, Walker JL, et al. Phase III study of valspodar (PSC 833) combined with paclitaxel and carboplatin compared with paclitaxel and carboplatin alone in patients with stage IV or suboptimally debulked stage III epithelial ovarian cancer or primary peritoneal cancer. *J Clin Oncol*. 2008;26(16):2674-2682. doi:10.1200/JCO.2007.14.9807

250. Cripe LD, Uno H, Paietta EM, et al. Zosuquidar, a novel modulator of P-glycoprotein, does not improve the outcome of older patients with newly diagnosed acute myeloid leukemia: A randomized, placebo-controlled trial of the Eastern Cooperative Oncology Group 3999. *Blood*. 2010;116(20):4077-4085. doi:10.1182/blood-2010-04-277269

251. Shukla S, Ohnuma S, V. Ambudkar S. Improving Cancer Chemotherapy with Modulators of ABC Drug Transporters. *Curr Drug Targets*. 2011;12(5):621-630. doi:10.2174/138945011795378540

252. Dohse M, Scharenberg C, Shukla S, et al. Comparison of ATP-binding cassette transporter interactions with the tyrosine kinase inhibitors imatinib, nilotinib, and dasatinib. *Drug Metab Dispos*. 2010;38(8):1371-1380. doi:10.1124/dmd.109.031302

253. Wu L, Zhang Z, Yao H, Liu K, Wen Y, Xiong L. Clinical efficacy of second-generation tyrosine kinase inhibitors in imatinib-resistant gastrointestinal stromal tumors: a meta-analysis of recent clinical trials. *Drug Des Devel Ther*. 2014;8:2061-2067. doi:10.2147/DDDT.S63840

254. Wang F, Wang X-K, Shi C-J, et al. Nilotinib Enhances the Efficacy of Conventional Chemotherapeutic Drugs in CD34+CD38− Stem Cells and ABC Transporter Overexpressing Leukemia Cells. *Molecules*. 2014;19(3):3356-3375. doi:10.3390/molecules19033356

255. Zhao XQ, Dai CL, Ohnuma S, et al. Tandutinib (MLN518/CT53518) targeted to stem-like cells by inhibiting the function of ATP-binding cassette subfamily G member 2. *Eur J Pharm Sci*. 2013;49(3):441-450. doi:10.1016/j.ejps.2013.04.015

256. Koppaka V, Thompson DC, Chen Y, et al. Aldehyde dehydrogenase inhibitors: A comprehensive review of the pharmacology, mechanism of action, substrate specificity, and clinical application. *Pharmacol Rev*. 2012;64(3):520-539. doi:10.1124/pr.111.005538

257. Pors K, Moreb JS. Aldehyde dehydrogenases in cancer: An opportunity for biomarker and drug development? *Drug Discov Today*. 2014;19(12):1953-1963. doi:10.1016/j.drudis.2014.09.009

258. Chen D, Cui QC, Yang H, Dou QP. Disulfiram, a clinically used anti-alcoholism drug and copper-binding agent, induces apoptotic cell death in breast cancer cultures and xenografts via inhibition of the proteasome activity. *Cancer Res*. 2006;66(21):10425-10433. doi:10.1158/0008-5472.CAN-06-2126

259. Duan L, Shen H, Zhao G, et al. Inhibitory effect of Disulfiram/copper complex on non-small cell lung cancer cells. *Biochem Biophys Res Commun*. 2014;446(4):1010-1016. doi:10.1016/j.bbrc.2014.03.047

260. Hothi P, Martins TJ, Chen LP, et al. High-Throughput chemical screens identify disulfiram as an inhibitor of human glioblastoma stem cells. *Oncotarget*. 2012;3(10):1124-1136. doi:10.18632/oncotarget.707

261. Wang Y, Li W, Patel SS, et al. Blocking the formation of radiation-induced breast cancer stem cells. *Oncotarget*. 2014;5(11):3743-3755. doi:10.18632/oncotarget.1992

262. Nechushtan H, Hamamreh Y, Nidal S, et al. A Phase IIb Trial Assessing the Addition of Disulfiram to Chemotherapy for the Treatment of Metastatic Non-Small Cell Lung Cancer. *Oncologist*. 2015;20(4):366-367. doi:10.1634/theoncologist.2014-0424

263. Sharma S, Kelly TK, Jones PA. Epigenetics in cancer. *Carcinogenesis*. 2010;31(1):27-36. doi:10.1093/carcin/bgp220

264. Figueroa ME, Abdel-Wahab O, Lu C, et al. Leukemic IDH1 and IDH2 Mutations Result in a Hypermethylation Phenotype, Disrupt TET2 Function, and Impair Hematopoietic Differentiation. *Cancer Cell*. 2010;18(6):553-567. doi:10.1016/j.ccr.2010.11.015

265. Peddi PF, Ellis MJ, Ma C. Molecular basis of triple negative breast cancer and implications for therapy. *IntJ Breast Cancer*. 2012;2012(2090-3189):217185. doi:10.1155/2012/217185

266. Shipitsin M, Campbell LL, Argani P, et al. Molecular definition of breast tumor heterogeneity. *Cancer Cell*. 2007;11(1535-6108):259-273. doi:10.1016/j.ccr.2007.01.013

267. Gore SD, Baylin S, Sugar E, et al. Combined DNA methyltransferase and histone deacetylase inhibition in the treatment of myeloid neoplasms. *Cancer Res*. 2006;66(12):6361-6369. doi:10.1158/0008-5472.CAN-06-0080

268. Lyko F, Brown R. DNA methyltransferase inhibitors and the development of epigenetic cancer therapies. *J NatlCancer Inst*. 2005;97(1460-2105):1498-1506. doi:10.1093/jnci/dji311

269. Costa G, Barra V, Lentini L, Cilluffo D, Di Leonardo A. DNA demethylation caused by 5-Aza-2'-deoxycytidine induces mitotic alterations and aneuploidy. *Oncotarget*. 2016;7(4):3726-3739. doi:10.18632/oncotarget.6897

270. Goodyear O, Agathanggelou A, Novitzky-Basso I, et al. Induction of a CD8+ T-cell response to the MAGE cancer testis antigen by combined treatment with azacitidine and sodium valproate in patients with acute myeloid leukemia and myelodysplasia. *Blood*. 2010;116(11):1908-1918. doi:10.1182/blood-2009-11-249474

271. Almstedt M, Blagitko-Dorfs N, Duque-Afonso J, et al. The DNA demethylating agent 5-aza-2'-deoxycytidine induces expression of NY-ESO-1 and other cancer/testis antigens in myeloid leukemia cells. *Leuk Res*. 2010;34(7):899-905. doi:10.1016/j.leukres.2010.02.004

272. Chiappinelli KB, Strissel PL, Desrichard A, et al. Inhibiting DNA Methylation Causes an Interferon Response in Cancer via dsRNA Including Endogenous Retroviruses. *Cell*. 2015;162(5):974-986. doi:10.1016/j.cell.2015.07.011

273. Roulois D, Loo Yau H, Singhania R, et al. DNA-Demethylating Agents Target Colorectal Cancer Cells by Inducing Viral Mimicry by Endogenous Transcripts. *Cell*. 2015;162(5):961-973. doi:10.1016/j.cell.2015.07.056

274. Tsai HC, Li H, Van NL, et al. Transient low doses of DNA-demethylating agents exert durable antitumor effects on hematological and epithelial tumor cells. *Cancer Cell*. 2012;21(1878-3686):430-446. doi:10.1016/j.ccr.2011.12.029

275. Abáigar M, Ramos F, Benito R, et al. Prognostic impact of the number of methylated genes in myelodysplastic syndromes and acute myeloid leukemias treated with azacytidine. *Ann Hematol*. 2013;92(11):1543-1552. doi:10.1007/s00277-013-1799-9

276. Traina F, Visconte V, Elson P, et al. Impact of molecular mutations on treatment response to DNMT inhibitors in myelodysplasia and related neoplasms. *Leukemia*. 2014;28(1):78-87. doi:10.1038/leu.2013.269

277. Shen L, Kantarjian H, Guo Y, et al. DNA methylation predicts survival and response to therapy in patients with myelodysplastic syndromes. *J Clin Oncol*. 2010;28(4):605-613. doi:10.1200/JCO.2009.23.4781

278. Qin T, Castoro R, El Ahdab S, et al. Mechanisms of resistance to decitabine in the myelodysplastic syndrome. *PLoS One*. 2011;6(8):e23372. doi:10.1371/journal.pone.0023372

279. Damaraju VL, Mowles D, Yao S, et al. Role of human nucleoside transporters in the uptake and cytotoxicity of azacitidine and decitabine. *Nucleosides Nucleotides Nucleic Acids*. 2012;31(3):236-255. doi:10.1080/15257770.2011.652330

280. Rius M, Stresemann C, Keller D, et al. Human concentrative nucleoside transporter 1-mediated uptake of 5-azacytidine enhances DNA demethylation. *Mol Cancer Ther*. 2009;8(1):225-231. doi:10.1158/1535-7163.MCT-08-0743

281. Treppendahl MB, Kristensen LS, Grønbæk K. Predicting response to epigenetic therapy. *J Clin Invest*. 2014;124(1):47-55. doi:10.1172/JCI69737

282. Nair A, Jacob S. A simple practice guide for dose conversion between animals and human. *J Basic Clin Pharm*. 2016;7(2):27. doi:10.4103/0976-0105.177703

283. Derissen EJB, Beijnen JH, Schellens JHM. Concise Drug Review: Azacitidine and Decitabine. *Oncologist*. 2013;18(5):619-624. doi:10.1634/theoncologist.2012-0465

284. Cashen AF, Shah AK, Todt L, Fisher N, DiPersio J. Pharmacokinetics of decitabine administered as a 3-h infusion to patients with acute myeloid leukemia (AML) or myelodysplastic syndrome (MDS). *Cancer Chemother Pharmacol*. 2008;61(5):759-766. doi:10.1007/s00280-007-0531-7

285. Cerami E, Gao J, Dogrusoz U, et al. The cBio Cancer Genomics Portal: An Open

Platform for Exploring Multidimensional Cancer Genomics Data: Figure 1. *Cancer Discov*. 2012;2(5):401-404. doi:10.1158/2159-8290.CD-12-0095

286. Gao J, Aksoy BA, Dogrusoz U, et al. Integrative Analysis of Complex Cancer Genomics and Clinical Profiles Using the cBioPortal. *Sci Signal*. 2013;6(269):pl1-pl1. doi:10.1126/scisignal.2004088

287. Vera-Ramirez L, Sanchez-Rovira P, Ramirez-Tortosa CL, Quiles JL, Ramirez-Tortosa Mc, Lorente JA. Transcriptional Shift Identifies a Set of Genes Driving Breast Cancer Chemoresistance. Creighton C, ed. *PLoS One*. 2013;8(1):e53983. doi:10.1371/journal.pone.0053983

288. Coyle KM, Murphy JP, Vidovic D, et al. Breast cancer subtype dictates DNA methylation and ALDH1A3-mediated expression of tumor suppressor RARRES1. *Oncotarget*. June 2016. doi:10.18632/oncotarget.9858

289. Coyle KM, Maxwell S, Thomas ML, Marcato P. Profiling of the transcriptional response to all-trans retinoic acid in breast cancer cells reveals RARE-independent mechanisms of gene expression. *Sci Rep*. 2017;7(1):16684. doi:10.1038/s41598-017-16687-6

290. Hall SR, Toulany J, Bennett LG, et al. Jadomycins Inhibit Type II Topoisomerases and Promote DNA Damage and Apoptosis in Multidrug-Resistant Triple-Negative Breast Cancer Cells. *J Pharmacol Exp Ther*. 2017;363(2):196-210. doi:10.1124/jpet.117.241125

291. Pastor-Anglada M, Pérez-Torras S. Nucleoside transporter proteins as biomarkers of drug responsiveness and drug targets. *Front Pharmacol*. 2015;6:13. doi:10.3389/fphar.2015.00013

292. Ebrahem Q, Mahfouz RZ, Durkin L, et al. Mechanisms of Resistance to 5-Azacytidine/Decitabine in MDS-AML and Pre-Clinical In Vivo Proof of Principle of Rational Solutions to Extend Response. *Blood*. 2015;126(23). doi:10.1182/blood.V126.23.678.678

293. Esteller M, Herman JG. Cancer as an epigenetic disease: DNA methylation and chromatin alterations in human tumours. *J Pathol*. 2002;196(1):1-7. doi:10.1002/path.1024

294. Kohli RM, Zhang Y. TET enzymes, TDG and the dynamics of DNA demethylation. *Nature*. 2013;502(7472):472-479. doi:10.1038/nature12750

295. Díez-Villanueva A, Mallona I, Peinado MA. Wanderer, an interactive viewer to explore DNA methylation and gene expression data in human cancer. *Epigenetics Chromatin*. 2015;8(1):22. doi:10.1186/s13072-015-0014-8

296. Song X-Y, Li B-Y, Zhou E-X, Wu F-X. The clinicopathological significance of RUNX3 hypermethylation and mRNA expression in human breast cancer, a meta-

analysis. *Onco Targets Ther*. 2016;9:5339-5347. doi:10.2147/OTT.S77828

297. Esteller M, Silva JM, Dominguez G, et al. Promoter Hypermethylation and BRCA1 Inactivation in Sporadic Breast and Ovarian Tumors. *J Natl Cancer Inst*. 2000;92(7):564-569. doi:10.1093/jnci/92.7.564

298. Shargh SA, Sakizli M, Khalaj V, et al. Downregulation of E-cadherin expression in breast cancer by promoter hypermethylation and its relation with progression and prognosis of tumor. *Med Oncol*. 2014;31(11):250. doi:10.1007/s12032-014-0250-y

299. Kim T-Y, Zhong S, Fields CR, Kim JH, Robertson KD. Epigenomic profiling reveals novel and frequent targets of aberrant DNA methylation-mediated silencing in malignant glioma. *Cancer Res*. 2006;66(15):7490-7501. doi:10.1158/0008-5472.CAN-05-4552

300. Zhong S, Fields CR, Su N, Pan Y-X, Robertson KD. Pharmacologic inhibition of epigenetic modifications, coupled with gene expression profiling, reveals novel targets of aberrant DNA methylation and histone deacetylation in lung cancer. *Oncogene*. 2007;26(18):2621-2634. doi:10.1038/sj.onc.1210041

301. Heller G, Schmidt WM, Ziegler B, et al. Genome-wide transcriptional response to 5-aza-2'-deoxycytidine and trichostatin a in multiple myeloma cells. *Cancer Res*. 2008;68(1):44-54. doi:10.1158/0008-5472.CAN-07-2531

302. Yang X, Han H, De Carvalho DD, Lay FD, Jones PA, Liang G. Gene Body Methylation Can Alter Gene Expression and Is a Therapeutic Target in Cancer. *Cancer Cell*. 2014;26(4):577-590. doi:10.1016/j.ccr.2014.07.028

303. Strissel PL, Ruebner M, Thiel F, et al. Reactivation of codogenic endogenous retroviral (ERV) envelope genes in human endometrial carcinoma and prestages: Emergence of new molecular targets. *Oncotarget*. 2012;3(10):1204-1219. doi:10.18632/oncotarget.679

304. Schoggins JW, Rice CM. Interferon-stimulated genes and their antiviral effector functions. *Curr Opin Virol*. 2011;1(6):519-525. doi:10.1016/j.coviro.2011.10.008

305. Burger H, Foekens JA, Look MP, et al. RNA expression of breast cancer resistance protein, lung resistance-related protein, multidrug resistance-associated proteins 1 and 2, and multidrug resistance gene 1 in breast cancer: Correlation with chemotherapeutic response. *Clin Cancer Res*. 2003;9(2):827-836.

306. Santini V. How I treat MDS after hypomethylating agent failure. *Blood*. 2019;133(6):521-529. doi:10.1182/blood-2018-03-785915

307. Coston T, Pophali P, Vallapureddy R, et al. Suboptimal response rates to hypomethylating agent therapy in chronic myelomonocytic leukemia; a single institutional study of 121 patients. *Am J Hematol*. 2019;94(7):ajh.25488.

doi:10.1002/ajh.25488

308. Du M, Zhou F, Jin R, Hu Y, Mei H. Mutations in the DNA methylation pathway predict clinical efficacy to hypomethylating agents in myelodysplastic syndromes: a meta-analysis. *Leuk Res*. 2019;80:11-18. doi:10.1016/J.LEUKRES.2019.03.001

309. Bejar R, Lord A, Stevenson K, et al. TET2 mutations predict response to hypomethylating agents in myelodysplastic syndrome patients. *Blood*. 2014;124(17):2705-2712. doi:10.1182/blood-2014-06-582809

310. Voso MT, Niscola P, Piciocchi A, et al. Standard dose and prolonged administration of azacitidine are associated with improved efficacy in a real-world group of patients with myelodysplastic syndrome or low blast count acute myeloid leukemia. *Eur J Haematol*. 2016;96(4):344-351. doi:10.1111/ejh.12595

311. Wang H, Li Y, Lv N, Li Y, Wang L, Yu L. Predictors of clinical responses to hypomethylating agents in acute myeloid leukemia or myelodysplastic syndromes. *Ann Hematol*. 2018;97(11):2025-2038. doi:10.1007/s00277-018-3464-9

312. De Beck L, Melhaoui S, De Veirman K, et al. Epigenetic treatment of multiple myeloma mediates tumor intrinsic and extrinsic immunomodulatory effects. *Oncoimmunology*. 2018;7(10):e1484981. doi:10.1080/2162402X.2018.1484981

313. Yu G, Wu Y, Wang W, et al. Low-dose decitabine enhances the effect of PD-1 blockade in colorectal cancer with microsatellite stability by re-modulating the tumor microenvironment. *Cell Mol Immunol*. 2019;16(4):401-409. doi:10.1038/s41423-018-0026-y

314. Stone ML, Chiappinelli KB, Li H, et al. Epigenetic therapy activates type I interferon signaling in murine ovarian cancer to reduce immunosuppression and tumor burden. *Proc Natl Acad Sci U S A*. 2017;114(51):E10981-E10990. doi:10.1073/pnas.1712514114

315. Lucarini V, Buccione C, Ziccheddu G, et al. Combining Type I Interferons and 5-Aza-2′-Deoxycitidine to Improve Anti-Tumor Response against Melanoma. *J Invest Dermatol*. 2017;137(1):159-169. doi:10.1016/J.JID.2016.08.024

316. Chatterjee A, Rodger EJ, Ahn A, et al. Marked Global DNA Hypomethylation Is Associated with Constitutive PD-L1 Expression in Melanoma. *iScience*. 2018;4:312-325. doi:10.1016/j.isci.2018.05.021

317. Yang H, Bueso-Ramos C, DiNardo C, et al. Expression of PD-L1, PD-L2, PD-1 and CTLA4 in myelodysplastic syndromes is enhanced by treatment with hypomethylating agents. *Leukemia*. 2014;28(6):1280-1288. doi:10.1038/leu.2013.355

318. Baylin SB, Jones PA. A decade of exploring the cancer epigenome-biological and translational implications. *Nat Rev Cancer*. 2011;11(10):726-734.

doi:10.1038/nrc3130

319. Yan PS, Chen CM, Shi H, et al. Dissecting complex epigenetic alterations in breast cancer using CpG island microarrays. *Cancer Res*. 2001;61(23):8375-8380.

320. Graff JR, Herman JG, Lapidus RG, et al. E-Cadherin Expression Is Silenced by DNA Hypermethylation in Human Breast and Prostate Carcinomas. *Cancer Res*. 1995;55(22):5195-5199.

321. Morita S, Takahashi R u., Yamashita R, et al. Genome-wide analysis of DNA methylation and expression of microRNAs in breast cancer cells. *Int J Mol Sci*. 2012;13(7):8259-8272. doi:10.3390/ijms13078259

322. Faryna M, Konermann C, Aulmann S, et al. Genome-wide methylation screen in low-grade breast cancer identifies novel epigenetically altered genes as potential biomarkers for tumor diagnosis. 2008:4937-4950. doi:10.1096/fj.12-209502

323. Dobrovic A, Simpfendorfer D. Methylation of the BRCA1 gene in sporadic breast cancer. *Cancer Res*. 1997;57(16):3347-3350.

324. Cho YH, Shen J, Gammon MD, et al. Prognostic significance of gene-specific promoter hypermethylation in breast cancer patients. *Breast Cancer Res Treat*. 2012;131(1):197-205. doi:10.1007/s10549-011-1712-y

325. Roulois D, Yau HL, De Carvalho DD. Pharmacological DNA demethylation: Implications for cancer immunotherapy. *Oncoimmunology*. 2016;5(3):e1090077. doi:10.1080/2162402X.2015.1090077

326. Linnekamp JF, Butter R, Spijker R, Medema JP, van Laarhoven HWM. Clinical and biological effects of demethylating agents on solid tumours – A systematic review. *Cancer Treat Rev*. 2017;54:10-23. doi:10.1016/j.ctrv.2017.01.004

327. Stewart DJ, Issa J, Kurzrock R, et al. Decitabine Effect on Tumor Global DNA Methylation and Other Parameters in a Phase I Trial in Refractory Solid Tumors and Lymphomas. 2009;15(11):3881-3889. doi:10.1158/1078-0432.CCR-08-2196

328. Labuschagne CF, van den Broek NJF, Mackay GM, Vousden KH, Maddocks ODK. Serine, but Not Glycine, Supports One-Carbon Metabolism and Proliferation of Cancer Cells. *Cell Rep*. 2014;7(4):1248-1258. doi:10.1016/j.celrep.2014.04.045

329. Maddocks ODK, Labuschagne CF, Adams PD, Correspondence KHV, Vousden KH. Serine Metabolism Supports the Methionine Cycle and DNA/RNA Methylation through De Novo ATP Synthesis in Cancer Cells. *Mol Cell*. 2016;61:210-221. doi:10.1016/j.molcel.2015.12.014

330. Bidkhori G, Benfeitas R, Klevstig M, et al. Metabolic network-based stratification of hepatocellular carcinoma reveals three distinct tumor subtypes. *Proc Natl Acad*

Sci U S A. 2018;115(50):E11874-E11883. doi:10.1073/pnas.1807305115

331. Lehtinen L, Ketola K, Mäkelä R, et al. High-throughput RNAi screening for novel modulators of vimentin expression identifies MTHFD2 as a regulator of breast cancer cell migration and invasion. *Oncotarget*. 2013;4(1):48-63. doi:10.18632/oncotarget.756

332. Lin H, Huang B, Wang H, et al. MTHFD2 Overexpression Predicts Poor Prognosis in Renal Cell Carcinoma and is Associated with Cell Proliferation and Vimentin-Modulated Migration and Invasion. *Cell Physiol Biochem*. 2018;51(2):991-1000. doi:10.1159/000495402

333. Liu F, Liu Y, He C, et al. Increased MTHFD2 expression is associated with poor prognosis in breast cancer. 2014. doi:10.1007/s13277-014-2111-x

334. Nilsson R, Jain M, Madhusudhan N, et al. Metabolic enzyme expression highlights a key role for MTHFD2 and the mitochondrial folate pathway in cancer. *Nat Commun*. 2014;5:3128. doi:10.1038/ncomms4128

335. Noguchi K, Konno M, Koseki J, et al. The mitochondrial one-carbon metabolic pathway is associated with patient survival in pancreatic cancer. *Oncol Lett*. 2018;16(2):1827-1834. doi:10.3892/ol.2018.8795

336. Reina-Campos M, Linares JF, Duran A, Metallo CM, Moscat J, Diaz-Meco MT. Increased Serine and One-Carbon Pathway Metabolism by PKCλ/ι Deficiency Promotes Neuroendocrine Prostate Cancer. 2019. doi:10.1016/j.ccell.2019.01.018

337. Tedeschi PM, Vazquez A, Kerrigan JE, Bertino JR. Mitochondrial Methylenetetrahydrofolate Dehydrogenase (MTHFD2) Overexpression Is Associated with Tumor Cell Proliferation and Is a Novel Target for Drug Development. *Mol Cancer Res*. 2015;13(10):1361-1366. doi:10.1158/1541-7786.MCR-15-0117

338. Shao DD, Tsherniak A, Gopal S, et al. ATARiS: Computational quantification of gene suppression phenotypes from multisample RNAi screens. *Genome Res*. 2013;23(4):665-678. doi:10.1101/gr.143586.112

339. Reich M, Liefeld T, Gould J, Lerner J, Tamayo P, Mesirov JP. GenePattern 2.0. *Nat Genet*. 2006;38(5):500-501. doi:10.1038/ng0506-500

340. Qu K, Garamszegi S, Wu F, et al. Integrative genomic analysis by interoperation of bioinformatics tools in GenomeSpace. *Nat Methods*. 2016;13(3):245-247. doi:10.1038/nmeth.3732

341. Yuan M, Breitkopf SB, Yang X, Asara JM. A positive/negative ion–switching, targeted mass spectrometry–based metabolomics platform for bodily fluids, cells, and fresh and fixed tissue. *Nat Protoc*. 2012;7(5):872-881.

doi:10.1038/nprot.2012.024

342. Li B, Tang J, Yang Q, et al. NOREVA: Normalization and evaluation of MS-based metabolomics data. *Nucleic Acids Res*. 2017;45(W1):W162-W170. doi:10.1093/nar/gkx449

343. Chong J, Soufan O, Li C, et al. MetaboAnalyst 4.0: towards more transparent and integrative metabolomics analysis. *Nucleic Acids Res*. 2018;46(W1):W486-W494. doi:10.1093/nar/gky310

344. López-Boado YS, Tolivia J, López-Otín C. Apolipoprotein D gene induction by retinoic acid is concomitant with growth arrest and cell differentiation in human breast cancer cells. *J Biol Chem*. 1994;269(43):26871-26878.

345. Chen W, Qin Y, Wang D, et al. CCL20 triggered by chemotherapy hinders the therapeutic efficacy of breast cancer. Eaves C, ed. *PLOS Biol*. 2018;16(7):e2005869. doi:10.1371/journal.pbio.2005869

346. Su S, Sun X, Zhang Q, Zhang Z, Chen J. Ccl20 promotes ovarian cancer chemotherapy resistance by regulating abcb1 expression. *Cell Struct Funct*. 2019;44(1):21-28. doi:10.1247/csf.18029

347. Zhang N. Role of methionine on epigenetic modification of DNA methylation and gene expression in animals. *Anim Nutr*. 2018;4(1):11-16. doi:10.1016/j.aninu.2017.08.009

348. Kottakis F, Nicolay BN, Roumane A, et al. LKB1 loss links serine metabolism to DNA methylation and tumorigenesis. *Nature*. 2016;539(7629):390-395. doi:10.1038/nature20132

349. Jain M, Nilsson R, Sharma S, et al. Metabolite profiling identifies a key role for glycine in rapid cancer cell proliferation. *Science (80-)*. 2012;336(6084):1040-1044. doi:10.1126/science.1218595

350. Koufaris C, Gallage S, Yang T, Lau C-H, Valbuena GN, Keun HC. Suppression of MTHFD2 in MCF-7 Breast Cancer Cells Increases Glycolysis, Dependency on Exogenous Glycine, and Sensitivity to Folate Depletion. doi:10.1021/acs.jproteome.6b00188

351. Gustafsson Sheppard N, Jarl L, Mahadessian D, et al. The folate-coupled enzyme MTHFD2 is a nuclear protein and promotes cell proliferation. *Sci Rep*. 2015;5(1):15029. doi:10.1038/srep15029

352. Nishimura T, Nakata A, Chen X, et al. Cancer stem-like properties and gefitinib resistance are dependent on purine synthetic metabolism mediated by the mitochondrial enzyme MTHFD2. *Oncogene*. 2019;38(14):2464-2481. doi:10.1038/s41388-018-0589-1

353. Gustafsson R, Jemth AS, Gustafsson NMS, et al. Crystal structure of the emerging cancer target MTHFD2 in complex with a substrate-based inhibitor. *Cancer Res*. 2017;77(4):937-948. doi:10.1158/0008-5472.CAN-16-1476

354. Ben-Sahra I, Hoxhaj G, Ricoult SJH, Asara JM, Manning BD. mTORC1 induces purine synthesis through control of the mitochondrial tetrahydrofolate cycle. *Science (80-)*. 2016;351(6274):728-733. doi:10.1126/science.aad0489

355. Wong KK, Lawrie CH, Green TM. Oncogenic Roles and Inhibitors of DNMT1, DNMT3A, and DNMT3B in Acute Myeloid Leukaemia. *Biomark Insights*. 2019;14:1177271919846454. doi:10.1177/1177271919846454

356. Selcuklu SD, Donoghue MTA, Rehmet K, et al. MicroRNA-9 Inhibition of Cell Proliferation and Identification of Novel miR-9 Targets by Transcriptome Profiling in Breast Cancer Cells. *J Biol Chem*. 2012;287(35):29516-29528. doi:10.1074/jbc.M111.335943

357. Ducker GS, Chen L, Morscher RJ, et al. Reversal of Cytosolic One-Carbon Flux Compensates for Loss of the Mitochondrial Folate Pathway. *Cell Metab*. 2016;23(6):1140-1153. doi:10.1016/j.cmet.2016.04.016

358. Hu J, Locasale JW, Bielas JH, et al. Heterogeneity of tumor-induced gene expression changes in the human metabolic network. *Nat Biotechnol*. 2013;31(6):522-529. doi:10.1038/nbt.2530

359. Mehrmohamadi M, Liu X, Shestov AA, Locasale JW. Characterization of the Usage of the Serine Metabolic Network in Human Cancer. *Cell Rep*. 2014;9(4):1507-1519. doi:10.1016/j.celrep.2014.10.026

360. Graca I, Sousa E, Baptista T, et al. Anti-Tumoral Effect of the Non-Nucleoside DNMT Inhibitor RG108 in Human Prostate Cancer Cells. *Curr Pharm Des*. 2014;20(11):1803-1811. doi:10.2174/13816128113199990516

361. Valente S, Liu Y, Schnekenburger M, et al. Selective non-nucleoside inhibitors of human DNA methyltransferases active in cancer including in cancer stem cells. *J Med Chem*. 2014;57(3):701-713. doi:10.1021/jm4012627

362. Shao Z, Xu P, Xu W, et al. Discovery of novel DNA methyltransferase 3A inhibitors via structure-based virtual screening and biological assays. *Bioorganic Med Chem Lett*. 2017;27(2):342-346. doi:10.1016/j.bmcl.2016.11.023

363. Grandin M, Mathot P, Devailly G, et al. Inhibition of DNA methylation promotes breast tumor sensitivity to netrin-1 interference. *EMBO Mol Med*. 2016;8(8):863-877. doi:10.15252/emmm.201505945

364. Borges S, Döppler H, Perez EA, et al. Pharmacologic reversion of epigenetic silencing of the PRKD1 promoter blocks breast tumor cell invasion and metastasis. *Breast Cancer Res*. 2013;15(2):R66. doi:10.1186/bcr3460

365. Fan H, Lu X, Wang X, et al. Low-dose decitabine-based chemoimmunotherapy for patients with refractory advanced solid tumors: a phase I/II report. *J Immunol Res*. 2014;2014:371087. doi:10.1155/2014/371087

366. Fazio C, Covre A, Cutaia O, et al. Immunomodulatory Properties of DNA Hypomethylating Agents: Selecting the Optimal Epigenetic Partner for Cancer Immunotherapy. *Front Pharmacol*. 2018;9:1443. doi:10.3389/FPHAR.2018.01443

367. Kawai J, Ota M, Ohki H, et al. Structure-Based Design and Synthesis of an Isozyme-Selective MTHFD2 Inhibitor with a Tricyclic Coumarin Scaffold. *ACS Med Chem Lett*. 2019;10(6):893-898. doi:10.1021/acsmedchemlett.9b00069

368. Kawai J, Toki T, Ota M, et al. Discovery of a Potent, Selective, and Orally Available MTHFD2 Inhibitor (DS18561882) with in Vivo Antitumor Activity. *J Med Chem*. 2019. doi:10.1021/acs.jmedchem.9b01113

369. Shafee N, Smith CR, Wei S, et al. Cancer stem cells contribute to cisplatin resistance in Brca1/p53-mediated mouse mammary tumors. *Cancer Res*. 2008;68(9):3243-3250. doi:10.1158/0008-5472.CAN-07-5480

370. Diehn M, Cho RW, Lobo NA, et al. Association of reactive oxygen species levels and radioresistance in cancer stem cells. *Nature*. 2009;458(7239):780-783. doi:10.1038/nature07733

371. Takebe N, Miele L, Harris PJ, et al. Targeting Notch, Hedgehog, and Wnt pathways in cancer stem cells: Clinical update. *Nat Rev Clin Oncol*. 2015;12(8):445-464. doi:10.1038/nrclinonc.2015.61

372. Li X, Wan L, Geng J, Wu CL, Bai X. Aldehyde Dehydrogenase 1A1 Possesses Stem-Like Properties and Predicts Lung Cancer Patient Outcome. *J Thorac Oncol*. 2012;7(8):1235-1245. doi:10.1097/JTO.0b013e318257cc6d

373. Hartomo TB, Van Huyen Pham T, Yamamoto N, et al. Involvement of aldehyde dehydrogenase 1A2 in the regulation of cancer stem cell properties in neuroblastoma. *Int J Oncol*. 2015;46(3):1089-1098. doi:10.3892/ijo.2014.2801

374. Moreb JS, Ucar D, Han S, et al. The enzymatic activity of human aldehyde dehydrogenases 1A2 and 2 (ALDH1A2 and ALDH2) is detected by Aldefluor, inhibited by diethylaminobenzaldehyde and has significant effects on cell proliferation and drug resistance. *Chem Biol Interact*. 2012;195(1):52-60. doi:10.1016/j.cbi.2011.10.007

375. Van Den Hoogen C, Van Der Horst G, Cheung H, Buijs JT, Pelger RCM, Van Der Pluijm G. The aldehyde dehydrogenase enzyme 7A1 is functionally involved in prostate cancer bone metastasis. *Clin Exp Metastasis*. 2011;28(7):615-625. doi:10.1007/s10585-011-9395-7

376. Canino C, Luo YY, Marcato P, Blandino G, Pass HI, Cioce M. A STAT3-

NFkB/DDIT3/CEBPβ axis modulates ALDH1A3 expression in chemoresistant cell subpopulations. *Oncotarget*. 2015;6(14):12637-12653. doi:10.18632/oncotarget.3703

377. Khoury T, Ademuyiwa FO, Chandraseekhar R, et al. Aldehyde dehydrogenase 1A1 expression in breast cancer is associated with stage, triple negativity, and outcome to neoadjuvant chemotherapy. *Mod Pathol*. 2012;25(3):388-397. doi:10.1038/modpathol.2011.172

378. Wang K, Chen X, Zhan Y, et al. Increased expression of ALDH1A1 protein is associated with poor prognosis in clear cell renal cell carcinoma. *Med Oncol*. 2013;30(2):574. doi:10.1007/s12032-013-0574-z

379. Yang L, Ren Y, Yu X, et al. ALDH1A1 defines invasive cancer stem-like cells and predicts poor prognosis in patients with esophageal squamous cell carcinoma. *Mod Pathol*. 2014;27(5):775-783. doi:10.1038/modpathol.2013.189

380. Qian X, Wagner S, Ma C, et al. Prognostic significance of ALDH1A1-positive cancer stem cells in patients with locally advanced, metastasized head and neck squamous cell carcinoma. *J Cancer Res Clin Oncol*. 2014;140(7):1151-1158. doi:10.1007/s00432-014-1685-4

381. Yue L, Huang ZM, Fong S, et al. Targeting ALDH1 to decrease tumorigenicity, growth and metastasis of human melanoma. *Melanoma Res*. 2015;25(2):138-148. doi:10.1097/CMR.0000000000000144

382. Mahmoud MIE, Potter JJ, Colvin OM, Hilton J, Mezey E. Effect of 4-(Diethylamino)benzaldehyde on Ethanol Metabolism in Mice. *Alcohol Clin Exp Res*. 1993;17(6):1223-1227. doi:10.1111/j.1530-0277.1993.tb05233.x

383. Han D, Wu G, Chang C, et al. Disulfiram inhibits TGF-β-induced epithelial-mesenchymal transition and stem-like features in breast cancer via ERK/NF-κB/Snail pathway. *Oncotarget*. 2015;6(38):40907-40919. doi:10.18632/oncotarget.5723

384. Liu P, Wang Z, Brown S, et al. Liposome encapsulated Disulfiram inhibits NFκB pathway and targets breast cancer stem cells in vitro and in vivo. *Oncotarget*. 2014;5(17):7471-7485. doi:10.18632/oncotarget.2166

385. Zeng S, Kapur A, Patankar MS, Xiong MP. Formulation, characterization, and antitumor properties of trans- and cis-citral in the 4T1 breast cancer xenograft mouse model. *Pharm Res*. 2015;32(8):2548-2558. doi:10.1007/s11095-015-1643-0

386. Murphy JP, Everley RA, Coloff JL, Gygi SP. Combining amine metabolomics and quantitative proteomics of cancer cells using derivatization with isobaric tags. *Anal Chem*. 2014;86(7):3585-3593. doi:10.1021/ac500153a

387. Bailly C. Targets and pathways involved in the antitumor activity of citral and its

stereo-isomers. *Eur J Pharmacol*. 2020;871:172945. doi:10.1016/j.ejphar.2020.172945

388. Chaouki W, Leger DY, Liagre B, Beneytout JL, Hmamouchi M. Citral inhibits cell proliferation and induces apoptosis and cell cycle arrest in MCF-7 cells. *Fundam Clin Pharmacol*. 2009;23(5):549-556. doi:10.1111/j.1472-8206.2009.00738.x

389. Ueno T, Masuda H, Ho CT. Formation mechanism of p-methylacetophenone from citral via a tert-alkoxy radical intermediate. *J Agric Food Chem*. 2004;52(18):5677-5684. doi:10.1021/jf035517j

390. Fang X, Cai Y, Liu J, et al. Twist2 contributes to breast cancer progression by promoting an epithelial-mesenchymal transition and cancer stem-like cell self-renewal. *Oncogene*. 2011;30(47):4707-4720. doi:10.1038/onc.2011.181

391. Akrap N, Andersson D, Bom E, Gregersson P, Ståhlberg A, Landberg G. Identification of Distinct Breast Cancer Stem Cell Populations Based on Single-Cell Analyses of Functionally Enriched Stem and Progenitor Pools. *Stem Cell Reports*. 2016;6(1):121-136. doi:10.1016/j.stemcr.2015.12.006

392. Triscott J, Lee C, Hu K, et al. Disulfiram, a drug widely used to control alcoholism, suppresses self-renewal of glioblastoma and overrides resistance to temozolomide. *Oncotarget*. 2012;3(10):1112-1123. doi:10.18632/oncotarget.604

393. Liu P, Brown S, Goktug T, et al. Cytotoxic effect of disulfiram/copper on human glioblastoma cell lines and ALDH-positive cancer-stem-like cells. *Br J Cancer*. 2012;107(9):1488-1497. doi:10.1038/bjc.2012.442

394. Ye W, Chang HL, Wang LS, Huang YW, Shu S, Sugimoto Y, Dowd MK, Wan PJ LY. Induction of apoptosis by (-)-gossypol-enriched cottonseed oil in human breast cancer cells. *Int J Mol Med*. 2010;26(1):113-119. doi:10.3892/ijmm_00000442

395. Van Poznak C, Seidman AD, Reidenberg MM, et al. Oral gossypol in the treatment of patients with refractory metastatic breast cancer: a phase I/II clinical trial. *Breast Cancer Res Treat*. 2001;66(3):239-248. doi:10.1023/a:1010686204736

396. Patel PB, Thakkar VR, Patel JS. Cellular effect of curcumin and citral combination on breast cancer cells: Induction of apoptosis and cell cycle arrest. *J Breast Cancer*. 2015;18(3):225-234. doi:10.4048/jbc.2015.18.3.225

397. Greish K. Enhanced permeability and retention (EPR) effect for anticancer nanomedicine drug targeting. *Methods Mol Biol*. 2010;624:25-37. doi:10.1007/978-1-60761-609-2_3

398. Park SY, Lee HE, Li H, Shipitsin M, Gelman R, Polyak K. Heterogeneity for stem cell-related markers according to tumor subtype and histologic stage in breast

cancer. *Clin Cancer Res*. 2010;16(3):876-887. doi:10.1158/1078-0432.CCR-09-1532

399. Ricardo S, Vieira AF, Gerhard R, et al. Breast cancer stem cell markers CD44, CD24 and ALDH1: Expression distribution within intrinsic molecular subtype. *J Clin Pathol*. 2011;64(11):937-944. doi:10.1136/jcp.2011.090456

400. Dinavahi SS, Bazewicz CG, Gowda R, Robertson GP. Aldehyde Dehydrogenase Inhibitors for Cancer Therapeutics. *Trends Pharmacol Sci*. 2019;40(10):774-789. doi:10.1016/j.tips.2019.08.002

401. Majumder M, Xin X, Liu L, et al. COX-2 Induces Breast Cancer Stem Cells via EP4/PI3K/AKT/NOTCH/WNT Axis. *Stem Cells*. 2016;34(9):2290-2305. doi:10.1002/stem.2426

402. Andreasen PA, Egelund R, Petersen HH. The plasminogen activation system in tumor growth, invasion, and metastasis. *Cell Mol Life Sci*. 2000;57(1):25-40. doi:10.1007/s000180050497

403. Neman J, Termini J, Wilczynski S, et al. Human breast cancer metastases to the brain display GABAergic properties in the neural niche. *Proc Natl Acad Sci U S A*. 2014;111(3):984-989. doi:10.1073/pnas.1322098111

404. Aghili M, Zare M, Mousavi N, et al. Efficacy of gabapentin for the prevention of paclitaxel induced peripheral neuropathy: A randomized placebo controlled clinical trial. *Breast J*. 2019;25(2):226-231. doi:10.1111/tbj.13196

405. Corcoran CC, Grady CR, Pisitkun T, Parulekar J, Knepper MA. From 20th century metabolic wall charts to 21st century systems biology: Database of mammalian metabolic enzymes. *Am J Physiol - Ren Physiol*. 2017;312(3):F533-F542. doi:10.1152/ajprenal.00601.2016

406. Yuan M, Breitkopf SB, Yang X, Asara JM. A positive/negative ion-switching, targeted mass spectrometry-based metabolomics platform for bodily fluids, cells, and fresh and fixed tissue. *Nat Protoc*. 2012;7(5):872-881. doi:10.1038/nprot.2012.024

407. Warrack BM, Hnatyshyn S, Ott KH, et al. Normalization strategies for metabonomic analysis of urine samples. *J Chromatogr B Anal Technol Biomed Life Sci*. 2009;877(5-6):547-552. doi:10.1016/j.jchromb.2009.01.007

408. Cheng GZ, Chan J, Wang Q, Zhang W, Sun CD, Wang LH. Twist transcriptionally up-regulates AKT2 in breast cancer cells leading to increased migration, invasion, and resistance to paclitaxel. *Cancer Res*. 2007;67(5):1979-1987. doi:10.1158/0008-5472.CAN-06-1479

409. Vesuna F, Lisok A, Kimble B, et al. Twist contributes to hormone resistance in breast cancer by downregulating estrogen receptor-α. *Oncogene*.

2012;31(27):3223-3234. doi:10.1038/onc.2011.483

410. Bowery NG, Smart TG. GABA and glycine as neurotransmitters: A brief history. *Br J Pharmacol*. 2006;147(SUPPL. 1):S109. doi:10.1038/sj.bjp.0706443

411. Kennecke H, Yerushalmi R, Woods R, et al. Metastatic behavior of breast cancer subtypes. *J Clin Oncol*. 2010;28(20):3271-3277. doi:10.1200/JCO.2009.25.9820

412. Wang Y, Klijn JGM, Zhang Y, et al. Gene-expression profiles to predict distant metastasis of lymph-node-negative primary breast cancer. *Lancet (London, England)*. 365(9460):671-679. doi:10.1016/S0140-6736(05)17947-1

413. Bos PD, Zhang XHF, Nadal C, et al. Genes that mediate breast cancer metastasis to the brain. *Nature*. 2009;459(7249):1005-1009. doi:10.1038/nature08021

414. Ginestier C, Wicinski J, Cervera N, et al. Retinoid signaling regulates breast cancer stem cell differentiation. *Cell Cycle*. 2009;8(20):3297-3302. doi:10.4161/cc.8.20.9761

415. Llufrio EM, Wang L, Naser FJ, Patti GJ. Sorting cells alters their redox state and cellular metabolome. *Redox Biol*. 2018;16:381-387. doi:10.1016/j.redox.2018.03.004

416. Binek A, Rojo D, Godzien J, et al. Flow Cytometry Has a Significant Impact on the Cellular Metabolome. *J Proteome Res*. 2019;18(1):169-181. doi:10.1021/acs.jproteome.8b00472

417. Vogt K. Diversity in GABAergic Signaling. In: *Advances in Pharmacology*. Vol 73. Academic Press Inc.; 2015:203-222. doi:10.1016/bs.apha.2014.11.009

418. Brzozowska A, Burdan F, Duma D, Solski J, Mazurkiewicz M. γ-amino butyric acid (GABA) level as an overall survival risk factor in breast cancer. *Ann Agric Environ Med*. 2017;24(3):435-439. doi:10.26444/aaem/75891

419. Sizemore GM, Sizemore ST, Seachrist DD, Keri RA. GABA(A) receptor Pi (GABRP) stimulates basal-like breast cancer cell migration through activation of extracellular-regulated kinase 1/2 (ERK1/2). *J Biol Chem*. 2014;289(35):24102-24113. doi:10.1074/jbc.M114.593582

420. Chen X, Cao Q, Liao R, Wu X, Huang J, Dong C. Loss of ABAT-Mediated GABAergic System Promotes Basal-Like Breast Cancer Progression by Activating Ca 2+-NFAT1 Axis. *Theranostics*. 2019;9(1). doi:10.7150/thno.29407

421. Gumireddy K, Li A, Kossenkov A V., et al. The mRNA-edited form of GABRA3 suppresses GABRA3-mediated Akt activation and breast cancer metastasis. *Nat Commun*. 2016;7:10715. doi:10.1038/ncomms10715

422. El-Mabhouh AA, Nation PN, Kaddoura A, Mercer JR. Unexpected preferential

brain metastases with a human breast tumor cell line MDA-MB-231 in BALB/c nude mice. *Vet Pathol*. 2008;45(6):941-944. doi:10.1354/vp.45-6-941

423. Sayyad MR, Puchalapalli M, Vergara NG, et al. Syndecan-1 facilitates breast cancer metastasis to the brain. *Breast Cancer Res Treat*. 2019;178(1):35-49. doi:10.1007/s10549-019-05347-0

424. Kijewska M, Viski C, Turrell F, et al. Using an in-vivo syngeneic spontaneous metastasis model identifies ID2 as a promoter of breast cancer colonisation in the brain. *Breast Cancer Res*. 2019;21(1):1-14. doi:10.1186/s13058-018-1093-9

425. Gong X, Hou Z, Endsley MP, et al. Interaction of tumor cells and astrocytes promotes breast cancer brain metastases through TGF-β2/ANGPTL4 axes. *npj Precis Oncol*. 2019;3(1). doi:10.1038/s41698-019-0094-1

426. Yoneda T, Williams PJ, Hiraga T, Niewolna M, Nishimura R. A bone-seeking clone exhibits different biological properties from the MDA-MB-231 parental human breast cancer cells and a brain-seeking clone in vivo and in vitro. *J Bone Miner Res*. 2001;16(8):1486-1495. doi:10.1359/jbmr.2001.16.8.1486

427. Delaney LJ, Ciraku L, Oeffinger BE, et al. Breast Cancer Brain Metastasis Response to Radiation After Microbubble Oxygen Delivery in a Murine Model. *J Ultrasound Med*. 2019;38(12):3221-3228. doi:10.1002/jum.15031

428. Masiero M, Li D, Whiteman P, et al. Development of therapeutic anti-Jagged1 antibodies for cancer therapy. *Mol Cancer Ther*. 2019;18(11):2030-2042. doi:10.1158/1535-7163.MCT-18-1176

429. Ghoreishi Z, Keshavarz S, Asghari Jafarabadi M, Fathifar Z, Goodman KA, Esfahani A. Risk factors for paclitaxel-induced peripheral neuropathy in patients with breast cancer 11 Medical and Health Sciences 1112 Oncology and Carcinogenesis. *BMC Cancer*. 2018;18(1):958. doi:10.1186/s12885-018-4869-5

430. Mustafa Ali M, Moeller M, Rybicki L, Moore HCF. Long-term peripheral neuropathy symptoms in breast cancer survivors. *Breast Cancer Res Treat*. 2017;166(2):519-526. doi:10.1007/s10549-017-4437-8

431. Xiao W, Boroujerdi A, Bennett GJ, Luo ZD. Chemotherapy-evoked painful peripheral neuropathy: Analgesic effects of gabapentin and effects on expression of the alpha-2-delta type-1 calcium channel subunit. *Neuroscience*. 2007;144(2):714-720. doi:10.1016/j.neuroscience.2006.09.044

432. Tsavaris N, Kopterides P, Kosmas C, et al. Gabapentin monotherapy for the treatment of chemotherapy-induced neuropathic pain: A pilot study. *Pain Med*. 2008;9(8):1209-1216. doi:10.1111/j.1526-4637.2007.00325.x

433. Arai YCP, Matsubara T, Shimo K, et al. Low-dose gabapentin as useful adjuvant to opioids for neuropathic cancer pain when combined with low-dose imipramine.

J Anesth. 2010;24(3):407-410. doi:10.1007/s00540-010-0913-6

434. Ross JR, Goller K, Hardy J, et al. Gabapentin is effective in the treatment of cancer-related neuropathic pain: A prospective, open-label study. *J Palliat Med*. 2005;8(6):1118-1126. doi:10.1089/jpm.2005.8.1118

435. Sills GJ. The mechanisms of action of gabapentin and pregabalin. *Curr Opin Pharmacol*. 2006;6(1 SPEC. ISS.):108-113. doi:10.1016/j.coph.2005.11.003

436. Klajic J, Busato F, Edvardsen H, et al. Dnamethylation status of key cell-cycle regulators such as CDKNA2/P16 and CCNA1 correlates with treatment response to doxorubicin and 5-fluorouracil in locally advanced breast tumors. *Clin Cancer Res*. 2014;20(24):6357-6366. doi:10.1158/1078-0432.CCR-14-0297

437. Agrawal A, Murphy RF, Agrawal DK. DNA methylation in breast and colorectal cancers. *Mod Pathol*. 2007;20(7):711-721. doi:10.1038/modpathol.3800822

438. Sánchez-Carbayo M. Hypermethylation in bladder cancer: biological pathways and translational applications. *Tumor Biol*. 2012;33(2):347-361. doi:10.1007/s13277-011-0310-2

439. Dawson MA, Kouzarides T. Cancer epigenetics: From mechanism to therapy. *Cell*. 2012;150(1):12-27. doi:10.1016/j.cell.2012.06.013

440. Ordway JM, Budiman MA, Korshunova Y, et al. Identification of Novel High-Frequency DNA Methylation Changes in Breast Cancer. Jin D-Y, ed. *PLoS One*. 2007;2(12):e1314. doi:10.1371/journal.pone.0001314

441. Yu J, Zayas J, Qin B, Wang L. Targeting DNA methylation for treating triple-negative breast cancer. *Pharmacogenomics*. 2019;20(16):1151-1157. doi:10.2217/pgs-2019-0078

442. Heyn H, Esteller M. DNA methylation profiling in the clinic: applications and challenges. *Nat Rev Genet*. 2012;13(10):679-692. doi:10.1038/nrg3270

443. Qin T, Castoro R, El Ahdab S, et al. Mechanisms of Resistance to Decitabine in the Myelodysplastic Syndrome. Batra SK, ed. *PLoS One*. 2011;6(8):e23372. doi:10.1371/journal.pone.0023372

444. Tsesmetzis N, Paulin C, Rudd S, et al. Nucleobase and Nucleoside Analogues: Resistance and Re-Sensitisation at the Level of Pharmacokinetics, Pharmacodynamics and Metabolism. *Cancers (Basel)*. 2018;10(7):240. doi:10.3390/cancers10070240

445. Soriano AO, Yang H, Faderl S, et al. Safety and clinical activity of the combination of 5-azacytidine, valproic acid, and all-trans retinoic acid in acute myeloid leukemia and myelodysplastic syndrome. *Blood*. 2007;110(7):2302-2308. doi:10.1182/blood-2007-03-078576

446. Blum W, Klisovic RB, Hackanson B, et al. Phase I Study of Decitabine Alone or in Combination With Valproic Acid in Acute Myeloid Leukemia. *J Clin Oncol*. 2007;25(25):3884-3891. doi:10.1200/JCO.2006.09.4169

447. Li B, Gan A, Chen X, et al. Diagnostic Performance of DNA Hypermethylation Markers in Peripheral Blood for the Detection of Colorectal Cancer: A Meta-Analysis and Systematic Review. Green J, ed. *PLoS One*. 2016;11(5):e0155095. doi:10.1371/journal.pone.0155095

448. Nebbioso A, Carafa V, Benedetti R, Altucci L. Trials with "epigenetic" drugs: An update. *Mol Oncol*. 2012;6(6):657-682. doi:10.1016/j.molonc.2012.09.004

449. Gros C, Fleury L, Nahoum V, et al. New insights on the mechanism of quinoline-based DNA methyltransferase inhibitors. *J Biol Chem*. 2015;290(10):6293-6302. doi:10.1074/jbc.M114.594671

450. Bruzzese F, Rocco M, Castelli S, Di Gennaro E, Desideri A, Budillon A. Synergistic antitumor effect between vorinostat and topotecan in small cell lung cancer cells is mediated by generation of reactive oxygen species and DNA damage-induced apoptosis. *Mol Cancer Ther*. 2009;8(11):3075-3087. doi:10.1158/1535-7163.MCT-09-0254

451. Srivastava P, Paluch BE, Matsuzaki J, et al. Induction of cancer testis antigen expression in circulating acute myeloid leukemia blasts following hypomethylating agent monotherapy. *Oncotarget*. 2016;7(11):12840-12856. doi:10.18632/oncotarget.7326

452. Krishnadas DK, Bao L, Bai F, Chencheri SC, Lucas K. Decitabine facilitates immune recognition of sarcoma cells by upregulating CT antigens, MHC molecules, and ICAM-1. *Tumor Biol*. 2014;35(6):5753-5762. doi:10.1007/s13277-014-1764-9

453. Nie J, Wang C, Liu Y, et al. Addition of Low-Dose Decitabine to Anti–PD-1 Antibody Camrelizumab in Relapsed/Refractory Classical Hodgkin Lymphoma. *J Clin Oncol*. 2019;37(17):1479-1489. doi:10.1200/JCO.18.02151

454. Tibbetts AS, Appling DR. Compartmentalization of Mammalian Folate-Mediated One-Carbon Metabolism. *Annu Rev Nutr*. 2010;30(1):57-81. doi:10.1146/annurev.nutr.012809.104810

455. Christensen KE, MacKenzie RE. Chapter 14 Mitochondrial Methylenetetrahydrofolate Dehydrogenase, Methenyltetrahydrofolate Cyclohydrolase, and Formyltetrahydrofolate Synthetases. *Vitam Horm*. 2008;79:393-410. doi:10.1016/S0083-6729(08)00414-7

456. Villa E, Ali ES, Sahu U, Ben-Sahra I. Cancer cells tune the signaling pathways to empower de novo synthesis of nucleotides. *Cancers (Basel)*. 2019;11(5). doi:10.3390/cancers11050688

457. Zhang WC, Ng SC, Yang H, et al. Glycine decarboxylase activity drives non-small cell lung cancer tumor-initiating cells and tumorigenesis. *Cell*. 2012;148(1-2):259-272. doi:10.1016/j.cell.2011.11.050

458. Lane AN, Fan TWM. Regulation of mammalian nucleotide metabolism and biosynthesis. *Nucleic Acids Res*. 2015;43(4):2466-2485. doi:10.1093/nar/gkv047

459. Helleday T. Targeting MTHFD2 using first-in-class inhibitors kills haematological and solid cancer through thymineless-induced replication stress. In: *Virtual AACR Annual Meeting I*. American Association for Cancer Research; 2020.

460. Fu TF, Schirch V, Rife JP. The role of serine hydroxymethyltransferase isozymes in one-carbon metabolism in MCF-7 cells as determined by 13C NMR. *Arch Biochem Biophys*. 2001;393(1):42-50. doi:10.1006/abbi.2001.2471

461. Vazquez A, Tedeschi PM, Bertino JR. Overexpression of the mitochondrial folate and glycine- Serine pathway: A new determinant of methotrexate selectivity in tumors. *Cancer Res*. 2013;73(2):478-482. doi:10.1158/0008-5472.CAN-12-3709

462. Pikman Y, Puissant A, Alexe G, et al. Targeting MTHFD2 in acute myeloid leukemia. *J Exp Med*. 2016;213(7):1285-1306. doi:10.1084/jem.20151574

463. Fan J, Ye J, Kamphorst JJ, Shlomi T, Thompson CB, Rabinowitz JD. Quantitative flux analysis reveals folate-dependent NADPH production. *Nature*. 2014;510(7504):298-302. doi:10.1038/nature13236

464. Chen L, Zhang Z, Hoshino A, et al. NADPH production by the oxidative pentose-phosphate pathway supports folate metabolism. *Nat Metab*. 2019;1(3):404-415. doi:10.1038/s42255-019-0043-x

465. Ju H-Q, Lu Y-X, Chen D-L, et al. Modulation of Redox Homeostasis by Inhibition of MTHFD2 in Colorectal Cancer: Mechanisms and Therapeutic Implications. *J Natl Cancer Inst*. 2019;111(6):584-596. doi:10.1093/jnci/djy160

466. Shin M, Momb J, Appling DR. Human mitochondrial MTHFD2 is a dual redox cofactor-specific methylenetetrahydrofolate dehydrogenase/methenyltetrahydrofolate cyclohydrolase. *Cancer Metab*. 2017;5(1):11. doi:10.1186/s40170-017-0173-0

467. Meiser J, Tumanov S, Maddocks O, et al. Serine one-carbon catabolism with formate overflow. *Sci Adv*. 2016;2(10). doi:10.1126/sciadv.1601273

468. Koufaris C, Nilsson R. Protein interaction and functional data indicate MTHFD2 involvement in RNA processing and translation. *Cancer Metab*. 2018;6(1):12. doi:10.1186/s40170-018-0185-4

469. Zhu Z, Leung GKK. More Than a Metabolic Enzyme: MTHFD2 as a Novel Target for Anticancer Therapy? *Front Oncol*. 2020;10:658. doi:10.3389/fonc.2020.00658

470. Zeng X, Miura T, Luo Y, et al. Properties of Pluripotent Human Embryonic Stem Cells BG01 and BG02. *Stem Cells*. 2004;22(3):292-312. doi:10.1634/stemcells.22-3-292

471. Di Pietro E, Sirois J, Tremblay ML, MacKenzie RE. Mitochondrial NAD-Dependent Methylenetetrahydrofolate Dehydrogenase-Methenyltetrahydrofolate Cyclohydrolase Is Essential for Embryonic Development. *Mol Cell Biol*. 2002;22(12):4158-4166. doi:10.1128/mcb.22.12.4158-4166.2002

472. Nilsson R, Nicolaidou V, Koufaris C. Mitochondrial MTHFD isozymes display distinct expression, regulation, and association with cancer. *Gene*. 2019;716. doi:10.1016/j.gene.2019.144032

473. Bertucci F, Finetti P, Birnbaum D. Basal Breast Cancer: A Complex and Deadly Molecular Subtype. *Curr Mol Med*. 2011;12(1):96-110. doi:10.2174/156652412798376134

474. Rebollido-Rios R, Venton G, Sánchez-Redondo S, et al. Dual disruption of aldehyde dehydrogenases 1 and 3 promotes functional changes in the glutathione redox system and enhances chemosensitivity in nonsmall cell lung cancer. *Oncogene*. 2020;39(13):2756-2771. doi:10.1038/s41388-020-1184-9

475. Terenzi A, Pirker C, Keppler BK, Berger W. Anticancer metal drugs and immunogenic cell death. *J Inorg Biochem*. 2016;165:71-79. doi:10.1016/j.jinorgbio.2016.06.021

476. Galvin KC, Dyck L, Marshall NA, et al. Blocking retinoic acid receptor-α enhances the efficacy of a dendritic cell vaccine against tumours by suppressing the induction of regulatory T cells. *Cancer Immunol Immunother*. 2013;62(7):1273-1282. doi:10.1007/s00262-013-1432-8

477. Bazewicz CG, Dinavahi SS, Schell TD, Robertson GP. Aldehyde dehydrogenase in regulatory T-cell development, immunity and cancer. *Immunology*. 2019;156(1):47-55. doi:10.1111/imm.13016

478. Dinavahi SS, Gowda R, Bazewicz CG, et al. Design, synthesis characterization and biological evaluation of novel multi-isoform ALDH inhibitors as potential anticancer agents. *Eur J Med Chem*. 2020;187. doi:10.1016/j.ejmech.2019.111962

479. Yang SM, Yasgar A, Miller B, et al. Discovery of NCT-501, a Potent and Selective Theophylline-Based Inhibitor of Aldehyde Dehydrogenase 1A1 (ALDH1A1). *J Med Chem*. 2015;58(15):5967-5978. doi:10.1021/acs.jmedchem.5b00577

480. Kulsum S, Sudheendra HV, Pandian R, et al. Cancer stem cell mediated acquired chemoresistance in head and neck cancer can be abrogated by aldehyde dehydrogenase 1 A1 inhibition. *Mol Carcinog*. 2017;56(2):694-711. doi:10.1002/mc.22526

481. Morgan CA, Hurley TD. Characterization of two distinct structural classes of selective aldehyde dehydrogenase 1A1 inhibitors. *J Med Chem*. 2015;58(4):1964-1975. doi:10.1021/jm501900s

482. Zhou L, Sheng D, Wang D, et al. Identification of cancer-type specific expression patterns for active aldehyde dehydrogenase (ALDH) isoforms in ALDEFLUOR assay. *Cell Biol Toxicol*. 2019;35(2):161-177. doi:10.1007/s10565-018-9444-y

483. Muzio G, Maggiora M, Paiuzzi E, Oraldi M, Canuto RA. Aldehyde dehydrogenases and cell proliferation. *Free Radic Biol Med*. 2012;52(4):735-746. doi:10.1016/j.freeradbiomed.2011.11.033

484. Bista R, Lee DW, Pepper OB, Azorsa DO, Arceci RJ, Aleem E. Disulfiram overcomes bortezomib and cytarabine resistance in Down-syndrome-associated acute myeloid leukemia cells. *J Exp Clin Cancer Res*. 2017;36(1):1-14. doi:10.1186/s13046-017-0493-5

485. Cortes-Dericks L, Froment L, Boesch R, Schmid RA, Karoubi G. Cisplatin-resistant cells in malignant pleural mesothelioma cell lines show ALDHhighCD44+ phenotype and sphere-forming capacity. *BMC Cancer*. 2014;14(1):1-13. doi:10.1186/1471-2407-14-304

486. Kimble-Hill AC, Parajuli B, Chen CH, Mochly-Rosen D, Hurley TD. Development of selective inhibitors for aldehyde dehydrogenases based on substituted indole-2,3-diones. *J Med Chem*. 2014;57(3):714-722. doi:10.1021/jm401377v

487. Metwally K, Pratsinis H, Kletsas D, et al. Novel quinazolinone-based 2,4-thiazolidinedione-3-acetic acid derivatives as potent aldose reductase inhibitors. *Future Med Chem*. 2017;9(18):2147-2166. doi:10.4155/fmc-2017-0149

488. Crespo I, Giménez-Dejoz J, Porté S, et al. Design, synthesis, structure-activity relationships and X-ray structural studies of novel 1-oxopyrimido[4,5-c]quinoline-2-acetic acid derivatives as selective and potent inhibitors of human aldose reductase. *Eur J Med Chem*. 2018;152:160-174. doi:10.1016/j.ejmech.2018.04.015

489. Jiménez R, Pequerul R, Amor A, et al. Inhibitors of aldehyde dehydrogenases of the 1A subfamily as putative anticancer agents: Kinetic characterization and effect on human cancer cells. *Chem Biol Interact*. 2019;306:123-130. doi:10.1016/j.cbi.2019.04.004

490. Huddle BC, Grimley E, Buchman CD, et al. Structure-Based Optimization of a Novel Class of Aldehyde Dehydrogenase 1A (ALDH1A) Subfamily-Selective Inhibitors as Potential Adjuncts to Ovarian Cancer Chemotherapy. *J Med Chem*. 2018;61(19):8754-8773. doi:10.1021/acs.jmedchem.8b00930

491. Buchman CD, Mahalingan KK, Hurley TD. Discovery of a series of aromatic lactones as ALDH1/2-directed inhibitors. *Chem Biol Interact*. 2015;234:38-44.

doi:10.1016/j.cbi.2014.12.038

492. Moretti A, Li J, Donini S, Sobol RW, Rizzi M, Garavaglia S. Crystal structure of human aldehyde dehydrogenase 1A3 complexed with NAD+ and retinoic acid. *Sci Rep*. 2016;6(1):1-12. doi:10.1038/srep35710

493. Muramoto GG, Russell JL, Safi R, et al. Inhibition of aldehyde dehydrogenase expands hematopoietic stem cells with radioprotective capacity. *Stem Cells*. 2010;28(3):523-534. doi:10.1002/stem.299

494. Chute JP, Muramoto GG, Whitesides J, et al. Inhibition of aldehyde dehydrogenase and retinoid signaling induces the expansion of human hematopoietic stem cells. *Proc Natl Acad Sci U S A*. 2006;103(31):11707-11712. doi:10.1073/pnas.0603806103

495. Dinavahi SS, Gowda R, Gowda K, et al. Development of a Novel Multi-Isoform ALDH Inhibitor Effective as an Antimelanoma Agent. *Mol Cancer Ther*. 2020;19(2):447-459. doi:10.1158/1535-7163.MCT-19-0360

496. Yang SM, Martinez NJ, Yasgar A, et al. Discovery of Orally Bioavailable, Quinoline-Based Aldehyde Dehydrogenase 1A1 (ALDH1A1) Inhibitors with Potent Cellular Activity. *J Med Chem*. 2018;61(11):4883-4903. doi:10.1021/acs.jmedchem.8b00270

497. Pérez-Alea M, Mcgrail K, Sánchez-Redondo S, et al. ALDH1A3 is epigenetically regulated during melanocyte transformation and is a target for melanoma treatment. *Oncogene*. 2017;36(41):5695-5708. doi:10.1038/onc.2017.160

498. Liang D, Fan Y, Yang Z, et al. Discovery of coumarin-based selective aldehyde dehydrogenase 1A1 inhibitors with glucose metabolism improving activity. *Eur J Med Chem*. 2020;187:111923. doi:10.1016/j.ejmech.2019.111923

499. Sarvi S, Crispin R, Lu Y, et al. ALDH1 Bio-activates Nifuroxazide to Eradicate ALDH High Melanoma-Initiating Cells In Brief. *Cell Chem Biol*. 2018;25. doi:10.1016/j.chembiol.2018.09.005

500. Yamashita D, Minata M, Ibrahim AN, et al. Identification of ALDH1A3 as a viable therapeutic target in breast cancer metastasis-initiating cells. *Mol Cancer Ther*. March 2020:molcanther.0461.2019. doi:10.1158/1535-7163.mct-19-0461

501. Coyle, Krysta M.; Dean, Cheryl A.; Giacomantonio, Carman A.; Helyer, L.; Marcato P. DNA methylation is a predictive biomarker for all-trans retinoic acid therapy in triple-negative breast cancer. *under Rev Clin Can Res*. 2018.

502. Zhou GB, Zhang J, Wang ZY, Chen SJ, Chen Z. Treatment of acute promyelocytic leukaemia with all-trans retinoic acid and arsenic trioxide: A paradigm of synergistic molecular targeting therapy. *Philos Trans R Soc B Biol Sci*. 2007;362(1482):959-971. doi:10.1098/rstb.2007.2026

503. Moreb JS, Ucar-Bilyeu DA, Khan A. Use of retinoic acid/aldehyde dehydrogenase pathway as potential targeted therapy against cancer stem cells. *Cancer Chemother Pharmacol*. 2017;79(2):295-301. doi:10.1007/s00280-016-3213-5

504. Sutton LM, Warmuth MA, Petros WP, Winer EP. Pharmacokinetics and clinical impact of all-trans retinoic acid in metastatic breast cancer: A phase II trial. *Cancer Chemother Pharmacol*. 1997;40(4):335-341. doi:10.1007/s002800050666

505. Bryan M, Pulte ED, Toomey KC, et al. A pilot phase II trial of all-trans retinoic acid (Vesanoid) and paclitaxel (Taxol) in patients with recurrent or metastatic breast cancer. *Invest New Drugs*. 2011;29(6):1482-1487. doi:10.1007/s10637-010-9478-3

506. Yung WK, Kyritsis AP, Gleason MJ, Levin VA. Treatment of recurrent malignant gliomas with high-dose 13-cis-retinoic acid. *Clin Cancer Res*. 1996;2(12):1931-1935.

507. Michael A, Hill M, Maraveyas A, Dalgleish A, Lofts F. 13-cis-Retinoic Acid in Combination with Gemcitabine in the Treatment of Locally Advanced and Metastatic Pancreatic Cancer - Report of a Pilot Phase II Study. *Clin Oncol*. 2007;19(2):150-153. doi:10.1016/j.clon.2006.11.008

508. Vaishampayan U, Flaherty L, Du W HM. Phase II evaluation of paclitaxel, α-interferon, and cis-retinoic acid in advanced renal cell carcinoma. Cancer. doi:10.1002/1097-0142(20010801)92:3<519::aid-cncr1350>3.0.co;2-#

509. Enzinger PC, Ilson DH, Saltz LB, Martin LK, Kelsen DP. Phase II clinical trial of 13-cis-retinoic acid and interferon-α-2a in patients with advanced esophageal carcinoma. *Cancer*. 1999;85(6):1213-1217. doi:10.1002/(SICI)1097-0142(19990315)85:6<1213::AID-CNCR1>3.0.CO;2-N

510. Hallum A V., Alberts DS, Lippman SM, et al. Phase II study of 13-cis-retinoic acid plus interferon-α2a in heavily pretreated squamous carcinoma of the cervix. *Gynecol Oncol*. 1995;56(3):382-386. doi:10.1006/gyno.1995.1067

511. Davies KJ. The Complex Interaction of Matrix Metalloproteinases in the Migration of Cancer Cells through Breast Tissue Stroma. *Int J Breast Cancer*. 2014;2014. doi:10.1155/2014/839094

512. Duffy MJ, Maguire TM, Hill A, McDermott E, O'Higgins N. Metalloproteinases: Role in breast carcinogenesis, invasion and metastasis. *Breast Cancer Res*. 2000;2(4):252-257. doi:10.1186/bcr65

513. Köhrmann A, Kammerer U, Kapp M, Dietl J, Anacker J. Expression of matrix metalloproteinases (MMPs) in primary human breast cancer and breast cancer cell lines: New findings and review of the literature. *BMC Cancer*. 2009;9(1):188. doi:10.1186/1471-2407-9-188

514. Reimers N, Zafrakas K, Assmann V, et al. Expression of extracellular matrix metalloproteases inducer on micrometastatic and primary mammary carcinoma cells. *Clin Cancer Res*. 2004;10(10):3422-3428. doi:10.1158/1078-0432.CCR-03-0610

515. P. Mazar A, W. Ahn R, V. O'Halloran T. Development of Novel Therapeutics Targeting the Urokinase Plasminogen Activator Receptor (uPAR) and Their Translation Toward the Clinic. *Curr Pharm Des*. 2011;17(19):1970-1978. doi:10.2174/138161211796718152

516. Harbeck N, Schmitt M, Meisner C, et al. Ten-year analysis of the prospective multicentre Chemo-N0 trial validates American Society of Clinical Oncology (ASCO)-recommended biomarkers uPA and PAI-1 for therapy decision making in node-negative breast cancer patients. *Eur J Cancer*. 2013;49(8):1825-1835. doi:10.1016/j.ejca.2013.01.007

517. Harbeck N, Schmitt M, Vetter M, et al. Prospective biomarker trials chemo N0 and NNBC-3 Europe validate the clinical utility of invasion markers uPA and PAI-1 in node-negative breast cancer. In: *Breast Care*. Vol 3. S. Karger AG; 2008:11-15. doi:10.1159/000151734

518. Ellis V, Behrendt N, Dano K. Plasminogen activation by receptor-bound urokinase: A kinetic study with both cell-associated and isolated receptor. *J Biol Chem*. 1991;266(19):12752-12758.

519. Higazi AAR, Cohen RL, Henkin J, Kniss D, Schwartz BS, Cines DB. Enhancement of the enzymatic activity of single-chain urokinase plasminogen activator by soluble urokinase receptor. *J Biol Chem*. 1995;270(29):17375-17380. doi:10.1074/jbc.270.29.17375

520. O'Halloran T V., Ahn R, Hankins P, Swindell E, Mazar AP. The many spaces of uPAR: Delivery of theranostic agents and nanobins to multiple tumor compartments through a single target. *Theranostics*. 2013;3(7):496-506. doi:10.7150/thno.4953

521. Xing RH, Rabbani SA. Overexpression of urokinase receptor in breast cancer cells results in increased tumor invasion, growth and metastasis. *Int J Cancer*. 1996;67(3):423-429. doi:10.1002/(SICI)1097-0215(19960729)67:3<423::AID-IJC18>3.0.CO;2-8

522. Frandsen TL, Holst-Hansen C, Nielsen BS, et al. Direct evidence of the importance of stromal urokinase plasminogen activator (uPA) in the growth of an experimental human breast cancer using a combined uPA gene-disrupted and immunodeficient xenograft model. *Cancer Res*. 2001;61(2):532-537.

523. Mazar AP. Urokinase plasminogen activator receptor choreographs multiple ligand interactions: Implications for tumor progression and therapy. *Clin Cancer Res*. 2008;14(18):5649-5655. doi:10.1158/1078-0432.CCR-07-4863

524. Guo Y, Higazi AA, Arakelian A, Sachais BS, Cines D, Goldfarb RH, Jones TR, Kwaan H, Mazar AP RS. A peptide derived from the nonreceptor binding region of urokinase plasminogen activator (uPA) inhibits tumor progression and angiogenesis and induces tumor cell death in vivo. *FASEB J*. 2000;14(10):1400-1410. doi:10.1096/fj.14.10.1400

525. Xing RH, Mazar A, Henkin J RS. Prevention of breast cancer growth, invasion, and metastasis by antiestrogen tamoxifen alone or in combination with urokinase inhibitor B-428. *Cancer Res*. 1997;15;57(16):3585-3593.

526. Rabbani S, Harakidas P, Davidson DJ, Henkin J, Mazar AP. Prevention of prostate-cancer metastasis in vivo by a novel synthetic inhibitor of urokinase-type plasminogen activator (uPA). *Int J Cancer*. 1995;63(6):840-845. doi:10.1002/ijc.2910630615

527. Wang D, Yang Y, Jiang L, et al. Suppression of Tumor Growth and Metastases by Targeted Intervention in Urokinase Activity with Cyclic Peptides. *J Med Chem*. 2019;62(4):2172-2183. doi:10.1021/acs.jmedchem.8b01908

528. Pugh S, Thomas GAO. Patients with adenomatous polyps and carcinomas have increased colonic mucosal prostaglandin E2. *Gut*. 1994;35(5):675-678. doi:10.1136/gut.35.5.675

529. Rigas B, Goldman IS, Levine L. Altered eicosanoid levels in human colon cancer. *J Lab Clin Med*. 1993;122(5):518-523. doi:10.5555/uri:pii:002221439390010V

530. Schrey MP, Patel K V. Prostaglandin E2 production and metabolism in human breast cancer cells and breast fibroblasts. Regulation by inflammatory mediators. *Br J Cancer*. 1995;72(6):1412-1419. doi:10.1038/bjc.1995.523

531. Ayiomamitis GD, Notas G, Vasilakaki T, et al. Understanding the interplay between COX-2 and hTERT in colorectal cancer using a multi-omics analysis. *Cancers (Basel)*. 2019;11(10). doi:10.3390/cancers11101536

532. Xin X, Majumder M, Girish G V., Mohindra V, Maruyama T, Lala PK. Targeting COX-2 and EP4 to control tumor growth, angiogenesis, lymphangiogenesis and metastasis to the lungs and lymph nodes in a breast cancer model. *Lab Investig*. 2012;92(8):1115-1128. doi:10.1038/labinvest.2012.90

533. Kundu N, Yang Q, Dorsey R, Fulton AM. Increased cyclooxygenase-2 (cox-2) expression and activity in a murine model of metastatic breast cancer. *Int J Cancer*. 2001;93(5):681-686. doi:10.1002/ijc.1397

534. Liu B, Qu L, Yan S. Cyclooxygenase-2 promotes tumor growth and suppresses tumor immunity. *Cancer Cell Int*. 2015;15:106. doi:10.1186/s12935-015-0260-7

535. Half E, Tang XM, Gwyn K, Sahin A, Wathen K, Sinicrope FA. Cyclooxygenase-2 expression in human breast cancers and adjacent ductal carcinoma in situ. *Cancer*

Res. 2002;62(6):1676-1681.

536. Greenhough A, Smartt HJ, Moore AE, Roberts HR, Williams AC, Paraskeva C KA. The COX-2/PGE2 pathway: key roles in the hallmarks of cancer and adaptation to the tumour microenvironment. *Carcinogenesis*. 2009;Mar;30(3):377-386. doi:10.1093/carcin/bgp014

537. Ristimäki A, Sivula A, Lundin J, et al. Prognostic significance of elevated cyclooxygenase-2 expression in breast cancer. *Cancer Res*. 2002;62(3):632-635.

538. Wang T, Yan J, Xu W, Ai Q, Mai K. Characterization of Cyclooxygenase-2 and its induction pathways in response to high lipid diet-induced inflammation in Larmichthys crocea. *Sci Rep*. 2016;6(1):1-13. doi:10.1038/srep19921

539. Kirkby NS, Zaiss AK, Wright WR, et al. Differential COX-2 induction by viral and bacterial PAMPs: Consequences for cytokine and interferon responses and implications for anti-viral COX-2 directed therapies. *Biochem Biophys Res Commun*. 2013;438(2):249-256. doi:10.1016/j.bbrc.2013.07.006

540. Font-Nieves M, Sans-Fons MG, Gorina R, et al. Induction of COX-2 enzyme and down-regulation of COX-1 expression by lipopolysaccharide (LPS) control prostaglandin E 2 production in astrocytes. *J Biol Chem*. 2012;287(9):6454-6468. doi:10.1074/jbc.M111.327874

541. Liu CH, Chang SH, Narko K, et al. Overexpression of Cyclooxygenase-2 is Sufficient to Induce Tumorigenesis in Transgenic Mice. *J Biol Chem*. 2001;276(21):18563-18569. doi:10.1074/jbc.M010787200

542. Chang SH, Liu CH, Conway R, et al. Role of prostaglandin E2-dependent angiogenic switch in cyclooxygenase 2-induced breast cancer progression. *Proc Natl Acad Sci U S A*. 2004;101(2):591-596. doi:10.1073/pnas.2535911100

543. Timoshenko A V, Xu G, Chakrabarti S, Lala PK, Chakraborty C. Role of prostaglandin E2 receptors in migration of murine and human breast cancer cells. *Exp Cell Res*. 2003;289(2):265-274. doi:10.1016/s0014-4827(03)00269-6

544. Wang D, Fu L, Sun H, Guo L, Dubois RN. Prostaglandin E2 Promotes Colorectal Cancer Stem Cell Expansion and Metastasis in Mice. *Gastroenterology*. 2015;149(7):1884-1895.e4. doi:10.1053/j.gastro.2015.07.064

545. Li HJ, Reinhardt F, Herschman HR, Weinberg RA. Cancer-stimulated mesenchymal stem cells create a carcinoma stem cell niche via prostaglandin E2 Signaling. *Cancer Discov*. 2012;2(9):840-855. doi:10.1158/2159-8290.CD-12-0101

546. Wu M, Guan J, Li C, et al. Aberrantly activated Cox-2 and Wnt signaling interact to maintain cancer stem cells in glioblastoma. *Oncotarget*. 2017;8(47):82217-82230. doi:10.18632/oncotarget.19283

547. Kuroda H, Mabuchi S, Yokoi E, et al. Prostaglandin E2 produced by myeloid-derived suppressive cells induces cancer stem cells in uterine cervical cancer. *Oncotarget*. 2018;9(91):36317-36330. doi:10.18632/oncotarget.26347

548. Kurtova A V, Xiao J, Mo Q, et al. Blocking PGE 2-induced tumour repopulation abrogates bladder cancer chemoresistance. *Nature*. 2014. doi:10.1038/nature14034

549. Elwood PC, Pickering JE, Morgan G, et al. Systematic review update of observational studies further supports aspirin role in cancer treatment: Time to share evidence and decision-making with patients? *PLoS One*. 2018;13(9):e0203957. doi:10.1371/journal.pone.0203957

550. Wernli KJ, Hampton JM, Trentham-Dietz A, Newcomb PA. Use of antidepressants and NSAIDs in relation to mortality in long-term breast cancer survivors. *Pharmacoepidemiol Drug Saf*. 2011;20(2):131-137. doi:10.1002/pds.2064

551. Rothwell PM, Wilson M, Price JF, Belch JFF, Meade TW, Mehta Z. Effect of daily aspirin on risk of cancer metastasis: A study of incident cancers during randomised controlled trials. *Lancet*. 2012;379(9826):1591-1601. doi:10.1016/S0140-6736(12)60209-8

552. Murray LJ, Cooper JA, Hughes CM, Powe DG, Cardwell CR. Post-diagnostic prescriptions for low-dose aspirin and breast cancer-specific survival: A nested case-control study in a breast cancer cohort from the UK Clinical Practice. *Breast Cancer Res*. 2014;16(2). doi:10.1186/bcr3638

553. Kwan ML, Habel LA, Slattery ML, Caan B. NSAIDs and breast cancer recurrence in a prospective cohort study. *Cancer Causes Control*. 2007;18(6):613-620. doi:10.1007/s10552-007-9003-y

554. Holmes MD, Chen WY, Li L, Hertzmark E, Spiegelman D, Hankinson SE. Aspirin intake and survival after breast cancer. *J Clin Oncol*. 2010;28(9):1467-1472. doi:10.1200/JCO.2009.22.7918

555. Fraser DM, Sullivan FM, Thompson AM, McCowan C. Aspirin use and survival after the diagnosis of breast cancer: A population-based cohort study. *Br J Cancer*. 2014;111(3):623-627. doi:10.1038/bjc.2014.264

556. Chen WY, Holmes MD. Role of Aspirin in Breast Cancer Survival. *Curr Oncol Rep*. 2017;19(7). doi:10.1007/s11912-017-0605-6

557. Blair CK, Sweeney C, Anderson KE, Folsom AR. NSAID use and survival after breast cancer diagnosis in post-menopausal women. *Breast Cancer Res Treat*. 2007;101(2):191-197. doi:10.1007/s10549-006-9277-x

558. Coombes R, Tovey H, Kilburn L, et al. Abstract GS3-03: A phase III multicentre double blind randomised trial of celecoxib versus placebo in primary breast cancer

patients (REACT – Randomised EuropeAn celecoxib trial). In: *Cancer Research*. Vol 78. American Association for Cancer Research (AACR); 2018:GS3-03-GS3-03. doi:10.1158/1538-7445.sabcs17-gs3-03

559. Jin Y, Smith C, Hu L, et al. LY3127760, a Selective Prostaglandin E4 (EP4) Receptor Antagonist, and Celecoxib: A Comparison of Pharmacological Profiles. *Clin Transl Sci*. 2018;11(1):46-53. doi:10.1111/cts.12497

560. Li X, Yang B, Han G, Li W. The EP4 antagonist, L-161,982, induces apoptosis, cell cycle arrest, and inhibits prostaglandin E2-induced proliferation in oral squamous carcinoma Tca8113 cells. *J Oral Pathol Med*. 2017;46(10):991-997. doi:10.1111/jop.12572

561. Cherukuri DP, Chen XBO, Goulet AC, et al. The EP4 receptor antagonist, L-161,982, blocks prostaglandin E2-induced signal transduction and cell proliferation in HCA-7 colon cancer cells. *Exp Cell Res*. 2007;313(14):2969-2979. doi:10.1016/j.yexcr.2007.06.004

562. Minuk GY. Gaba and hepatocellular carcinoma. *Mol Cell Biochem*. 2000;207(1-2):105-108. doi:10.1023/A:1007062802164

563. He XB, Hu JH, Wu Q, Yan YC, Koide SS. Identification of GABAB receptor in rat testis and sperm. *Biochem Biophys Res Commun*. 2001;283(1):243-247. doi:10.1006/bbrc.2001.4732

564. Watanabe M, Maemura K, Kanbara K, Tamayama T, Hayasaki H. GABA and GABA receptors in the central nervous system and other organs. In: *International Review of Cytology*. Vol 213. Academic Press Inc.; 2002:1-47. doi:10.1016/S0074-7696(02)13011-7

565. Sigel E, Steinmann ME. Structure, function, and modulation of GABAA receptors. *J Biol Chem*. 2012;287(48):40224-40231. doi:10.1074/jbc.R112.386664

566. Enz R, Cutting GR. Molecular composition of GABA(C) receptors. In: *Vision Research*. Vol 38. Elsevier Ltd; 1998:1431-1441. doi:10.1016/S0042-6989(97)00277-0

567. Ansari SR, Jandial Z, Wu X, Liu X, Chen MY, Ansari KI. Journal of Cancer Metastasis and Treatment Synergistic inhibition of SCR1-and ERBB2-driven brain metastatic breast cancer cells. 2019. doi:10.20517/2394-4722.2018.68

568. Zafrakas M, Chorovicer M, Klaman I, et al. Systematic characterisation of *GABRP* expression in sporadic breast cancer and normal breast tissue. *Int J Cancer*. 2006;118(6):1453-1459. doi:10.1002/ijc.21517

569. Williams KC, Cepeda MA, Javed S, et al. Invadopodia are chemosensing protrusions that guide cancer cell extravasation to promote brain tropism in metastasis. *Oncogene*. 2019;38(19):3598-3615. doi:10.1038/s41388-018-0667-4

570. Kaupmann K, Malitschek B, Schuler V, et al. GABA(B)-receptor subtypes assemble into functional heteromeric complexes. *Nature*. 1998;396(6712):683-687. doi:10.1038/25360

571. Kau P, Nagaraja GM, Zheng H, et al. A mouse model for triple-negative breast cancer tumor-initiating cells (TNBC-TICs) exhibits similar aggressive phenotype to the human disease. *BMC Cancer*. 2012;12:120. doi:10.1186/1471-2407-12-120

572. Zhang D, Li X, Yao Z, Wei C, Ning N, Li J. GABAergic signaling facilitates breast cancer metastasis by promoting ERK1/2-dependent phosphorylation. *Cancer Lett*. 2014;348(1-2):100-108. doi:10.1016/j.canlet.2014.03.006

573. Kukkar A, Bali A, Singh N, Jaggi AS. Implications and mechanism of action of gabapentin in neuropathic pain. *Arch Pharm Res*. 2013;36(3):237-251. doi:10.1007/s12272-013-0057-y

574. Bockbrader HN, Wesche D, Miller R, Chapel S, Janiczek N, Burger P. A comparison of the pharmacokinetics and pharmacodynamics of pregabalin and gabapentin. *Clin Pharmacokinet*. 2010;49(10):661-669. doi:10.2165/11536200-000000000-00000

575. Grankvist N, Lagerborg KA, Jain M, Nilsson R. Gabapentin Can Suppress Cell Proliferation Independent of the Cytosolic Branched-Chain Amino Acid Transferase 1 (BCAT1). *Biochemistry*. 2018;57(49):6762-6766. doi:10.1021/acs.biochem.8b01031

576. Irizarry MC, Webb DJ, Boudiaf N, et al. Risk of cancer in patients exposed to gabapentin in two electronic medical record systems. *Pharmacoepidemiol Drug Saf*. 2012;21(2):214-225. doi:10.1002/pds.2266

577. Fauer AJ, Davis MA, Choi SW, Wallner LP, Friese CR. Use of gabapentinoid medications among US adults with cancer, 2005–2015. *Support Care Cancer*. 2020;28(1):5-8. doi:10.1007/s00520-019-05100-9

578. Bassik MC, Kampmann M, Lebbink RJ, et al. A systematic mammalian genetic interaction map reveals pathways underlying ricin susceptibility. *Cell*. 2013;152(4):909-922. doi:10.1016/j.cell.2013.01.030

579. Williams SA, Anderson WC, Santaguida MT, Dylla SJ. Patient-derived xenografts, the cancer stem cell paradigm, and cancer pathobiology in the 21st century. *Lab Investig*. 2013;93:970-982. doi:10.1038/labinvest.2013.92

580. Sun M, Yang Z. Metabolomic Studies of Live Single Cancer Stem Cells Using Mass Spectrometry. *Anal Chem*. 2019;91(3):2384-2391. doi:10.1021/acs.analchem.8b05166

581. Waki M, Ide Y, Ishizaki I, et al. Single-cell time-of-flight secondary ion mass spectrometry reveals that human breast cancer stem cells have significantly lower

content of palmitoleic acid compared to their counterpart non-stem cancer cells. *Biochimie*. 2014;107(Part A):73-77. doi:10.1016/j.biochi.2014.10.003

582. Rusu P, Shao C, Neuerburg A, et al. GPD1 Specifically Marks Dormant Glioma Stem Cells with a Distinct Metabolic Profile. *Cell Stem Cell*. 2019;25(2):241-257.e8. doi:10.1016/j.stem.2019.06.004

583. Yip NC, Fombon IS, Liu P, et al. Disulfiram modulated ROS-MAPK and NFB pathways and targeted breast cancer cells with cancer stem cell-like properties. *Br J Cancer*. 2011;104(10):1564-1574. doi:10.1038/bjc.2011.126

APPENDIX 1: COPYRIGHT PERMISSIONS

6.8.1 *CHAPTER 1*

Thomas ML, P Marcato. Epigenetic Modifications as Biomarkers of Tumour Development, Therapy Response, and Recurrence Across the Cancer Care Continuum (2018). *Cancers* doi:10.3390/cancers10040101

No special permission is required to reuse all or part of article published by MDPI, including figures and tables. For articles published under an open access Creative Common CC BY license, any part of the article may be reused without permission provided that the original article is clearly cited. Reuse of an article does not imply endorsement by the authors or MDPI.

Thomas ML, Krysta M Coyle, Mohammad Sultan and Paola Marcato. (2015) Cancer Stem Cells and Chemoresistance: Strategies to Overcome Therapeutic Resistance (Chapter 26). Cancer Stem Cells: Emerging Concepts and Future Perspectives in Translational Oncology. Springer.

Authors have the right to reuse their article's Version of Record, in whole or in part, in their own thesis. Additionally, they may reproduce and make available their thesis, including Springer Nature content, as required by their awarding academic institution. Authors must properly cite the published article in their thesis according to current citation standards.

6.8.2 *CHAPTER 2*

Dahn ML, BM Cruickshank, A Jackson, C Dean, R Holloway, SR Hall, KM Coyle, DM Waisman, KB Goralski, CA Giacomantonio, P Marcato (2020). Decitabine response in breast cancer requires efficient drug processing, induction of genes mediating cell cycle arrest and apoptosis, and is not limited by multidrug resistance. Molecular Cancer Therapeutics. doi: 10.1158/1535-7163.MCT-19-0745

Authors of articles published in AACR journals are permitted to use their article or parts of their article in the following ways without requesting permission from the AACR. All such uses must include appropriate attribution to the original AACR publication. Authors may do the following as applicable:

1. Reproduce parts of their article, including figures and tables, in books, reviews, or subsequent research articles they write;
2. Use parts of their article in presentations, including figures downloaded into PowerPoint, which can be done directly from the journal's website;
3. Post the accepted version of their article (after revisions resulting from peer review, but before editing and formatting) on their institutional website, if this is required by their institution. The version on the institutional repository must contain a link to the final, published version of the article on the AACR journal website so that any subsequent corrections to the published record will continue to be available to the broadest readership. The posted version may be released publicly (made open to anyone) 12 months after its publication in the journal;
4. **Submit a copy of the article to a doctoral candidate's university in support of a doctoral thesis or dissertation**.

6.8.3 *CHAPTER 4*

Thomas ML, R De Antueno, KM Coyle, M Sultan B Cruickshank, M Giacomantonio, R Duncan CA Giacomantonio, P Marcato (2016). Citral reduces breast tumour growth by inhibiting cancer stem cell marker ALDH1A3. Molecular Oncology doi: 10.1016/j.molonc.2016.08.004